TECHNISCHE UNIVERSITÄT MÜNCHEN

Lehrstuhl für Humanbiologie

The role of IKKalpha in sporadic and familial colorectal tumorigenesis

Serkan İsmail Göktuna

Vollständiger Abdruck der von der Fakultät Wissenschaftszentrum Weihenstephan für Ernährung, Landnutzung und Umwelt der Technischen Universität München zur Erlangung des akademischen Grades eines

Doktors der Naturwissenschaften

genehmigten Dissertation.

Vorsitzende(r):	Univ.-Prof.Dr. J. J. Hauner
Prüfer der Dissertation:	1. Univ.-Prof. Dr. M. Schemann
	2. Priv.-Doz. Dr. F. R. Greten

Die Dissertation wurde am 02.11.2009 bei der Technischen Universität München eingereicht und durch die Fakultät Wissenschaftszentrum Weihenstephan für Ernährung, Landnutzung und Umwelt am 05.02.2010 angenommen.

ABSTRACT

In this thesis, the role of IKKα in colorectal tumorigenesis was investigated by the use of chemical and genetic mouse models of colorectal tumors. To do this, an inactive IKKα mutant mouse was used in conjunction with these tumor models and the development of colorectal tumors were monitored for morphological and physiological differences. As a result of these experiments, a distinct phenotype of tumor growth retardation and extended survivals of the animals were observed in all tumor models with IKKα inactivation.

Molecular analysis of reduced tumor growth in IKKα mutants resulted in a clear IFNγ upregulation due to myeloid cell recruitment by epithelial secreted factors and autocrine myeloid cell activation by intrinsic factors like MCP-1 and IL-12. NF-κB activity was found to be crucial for activation of myeloid cells to release IFNγ, which further caused growth arrest in IKKα mutant enterocytes.

In conclusion, phospho-activation of IKKα is characterized as an important regulator of immune responses in colorectal tumorigenesis. Therefore, the primary role of IKKα in colorectal tumorigenesis is to suppress IFNγ release. However, this role adversely promotes tumor growth in colorectal cancers. In this respect, these results strongly suggest that IKKα phospho-inactivation can be a potent therapeutic strategy for the therapy of colorectal tumors.

ZUSAMMENFASSUNG

In der vorliegenden Arbeit die Funktion von IKKα bei der Tumorentstehung wurde durch chemische und genetische murine kolorektale Karzinom-Modelle untersucht. Inaktivierung von IKKα führte in allen Modellen durch eine Verzögerung des Tumorwachstums zu einer signifikanten Verlängerung des Überlebens der Versuchstiere.

Molekularbiologische Untersuchungen zeigten in IKKα defizienten Mäusen eine deutlich gesteigerte IFNγ Hochregulation aufgrund der Rekrutierung von myeloischen Zellen durch epithelial sekretierte Faktoren sowie durch autokrine myeloische Zell-Aktivierung durch intrinsische Faktoren wie MCP-1 und IL-12. Die NF-κB Aktivität ist von entscheidender Bedeutung, für die Aktivierung der myeloischen Zellen zur Freisetzung von IFNγ, was in Folge zu konsekutivem Wachstumsstop in IKKα defizienten Enterozyten führt.

Zusammenfassend demonstrieren die Ergebnisse dieser Arbeit, dass die Aktivierung von IKKα die kolorektale Karzinomentstehung durch Suppression der IFNγ Expression maßgeblich fördert. Die Möglichkeit einer pharmakologischen Inhibition der IKKα abhängigen IFNγ Suppression könnte demnach in Zukunft eine neue potentielle Strategie in der Therapie des kolorektalen Karzinoms darstellen.

ACKNOWLEDGMENTS

First of all, I want to thank Prof. Florian R. Greten for providing this research position in which I have found plenty of opportunity to develop my technical skills, my theoretical background on various subjects and my scientific approach to different issues. He is a model scientist for hard-working, commitment to oneself job, critical thinking and innovative problem solving abilities. He helped me a lot to be able to look subjects from different angles, in developing skeptic thinking abilities and in finding way out when I was hindered by certain experimentation. It would not be possible for me to finish this project without his profound guidance. I have every confidence in him that he will be a leading scientist in his area in the near future. The experience I gained from his advisership will be one of the most powerful earnings to build up my future academic career. For this reason and many others, it was a great pleasure and honor for me to have a chance to make research together with him.

I am also thankful to Prof. Roland M. Schmid for being a very good Chief to our department, providing us with such good facilities and hosting social activities which made each other know.

I am grateful to Prof. Michael Schemann for accepting me as a student in his faculty, being my Doktorvater and advising me with academic and bureaucratic requirements that helped a lot while preparing this thesis.

I am also thankful to Dr. M. Canan Arkan for her kind collaboration in our research projects and every other help she gave while I am working in the lab. Moreover, I was benefited from her essential advises both in academic and personal issues that made my life easier.

Furthermore, I am grateful to Dr. Hana Algül, Dr. Jens Siveke, Dr. Dieter Saur, Dr. Günther Schneider and Dr. Hassan Nakhai, for their collaboration, advises in research and in personal issues.

I am especially thankful to Dr. Frank Schmidt for invaluable helps in dendritic cell experiments; Dr. Jörg Magesand Angela Servatius for generating and analyzing Microarray data; Julia Bollrath for excellent and enormous amount of FACS data that helped a lot in finishing this project; Özge Canlı for exceptional ELISA and macrophage stimulation data; Tim Nebelsiek for vital kinase assay data and completing expression analysis with double knockouts; Kristin Retzlaff for brilliant technical assistance for dealing mice genotypes and matings; similarly Birgit Wittig and Rabea Könitschke for technical assistance and the rest of the lab for providing assistance whenever I was in the need.

My personal thanks go to my comrades Jamil Khasawneh, Dr. Alexander A. Fingerle, (soon to be Dr.) Moritz Bennecke, Tim Nebelsiek, Dr. Arun K. Mankan and Özge Canlı for their friendship and assistance in technical and

practical problems. I am grateful to them not only being the best colleagues one can have but also being such good friends. Especially their kind advises and limitless humor helped me a lot in coping with the difficulties of the research life and persuading me to go on no matter how hard the difficulties I faced.

My other lab mates Julia Bollrath, Sarah Schwitalla, Vivian Daer, Simone Zach, Manon Schulz and Çiğdem Atay, I am also thankful to you for countless helps and the good times we had in the lab and in extracurricular activities. Thank you so much all other people from 2nd Internal Medicine who helped me in any single way or just shared their friendship.

I am thankful to Prof. Michael Karin (Univ. of Calif. San Diego, USA), Prof. Yinglin Hu (Univ. of Texas MD Anderson Cancer Centre, USA), Roland M. Schmid, Prof. Falk Weih (Leibniz Institut für Alterforschung, Germany), Prof. Makato M. Taketo (Kyoto University, Japan), and Prof. Sylvie Robin (Institut Curie, France) for kindly providing the mouse models we used in this study. Moreover, I thank Prof. Davis Artis for providing IL-12b neutralizing antibody.

I am thankful to my friends Dr. Özgür Şahin (DKFZ, Heidelberg), Özlem Sener Şahin (Univ. Heidelberg), Ufuk Bayburt (METU, Ankara), Dr. Çetin Baloğlu (Cambridge Univ., UK), Dr. Günseli Bayram Akçapınar (Sabancı Univ., İstanbul), Dr. Çağhan Kızıl (MPI Dresden), Dr. Güneş Özhan Kızıl (MPI Dresden) for personal assistance they provided to complete my documents, being there whenever I needed somebody to talk and infinite support and trust they provided.

Lastly, I cannot find words to describe my gratefulness for my parents Nesrin and Mete and my sister Canan Sezin for providing support in every possible way one can imagine. I am also thankful to my uncle Fethi Göktuna for his limitless supports and trust that made this thesis possible. And the rest of my family and cousins I could not mention specifically here, thank you very much.

I am dedicating this thesis to my family and to my beloved cousins Güzide and Levent who were like elder sister and elder brother to me and have departed from this world to leave me in solitude. I hope you are in peace wherever you went.

Serkan İsmail Göktuna

Munich, October 2009

Güzide Ablama,

Levent Ağabeyime,

Öncü Dayıma,

ve hiçbir zaman desteklerini

eksik etmeyen aileme

Imagination will often carry us to worlds that never were.
But without it we go nowhere.

Carl Sagan

INDEX

INDEX OF FIGURES

INDEX OF TABLES

ABBREVIATIONS

Ab	antibody
APC	antigen presenting cell/adenomatosis polyposis coli (context dependent)
ASCL2	achaete-scute complex homolog 2
b.m.	bone marrow
BMD	bone marrow derived
CA	continuously active
CAC	colitis associated carcinoma
CCL	chemokine (C-C motif) ligand
CXCL	chemokine (C-X-C motif) ligand
CD	cluster of differentiation
chIP	chromosomal immunoprecipitation
CK-I	casein kinase I
coIP	co-immunoprecipitation
CR	colorectal
CRC	colorectal cancer
DC	dentritic cell
DMEM	Dulbecco's modified Eagle's medium
DN	dominant negative
EGFR	endothelial growth factor receptor
ELF3	E74-like factor 3
EMSA	enzyme mobilized shift assay
ES	embryonic stem cell
FACS	fluorescence assisted cell sorter
FAP	familial adenopolyposis
FCS	fecal calf serum
GI	gastrointestinal
GSH	glutathione
GST	glutathione S -tranferase
HA	hemagglutinin
HCC	hepatocellular carcinoma
HCT	hematocrit
HES1	hairy and enhancer of split 1
HGB	hemoglobin
HNNP	human nonpolyposis neoplasia

Abbreviations

i.p.	intraperitoneal
IB	immunoblotting
IEC	intestinal epithelial cell
IFN	interferon
IF	immunoflorescence
IHC	immunohistochemistry
IκB	inhibitor of kappa B
IKDC	interferon producing killer dendritic cell
IKK	inhibitor of kappa B kinase
IL	interleukin
IP	immunoprecipitation
KC	Kupfer cells
KD	knockdown/kinase deficient (context dependent)
KLF4	Kruppel-like factor 4
KO	knock-out
LEF	lymphocyte enhancing factor
LGR5	leucine rich repeat containing G protein coupled receptor 5
LPS	lipopolysaccharide
MAPK	mitogen-activated protein kinase
MATH1	atonal homolog 1
MCP-1	monocyte chemoactractant protein-1
mDC	myeloid denritic cell
MDSC	macrophage derived stromal cell
MEF	murine embryonic fibroblast
MHC	major histocompability complex
MLN	mesenteric lymph node
MMP	matrix metallo proteinase
Mt	mutant
NF-κB	nuclear factor-kappa B
NGN3	neurogenin 3
NK	natural killer
NSAID	non-steroidal anti-inflammatory drug
OLFM4	olfactomedin 4
PAX	paired box gene
pDC	plasmocytoid dendritic cell
PI	propidium iodide
ROS	reactive oxygen species
RTK	receptor tyrosine kinase
siRNA	small interfering RNA

Abbreviations

SMAD	sma and mothers against decapentaplegic homolog
STAT	signal transducer and activator of transcription
TAA	tumor associated antigen
TCF	transcription factor (T-cell specific, HMG-box)
TCR	T-cell receptor
TDSF	tumor derived soluble factors
Th	helper T-cell
TNF	tumor necrosis factor
TiDC	tumor infiltrating dendritic cell
TRAIL	tumor necrosis factor-related apoptosis inducing ligand
Treg	regulatory T-cell
TSLP	thymic stromal lymphopoietin
VEGFR	vascular endothelial growth factor receptor
WB	western blotting
WT	wild type

1. INTRODUCTION

Medicine is an important division of the life sciences which enables us to apply the knowledge we obtained from basic research to patients to save their lives or to improve their life quality. Before the establishment of aseptic theory or discovery of microscopes to find out basic organization units of life, cells, medicine and molecular biology evolved quite separately. Traditional medicine relied on symptomatic treatment of diseases or surgical removal of the parts that cause problem. Although improvements in surgery enjoyed many patients, the real breakthrough of medicine came after aseptic theory and identifying microscopic pathogens by the studies of Lister, Koch and Pasteur (Exner et al., 2001). Then molecular biology and medicine united to form today what we know as molecular medicine. Studies in biochemistry and cell biology proved very important findings in understanding cellular or molecular origins of human diseases. However, it was only after the discovery of genetic material (its structure (Watson and Crick, 1953) and function (Watson and Crick, 1953)) and understanding the importance of mutations (Freese, 1959), humankind started to truly understand very basis of every disease. Use of mutational models in experimental animals (Capecchi, 1989) and use of stem cells (Evans and Kaufman, 1981) enabled us to understand development of many diseases and now even make it possible to find non-symptomatic therapeutic interventions at the molecular level to treat diseases. The future of molecular medicine lies within understanding initiation and development of diseases by very good understanding of molecular pathways to give rise to pathological conditions. Only after then we will be successfully addressing our treatments specifically and personally to deal with today's dreadful diseases.

Once learnt the importance of molecular medicine in finding therapies to the diseases, let us turn our attention to the very basis of molecular machinery that give rise to pathological disorders. Within any organisms organ systems are the important labor of division to handle daily requirements of living (Sadava et al., 2006). Although there are problems with physical

obstructions or traumatically injuries, most of the problems occurring in the systems are affected from molecular problems that occur in the basic building blocks of tissues and organs, cells. Cells manage complex molecular functions that vary from metabolism to growth, signaling to interaction with different cells or environment. All these functions are made by the use of thousands of proteins whose interaction is controlled via absolute concentrations that is managed via genetic material again by the use of regulatory enzymes. Cellular functions are orchestrated with a group of molecules called transcription factors (Karin, 1990) that are able to translocate into nucleus upon delivery of upstream stimuli in the form of effectors molecules or direct interaction with receptors (Rensing, 1972). Collectively these molecules form the signaling pathways to deliver messages into nuclear response elements via transcription factors. According to concentration and the strength of the stimuli one pathway may dominate or alternative signaling pathways can collaborate in cellular functions. Transcription factors are the key elements of any signaling machinery and their regulation is utmost importance to cellular functions or survival (Latchman, 1997). A loss of a structural protein may have profound effects in a specific genetic disease while loss or dysfunction of molecules in signaling pathways can have dramatic effects in many different mechanisms and can threaten the life of whole organisms in several different ways (Karin and Greten, 2005; Li et al., 2006; Massagué, 1998). Therefore understanding signaling pathways and crosstalk between each other is indispensable to understand development of diverse pathological outcomes (Chen et al., 2003; Greten et al., 2004).

NF-κB Signaling is central to many signaling mechanisms connecting inflammation to cell survival in pro and anti-apoptotic responses (Karin and Greten, 2005). According to the source and latency of the upstream signal, the downstream effects of NF-κB can be tumor promoting or suppressing as shown in different cancer models (Greten et al., 2004; Lawrence et al., 2005). IKKβ is widely studied regulator or canonical NF-κB activation and known to have important roles in inflammation and cancer (Greten et al., 2004). IKKα is on the other hand is less studied and known to have roles in dominantly in alternative NF-κB activation (Senftleben et al., 2001). Recent studies have shown that IKKα has significant roles in cell differentiation (Descargues et al., 2008), immune regulation (Lawrence et al., 2005) and cancer formation (Lamberti et al.,

2001) related to alternative or canonical NF-κB activation (Häcker and Karin, 2006). Especially, it has been shown to translocate into cell nuclei (Lamberti et al., 2001), regulate proliferative proteins like β-catenin (Carayol and Wang, 2006), repress NF-κB subunit binding (Lawrence et al., 2005) to their respective promoters to resolve inflammation gave us the idea that IKKα has a great potential to regulate cancer initiation and development especially related to immune activation.

After all these observations, we were convinced that IKKα is a potentially important molecule which is at the junction of molecular pathways leading to diverse background of cancers. Therefore, we believed that IKKα should have a major contribution to the development of colorectal tumorigenesis due to its potent regulatory function on NF-κB dependent or non-dependent pathways leading to proliferation or the control of inflammation. For this purpose, we used CRC models where IKKα is inactivated or totally removed. By doing so, we will learn how this molecule is regulating the course of CRC development. In the following sections we will give basic information regarding colorectal tumorigenesis and its association with inflammation in the context of NF-κB or IKKα activation. Finally, we will present our experimental results and discuss them in the light of current literature to address the role of IKKα in colorectal tumorigenesis.

1.1. BACKGROUND

1.1.1. Intestinal Cell Development and Differentiation

Intestine is the place where nutritious polymers are digested into basic subunits and absorbed along with water, minerals and vitamins for energy and catalysts requirements (Sizer and Whitney, 2005). Being one of the most important bodily functions, digestion requires a lot of energy and maintenance (Sadava et al., 2006). Yet maintenance of gastrointestinal (GI) track is another vital issue since it is an important place after our skin which is continuously in contact with outside pathogens. Unlike to most other tissues, GI epithelial cells needs to be renewed since they are more prone to mechanical wearing (Sadava et al., 2006). Although innate immune system has a series of physical barriers and measures against potentially invading pathogens, there are still possibilities of leakages in the system that may lead to immune activation to cause inflammation (Sadava et al., 2006). Although inflammation is marked by an important mediator of adaptive immune activation, it is still one of the most important causes of diverse pathological problems including inflammatory diseases and cancer (Greten et al., 2004). For these reasons learning about GI system its interaction with the surrounding environment and other tissues like immune cells has utmost importance in developing our understanding for the cause of these problems.

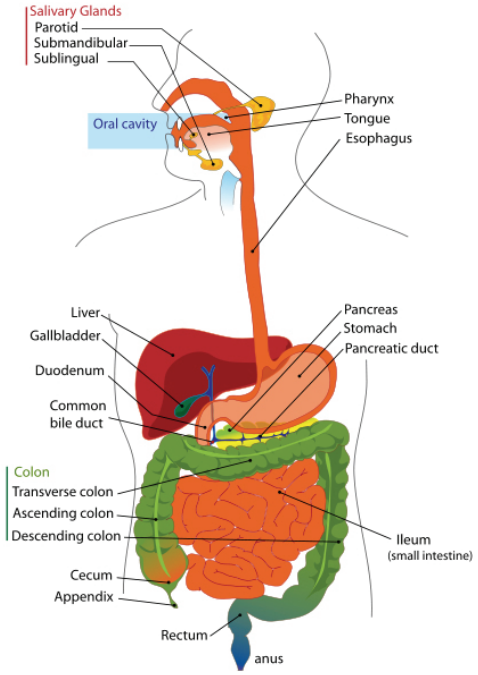

Figure 1.1: Human Gastrointestinal System. (Wikipedia, 2009)

Intestine in human and mice shows similar morphology, physiology and differentiation pattern from embryonic layers. Basically intestine is divided into two morphologically distinct parts as small intestine and colon. Intestine is composed of at least four different tissue; epithelia, surrounding smooth muscle tissue, blood vessel endothelia and hematopoietic cells (Sadava et al., 2006). Lamina propria is the loose connective tissue lies beneath the epithelia and is rich in muscle cells and also blood vessels. Epithelia together with lamina propria are collectively called as mucosa (Sadava et al., 2006). The plane that removes epithelia from lamina propria is called basal membrane. There are also numerous capillary growth into epithelia outgrows and lymph nodes are frequently seen between epithelia and lamina propria (Sadava et al., 2006). Small intestine shows a specific organization outgrowing hair like structure of cells called as villi while cavities called crypts are shared characteristic of small intestine and colon (Sadava et al., 2006). Here crypt contains epithelial stem cells and is the place for proliferating and differentiating cells. Villi are mostly composed of differentiated cells (Gregorieff and Clevers, 2005). Colon does not have villi but only consist of crypts and has a smoother surface (Sadava et al., 2006).

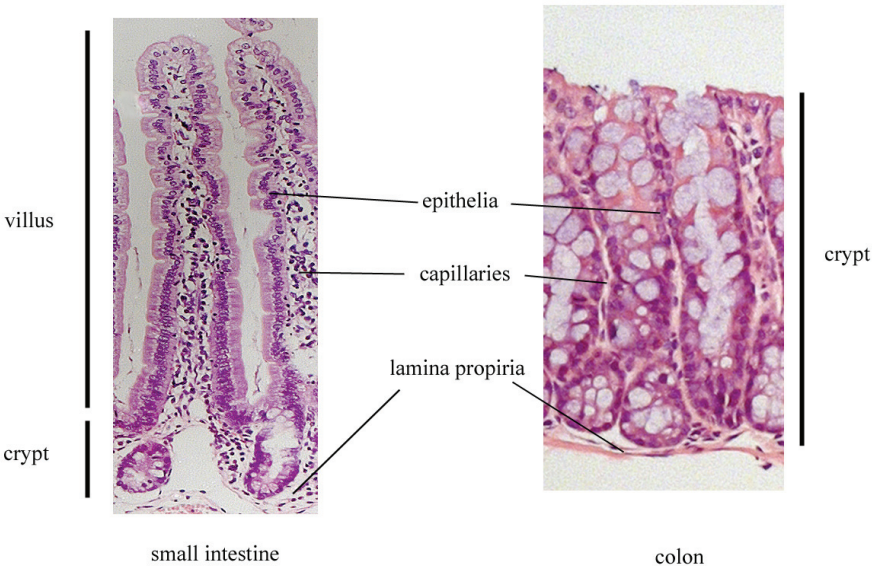

Figure 1.2: Architecture of Small Intestine and Colon: H&E staining of mouse small intestine and colon showing general morphology of the crypts in both tissues and villus only in duodenum.

The different cell types that can be observed in intestinal epithelia are stem cells, paneth cells, enterocytes, enteroendocrine cells and goblet cells (Gregorieff and Clevers, 2005). As mentioned above stem cells are the progenitor cells of any other cell type in the intestine and they have high potential to proliferate to renew of all cells from crypt to villus in 5-7 days (Gregorieff and Clevers, 2005). Wnt signaling plays important role in the development and differentiation of intestinal cell lineages. Wnt is signaling is highly active during embryogenesis and in the differentiation of intestinal epithelial stem cells. Wnt signaling is constitutively active in stem cells and recently discovered stem cell markers like LGR5, OLFM4 and ASCL2 are all targets of Wnt signaling and β-catenin (Barker et al., 2007; van der Flier et al., 2009; van der Flier et al., 2009). LGR5 is the first marker for stem cells and made us possible to track stem cells and their localization (Barker et al., 2007). It was found that 6-8 stem cells are found in the bottom of the crypts and are surrounded by paneth cells as one cell apart with neighboring paneth cells (Barker et al., 2007; van der Flier et al., 2009). Then OLFM4 a target of Wnt signaling is also

discovered as stem cell marker and this protein gives colocalization in intestinal epithelial stem cells only (van der Flier et al., 2009). The last stem cell marker, ASCL2 is actively expressed in stem cells and its absence in the animals via conditional knockout may cause the loss of stem cells within days from intestine (van der Flier et al., 2009). Therefore, ASCL2 is the ultimate target of Wnt signaling to give cells stem cell properties. We also recently discovered that highly proliferating cells in β-catenin and NF-κB constitutively active cells retain ASCL2, OLFM4 and LGR5 expression and show dysfunctional differentiation in crypt like pockets (Fingerle et al., 2009).

Stem cell give rise to transit amplifying cells which will form all other cell lineages in intestinal epithelia. These cells bear cyclins and c-Myc as marker for identification and these cells have high rate of proliferation. Transit amplifying cells give rise to secretory lineage of cells like paneth, goblet or enteroendocrine cells via Wnt signaling and specific marker for them is MATH1 (Yang et al., 2001). The remaining transit amplifying cells will form enterocytes by Notch signaling but not by Wnt signaling anymore (Jensen et al., 2000). The first cell lineage in secretory transit amplifying cell lineage is paneth cells and they are restricted to the bottom of the crypts with their bactericide production function (Sadava et al., 2006) for the defense of crypts from invading pathogens. Paneth cell lineage have specific markers of Wnt targets cryptidin and defensin (Andreu et al., 2005; Van Es et al., 2005). The second secretory cell type, goblet cells, are ubiquitous to whole crypt to villus axis and are best known with their mucous production which provides protection of epithelial cells from chemical and mechanical stress of stool via neutralizing or softening (Sadava et al., 2006). They share the common secretory cell marker MATH1 with enteroendocrine and Paneth cells (Yang et al., 2001) but KLF4 and ELF3 mutants were found to be specifically lacking goblet cells (Katz et al., 2002; Ng et al., 2002). Enteroendocrine cells are another secretory cell type which produces hormones that initiate enzyme secretion into intestine (Sadava et al., 2006). They have specific markers of lineage commitment such as NGN3, BETA2, PAX4 and PAX6 in the absence of which this cell lineage is diminished (Schonhoff et al., 2004). The remaining cells are called enterocytes and they are basic structural connective cells between all others cell types and they are responsible from the absorption of digested food, mineral, vitamins and water from intestinal cavity (Sadava et al., 2006). They are noted by extensive microvilli formation on their cell membranes to increase

diffusion efficiency (Sadava et al., 2006). They have cell specific marker HES1, a Notch signaling target which antagonizes MATH1 of secretory cell lineages (Jensen et al., 2000).

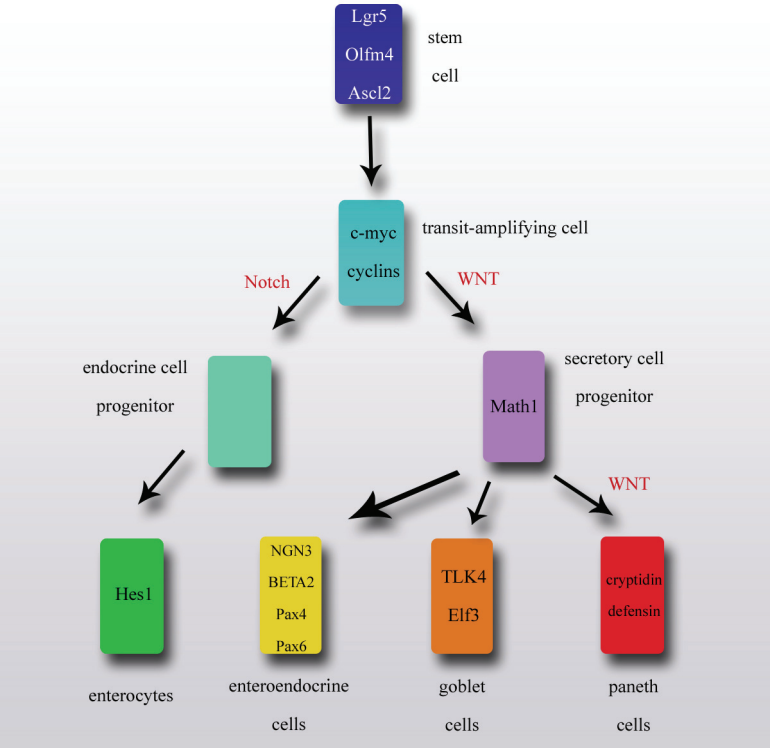

Figure 1.3: Intestinal Epithelial Cell Differentiation. Cell specific markers are indicated inside the boxes. Please see the main text for specific reference of each molecule and pathway involved. Adapted from (Gregorieff and Clevers, 2005).

Overall, intestinal architecture shows quite simple organization of cells from well defined precursor cells which make it easier to follow the initiation and progression of tumors and to target different genes and pathways with high precision in favor of developing promising therapeutic interventions (Clarke, 2006). Colorectal carcinogenesis is well studied and there exist sound information about genes that are involved in the initiation and development of tumors from single benign adenoma to metastatic adenocarcinoma (Fodde et al., 2001; Schneikert and Behrens, 2007). For these purposes, colorectal carcinogenesis is a very good model to generate

gene specific tumor models to understand underlying mechanism of tumorigenesis not only in CRC but also in any other cancer with epithelial origin.

1.2. COLORECTAL CANCER

1.2.1. Epidemiology of CRC

Colorectal cancer is among the leading causes of death in the developed/developing countries (Jemal et al., 2008; Parkin et al., 2005). According to statistics it is 4th most lethal cancer in western countries and its incidence is increasing in the rest of the World as well with over 1 million cases every year (9.4% all cancers in 2002) (Parkin et al., 2005). Although mortality rates are decreasing due to new therapeutic interventions especially in developed countries (529 thousand deaths in 2002) (Parkin et al., 2005), incidence rates are still on the rise especially in the developing countries (Parkin et al., 2005). It ranks 4th in men and 3rd in women incidence frequency in all cancers (Parkin et al., 2005). Average onset of incidence is higher than 60 in most countries but it is decreasing due to environmental and socioeconomic differences (Jemal et al., 2008; Parkin et al., 2005). Especially higher socioeconomic classes have higher incidence rate than that of lower classes (Tappenden et al., 2007). Although diagnostic tools and therapeutic techniques have improved considerably in the last decades, average diagnosis of treatable colorectal tumors, which is the leading cause for 50% life expectancy 5 years after diagnosis, is still as low as 37%. Understanding the molecular pathways which leads to initiation, development and metastasis of colorectal carcinogenesis is invaluable to develop therapeutic agents to treat this noteworthy disease.

1.2.2. Etiology of CRC

Colorectal cancers arise from a diverse background of cases. There is a 20 fold difference between high and low-geographical risk areas which makes us think that environmental and dietary factors play and important role in predisposition of mutations that lead to colorectal tumorigenesis. Sporadic CRC is predominantly caused by environmental factors that result in mutations in genetic material (being exposed to carcinogenic chemicals and cigarette smoking) or increased oxidative stress which results in inflammation or DNA damage as well (such as high fat intake, obesity, lack of physical activity) (Fodde et al., 2001; Martínez et al., 2008; Tappenden et al., 2007). Hereditary susceptibility, on the other hand, only has a small percentage in all colorectal tumorigenesis yet can dramatically increase chances of developing metastatic colorectal tumors in affected individuals.

Sporadic colorectal carcinoma are 85% of the cases (some of which is associated with history of colitis for more than 5 years) while hereditary colorectal carcinomas comprise remaining 15% (Fodde et al., 2001) including nonpolyposis CRCs (Tappenden et al., 2007). Incidence rate is very high in older adults especially with sporadic CRCs. Sporadic CRCs usually requires complex interaction of environmental factors and hereditary background over a long time period. It is believed that it takes about 10 years to form evasive CRC from preexisting adenomas. Mutations that alter genetic material are effective in several mechanisms that regulate cell survival and proliferation which give rise to colorectal carcinogenesis. Generally, mutations leading to chromosomal instability (CI) increase the susceptibility to further mutations. CI was first described as a result of cell cycle checkpoint genes *Bub1* and *Trp53* mutations (Cahill et al., 1998) yet later on evidence suggested that CI occurs early in the adenoma formation (Shih et al., 2001) suggesting the important role of *Apc* gene. Following the loss of chromosomal instability further mutations can block apoptosis, increase proliferation via deregulation of protooncogenes or can increase mutational rate by targeting oncogenes or tumor suppressors (Cahill et al., 1999; Stoler et al., 1999). Chromosomal instability is very common in sporadic cancers and is the leading cause of FAP disease due to loss of *Apc* gene (Kinzler et al., 1991). Microsatellite

instability (MSI) is another common problem that is observed in CRC. On the other hand, MSI is caused by dysfunction or deletions of DNA mismatch repair enzymes like *Msh2* or *Mlh1* via hereditary or sporadic mutations. Since these regions are the simple repeats of several nucleotides any problem with mismatch repair machinery provides susceptibility to accumulate mutations as in the case of CI. MSI leads to a hereditary disease called HNPCC (Potter, 1999). HNPCC disease is related to mutations in DNA mismatch repair genes and more likely to be associated with family history of CRC in predicting risk factor (Potter, 1999; Tappenden et al., 2007).

Since complex interactions and accumulation of genetic problems are required, incidence of sporadic tumor formation is very low with younger population (0-49 years). However, most CRCs observed in younger people are hereditary origin like FAP or HNPCC (Fodde et al., 2001). In FAP disease, due to loss of *Wnt* signaling regulation by a truncation mutation in APC protein, development of a tumor burden with hundreds of polyps throughout the intestine is a common feature within the ages of 10 to 30 in affected patients. From these polyps a significant percentage can turn into carcinoma in the colons of affected individuals by the age of 40 (Fodde et al., 2001; Tappenden et al., 2007).

1.2.3. Genetics and Pathology of CRC

Sporadic colorectal carcinogenesis occurs via a well defined sequence of genetic alterations which were first described by Fearon and Vogelstein (Fearon and Vogelstein, 1990). Normal intestinal epithelia is formed by continuously dividing pluripotent intestinal stem cells (Fearon and Vogelstein, 1990) which sit at the base of crypts and sequestered by paneth cells (Barker et al., 2007). Without any genetic abnormality these cells produce all other intestinal cell types. There are four common genes as targets of mutations that give rise to colorectal carcinogenesis (Fodde et al., 2001). Mutations in one oncogene (K-ras) and three tumor suppressor genes (Apc, Smad3/4 and Trp53) are enough to predispose intestinal malignancy (figure 1.4). Usually Apc mutation is the priming event that initiate cascade of events that leading to chromosomal instability and deregulation of Wnt signaling (Fearon and Vogelstein, 1990). Once *Apc* gene is lost mutational rates are increased due to chromosomal instability which may result in the

mutation of further genes like *K-Ras* (activating), *Smad* or *Trp53* (deactivating) (Fodde et al., 2001; Pinto and Clevers, 2005). Deregulated Wnt signaling leads to increase in the proliferation of intestinal cells and formation of aberrant crypt foci by the fusion or duplication of crypts (Fearon and Vogelstein, 1990; Fodde et al., 2001).

As described in Vogelstein model, proliferating cells follow a top-down model of proliferation (Shih et al., 2001). According to this model, mutations in proliferating cancer stem cells up in the villi increase in number in the villi and move into crypts to replace proliferating crypts or to form new ones. However, others also argued that proliferating undifferentiated cells can move from crypt to villi and form microadenomas (Preston et al., 2003). The latter model is called as bottom-up model of proliferation and it is generally accepted mechanism of adenoma formation. We have recently show that NF-κB signaling acting on Wnt signaling via β-catenin and p65 interaction may regulate a de-differentiation program in which adenomatous crypts in villi are observed (Fingerle et al., 2009). These adenomatous crypts regain stem cell properties and can expand tumor cell numbers while retaining intestinal stem cell marker expression (Fingerle et al., 2009). Our recent work has revealed that these two models do not exclude each other and can co-exist where this alternative model is also possible in proliferation of cancer stem cells (Fingerle et al., 2009).

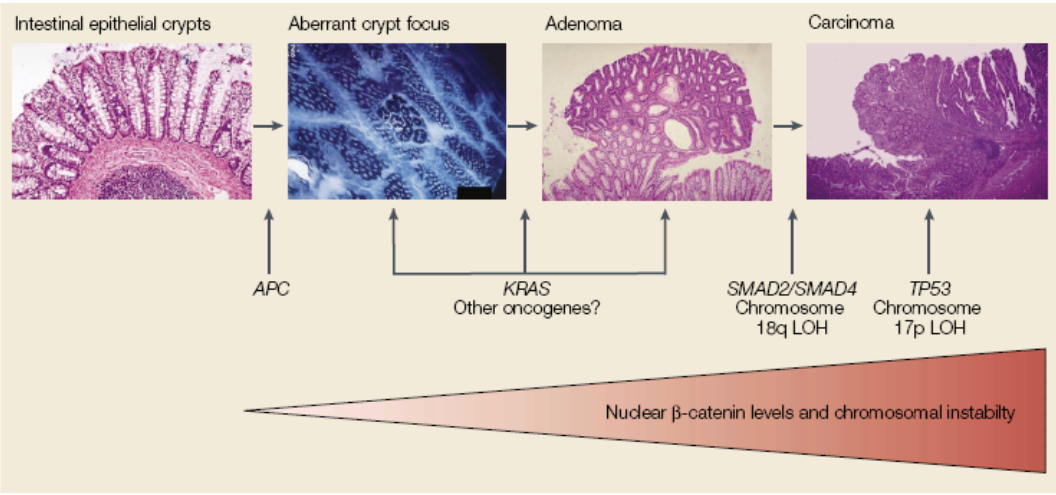

Figure 1.4: Genetics of CRC. Apc mutation is usually the first step for sporadic colorectal tumorigenesis. Mere Apc mutation is enough for increased proliferation and aberrant crypt foci. However, further mutations are required to complete adenoma to carcinoma shift (taken from (Fodde et al., 2001)).

An extra K-ras activating mutation is required for the increased apoptosis leading to adenoma formation (Fearon and Vogelstein, 1990). Adenomatous polyps or non-adenomatous tumors require further modifications in pro-apoptotic tumor suppressor genes (like Smad2/4 and Trp53), which prevent metastasis, to exceed the barrier between adenoma and carcinoma (Fodde et al., 2001). All of these proteins are involved in the control of critical mechanisms like proliferation, apoptosis or anchorage factors, which are important in vascularization, metastasis and resulting carcinoma formation.

1.2.3.1. *Apc* and Wnt Signaling

Most frequently the first step in familial and sporadic CRC is the deactivation of *Apc* gene, which comprises about 90 per cent of all cases (Fodde et al., 2001). *Apc* (adenomatosis polyposis coli) is an important tumor suppressor gene and is named after familial adenomatous polyposis (FAP) due this hereditary disease of multiple polyp formation in the absence of this gene (Gardner, 1951; Groden et al., 1991; Moser et al., 1990). Its product APC protein is one of the components of β-catenin destruction complex under Wnt signaling which drives cells into hyperproliferation when activated (Fodde et al., 2001). APC also interact with microtubules that take part in chromosome attachment to spindle fibers during cell division (Mimori-Kiyosue et al., 2000; Munemitsu et al., 1994). Any problem or mutation that prevents this interaction causes chromosomal instability and increased mutation rate that increases tumor initiation or progression susceptibility (Shih et al., 2001). Altogether, *Apc* is the major target of different mutations that give rise to colorectal adenoma formation yet further mutations are required to complete tumor progression towards carcinoma. Since we have discussed the importance of CI in increased mutational rate in CRC etiology chapter, here we will focus on increased proliferation due to deregulated Wnt signaling in the absence of APC.

To better understand the role of APC we should first acquire an overall understanding of Wnt signaling and its importance in the cell cycle and proliferation. Wnt signaling is a key molecular pathway in development and cell differentiation in a number of different tissues including hematopoietic, skin, mammary and gastrointestinal epithelia (Clarke, 2006; Kenny et al., 2005; Pinto and Clevers, 2005; Pinto et al., 2003; Schneikert and Behrens, 2007). As we have previously described, Wnt signaling is crucial for the development of intestinal architecture and it is also important for the maintenance of stem cells which give rise to different cell types of the intestinal epithelia (Batlle et al., 2002; Pinto et al., 2003; Van de Wetering et al., 2002). This role in cell differentiation inevitably brings about its proliferative potential in many tissues primarily including intestinal epithelia (Korinek et al., 1997; Morin et al., 1997; Van Es et al., 2005). Cell differentiation requires cell division and any deviation from cell division machinery will result in malignancy (Andreu et al., 2005). For this reason, loss of control in Wnt signaling machinery is the most common point for tumor initiation for sporadic intestinal cancers (Fodde et al., 2001). In normal intestinal epithelia Wnt signaling is usually kept under control by a group of proteins whose primary role is to bind or phosphorylate transcription factor β-catenin (Clarke, 2006) (see figure 1.5.A). β-catenin is a membrane bound protein in interaction with E-cadherin (Kitagawa et al., 1999) yet it is cycled to cytoplasm where it is controlled via destruction complex consisting of APC, axin and GSK3β (Amit et al., 2002). Phosphorylation primes β-catenin for ubiquitionation and proteasomal degradation. In the presence of Wnt ligand (figure 1.5.B), activated GBP inhibits GSK3β phosphorylation of β-catenin (Amit et al., 2002; Liu et al., 2002) which leads to β-catenin accumulation in the cytoplasm and finally β-catenin translocates to nucleus where it binds to TCF/LEF to act as a transcriptional coactivator to drive cell into proliferation (Behrens et al., 1996). Here APC is a structural protein which directly binds to β-catenin (Rubinfeld et al., 1996) and provides its recruitment to principal β-catenin kinases CKI and GSK3β for sequential phosphorylation (Amit et al., 2002). This association is the priming event of β-catenin degradation and without this event β-catenin degradation complex cannot form.

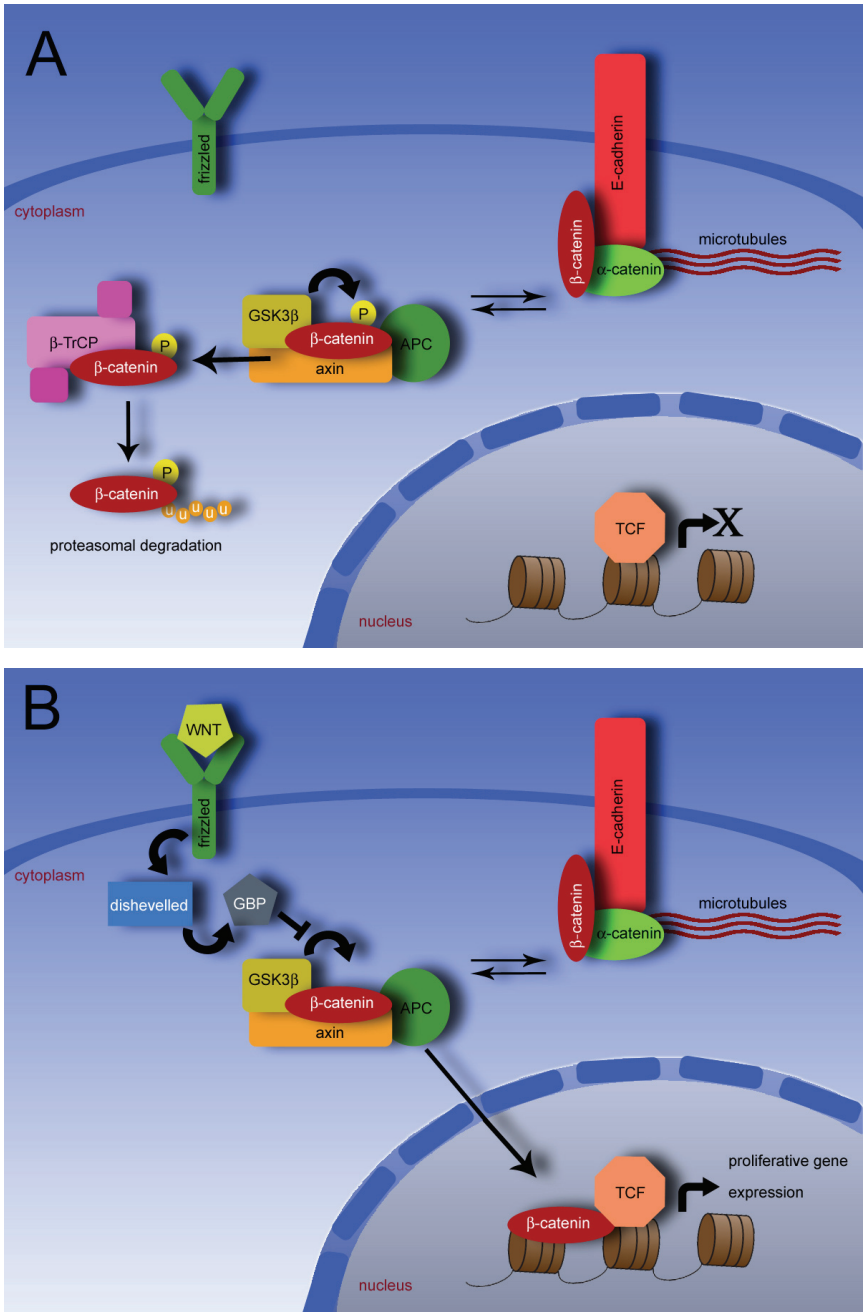

Figure 1.5: WNT signaling. (A) In the absence of Wnt ligand cytoplasmic β-catenin levels are kept under the control of destruction complex and proteasomal degradation after ubiquitination (Gregorieff and Clevers, 2005). (B) When Wnt ligand binds to its receptor downstream effectors repress β-catenin phosphorylation (Chen et al., 2003; Wong et al., 2003; Yost et al., 1998) and its cytoplasmic concentration is elevated to help its nuclear translocation (Waterman, 2004).

As we described in previous sections, Wnt signaling is important for the intestinal cell polarization, differentiation and proliferation. All these functions are passing through β-catenin activation and nuclear localization. The intestinal cell polarization is specifically dependent on

TCF4 activation (Van de Wetering et al., 2002) while the rest of the machinery in intestines is dependent on oncogenic c-Myc protein. c-Myc has been shown to be important for the crypt progenitor cell formation (Muncan et al., 2006) so all Wnt signaling in stem cell targets pass through c-Myc dependent manner. Eventually, c-Myc deletion can revert all the phenotype associated with *Apc* loss in a $Apc^{fl/fl}$ mouse model of adenoma formation (Sansom et al., 2007).

1.2.4. Inflammation and Colorectal Cancer

As early as 19th century, Virchow noted that association of inflammation with increased cancer predisposition (cited in (Karin, 2008)). With recent findings, we understood that inflammation is a driving force for a number of different cancers and has an important share in the initiation and progression process. Especially persistent inflammation paves the way to tumor tolerance and tumor promotion via production of immune cell derived factors like angiogenic cytokines and matrix remodeling enzymes (reviewed in (Balkwill and Mantovani, 2001; Prendergast and Jaffee, 2007)). Up to date, the relation between inflammation and cancers in Stomach due to *H. pylori* infection (Roder, 2002), HCC due to HCV infection (Fattovich et al., 2004) and CAC (Ekbom, 1998) has been clarified via epidemiological associations. Moreover, early data suggested strong association of inflammatory factors with skin (Moore et al., 1999), SCC (Arnott et al., 2002) and mammary carcinoma (Lin et al., 2002) regardless of the lack of epidemiological support (Karin, 2008).

So far different experiments have shown the association of various inflammatory factors and immune cells with cancer initiation or progression in different cancer models (Karin, 2008). The first molecular association of inflammation with CRC was suggested by showing that NSAIDs that inhibit COX-2 activation has blocked the adenoma to carcinoma progression and reduced overall tumor burden in $Apc^{min/+}$ model of CRC (Oshima et al., 1996). Then the basis of this association was identified as NF-κB (COX-2 upstream) activation in a colitis associated CRC (CAC) model by Greten et al. They describe this association such that IKKβ links inflammation to CRC (Greten et al., 2004). Although it was suggested in the same paper that proliferative

potential of intestinal epithelia is arising from inflammatory factors like IL-6, this phenomenon was later confirmed by IL-6 and Stat3 KO mice (Grivennikov et al., 2009). Finally, Bollrath et al. showed that Stat3 activation is important not only in proliferation but also in the survival of the epithelial cells in a similar CAC model (Bollrath et al., 2009). Other factors like TNF-α (Eckmann et al., 2008; Nenci et al., 2007) and IL-1 (Greten et al., 2007) are also suggested to be important in immune activation that can be pronounced in CRC development in the case of colitis.

In summary, these experiments and many others not only provided us to associate inflammation to colorectal tumorigenesis but also provided underlying mechanistic details how inflammation is related to tumor initiation and promotion in CRC. The common point in all these mechanisms that regulates the association between inflammation and CRC is NF-κB signaling. NF-κB signaling is central to cytokine production related to inflammation, immune regulation and apoptosis. Therefore understanding about NF-κB regulation in inflammatory pathways is crucial to develop alternative therapies tipping the balance between persistent inflammation and tumor specific responses. In the following sections we will briefly explain recent findings about general immune regulation pathways in relation to the cancer and finally we will finish our introduction with the specific roles of NF-κB and its regulatory kinases in inflammation and cancer.

1.2.4.1. Tumor Immunosurveillance, Immunotolerance and Escape

The concept of tumor immunosurveillance is rooted from numerous experimental observations in which it was evident that immune system can effectively eliminate tumor cells before they are clinically identified, which was first described as early as Ehrlich in 1909 (Prendergast and Jaffee, 2007). Moreover, experiments with elimination of certain immune cells or immune activation specific models promoted tumor growth in sporadic and chemical models of tumor formation nearly a century later than Ehrlich's initial proposal (Street et al., 2001). Most sporadic tumors are highly immunogenic and effectively eliminated by immune cells via

different pathways of molecular processing (Smyth et al., 2006). However, tumors usually evolve in such a way that they can suppress immunogenic activity of hematopoietic cells (Darrasse-Jèze et al., 2009) in their advantage to suppress their antitumor activity or to provide growth advantage to tumor cells (Zitvogel et al., 2006). By understanding mechanism leading to immune activation and suppression we may direct immune responses towards tumor growth regression or complete tumor elimination. Below we will explain the involvement of different hematopoietic cell lines in initial elimination of tumor cells to tolerate or promote them to prevent self destruction of own tissues.

1.2.4.1.1. Innate Immunity in Tumor Surveillance

Most tumors bear tumor specific antigens which are recognized by innate immune system and processed for antigen presentation to invoke further adaptive immune responses. Tumor associated antigens (TAA for short) (Burnet, 1958) are usually proteins overexpressed in transformed cells or highly induced tumor derived soluble factors (TDSF) in malignant cells to promote growth, mobility, migration, vascularization or matrix deformation (Kim et al., 2006). APCs may recognize elevated levels of these proteins or transformed cells can also present them via MHC class I dependent manner to provoke adaptive immune cell activation (Smyth et al., 2001).

APCs like macrophages or dendritic cells complete their maturation and produce further cytokines or translocate to myeloid organs to induce adaptive immunity towards tumor cells (Prendergast and Jaffee, 2007). In different tumors dendritic cells or macrophages can directly evoke antitumor responses to eliminate tumor cells. Phagocytosis or cytokine induced cytotoxicity by macrophages (Hicks et al., 2006) or TRAIL mediated apoptosis via IKDCs (Taieb et al., 2006) can directly eliminate tumor without further adaptive immune response in some cancers. Macrophages have two distinct phenotypes according to the source of stimuli or the stage of external events. These phenotypes are called M1 and M2 and the neutral phase is usually called as M0 (Condeelis and Pollard, 2006). M1 macrophages are proinflammatory macrophages that

produce cytokines that can induce Th1 lymphocytes to produce higher amounts of IFNγ . They can be induced by bacteria derived factors like LPS (Martinez et al., 2008). Moreover, activation of M1 macrophages makes them more proficient in phagocytosis and they can produce cytokines like MCP-1 and IL-8 for further recruitment of other macrophages or neutrophils to the site of inflammation (Condeelis and Pollard, 2006; Lu et al., 1998). They are characterized by their increased iNOS, TNF-α, IL-6 and IL-12 production (Condeelis and Pollard, 2006; Kopf et al., 1994; Martinez et al., 2008). Alternatively activated macrophages, also called as M2 macrophages, are regulatory macrophages that take role in alternative immune processes (Condeelis and Pollard, 2006). They are analogous to Th2 lymphocytes and they are activated as a feedback regulation of immune responses by IL-4 (Martinez et al., 2008). Their alternative functions regulate other immune reactions that usually oppose M1 phenotype while important for the regulation of immune responses and tissue repair after inflammatory reactions (Van Ginderachter et al., 2006). They are marked by the production of cytokines like IL-10 and IL-13 (Ma et al., 2004; Martinez et al., 2008). M1 macrophages can promote tumor suppression by the activation of Th1 cells while M2 macrophages have an opposite role and they promote tumor growth (Condeelis and Pollard, 2006; Van Ginderachter et al., 2006). Neutrophils, albeit less common, can also activate adaptive immune responses or tumor cytotoxicity early in tumor development (Curcio et al., 2003) yet their antitumor potential is surpassed by tumor promoting activities by them in extended inflammation via tissue remodeling and angiogenic cytokines (Prendergast and Jaffee, 2007). Some innate immune cells like NK cells can also directly recognize tumor antigens via NKG2D receptor dependent manner (Smyth et al., 2000) to mount perforin or TRAIL dependent assault (Smyth et al., 2000). NK cells and γδT cells are other first line defense against tumor cells with their unique ability to recognize cells via MHC Class I dependent antigen presentation (Raulet, 2003). NK cells recognize tumor cells via MHC or NKG2D dependent manner and they respond via IFNγ, perforin, granzyme or TRAIL secretion to eliminate tumor cells directly (Dunn et al., 2004). Also, IFNγ production may further induce adaptive immune cells infiltration especially $CD8^+$ T-cells to extend adaptive immunity against tumor cells (Dunn et al., 2002). γδT cells are on the other hand are localized within the tissue and can recognize tumor cells via NKG2D dependent manner and they can

secrete IFNγ or localize to lymph nodes to further activate adaptive immune responses towards tumor (Brandes et al., 2005).

1.2.4.1.2. Adaptive Immunity in Tumor Surveillance

Adaptive immune responses heavily depend on induction via dendritic cells. DCs are the pioneers of adaptive immune activation via IL-12 production (Dunn et al., 2002). In other cases IFNα or TNFα production may also weakly induce adaptive immune responses (Prendergast and Jaffee, 2007). Upon activation by IL-12, $CD4^+$ T-cells starts to produce a large array of cytokines which further induce adaptive immune responses by T-cells especially towards Th1 phenotype (Smyth et al., 2006). On the other hand, $CD4^+$ T-cells can also induce B-cell activation via antigen presentation and B-cells can mount anti-tumor antibodies which may contribute better activation of T-cell responses (Dhodapkar et al., 2002). $CD8^+$ T-cells shift to cytotoxic phenotype and can directly mount tumor cell specific killing via granzymes and perforin (Smyth et al., 2000). Both cell types can secrete large amounts of IFNγ to suppress tumor growth, to propagate further adaptive immune cell activation and to complete DC maturation to increase IL-12 production efficiency (Hung et al., 1998). In turn, tumor specific immunity via adaptive immune cells provides the most effective and long lasting antitumor responses to remove most tumors before they become a threat (Hung et al., 1998).

Most tumor cells are eliminated via innate or adaptive immune cells and this may lead to complete elimination or regression of tumor (Prendergast and Jaffee, 2007). Here vast amount of data accumulated to support that molecules like RAG2 (Shankaran et al., 2001) (for T-cell and B-cell maturation (Shinkai et al., 1992)), NKG2D (Smyth et al., 2000) (for NK and NKT activity via FasL dependent (Zou, 2005) or perforin dependent apoptosis (Street et al., 2001)), IFNγR1 (Billiau et al., 1988) (for NK activity, T-cell activation or tumor specific suppression), STAT1 (Kaplan et al., 1998; Shankaran et al., 2001) (for IFNγ downstream activation (Shankaran et al., 2001)), IL-12p35 (Langowski et al., 2006; Smyth et al., 2005) (for tumor specific T-cell activity), TNFα (Takeda et al., 2002) (for T-cell activation and TRAIL dependent

apoptosis), TCRγ and TCRβ (Girardi et al., 2001) (for γδT and αβT cell activation respectively) are important for tumor elimination and when they are absent tumor rejection is significantly reduced or completely abrogated in different cancer models (reviewed in (Prendergast and Jaffee, 2007; Zitvogel et al., 2006)).

1.2.4.1.3. Immunotolerance and Immune Escape

Not all tumor cells in a tumor are composed of uniformly immunogenic cells. Instead the tumor cells are evolved in such a way that highly immunogenic and less immunogenic tumor cells coexist and immune cells usually eliminate highly immunogenic tumor cells while tolerating less immunogenic species (Dunn et al., 2002). This phenomenon is called as equilibrium. In extreme cases, immune cells may promote their growth as well. This phenomenon of selection is called immunotolerance and immune cells favor growth of some tumor cells while inhibit others according to effectiveness of antigen presentation, recognition and complications to avoid autoimmune disorders (Willimsky and Blankenstein, 2005). This is most likely due to overlapping signaling mechanisms and activation of immune cells in different roles like infection or wound healing which in turn compete each other for addressing best suitable response (Zitvogel et al., 2006). It is known that elongated inflammation may cause tumor formation in different tissues while wound healing process is also a very good model of immune tolerance for promoting tumor growth (Condeelis and Pollard, 2006). Here tumor cells are the key factor to manipulate immune reactions against them and they can change the series of immune reactions from tumor eliminating factors to tumor promoting factors. Less immunogenic tumor cells are usually tolerated by immune cells and their growth are promoted due to unresolved inflammation (Balkwill and Mantovani, 2001). Further, they can synthesize or induce immune cells to secrete factors like EGF, VEGF (Toi et al., 1996), TGFβ (Hasegawa et al., 2001; Saito et al., 1999; Shariat et al., 2001), MMPs and their receptors to remodel extracellular matrix which enhance tumor growth and metastasis (Kim et al., 2006; Li et al., 2001). They are important in growth

and vascularization of the tumor to meet high nutrition requirements of fast growing tumor cells (Prendergast and Jaffee, 2007).

The last important concept of immunoediting is the escape of tumor cells from immune attack. It is a known fact that specific Th1 activation and downstream activation of IFNγ related factors are very important in tumor regression and in most tumors it was observed that cytokines that inhibit Th1 activation are highly increased the tumor growth (Prendergast and Jaffee, 2007). Actually inhibition of adaptive immune cells specific tumor regression may occur in several different ways. One of them is Th2 activation in which Th2 cells inhibit tumor specific reaction via cytokines like IL-4 and IL-10 dependent manner (Fiorentino et al., 1989). Innate immune cells can also inhibit T-cell activation via IL-23 (Hunter, 2005). IL-23 is an important cytokine that can transform T-cells into a specific subset called Th17 which is able to produce proinflammatory cytokines such as IL-17, IL-6 and TNF-α. Especially IL-23 is reported to be important regulator of Th1 and Th2 activities and IL-23 specifically inhibits IL-12 dependent T-cell activation (Hunter, 2005). Even loss of function experiments have shown that IL-12p40 is dominant over IL-12p35 and IL-12p40 depletion has positive effect on tumor regression while IL-12p35 depletion has reserved effect (Langowski et al., 2006) which shows that IL-23 can successfully antagonize IL-12 stimulation and its role in tumor progression is more prominent (Prendergast and Jaffee, 2007). On the other hand, TGF-β is an important factor which promotes tumor growth and regulatory $CD4^+CD25^+$ T-cell activation and its production can be upregulated via tumor cells to promote regulatory T-cell activity via TGF-β production (Curiel et al., 2004). Moreover, tumor environment contains factors that interferes APC differentiation and lead to APC dysfunction which results in Treg infiltration. DCs can also induce Treg infiltration in tumors and draining lymph nodes (Sakaguchi et al., 2001; Shevach, 2004). Also, regulatory T-cells are capable of expressing cytokines like CCL22 and its receptor CCR4 (Curiel et al., 2004) to further propagate conversion of normal T-cells into Tregs and infiltration of Treg to the tumors as evident in numerous cancers (Liyanage et al., 2002).

Although many immune activation mechanisms favor tumor clearance, the most important challenge is immune tolerance towards destruction of self cells which in turn results in suppression of tumor specific immunity. Tumor cells produce different cytokines which favor

immune suppression and tip the balance from immunosurveillance to immunotolerance which end up escape of tumor cells from specific immune targeting. Therefore, understanding about immune regulation at different regulatory levels is crucial to develop strategies favoring specific immune reactions in different diseases. As for cancer, we should focus on activation of adaptive immunity by better antigen presentation or by activated cytokine production via eliminating regressive anti-inflammatory signaling pathways. Hence, understanding the control mechanisms over cytokine production is invaluable to develop tools for specific immune activation against cancer.

1.2.4.2. NF-κB Signaling

Central hub of signal transduction machinery governing inflammatory responses, the regulation of cell growth and apoptosis is known as Rel or nuclear factor-kappa B (NF-κB) family of transcription factors. These factors are activated via many different signals such as proinflammatory cytokines, bacterial lipopolysaccharide (LPS), UV radiation, oxidative stress, viral proteins, double-stranded RNA and mitogens (Ghosh et al., 1998; Miyamoto and Verma, 1995; Pahl, 1999; Siebenlist et al., 1994). NF-κB can increase the expression of inhibitory proteins of apoptotic machinery (c-IAP 1 and c-IAP 2) and it also affects the proteins involved in cell cycle (Chu et al., 1997; Guttridge et al., 1999; Wang et al., 1998). Moreover, NF-κB controls the expression of genes involved in invasion and metastasis (Huang et al., 2000; Huang et al., 2001; Wang et al., 1996).

In the cell, NF-κB may be found as a homodimer or heterodimer made up of Rel family member proteins p50/105, p52/p100, RelA (p65), RelB and c-Rel (figure 1.6). However, it is not active in these forms since its activity is blocked by an inhibitory protein family called IκB which in turn regulate the activity of NF-κB (Baeuerle and Baltimore, 1996; Baldwin, 1996; Gilmore, 1999). Phosphorylation of these inhibitory molecules are required for subsequent proteolytic activity of proteasome for complete or partial degradation certain subunits (like p105 to p50 and p100 to p52) to activate NF-κB dimers to translocate into nucleus (Senftleben et al., 2001).

These phosphorylations are regulated via different effector proteins (according to the type of receptor) which in turn activate IKK complex. Phospho-activation of IKK catalytic subunits prime the events starting with IκB phosphorylation, ubiquitination and degradation leading to activation of NF-κB subunits (figure 1.7).

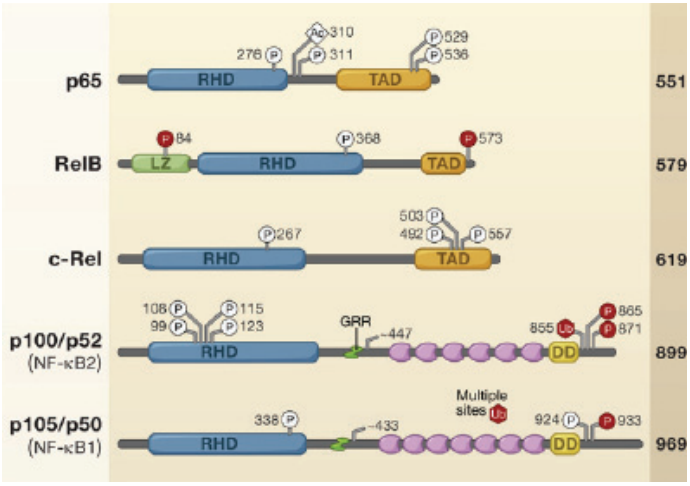

Figure 1.6: Rel Family of Proteins. Taken from (Hayden and Ghosh, 2008)

The source signal and activated effector proteins determine which NF-κB subunits to be activated. According to effector proteins different combinations of NF-κB heterodimers are activated while others are suppressed (reviewed in (Hayden and Ghosh, 2008; Häcker and Karin, 2006)). Canonical NF-κB activation via death receptors, toll like receptors and DNA damage strongly induce activation of RelA/p50 heterodimers through phosphoactivation of IKKβ (Karin and Greten, 2005). Though active IKKα can also induce canonical NF-κB activation albeit much weakly, its major function is to determine promoter specificity of NF-κB heterodimers to various NF-κB target promoters (Chariot, 2009; Gloire et al., 2007). Depending on the signal IKKα can promote or regress promoter activity of these dimers (Gloire et al., 2007; Lawrence et al., 2005). On the other hand IKKα is the major IKK subunit which governs alternative NF-κB activation through cytokine and growth receptor signaling pathways (Hayden and Ghosh, 2008). The specific examples of each of these activation pathways will be given in the following sections.

In cancer, NF-κB can act as tumor promoting or repressing according to the source of signal and the mechanisms involved in tumorigenesis (Hayden and Ghosh, 2008). In most cancers NF-κB is regarded as a tumor promoter due to its role its role in proliferation and survival (Karin and Greten, 2005). It is well established that NF-κB co-regulates proliferative pathways in Wnt signaling in CRC and breast cancer (Fingerle et al., 2009). On the other hand, NF-κB is also take role in the regulation of p53 regulation (Huang et al., 2007; Tergaonkar et al., 2002) in addition to its anti-apoptotic role in most cancers. Only, this potential explains why NF-κB inhibition is targeted in most cancers to overcome apoptotic resistance in tumor cells. Especially, in CRC, NF-κB is an important target for elimination of drug (Greten and Karin, 2004) or radiation resistance (Egan et al., 2004). NSAIDs, especially acetylsalicylic acid (Elwood et al., 2009), are reported to have protective effect on CRC through suppression of NF-κB targets like COX-2 (Oshima et al., 1996). Similarly, NF-κB is reported to be important in association of persistent inflammation with cancer in a model of CAC where tissue specific IKKβ deletion from epithelia induced increased apoptosis (Greten et al., 2004). In a similar setting we have also observed that tissue specific IKKβ deletion or pharmacologic inhibition improved effectiveness of chemotherapeutic agents and prolonged the survival of animals through increased apoptotic rate in a genetic model of CRC (unpublished data). Although inflammation is regarded as tumor promoting in persistent forms, it is also crucial for initiation of adaptive immune responses against tumors (Hung et al., 1998). Moreover, NF-κB has been shown to regulate adaptive immune responses in immunosurveillance and tumor rejection (Karin and Greten, 2005). Activation of tumor specific responses by macrophages and lymphocytes are strictly regulated by NF-κB by these cytokines and absence of NF-κB signaling may promote tumor progression in other circumstances (Karin and Greten, 2005; Li et al., 2001; Li et al., 2005).

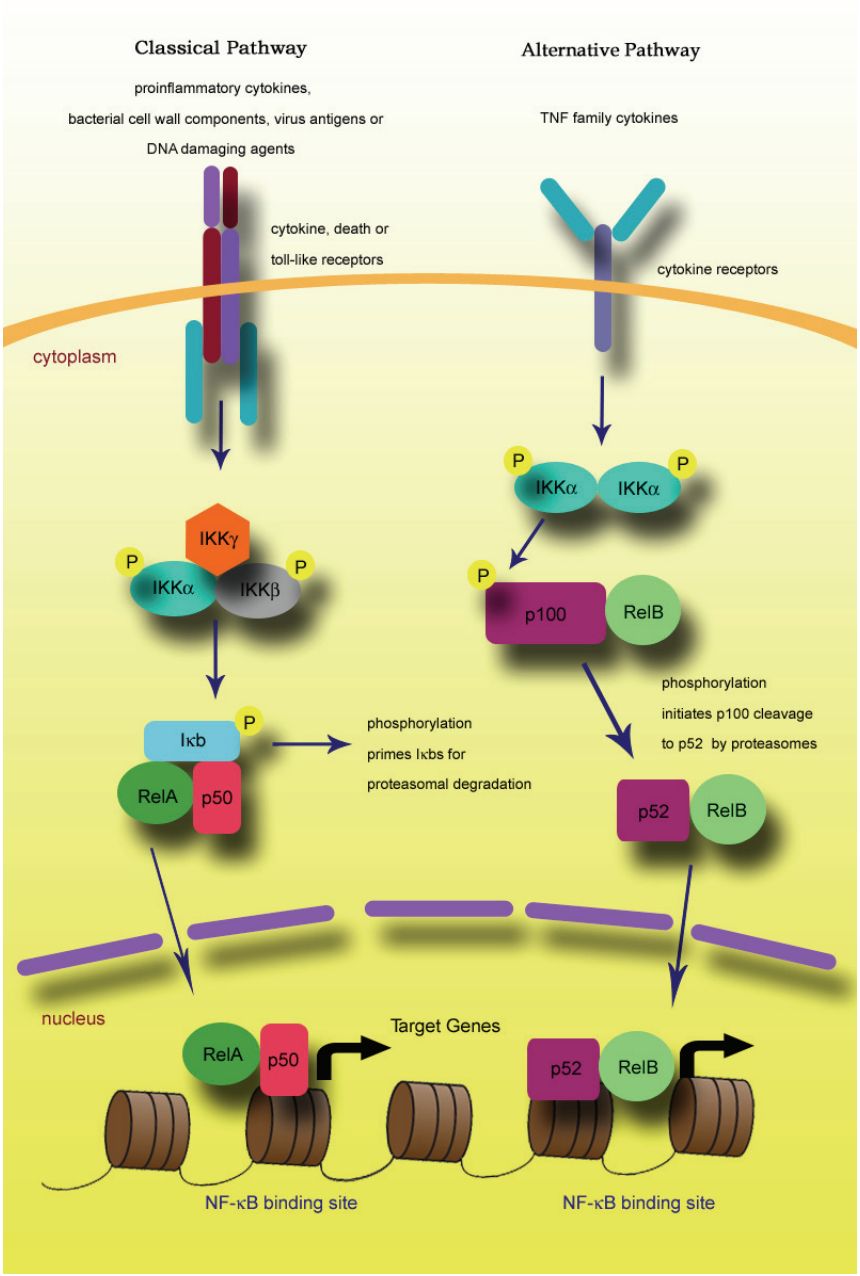

Figure 1.7: NF-κB Activation Pathways. Schematic representation of classical and alternative pathway of NF-κB activation. IKK complex and primarily IKKβ is responsible for the classical pathway in which IκB is phosphorylated and further degraded via proteasome. On the other hand, IKKα homodimers phosphorylate p100 to degrade p52 and p52/RelB dimer goes into nucleus where it activates alternative NF-κB signaling cascades. Adapted from (Senftleben et al., 2001).

Although NF-κB is described as proinflammatory and anti-apoptotic in general, these two mechanisms can cause diverse results according to the target tissue and other factors involved. For example, the loss of IKKβ in myeloid cells is associated with reduction in inflammation and tumor sizes through suppression of epithelial proliferation (Greten et al., 2004) due to decline in factors like IL-6 and STAT3 as previously described (Bollrath et al., 2009; Grivennikov et al., 2009). However, the same mutation in myeloid cells in DEN induced HCC had totally different outcome where the loss of NF-κB increased tumor growth and metastasis due to elevated inflammation (Maeda et al., 2005). Here anti-apoptotic potential of NF-κB protects kupfer cells from anti-oxidant caused apoptotic stress while in the absence of active NF-κB they actively undergo apoptosis leading to exerbated inflammation which ultimately resulted in increased tumor development (Maeda et al., 2005). Other experiments prove opposing functions of NF-κB in acute and chronic inflammation in the colon (Eckmann et al., 2008). Inhibition of NF-κB through IKKβ led to exerbated inflammation in acute colitis model due to the loss of NF-κB which would otherwise provide apoptotic protection in epithelial cells and would facilitate recruitment of immune cells that can produce cytoprotective agents for mucosal regeneration. On the other hand, inhibition of IKKβ in myeloid cells in chronic inflammation reduced proinflammatory immune cell recruitment which make the tissue damage (Eckmann et al., 2008). Yet there are evidence that NF-κB is an important partner in activation of tumor specific immunity and loss of NF-κB activity may abrogate innate and adaptive immune responses through elimination of NF-κB target proinflammatory cytokines and rapid elimination of activated immune cells via apoptosis (Lawrence et al., 2005; Maeda et al., 2005). All these examples make it clear that even basic roles of NF-κB in proinflammatory and anti-apoptotic functions can be diverse and have opposing effects in immune reactions regarding inflammatory diseases and cancer. These and other examples of NF-κB activations will be discussed in detail in the context of the source IKK complex.

1.2.4.2.1. IKK Complex

As we have described above the primary role of the IKK complex is to phosphorylate IκB or IκB like proteins for the activation of different NF-κB dimers (Mercurio et al., 1997). However, their function is not limited to this important cellular signaling machinery (Häcker and Karin, 2006). Before going into further details of its specific roles, we want to give an introduction in the structure and functioning of IKK complex. Inhibitory κB kinase complex or IKK for short is a multi-protein complex that consists of two serine/threonine kinase named IKKα and IKKβ (Mercurio et al., 1997; Zandi et al., 1997) and a structural subunit called IKKγ or NEMO (Rothwarf et al., 1998; Yamaoka et al., 1998). Structural association of two catalytic subunits and attachment of structural subunit is found to be essential for the proper functioning of the complex (Yamaoka et al., 1998) and also for individual roles of the subunits (Häcker and Karin, 2006; Karin, 2008) (with the exception of IKKα homodimers which is able to translocate to nucleus in different circumstances (Karin, 2008)).

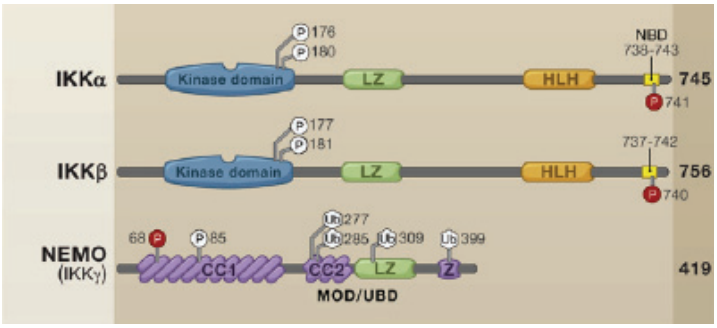

Figure 1.8: IKK Subunits. Taken from (Hayden and Ghosh, 2008)

Catalytic subunits IKKα and IKKβ show a high degree of sequence, structural and functional similarities (Häcker and Karin, 2006), perhaps most notable difference being in the substrate specificity (Karin, 2008). They both contain N-terminal kinase domains and C-terminal leucine zipper (LZ), helix-loop-helix (HLH) and NEMO binding domain (NBD) structures (Häcker and Karin, 2006). 50% sequence and 70% amino acid similarity and being able to coprecipitate in larger complexes of 3 or 4 make them very unique among all other kinases (Häcker and Karin,

2006). They associate IKKγ by NBD (May et al., 2000) and they polymerize by binding with LZ domains (May et al., 2002). Further IKKγ can form oligomers of 3 or 4 in a similar fashion which can account for 700-900kDa (3-4x 220kDa of single complex) size of the complexes in the cell (Agou et al., 2002; Rothwarf et al., 1998) which may incorporate other proteins like Hsp90 as well (Häcker and Karin, 2006). However the role of this multi oligomer association is yet to be identified (Tegethoff et al., 2003). Kinase domains of catalytic subunits contain an activation loop that contains two serine residues 4 amino acids apart (S177&S181 in IKKβ and S176&S180 in IKKα) (Delhase et al., 1999; Johnson et al., 1996). Phosphorylation of these residues are crucial for activation of IKK complex (Delhase et al., 1999). Mutational studies have shown that replacement of serines by alanines inactivates IKKβ while replacement by phospho-mimicking glutamates renders it constitutively active (Delhase et al., 1999). The same replacements in IKKα have no effect on classical but alternative NF-κB activation (Hu et al., 1999; Takeda et al., 1999). While HLH domain contain other serine residues phosphorylation of which negatively regulates IKK activity, which is considered as a control to terminate transient activation of IKK catalysts (Zandi et al., 1997; Zandi et al., 1998).

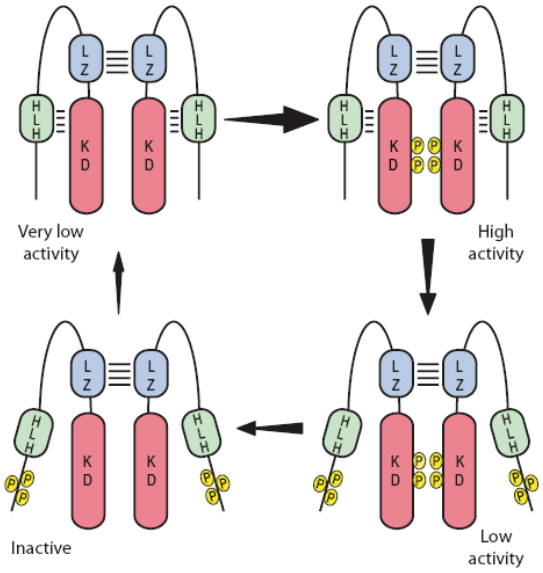

Figure 1.9: Model for IKK dimerization and phospho-activation. Taken from (Häcker and Karin, 2006)

1.2.4.2.2. IKKβ Specific Roles

Having discussed the major role of IKKβ (a.k.a. IKK2) in NF-κB activation, here we will give some further information about IKKβ specific roles in cancer, inflammation and immune cell modulation. The role of IKKβ is almost always exclusively associated to NF-κB activation. Yet there are also NF-κB independent targets for IKKβ like TCR and apoptotic factors (reviewed in (Chariot, 2009)). The difference in the downstream targets is usually dependent on the upstream source of activation that leads to different responses depending on the situation and cell type (Hayden and Ghosh, 2008). IKKβ can be activated by numerous upstream stimuli including death receptors, cytokine receptors and toll like receptors to activate downstream targets of various cytokines, transcription factors, immune cell markers and inhibitors of apoptosis to orchestrate major pathways in inflammation, immune cell interactions and maturation, cell growth and survival (Häcker and Karin, 2006).

IKKβ is important in cytokine signaling and survival of the cells to different stimuli like opposing IL-1β or TNF-α induced apoptosis (Greten et al., 2007). These stimuli also induce IKKβ and following NF-κB activation opposes these pro-apoptotic signals by the elevation of anti-apoptotic Bcl-2 family of proteins (Bax, Bad, Bcl-x_L) or inhibitors of apoptosis like c-FLIP (Häcker and Karin, 2006). These proteins basically prevent caspase activation and leading mitochondrial apoptotic pathway (Karin and Greten, 2005). Another important role of IKKβ activation is seen in immune cells upon induction by various stimuli including toll-like receptors or cytokines NF-κB activation leads to production of further proinflammatory cytokines like IL-1, IL-2, IL-12 and even TNF-α (Häcker and Karin, 2006).

NF-κB activation is prominent in most tumors and is one of the leading causes of resistance towards drug or radiotherapy. NF-κB is important in blocking necrotic pathway that is induced by these factors (Karin, 2008). For similar reasons, IKKβ activation is crucial for suppressing inflammation in different pathological conditions which lead to more severe conditions like colitis induced cancer when NF-κB signaling is active. In a CAC model of CRC induced by AOM and DSS in distal colon, conditional epithelial IKKβ knock-out has reduced tumor burden 80% (Greten et al., 2004). However, the reduction in tumor occurrence was not due to reduced

proliferation but increased apoptosis due to downregulation in the expression of inhibitors of apoptosis like Bcl-x_L (Greten et al., 2004). The proliferation is later found out to be driven by macrophages which produce tumor growth cytokines in response to inflammation and macrophage specific IKKβ deletion reduced tumor sizes and numbers dramatically (Greten et al., 2004). Recently it was suggested that IL-6 produced by macrophages promotes tumor growth by STAT3 activation (Grivennikov et al., 2009). STAT3 has also shown to be an important regulator of tumor growth in CAC tumor model (Bollrath et al., 2009) which can explain increased tumor growth due to IL-6 production as a result of IKKβ action.

As a contrasting example, IKKβ plays an important role in inhibiting DEN induced HCC (Karin, 2008; Maeda et al., 2005). DEN is a carcinogen which causes cell death by DNA damage and necrosis of hepatocytes (Fausto, 1999). However, IKKβ deletion in hepatocytes increased HCC burden dramatically (Maeda et al., 2005). It was understood that this mechanism differs from CAC model due to higher regeneration potential of hepatocytes where NF-κB plays an important protective role against damage induced cell death and following compensatory proliferation in liver injury (Maeda et al., 2005). DNA damage triggers p53 induced apoptosis (Tergaonkar et al., 2002) and NF-κB represses this mechanism in hepatocytes (Maeda et al., 2003; Maeda et al., 2005). NF-κB activates SOD which removes ROS stress in the cell (Pham et al., 2004), in the absence of NF-κB activation ROS leads to activation of JNK (Sakurai et al., 2006) which leads cells to undergo apoptosis. Extensive hepatocyte death triggers proliferation of others to regenerate and to protect the liver from chemical induced injury and function efficiently (Maeda et al., 2005). Due to increased DNA damage and mutations, compensatory proliferation may lead to HCC in the absence of control (Karin, 2008). However, like in CAC model, DEN induced HCC is also inhibited by macrophage specific deletion of IKKβ (Maeda et al., 2005). Kupfer cells are resident liver macrophages and they are induced by dying hepatocytes to secrete inflammatory cytokine IL-6 which drives proliferation of hepatocytes similar to CAC (Maeda et al., 2005; Naugler et al., 2007).

IKKβ has also shown to be an important negative regulator of IL-1β secretion in macrophages (Greten et al., 2007). Lately we have shown that IKKβ has opposing roles in acute and chronic colitis (Eckmann et al., 2008). The outcome can be protection from apoptosis in intestinal

epithelial cells coupled to activation of inflammatory cell that take part in the tissue regeneration as in the case of acute proliferation. However, this mechanism has negative effect on CAC as we explained above. On the other hand, in chronic colitis (via *Il10*$^{-/-}$) the effect is reversed and IKKβ in myeloid cells increase proinflammatory activities of immune cells that cause extended tissue damage (Eckmann et al., 2008). Altogether IKKβ is a major player in inflammatory pathways to which leads to different outcomes according to source of the signal and the target tissues involved. In conclusion, these observations clearly suggest that IKKβ has opposing but not exclusive functions in inflammation or cancer in a context, upstream signal and time dependent manner.

1.2.4.2.3. IKKα Specific Roles

Recent evidence shows that IκB kinases (IKKs) may have other substrates than IκBs (i.e., alpha and beta variants). Especially, IKKα (a.k.a. IKK1, CHUK) has been shown to play wide variety of other roles in diverse other mechanisms (Karin, 2008). One of the first identified roles was phosphorylation of p100 to degrade into p52 by IKKα homodimers in alternative NF-κB activation (Senftleben et al., 2001). This mechanism is observed downstream of different TNF family receptors; BAFF-R (Claudio et al., 2002) or CD40 (Coope et al., 2002) or in B-cells or LTβR (Dejardin et al., 2002) in spleenic cells (Bonizzi and Karin, 2004). Upon stimulation of BAFF-R, NIK is released and can phospho-activate IKKα dimers (Ling et al., 1998) which results in downstream phosphorylation of p100 and translocation of p52/RelB heterodimers to induce genes related to B-cell maturation and activation (Claudio et al., 2002; Xiao et al., 2001). Actually this mechanism has been first time shown in RANK signaling where in the absence of IKKα activation (provided by previously described alanine replacements) mammary epithelia cannot complete development (Cao et al., 2001; Senftleben et al., 2001). Consequently, adult female mice were found to be deficient in milk production due to impaired cyclin D1 activation (Cao et al., 2001). With this publication it has been shown that RANK-L activated NF-κB signaling and cyclin D1 production is linked by alternative NF-κB activation but TNF-α

activated NF-κB signaling remained intact in cultured mammary gland cells (Cao et al., 2001). Close examination of this alternative signaling revealed that this mechanism occurs regardless of the absence of IKKβ or NEMO and exclusively depends on activation of kinase activity of IKKα (Senftleben et al., 2001). Interaction of IKKα dimers with NIK is not clear and yet to be clarified (Häcker and Karin, 2006).

Keeping in mind that effect of NF-κB on cyclin D1 expression is rather indirect (Cao et al., 2001); to further understand this association and underlying mechanism, another group presented that IKKα and IKKβ physically interact (coIP studies) and phosphorylate β-catenin (Lamberti et al., 2001). However, IKKα is more important for the activation of β-catenin as suggested by absence of β-catenin nuclear localization in $IKK\alpha^{-/-}$ MEFs (Lamberti et al., 2001). Further analysis of IKKα and IKKβ deficient MEF cells with luciferase activity assays has shown that IKKα is required for the normal levels of β-catenin expression while its overexpression does not alter TCF/LEF activity (Lamberti et al., 2001). In the light of these findings, they expanded their findings to activation of TCF/LEF and cyclin D1 are both increased with active form of $IKK\alpha^{S182E/S186E}$ overexpression in DU145 cells (Albanese et al., 2003). Given the fact that IKKα phosphorylates (most probably stabilizes β-catenin) and cyclin D1 is important for cell cycle entry upon mitogenic induction, they have hypothesized that IKKα associates the regulation of mitogenic signaling through transcriptional induction of cyclin D1 via TCF (Albanese et al., 2003). Furthermore, another group has presented evidence that IKKα stabilizes β-catenin in both canonical and non-canonical degradation pathways (Carayol and Wang, 2006).

Although these findings shed light onto the role of IKKα in mammary gland development via cyclin D1 regulation and also given the fact that WNT signaling is important for the development of many different cancers, the role of phospho-stabilization of β-catenin by IKKα or other specific roles in different cancers still need to be clarified via in vivo and in vitro models. To do so, Schneider and his colleagues proposed that IKKα controls p52/RelB at the *Skp2* gene promoter to regulate G1 to S progression (Schneider et al., 2006). In their model they have transfected pancreatic cancer cell line MiaPaCa2 with siRNA for IKKα and they have observed increased levels of cyclin-dependent kinase inhibitor $p27^{kip1}$ (Schneider et al., 2006). This increase was due to downregulation of $p27^{kip1}$ regulating F-box protein S-phase kinase associated

protein (Skp2) as shown by promoter activity assay coupled to IKKα knockdown (Schneider et al., 2006). By doing so, they have identified a role for IKKα in pancreatic cancer where alternative NF-κB activation regulates p27 via SKP2 rather than cyclin D1 as shown in mammary gland development (Cao et al., 2001).

IKKα has very unique roles in the skin cells unrelated to NF-κB signaling or its catalytic ability. *Ikkα*$^{-/-}$ mice found to be seriously defected in skin and limb development (Hu et al., 1999). Then It was reported that IKKα is found to be mutated in melanomas (Liu et al., 2006). Recent publications have shown that skin problems in *Ikkα*$^{-/-}$ mice are due to differentiation problem in keratinocytes (Descargues et al., 2008). Basal cells cannot complete their differentiation into keratinocytes. Instead, they continue to proliferate in undifferentiated state which explains the melanoma formation in the absence of IKKα (Descargues et al., 2008). Here IKKα is described as a cofactor of TGFβ/Smad4 signaling which regulates terminal differentiation of keratinocytes that gives rise to keratin accumulation and basal membrane formation (Descargues et al., 2008). Another group has reported that epithelial specific ablation of IKKα has resulted in normal epidermal differentiation yet impaired basal membrane formation due to regulation of retinoic acid receptor targets (Gareus et al., 2007). This supports the structural role of IKKα in complete development of keratinocytes and suppression of skin cancer yet showing that kinase function is important in the basal membrane formation of the skin.

For the involvement of IKKα in prostate cancer and interaction of immune system with normal cancer environment, very recently, it has been shown that nuclear mitogen activated IKKα controls prostate cancer metastasis via suppressing metastatic inhibitory protein Maspin in a RANKL dependent manner (Luo et al., 2007). In a mouse model of prostate cancer with TRAMP mice, it was observed that mice lacking IKKα phospho-activation (*Ikkα*$^{S182A/S186A}$ or *Ikkα*$^{AA/AA}$) were bearing less distant site metastasis than WT mice although all mice died eventually (Luo et al., 2007). Close examination revealed that tumor initiation was not affected whereas WT mice have more RANKL and LTα expression (Luo et al., 2007). Furthermore, IKKα nuclear translocation correlated with decreased levels of Maspin (Luo et al., 2007). Eventually they hypothesized that upon the necrosis of core tumor cells in a progressing tumor T-cells are attracted to the site and they produce pro-inflammatory cytokines including RANKL

which further initiates nuclear localization of IKKα where it associates with the maspin promoter as shown by ChIP studies (Descargues et al., 2008; Luo et al., 2007). This study has shown how important the immune cell interaction with cancer cells to provide upstream activation for IKKα via proinflammatory cytokines.

After observing the importance of IKKα in the downstream of proinflammatory signals in the cancer cells, we will describe how IKKα regulates inflammatory signals in the immune cells with specific examples. As we have described above IKKα was found to be essential in regulation of immune cells bearing TNF family of receptors, yet its role is not limited with those cells. Recent evidence shows that IKKα limits macrophage activation and contributes to the resolution of inflammation (Lawrence et al., 2005). They have used an activation deficient *Ikkα* knock-in mouse model which is not able to be phosphorylated via upstream targets to activate downstream events. These mice when challenged with bacteria were better in clearing bacteria from the blood but more prone to get septic shock due to elevated proinflammatory response (Lawrence et al., 2005). They have found that IKKα is crucial in limiting macrophage activity via limiting extended promoter binding of RelA and c-Rel (Lawrence et al., 2005). Their turnover rate increased in the nucleus and cytoplasm. When IKKα upstream activation is not possible, increased promoter binding of these NF-κB subunits on proinflammatory genes like *iNos, IL-12p40* and *Bfl-1* causes an increased macrophage activation while macrophages are protected from apoptosis which in turn leads to prolonged inflammation resulting in septic shock which causes loss of animals regardless of better bacterial clearance (Lawrence et al., 2005).

All above examples in IKKα specific roles clearly show that IKKα is a very potent molecule in any cancer at different stages due to its power to regulate differentiation and inflammatory signaling through NF-κB. Although, IKKβ is well studied and targeted for pharmacological inhibition, there is little evidence for the outcomes of IKKα specific inhibition in disease models. Given that intestinal epithelia have very simple organization and differentiation pattern and colon cancer is very well defined in pathological development and genetic basis in terms of sequence of mutational alterations occurred, looking the role of IKKα in this model of cancer will both ease our job in understanding cancer development and will give idea to reflect our knowledge to more complicated cancers where immune system regulation is predominantly involved.

2. PURPOSE OF THE STUDY

Colorectal cancer is an important disease with over 1 million new diagnosis and over half million mortality every year. Regardless of improvements in diagnosis and therapy, the 5-year-survival is as low as 50% which forces us to develop better therapeutic interventions to deal with this bitter disease. To develop superior therapies we need to know about initiation and development of colorectal carcinogenesis. The relation between inflammation and cancer is well established in CRC and in many others yet the power of immunotherapy has been proven with numerous experimental trials. For this purpose, understanding immune regulation in inflammation and cancer is crucial in expanding our possibilities with new therapeutic strategies.

NF-κB is an important transcription factor that regulates cytokine production that governs immune cell maturation, survival and inflammation. For this reason, any machinery that controls NF-κB signaling can have gross regulatory effect on immune system leading to control of tumor suppression or growth. IKKα is a molecule that is known to regulate both canonical and alternative NF-κB signaling under different upstream signals. It has been shown to have significant roles in cell differentiation, immune regulation and proliferation in NF-κB dependent or independent manner. For this reason, understanding the role of IKKα in colorectal tumorigenesis can prove to be crucial in understanding immune cell regulation leading to tumor specific responses that are controlled via NF-κB. Therefore, we aimed to understand the role of IKKα in CRC by the use of IKKα inactivation within chemical or genetic murine models of colorectal tumorigenesis.

3. MATERIALS AND METHODS

3.1. MATERIALS

3.1.1. Chemicals

All chemicals were supplied by Amresco, Applichem, Fluka (Switzerland), CalBiochem (USA), Merck (Germany), Riedel de Haen (Germany), and Sigma-Aldrich (Germany)

Antibiotics: Ciprobay 500mg (Bayer, Germany) #8242.02.00; penicillin, ampicillin, kanamycin (Sigma, Germany) Penicillin-Streptomycin (Gibco)

3.1.2. Mouse Models

Mouse Model	Reference
Apc$^{min/+}$	(Moser et al., 1990)
Vil-Cre-ER^{T2}	(El Marjou et al., 2004)
Ctnnb1$^{+/lox(ex3)}$	(Harada et al., 1999)
Ikka$^{AA/AA}$	(Cao et al., 2001)
Ikka$^{fl/fl}$	(Liu et al., 2008)
Ikkb$^{fl/fl}$	(Park et al., 2002)
Nfkb2$^{-/-}$	(Paxian et al., 2002)
Relb$^{fl/fl}$	Unpublished
Ifnar1$^{-/-}$	(Müller et al., 1994)
Ifng$^{-/-}$	(Dalton et al., 1993)

Table 3.1: Mouse Models used in this Study.

Ikka$^{AA/AA}$ and *Ikkb*$^{fl/fl}$ mice by Prof. Michael Karin (Univ. of Calif. San Diego, USA), *Ikka*$^{fl/fl}$ by Prof. Yinglin Hu (Univ. of Texas MD Anderson Cancer Centre, USA), *Nfkb2*$^{-/-}$ mice by Roland M. Schmid (TUM Klin. r. d. Isar, Germany), *Relb*$^{fl/fl}$ by Prof. Falk Weih (Leibniz Institut für Alterforschung, *Ctnnb1*$^{fl/fl\ ex3}$ mice by Makato M. Taketo (Kyoto University, Japan), and *Vil-Cre-ER*^{T2} mice by Prof. Sylvie Robin (Institut Curie, France) were kindly provided. All other mouse models were purchased from Jackson Laboratories (USA).

3.1.3. Cell Lines

Cell Line	Grown in
CT26	RPMI1640
HT116	DMEM
HEK293	DMEM
CaCo2	DMEM
SW48	DMEM
SW480	DMEM
MEF	DMEM
MEF-*Ikkα*$^{-/-}$	DMEM
MEF-*Ikkβ*$^{-/-}$	DMEM
MEF-*Ikkγ*$^{-/-}$	DMEM
BMD macrophages	RPMI1640
BMD dendritic cells	RPMI1640
Peritoneal macrophages	RPMI1640

3.1.5. Commercial Kits

Apo Alert DNA Fragmentation Kit (Clontech)

Streptovivin/Biotin Blocking Kit (Vector Lab)

Peroxidase Sustrate DAB Kit (Vector Lab)

Vectastain ABC Kit (Vector Lab)

Super Signal West Pico WB Chemiluminescence Kit (Thermo)

Qiaquick Gel Extraction Kit (Qiagen)

Qiaprep Spin Miniprep Kit (Qiagen)

DNeasy Blood and Tissue Kit (Qiagen)

RNeasy Mini Kit (Qiagen)

PurelinkTM HiPure Plasmid Maxiprep Kit (Invitrogen)

QuikChange Site Directed Mutagenesis Kit (Stratagene)

Luciferase Assay System 10 Pack (Promega)

Luciferase Assay System with Reporter Lysis Buffer (Promega)

Super Signal West Pico-Stable Chemiluminescence Kit (Thermo)

3.1.6. Bacterial Strains

Strain	*Use*
E.coli DH5	for general cloning and re-transformation
E.coli XL-1 Blue	super-competent for first line cloning and blunt-ended ligation cloning
E.coli BL21	for overexpression of proteins

3.1.7. Buffers and Solutions

3.1.7.1. Culture Media

3.1.7.1.1. LB broth

Luria Bertani (LB) broth (Sigma, Merck or Applichem) is used as the liquid culture for the bacteria. It contains tryptone, yeast extract, and chemical salts in appropriate amounts. For 1l of LB broth, 20g of the LB powder is added to distilled water and mixed well. Then the culture is autoclaved for sterility. In case a selective media is required, ampicillin or kanamycin is added to obtain a final concentration of 100μM or 50μM respectively.

3.1.7.1.2. LB agar

LB agar is used as solid media for the bacteria. It is used as differential screening of bacteria in transformation by the use of appropriate antibiotics. 1l LB agar is prepared by mixing 40g LB-broth-mix with 1l distilled water. After sterilization in the autoclave, liquid agar is cooled for antibiotic addition if required. Before solidifying, the liquid agar must be poured into appropriate plates in 20-25ml amounts. Then they should be let harden in the fume hood. Then these plates are sealed and can be stored at 4°C for months. In case a selective media is required, ampicillin or kanamycin is added to obtain a final concentration of 100 M or 50 M respectively.

3.1.7.2. Buffers

All buffers indicated in this section are filter-sterilized as otherwise stated.

3.1.7.2.1 DNA Assay Buffers

3.1.7.2.1.1 TE Buffer

10mM	TrisHCl pH 8.0

3.1.7.2.1.2 Tail Lysis Buffer

100mM	TrisHCl
200mM	NaCl
5mM	EDTA
0.2%	SDS

3.1.7.2.1.3 Agarose Gel Buffer: TAE (50x)

2M	Tris
5.71%	Acetic acid
50mM	EDTA

3.1.7.2.2 Protein Assay Buffers

3.1.7.2.2.1 Lysis Buffer (for Protein Isolation)

For Stock preparation:

50mM	TrisHCl pH 7.5
250mM	NaCl
3mM	EDTA
3mM	EGTA
1%	Triton
0.5%	NP40 (Igepal)
10%	Glycerol
25mM	Sodium pyrophosphate

Freshly add:

25mM	Sodium fluoride
5mM	Sodium orthovanadate
5mM	Glycerol-2-phosphate
1mM	DTT
2mM	PMSF

3.1.7.2.2.2. Western Blot Buffers and Gels

3.1.7.2.2.2.1. SDS-PAGE Running Buffer (10x)

250mM	Tris
2M	Glycine
1%	SDS

3.1.7.2.2.2.2. Western Blotting Buffer (10x)

12mM	Tris
96mM	Glycine

*add methanol to make 20% of the final concentration while preparing 1x buffer

3.1.7.2.2.2.3. Sample Buffer (Laemmli Buffer)

62.5mM	TrisHCl pH 6.8
25%	Glycerol
2%	SDS
5%	β-mercaptoethanol
0.01%	Bromophenol blue

3.1.7.2.2.2.4. SDS-PAGE Buffers and Gels

Running Gel Buffer

1.5M	TrisHCl pH 8.8
0.4%	SDS

Stacking Gel Buffer

0.5M	TrisHCl pH 6.8
0.4%	SDS

Running Gel

Percentage of the Gel	Acrylamide-bisacrylamide (40% stock) in ml	Running Gel Buffer in ml	Distilled water in ml	TEMED (in µl)	10% APS (in µl)
8%	2	2.5	5.5	5	50
10%	2.5	2.5	5	5	50
12%	3	2.5	4.5	5	50
15%	3.75	2.5	3.75	5	50

Stacking Gel

Percentage of the Gel	Acrylamide-bisacrylamide (40% stock) in ml	Stacking Gel Buffer in ml	Distilled water in ml	TEMED (in µl)	10% APS (in µl)
5%	1.25	2.5	6.25	5	50

Table 3.2: SDS-PAGE Buffer Recipes.

3.1.7.2.2.3. Kinase Assay Buffers

3.1.7.2.2.3.1. Kinase Assay Reaction Buffer (10x)

0.25M	HEPES pH 7.5
1.5M	NaCl
0.25M	β-Glycerophosphate
0.1M	$MgCl_2$ (0.95g/100ml)

3.1.7.2.2.3.2. Kinase Assay ATP Solution

10mM	ATP
100mM	Tris pH 7.5
50mM	$MgCl_2$
10mM	DTT

3.1.7.2.2.4. Enzymatic Mobility Shift Assay (EMSA) Buffers

3.1.7.2.2.4.1. EMSA Reaction Buffer (10x)

100mM	TrisHCl pH 7.6
500mM	KCl
10mM	EDTA
50%	Glycerol

3.1.7.2.2.4.2. EMSA Loading Buffer (10x)

250mM	TrisHCl pH7.6
40%	Glycerol
0.2%	Bromophenol blue

3.1.7.2.2.4.3. TBE Buffer (5x)

500mM	Tris
500mM	Boric acid
10mM	EDTA

3.1.7.2.2.4.4. EMSA Gel (5%)

Concentration	amount in 50ml	chemical
20%	10ml	5x TBE
12.5%	6.25ml	40% acrylamide/bisacrylamide
0.069%	34.5µl	TEMED
0.674%	337µl	10% APS

3.1.7.2.2.5. Protein Overexpression and Dialysis Buffers

3.1.7.2.2.5.1. Base buffer

1mM	EDTA
5mM	DTT
0.5%	TritonX100

dissolved in 1x PBS

3.1.7.2.2.5.2. Buffer I

0.3M	Ammonium sulfate

dissolved in the Base Buffer

3.1.7.2.2.5.3. Suspension Buffer

1mM	PMSF

Protease inhibitor tablet (1tablet in 50ml buffer)

dissolved in the Buffer I

3.1.7.2.2.5.4. Elution buffer

100mM	Tris
20mM	Glutathione

dissolved in PBS and adjusted to pH 8.0

3.1.7.2.2.5.5. Dialysis Buffer

20mM	TrisHCl pH 8.0
0.1M	NaCl
0.2mM	EDTA
10mM	β-Glycerophosphate
10%	Glycerol

3.1.7.2.2.6. Coomassie Staining Solutions

3.1.7.2.2.6.1. Staining Solution

50%	methanol
10%	acetic acid
0.025%	coomassie brilliant blue

3.1.7.2.2.6.2. Destaining Solution

50%	methanol
10%	acetic acid

3.1.7.2.2.6.3. Quick Coomassie Staining Solution

35mM	HCl
0.006%	Coomassie Brillant Blue

let Coomassie dye water mixture stay at RT for 2-3 hours before addition of HCl and keep in the dark for later uses.

3.1.7.3. Histological Staining Buffers and Solutions

3.1.7.3.1. Alcian Blue Solution

3%	glacial acetic acid
1%	Alcian blue 8GX

Mix well and adjust to pH2.5 with acetic acid

3.1.7.3.2. Nuclear Fast Red Solution

1%	Nuclear Fast Red
5%	Ammonium sulfate

Dissolve ammonium sulfate in the water and add nuclear fast red slowly while boiling. Cool down the mixture, filter and add a grain of thymol as preservative (use commercially available nuclear fast red solution)

3.1.7.3.3. Azure-Eosin Solution

20ml	0.1% eosin solution
18 drops	of acetic acid
10ml	0.1% azure II solution
170ml	distilled water

Mix well and filter

3.1.7.4. Solutions for Animal Experiments

3.1.7.4.1. Bromo Uridine Solution

25mM	Bromo uridine in PBS

76.7mg bromouridine is dissolved in 10ml PBS and filter sterilized. It is stored at 4°C until use.

3.1.7.4.2. Tamoxifen solution

1% (w/v)	Tamoxifen
15% (v/v)	Ethanol

all dissolved in plant based oil

50mg tamoxifen is dissolved in 750µl ethanol via vortexing and the total volume is completed to 5ml with plant based oil and aliquoted in microcentrifuge tubes and stored at -20°C.

3.1.7.4.3. Azoxymethane (AOM)

0.05%	AOM in PBS

50mg AOM is dissolved in 100ml sterile PBS (0.5mg/ml) and aliquoted in 5ml and stored at -20°C.

3.1.7.4.4. Thioglycollate

3% thioglycollate

dissolved in water, filter sterilized and stored at RT and in a dark place

3.2. METHODS

3.2.1. Animal Treatments

3.2.1.1. Animal Handling

All mice are grown and treated in pathogen free environment in dedicated animal facility according to German national and EU regulations. All mice are fed with rodent food with 5% fat and handled in pre-sterilized cages with autoclaved water. Bone marrow transplanted mice are handled in special air filtered units throughout the experiment. All injections are done with sterile injectors. All chemical for feeding and injection are pre-sterilized via filtering before administration.

3.2.1.2. Genotyping of Mice

DNA obtained from tail or any other tissues were used or genotyping PCR with the following recipe (all reagents from Invitrogen):

10xPCR buffer	2µl
50mM MgCl2	0.8µl
10mM dNTP mix	0.4µl
20mM forward primer	0.5µl
20mM reverse primer	0.5µl
Taq polymerase (5U/µl)	0.15µl
DNA (20-100ng/ml)	1.5µl
Distilled water	14.15µl
Total	20µl

Additional primers were added (where it is possible) to make genotyping for mutant and wild type alleles together. All reaction conditions for each gene will be given in the appendixes (see appendix xx). Finally, each sample is loaded to 1.5-2% agarose gel containing 0.005% ethidium bromide and visualized under UV light to check the size of the bands.

3.2.1.3. Proliferation Index via Bromouridine Injections

100µl 25mM BrdU is injected i.p. to achieve a concentration of 75mg BrdU/kg body weight 90 minutes pre-sacrifice of the animals to incorporate BrDU into S-phase cells.

3.2.1.4. Inducing Distal Colon Tumors via Azoxymethane (AOM)

200µl of 0.5mg/ml AOM stock per 10g body weight is injected i.p. to mice to obtain a concentration of 10mg/kg body weight once a week for six consecutive weeks. Then mice are controlled for 20 weeks by weighing and physical examination. Finally, mice are sacrificed and their colon are collected, rolled and fixed in 4% PFA for immunohistological practices.

3.2.1.5. Induction of Cre Recombinase via Tamoxifen

As described in materials conditional knock-out model *VilCreER^{T2}* mice requires tamoxifen as estrogen analog to activate Cre recombinase in villin expressed tissues (intestinal enterocytes here). To achieve this activation *VilCreER^{T2}* mice are orally fed with 100µl oil containing 15% ethanol (to dissolve tamoxifen) and 1% (w/v) tamoxifen for 5 consecutive days so each animal gets 1mg tamoxifen per day. This solution is prepared by dissolving tamoxifen in ethanol via vigorous shaking and completing the volume by oil to have 1 mg tamoxifen per 100µl solution.

3.2.1.6. Blood Serum and Culture Media Supernatant Isolation

For ELISA of circulating cytokines or cytokines produced in the intestinal tissue in a given time, we have gathered blood sera or IEC culture media supernatants. Blood samples are collected from tail or from aorta (post-mortem). Then centrifuged 3krpm for 10 min to precipitate blood cells and clot. Serum is collected, aliquoted and frozen at -80°C before use. For IEC culturing, half of the duodenum is minced into small pieces and cultured in 400ml DMEM containing 10%FCS and 1%P/S for 2 hours in an incubator with 5% CO2 supply at 37°C. Then all

intestine and media are collected in a microcentrifuge tube and centrifuged at 5krpm for 5 minutes. The supernatants are collected, aliquoted and frozen at -80°C. Intestinal pellets are weighed for mass normalization.

3.2.1.7. Cell Isolation and Primary Cell Culturing

3.2.1.7.1. Epithelial Cell and Lamina Propria Isolation

After sacrifice of the animals, intestine is divided into four parts as duodenum, jejunum, ileum and colon and each part is treated separately. Each part is flushed with PBS at RT. Then intestines are cut open along their long axis washed more to get rid of fecal remnants then they are cut into two along their long axis half is used for histological fixation while the remaining half is minced into small pieces by the help of an operation scissor. These pieces are put into 5-10ml of HBSS-EDTA (30mM) and shaken at 37°C for 10 minutes to get epithelial tissue softened and easy to remove by physical effect. After that, the tube containing epithelia were vortexed vigorously for 30 seconds to remove lamina propria and epithelia. Epithelia are suspended in the buffer while lamina propria forms precipitate quickly. By pipetting suspension epithelia are collected in a 15ml tube while lamina propria remaining in the bottom can be collected in microcentrifuge tubes and frozen in liquid nitrogen directly. Epithelial cells are harvested at 1.5krpm for 5 minutes at 4°C and washed with ice-cold PBS and recollected in microcentrifuge tubes at 5krpm for 5 minutes at 4°C. Washouts are discarded and dry pellet of the cells are frozen in liquid nitrogen and stored at -80°C until use.

3.2.1.7.2. Peritoneal Macrophage/Neutrophil Isolation

Mice are injected i.p. with 2ml 3% thioglycollate 3 days/3 hours (macrophages and neutrophils respectively) before to induce peritoneal inflammation and macrophage accumulation. Then mice are sacrificed and their fur is skinned without damaging peritoneal membrane. Peritoneal cavity is filled with 10ml ice cold PBS by injection. Then peritoneal suspension is drawn back via using a syringe and cells are harvested at 1.5krpm for 5 minutes at RT. Then cells are washed with PBS, harvested and counted before seeding for desired assay. For cytokine induction assays, 10^6 macrophages/vial for 6-well plate were seeded in RPMI1640 while neutrophils are not stable for extended assays and used for FACS analysis only.

3.2.1.7.3. Isolation of MEF from mouse embryos

MEF cells should be isolated from D12-D14 embryos. For this purpose pregnant female mice are sacrificed and their whole uterus is excised from the peritoneal cavity. Uterus is placed into a Petri dish containing PBS and washed in PBS under sterile flow. One embryo at a time is homogenized by putting embryo into a 20G needle with 2ml typsin. By drawing in and out of the needle several times the embryo is homogenized. Then embryo trypsin suspension is incubated 5 min in the 37°C incubator for complete detachment of the cells. Then 5 ml DMEM with 10%FCS and 1%P/S is added to inactivate trypsin and cells are harvested at 1.5krpm for 5 minutes. Finally cells are resuspended in fresh DMEM with FCS and P/S and seeded to 6 well plates to expand their numbers (one embryo per well).

3.2.1.7.4. Bone Marrow Isolation and Transplantation

Ikkα$^{AA/AA}$ mice are backcrossed to FVB line mice at least x generation and these mice are used as donors for bone marrow transplantation. After sacrificing the mice femoral bones are removed from the ilium without damaging the head of femur and cleaned from skin and fur and placed in

ice cold PBS. Then moved to a sterile hood and rest of isolation is performed there. All remaining muscles are removed carefully and the joint under patella (connecting femur and tibia) is dislocated without damaging the head of the bones. Then by the use of an alcohol sterilized scissors head and the bottom of femur are cleaved to expose bone marrow. By using a 24G needle, bone marrow is flushed out into a falcon tube with 5ml PBS. This procedure can be repeated with tibial bone marrow as well. Bone marrow is resuspended in PBS and filtered with a 70µm filter to get rid of skeletal particles and stromal cells. The volume of suspension is completed to 20ml with extra PBS and cells are counted to determine total number of nucleated cells. Then cells are harvested at 1.5krpm for 5 minutes at 4°C and resuspended in an appropriate volume of PBS to achieve $4{\cdot}10^6$ cells/100µl PBS concentration prior to transplantation. On the other hand mice to be transplanted are pre-radiated with lethal 9Gy radiation to clear immune cells in their body. Then $4{\cdot}10^6$ bone marrow cells in 100µl PBS are injected into the tail veins of the receiver mice. The mice are directly put into air ventilated sterile mice facility and given with large spectrum antibody (Ciprobay, Bayer) in their drinking water to protect from infections for two weeks post-transplantation. After two weeks they were returned to normal drinking water and their cages were changed with other mice periodically every two days to regenerate their intestinal flora for two weeks prior to experiments.

3.2.1.7.5. Isolation and Culture of Mouse Bone Marrow-Derived Macrophages

Mononuclear phagocyte progenitor cells derived from femoral and tibial bone marrow are propagated in the presence of M-CSF. This macrophage growth factor is secreted by L929 cells and is used in the form of L929 cell conditioned medium. The progenitor cells proliferate and differentiate through monoblast, promonocyte and monocyte stages before maturing to macrophages. At this time the cells become firmly adhered to the culture vessel.

Day 1:

Animals are sacrificed and bone marrows are isolated as described in the previous section. Then bone marrow cells are resuspended in 50ml RPMI (with 10%FCS, 1%Antibiotics and 20% M-CSF (L929 cell supernatant). Cells are seeded into 10 15cm plates per mice and an additional 10ml medium is added to each plate.

Day 4:

Growth and adherence of the cells are checked under microscope and the media are refreshed.

Day7:

Cells are washed with PBS and cells are trypsinized with 3ml trypsin per plate for 5 minutes in the incubator. Cells are collected and resuspended in 10ml RPMI1640. Cells are harvested at 1.5krpm for 5 minutes and counted to determine their numbers. Then 5.10^6 cells are seeded into plate one day before stimulation experiments.

3.2.1.7.6. Isolation and Culture of Mouse Bone Marrow-Derived Dendritic Cells

Dendritic cell progenitors derived from femoral and tibial bone marrow are propagated in the presence of GM-CSF or Flt3L. The progenitor cells proliferate and differentiate to form immature mDC or pDC populations respectively. At this time pDC become firmly adhered to the culture vessel or form suspensions like mDCs.

Day1:

Animals are sacrificed and their bone marrows are isolated as described in BMD macrophage isolation. mDCs can strongly attach to normal tissue flasks and should be kept in suspensions. For this purpose we used bacterial Petri dishes for culturing mDCs. To induce dendritic cell propagation from immature bone marrow cells, we used either GM-CSF or Flt3L to induce mDC or pDC maturation respectively. For mDCs maturation, we seeded half of the BMD cells in 10ml GM-CSF (10ng/ml) containing RPMI1640 into a Petri dish and incubated o/n. On the other hand remaining BMD cells are incubated in 1ml RBC lysis buffer for 5 minutes at RT and washed in PBS, counted and seeded 3.10^6 cells/vial on 6-well plates in Flt3L (100ng/ml) containing RPMI1640 and incubated a week for pDC growth.

Day 2:

mDC suspension are flushed in their own medium and harvested at 1.5krpm for 5 minutes at 4°C and counted. Then they are seeded 7.10^6cells/well into bacterial petridishes in 1:10000 GM-CSF containing 10ml RPMI1640.

Day 5:

Another 10ml 1:10000 GM-CSF containing RPRMI1640 media are added into each culture for mDCs.

Day 8:

Both mDCs and pDCs are flushed to remove from their dishes, harvested at 1.5krpm for 5 minutes at 4°C, counted and seeded 10^6cells/well of 12-well plates in RPMI1640 before cytokine stimulations.

3.2.1.7.7. Cell Stimulations

Working Concentrations of Chemokines and Cytokines:

GM-CSF	10ng/ml
Flt3L	100ng/ml
LPS	100ng/ml
Poly I: C	125µg/ml
Pam3CSK4	1µg/ml
A type CpG	1µM
B type CpG	1µM

3.2.2. Histological Protocols

3.2.2.1. General Histological Preparations

3.2.2.1.1. Preparation of Tissues for Histological Examinations

After the sacrifice of the animals, tissues are collected and fixed overnight in 4% paraformaldehyde (PFA) at 4°C. The following day the fixed samples were dehydrated in Leica dehydrator with the following program:

70% ethanol for 45 minutes
86% ethanol 45 minutes
96% ethanol 45 minutes
96% ethanol 60 minutes
100% ethanol 60 minutes
100% ethanol 60 minutes
100% ethanol 60 minutes
xylene 45 minutes
xylene 70 minutes
xylene 75 minutes
paraffin wax 60 minutes at 62°C
paraffin wax 60 minutes at 62°C
paraffin wax 60 minutes at 62°C

and dehydrated samples are paraffin embedded and stored at RT. Before histological examination 3-5µm thick sections were cut via a microtome and these sections are fixed on glass slides prior to histological preparations.

3.2.2.1.2. H&E Staining

Rehydrate the slides through washing

2x in xylol for 5 minutes each
2x in 100% ethanol 2 minutes each
2x in 96% ethanol 2 minutes each
2x in 80% ethanol 2 minutes each
2x in 70% ethanol 2 minutes each
2x in 50% ethanol 2 minutes each
Once in PBS for 5 minutes

Stain slides in hematoxylin for 2 minutes and rinse them with distilled water and stain them in eosin solution (1% eosin and 20 drops of glacial acetic acid in 200ml) for 30 seconds and rinse in two different distilled water bath thoroughly. Then dehydrate the slides through washing:

2x in 50% ethanol 2 minutes each
2x in 70% ethanol 2 minutes each
2x in 80% ethanol 2 minutes each
2x in 96% ethanol 2 minutes each
2x in 100% ethanol 2 minutes each
2x in xylol for 5 minutes each

Dry the slides in air and mount them with coverslips

3.2.2.1.3. Alcian Blue Staining

Rehydrate slides as described in H&E staining. Stain in Alcian blue solution for 30 minutes. Wash under tap water (carefully not rip off the tissue) for 2 minutes. Rinse thoroughly in distilled water. Counter stain in nuclear fast red solution for 5 min (use a few drops per slide). Wash under tap water (carefully not rip off the tissue) for a minute. Dehydrate the slides as described in H&E staining. Finally, dry the slides in air and mount them with coverslips.

3.2.2.1.4. Azure Eosin Staining

Rehydrate slides as described in H&E staining. Stain in Azure-Eosin solution for 2 hours and dehydrate the slides through washing

2x in 96% ethanol 2 minutes each
2x in 100% ethanol 2 minutes each
2x in xylol for 5 minutes each

Dry the slides in air and mount them with coverslips.

3.2.2.2. Immunohistochemistry

Slides are rehydrated as described in H&E staining. Then slides are washed 5 minutes in PBS; 10 minutes in 3% hydrogen peroxide in PBS and again 5 minutes in PBS. Slides are heated to just under boiling temperature (e.g., 95°C) for 20 minutes in unmasking solution prepared with 3.75ml unmasking solution (Vector Lab)/400ml distilled water. Slides are let cooling in the unmasking solution up to RT and washed 5 min in PBS. Slides were blocked first with Avidin-biotin Blocking Kit (as instructed in manufacturer's manual-Vector Lab) and then washed in PBS for another 5 minutes. Then they are blocked again 30 minutes in 3% BSA in PBS and slides are incubated with primary antibody (normal or biotinylated) 1:100 to 1:400 in 3% BSA for 90 minutes or overnight. Slides are washed 3 times 5 minutes in PBS and (incubated with ABC solution if it is a biotinylated antibody) incubated with biotinylated secondary antibody of 1:1000 dilution in 3% BSA for 30 minutes. Slides are washed three times 5 minutes in PBS. Then apply slides with ABC mixture (prepared 15 minutes prior to application) for 30 minutes. Then slides are washed three times 5 minutes in PBS. Finally slides are stained with coloring reagent DAB (which is prepared from DAB coloring reagent kit (Vector Labs)) for 30-180 seconds until desired part of the cells are specifically stained. Slides are washed in distilled water and counterstained with hematoxylin for 2 minutes. Finally, they are dehydrated as described in H&E staining and covered with coverslips before examination under microscope.

3.2.2.3. Immunohistofluorescence

Rehydrate slides as described in H&E staining. Then permeabilize and block the slides as described in normal immunohistochemistry protocol. Primary antibody is used either directly fluorescent tag or without if it has fluorescent tag then 2° antibody is unnecessary. Otherwise fluorescent tagged 2° antibody is used to detect specific primary antibody. 1° antibody with 1:100 to 1:200 dilutions used for various nonfluorescent antibodies otherwise 1:400 of lesser dilutions preferred for fluorescent antibodies. Antibodies are diluted in 3% BSA and incubated 90 minutes to overnight for binding. Then wash 3 times in PBS for 5 minutes each. 2° antibody (if necessary) is diluted 1:500 to 1:1000 according to primary antibody dilution and incubated 30 minutes. Here all fluorescent antibodies are bound in the dark and the rest of the experiment carried in the dark to preserve light sensitive fluorescent tags. Finally the slides are washed 3x in PBS for 5 minutes each and tissues are covered with a small drop of DAPI for nuclear counterstaining. Usually FITC, PE, PC-tagged antibodies are used for detection of specific proteins.

3.2.2.4. TUNEL Assay

This assay makes use of fluorescent nucleotide binding to defragmenting DNA via terminal transferase activity to visualize them. Rehydrate slides as described in H&E staining. Then wash them 5 minutes in 0.85% NaCl and 5 minutes in PBS. Then fix the slides 15 minutes in 4%PFA and wash them 5 minutes in PBS. Then cellular DNA disfragmentation is labeled by the use of DNA fragmentation kit (Clontech) (the rest of the procedure is also performed in the dark). The reaction is stopped by the addition of equal amount of 2xSSC buffer and kept another 15 minutes in the dark. Finally slides are washed in PBS for 5 more minutes and samples are covered with a small drop of DAPI for nuclear counter staining. Slides examined under UV light with FITC filter for apoptotic cells.

3.2.3. Cell Based Assays

3.2.3.1. Mammalian Cell and Tissue Culture Based Assays

3.2.3.1.1. Mammalian Cell Culture

All cell lines are grown in their specific cell media supplied with 10%FCS and 1% penicillin-streptomycin. Then they are grown in an incubator at 37°C and providing 5% CO_2. The cells were washed with 1xPBS prior to trypsinizing and they are detached at confluency by cell culture grade trypsin. As required, they are frozen in FCS with 10% DMSO (Sigma). After trypsinization, the cells and harvesting them in an Eppendorf 5702R centrifuge at 1.5krpm. The frozen stocks were kept at -80°C for short term and in liquid nitrogen for longer periods. These stocks were thawed in 37°C water bath to avoid damage from crystallization.

3.2.3.1.2. Transfection

3.2.3.1.3. Lipovesicle Based Chemical Transfection

All cell lines are transfected by the use of Lipofectamine 2000 (Invitrogen) transfection reagent transfection kit (Invitrogen). For Lipofectamine transfection, cells were inoculated into 6-well (at $2\text{-}5\cdot10^5$ cells per well), 12-well ($1\text{-}2\cdot10^5$ cells) or 24-well (at $5\text{-}10.10^4$ cells) to guarantee the cells will be still in the growth phase at the day of transfection and not confluent more than 50-60%. For the transfection antibiotic free OptiMEM (Gibco) is used in place of the media mentioned in the previous section. The transfection is carried according to the manufacturer's protocol by putting transfection reagent (2-10µl) directly into serum and antibiotic free medium. Then appropriate amount of (0.5-5µg) plasmid vector or 25-100nM siRNA (final concentration

in the cell culture) is added into another vial of medium and they were let for standing 5 minutes at RT. Once they are equilibrated with the room temperature plasmid or siRNA and Lipofectamine 2000 containing media are mixed and tapped to assure homogenous dispersal. Then the mixture was incubated further 20 minutes for the incorporation of the plasmids to the Lipofectamine 2000 reagent. This mixture is added into the medium containing the cells to be transfected drop wisely. The plate or the dish is lent back and forward to provide even dispersal. The cells were left to grow in an incubator for 6 hours and their media are changed with normal antibiotics one. A total of 24 or 48 hours waited for the expression of the vectors or knockdown of the target genes respectively. Then cells are harvested and lysed. The transfection efficiency is indirectly measured by the use of EGFP containing plasmid. Then the transfection efficiency is assumed to be comparable to the cells expressing GFP which was observed under fluorescent microscope. Also, the success of the transfection was checked via expression of overexpressed or knockdowned proteins indirectly.

3.2.3.2. Bacterial Cell Based Methods

3.2.3.2.1. Chemically Competent Bacterial Cell Preparation

Overnight grown bacterial plates are used to pick up a single colony and it is transferred to 100ml LB medium. The culture is incubated at 37°C for 3 hours to obtain an OD_{600} of 0.4 for 10^8 cells/ml. Then the culture is cooled on ice for 10 minutes and aliquoted into 50ml tubes before harvesting cells at 2700g for 10 minutes at 4°C. All traces of medium are removed by decanting the supernatant and inverting the flask at least one minute on a piece of paper. The cells are resuspended in 30ml ice cold $MgCl_2$-$CaCl_2$ solution (80mM: 20mM). Cell are harvested again at 2700g for 10 minutes at 4°C and supernatant are decanted and removed as described before. Finally cells are resuspended in in 2ml $CaCl_2$ solution per tube and either directly used for transformation or mixed with 200 l DMSO, aliquoted in 100 l and snap frozen for longer storage at -80°C.

3.2.3.2.2. Transformation of E.coli

E.coli DH5α, XL-1 Blue or BL-21 chemically competent cells were used for transformation. Competent stock were removed from freezer and thawed on ice. Each of the vials was divided into two prechilled microcentrifuge tubes and 2-50ng of each plasmid was added to competent bacteria. These mixtures were incubated on ice for 45 minutes and they heat shocked at 42°C water bath for 30-90 seconds. After heat shock, tubes are immersed into ice and rested for 5 minutes. Then 1ml of LB broth (non-selective) was added to each tube and they were incubated 1 hour at 37°C at 250rpm for the expression of the plasmid DNA. Finally, bacteria were plated onto selective LB agar for the selection of transformants.

3.2.4. Nucleic Acid Based Assays and Preparations

3.2.4.1. DNA Isolation Mouse Tails and Tissues

Tails from 3-4 weeks old mice are collected and lysed 4 hours to overnight in 100µl tail lysis buffer containing 5% Proteinase K at 56°C. Then the tail lysates are vortexed vigorously for 15 seconds and diluted with 900µl of distilled water and mixed well. Cell debris and hair remnants are collected via centrifugation at 13.2krpm for 10 minutes at 4°C. Supernatants containing DNA were transferred to new tubes and cleaned-up with Qiagen Blood & Tissue kit as described by the manufacturer and used for genotyping. All other tissues are used with Qiagen Blood & Tissue kit as described by the manufacturer.

3.2.4.2. Mini and Maxiprep of Plasmid DNAs

Transfectant bacterial cells were inoculated into appropriate amount of selective medium with antibiotics (5-100ml) in appropriate aerated containers. They were incubated overnight at 37°C at 250rpm. After an absorbance value of about 3 is obtained at OD_{600}, the cells were removed from the incubator and harvested at 4.4krpm in an Eppendorf 5702R centrifuge. Then we followed the instruction manual's directions for Qiagen mini and Invitrogen maxiprep kits for the isolation of the plasmid DNAs.

3.2.4.3. RNA Isolation

Animal tissues are homogenized via microcentrifuge pistils or dedicated electronic homogenizers in RLT buffer (Qiagen RNeasy kit) containing 1% β-mercaptoethanol. RNAs are isolated with Qiagen RNeasy kit as described in manufacturer's manual. RNAs are stored at -80°C until use.

3.2.4.4. cDNA Synthesis

500ng to 1µg RNA is used per sample and pipetted into a clean tube via using filter tips. Then following mixture is prepared

0.5-1µg	RNA
1µl	oligodT
1µl	dNTP

total volume is completed to 13µl with RNase free water

This mixture is incubated at 65°C for 5 min for binding of oligodT primers to mRNAs. Immediately they were centrifuged shortly to preserve condensed water and immersed in ice at least for a minute. On the other hand a mixture containing

4µl	distilled water
1µl	0.1M DTT
1µl	RNaseOUT
1µl	DS III reverse transcriptase

is prepared per each sample and added to the annealed primer-RNA mixture to complete volume to a working volume of 20µl and incubated at 50°C for 1 hour. Finally, they are diluted 1:4 with 60µl distilled water and stored at -20°C.

3.2.4.5. Real Time PCR (RT-PCR)

Specific TaqMan primers were designed for each gene using PrimerExpress™ software (see appendixes fort he list of primers). After reconstitution in distilled water forward and reverse primers are combined in 20mM and these will be used as 10x primer stocks. Then for each sample following mixture is prepared for the PCR reaction:

10µl	2x Sybr mix
0.5µl	cDNA
2µl	10x primer
7.5µl	dH_2O

These mixes are transferred to an optically transparent 96 well plates and PCR reactions run with the following protocol:

Step1	50°C	2min
Step2	95°C	10min
Step3	95°C	30sec
Step4	60°C	1 min
Step5	Return to Step3	40 times
Step6	Keep at 25°C	

Reading from the RT-PCR machine is analyzed in ABI's StepOne™ Software to obtain Ct values which were used to calculate absolute expressions of each probe and these data is normalized with housekeeping Cyclophilin expressions with following formula:

(1) Absolute expression = $2 \wedge (C_{T(housekeeping)} - C_{T(gene)})$

3.2.4.6. Restriction Enzyme Digestion of Plasmids

For cloning of different genes and to make various expression vectors restriction enzymes from NEB was used as instructed in their specific manuals. Digestions were carried for 1-1.5 hours depending on DNA amount and 3 hours for double digests. The digestions were stopped by insertion of reaction tubes into ice and the digests were analyzed on 0.8% agarose gel.

3.2.4.7. Agarose Gel Electrophoresis

Agarose gel was prepared by mixing 1xTAE buffer with 0.8-2% (w/v) agarose and by cooking the mixture in a microwave oven at 600W for 3 minutes (seldom shaken). The gel was left to cold-down to about 60°C for the addition of ethidium bromide (0.005%). Then immediately gel was poured into its tray to cast and appropriate combs were placed for the formation of wells. On the other hand, samples were prepared by mixing 6x loading dye with appropriate plasmid DNA and water volumes (loading dye: plasmid DNA 1:5 mixtures were applied). Once the gel gets polymerized, combs were removed and the gel was put into electrophoresis chamber. After the addition of 1xTAE to cover the gel, samples along with 10µl 1:10 diluted 1kb marker (Invitrogen) was loaded to wells and gel was run at 100V for 30-60 minutes. Then the DNA bands were observed under UV-light and they were photographed by using appropriate imaging system (Biorad).

3.2.4.8. DNA Chip Assay and Evaluation of Microarray Data

Mouse duodenal epithelia from 1 cm after stomach to 6 cm after stomach is isolated as described before. Then RNA was isolated with Qiagen RNeasy kit with manufacturer's protocol. Then RNA is labeled as recommended by the manufacturer. 1-5µg of labeled RNA was hybridized to mouse expression gene chip arrays (Affymetrix Mouse Genome 430A 2.0 Array) according to Affymetrix protocols. Gene chips were scanned and analyzed using Affymetrix Microarray Suite 5.0 software (MAS 5.0). K-means clustering is used to group significantly altered genes. Then raw data is also analyzed in GSEA to question association of our significantly regulated genes to major pathways.

3.2.5. Protein Based Assay and Preparations

3.2.5.1. Protein Isolation

3.2.5.1.1. Total Protein Isolation

Freshly collected or frozen animal tissues are homogenized via a small microcentrifuge tube type pistil or electronic homogenizer properly in an adequate amount of cell lysis buffer. Homogenized animal tissues were let stand on ice for complete lysis for 20 minutes. For cell cultures, cells grown on culture plates were washed thoroughly with ice-cold PBS. Appropriate amount of cell lysis buffer (100µl for 6 well plates) is added and the culture plates were rocked to evenly disturb the buffer. Then cells are scrapped from the plates and collected in microcentrifuge tubes and lysed on ice for 20 minutes. After cell lysis vials were vortexed vigorously to burst remaining intact cells. Cell debris was removed by centrifugation 10 min at 13krpm and supernatant contains total proteins. These proteins should be stored at -80°C.

3.2.5.2. Protein Content Assay

Protein concentrations were determined with Bradford protein assay (Biorad). Bradford reagent is diluted 1:5 with distilled water. 1ml of the diluted Bradford reagents were put into microcentrifuge tubes and 2µl of each protein samples are added to them. Additionally, a group of vials should be prepared as standards from known concentration of BSA solution. Then protein concentrations are determined via measurement in a spectrophotometer (Biorad) at 595nm wavelength.

3.2.5.3. SDS-PAGE

Biorad Mini Protean gel systems were used for protein electrophoresis. 8-15% running gels were casted by mixing the ingredients that were given before (table 3.2). Here APS should be added last to prevent immature polymerization. Then gels were overlaid with isopropanol. Once the gel was formed then the isopropanol was removed and 5% stacking gel (table 3.2) was poured onto the running gel. Finally well combs were placed for the formation of wells. Fully polymerized gels were put into gel tanks and 10x running buffer is diluted to 1x with distilled water and added into the tanks. Equal volumes of 2x sample buffer was added to each sample (10-40µg proteins) and proteins were denatured in a 95°C water bath for 5 minutes. Then each of the samples was loaded to SDS-PAGE gel along with a 10µl of appropriate marker. Stacking of the gels was performed at 60V for 30 minutes while the complete run of the proteins were performed at 120V for 1-1.5 hours with the help of a proper power supply.

3.2.5.4. Immunoblotting

Once the proteins were run on a SDS-PAGE, gels are removed from the electrophoresis tanks and put into a blotter surrounded by one PVDF membrane, two Whatman papers and finally with two sponges (membrane facing towards anode). Here all these components were prewetted with transfer buffer while activation of the PVDF membrane was achieved by 30 seconds methanol wash followed by rinsing in distilled water. Then proteins were blotted onto PVDF membranes by applying 300-350mA current. The membranes were then blocked with 3% skim milk in PBS-Tween 20 (0.1%) for 2 hours at RT and incubated with appropriate primary and horseradish peroxidase (HRP)-conjugated secondary antibodies. After required washes with PBS-Tween 20 (3x10 minutes after blocking and primary antibody and 3x10 minutes after secondary antibody), membranes were overlaid with enhanced chemiluminescence mixture (Thermo) for 5 min and exposed to x-ray film for 10 seconds to10 minutes to obtain specific bands for the protein of interest which will be further obtained via chemical development of the films in an automated developer.

3.2.5.5. EMSA

3.2.3.5.1. Probe Preparation:

i. Annealing

Oligonucleotide stocks (40nM) are diluted 1:10 in distilled water (10µl each forward and reverse oligos and 80µl distilled water). Then they are annealed at 80°C for 10 minutes and cooled down to RT and stored at -20°C.

ii. Oligo Labeling

Reaction mixture is prepared as follows

2µl	annealed oligos
2µl	10x PNK buffer
1µl	^{32}P-γ-ATP
1µl	T4 PNK
14µl	dH_2O

Above mixture is mixed well and incubated 20 minutes at 37°C. The reaction mixture is applied into the middle of resin in the prespinned sepharose columns for size exclusion and spinned at 3krpm for 2 minutes. Elute contains labeled oligos while free ATPs are mostly retained in the resin.

3.2.5.5.1.2. Binding Assay:

Protein concentrations are determined and total volume of each sample with proteins should be adjusted to 10-12 µl with lysis buffer (this part is called protein mixture). On the other hand reaction mixture is prepared as follows

2µl	10x EMSA reaction buffer
2µl	polydI:dC
1µl	20mM DTT
0.2µl	^{32}P-γ-labeled oligo
2.8-4.8µl	dH_2O

These two mixtures are mixed and assay mixture is incubated at RT for 30 minutes. Reaction is concluded by the addition of 2µl 10x EMSA loading buffer to each sample. All reaction mixture is loaded into a native 5% EMSA gel (which was prerun at 120V for 20 minutes in 0.5x TBE

buffer) and run for 1-1.5 hours at 200V. Then the gel should be removed carefully and be stuck on a Whatman paper and covered with a saran wrap from one side facing up and placed into gel dryer and dried for 90 min at 80°C. Finally, dried gel is put into a cassette containing intensifying screen and exposed to radioactivity film overnight or longer and the film is developed in an automated developer.

3.2.5.6. Coomassie Staining

After SDS-gels are run they are stained for 4 hours in Coomassie Staining solution and destained in destaining solution overnight with continuous shaking at 30-50rpm.

3.2.5.7. Quick Coomassie Staining

The SDS-PAGE is removed from the chamber after the run and it is washed 3x in distilled water for 5 minutes. At the beginning of each wash it is heated in the microwave oven for 30 seconds at 600W power without boiling. After the last wash the Quick Coomassie Staining is added and heated for 10 seconds in the microwave oven. And let washing on a shaker for at least 15 minutes before the protein bands are observable.

3.2.5.8. Co-Immunoprecipitation

To identify physical interaction between two proteins (denoted by X and Y here for simplicity) immunoprecipitation is performed. The first step is to immunoprecipitate the protein of interest. For this purpose about 500 g total protein of cell lysate for protein Y of interest (endogenous or overexpressed protein) is immunoprecipitated with specific antibody against protein X whose interaction is questioned as follows:

15µl	protein A sepharose beads (Roche)
2µg	anti-protein X antibody
50µl	lysis buffer

Protein A sepharose beads are prewashed in fresh lysis buffer and centrifuged 1 minute at 3krpm to collect the beads. Above mixture is mixed well and pipetted to each sample with protein Y via a cut-tip. Then total volume is adjusted to 600µl and the tubes are rotated at least 4 hours to overnight at 4°C. After immunoprecipitation, samples are added with 10µl sample buffer heated 5 min at 95°C and 20µl of each sample is loaded to a suitable SDS-gel. Immunoblotting is performed as described before and specific antibody for protein Y is used to investigate if this protein is also precipitated along with the protein X which was precipitated with specific antibody before. If any interaction is observed, the reverse co-immunoprecipitation is done. It is performed by precipitation of protein Y with its specific antibody and detection of protein X in immunoblot.

3.2.5.9. Kinase Assay

To measure activity of endogenous kinases or to identify unique phosphorylation events kinase assays are utilized. The first step is to immunoprecipitate the kinase of interest. For this purpose about 500µg of cell lysate is immunoprecipitated with specific antibody against our kinase with the following recipe:

15µl	protein A sepharose beads (Roche)
2µg	anti-kinase of interest antibody
50µl	lysis buffer

as described above. Then they are added with 500µl 1x kinase buffer and beads are equilibriated to this buffer 30 minutes in a rotating wheel at 4°C. Then the beads are harvested at 3krpm for 1 minute and added with 15µl 2x kinase buffer prior to kinase assay. For the kinase assay following kinase reaction mixture is prepared:

0.3µl	ATP
0.5µl	^{32}P-γ-ATP
1-1.5µg	substrate
completed to	15µl with distilled water

This mixture is added to each of the beads containing 2x kinase assay buffer and the kinase reaction is run 30 minutes at 30°C. The reaction is concluded via addition of 10µl sample buffer to each vial and samples are denaturated via heating to 95°C for 5 minutes. The beads are collected via centrifugation at 14krpm for 2 minutes and 20µl of supernatants from each sample is loaded to a suitable percentage of SDS-PAGE along with 10µl protein molecular weight marker. Then the gel is run as described in normal immunoblotting procedure. The run is stopped before the free radioactivity probes run into the buffer (usually a red color guides the place of free probes). Then the gel is cut to get rid of free probes and blotted onto a PVDF membrane as described previously and the blotted membrane is wrapped with a saranwrap and exposed to an X-ray film (Kodak BioMax etc.) overnight or longer at -80°C. After development of the film the membrane can be used for immunoprobing of kinases to check loading.

4. RESULTS

To understand the role of IKKα in colorectal tumorigenesis, three independent tumor models were utilized to create pharmacological and genetic models of colorectal tumorigenesis. AOM was the chemical/pharmacological model of colorectal tumorigenesis to mimic sporadic tumor formation in distal colon while *Apc*$^{min/+}$ and *Vil-Cre-ER*^{T2}*Ctnnb1*$^{+/lox(ex3)}$ models were inducing sporadic tumorigenesis through genetic basis. Regardless of the model used, distinct phenotypes associated with IKKα activation deficient mice were observed. In this chapter, all the observations regarding the loss of IKKα activation will be presented and further evidence will be given to explain underlying mechanism behind IKKα involvement in colorectal tumorigenesis. In the beginning, a short description of *Ikkα*$^{AA/AA}$ and wt mice will be presented by the use of histological observations. Then basic observations with three different colorectal cancer models will be shown to present detailed phenotypical observations related to IKKα activation loss. Finally, molecular evidence that explains the detailed machinery of IKKα involvement in the described phenotype will be given to propose a model to explain the role of IKKα in the context of colorectal cancer initiation and progression.

4.1. CHARACTERIZATION OF *Ikkα*$^{AA/AA}$ MICE

Ikkα$^{AA/AA}$ mice are born healthy and fertile. However, they are characterized as having problems in mammary gland development and deficiency in intestinal Peyer's patches formation yet no other anomaly is observed during the course of intestinal development or function. H&E stainings show normal architecture of crypts and villi while basic histological markers for goblet cells, paneth cells or proliferating cells which do not show any difference to wild type animals (figure 4.1). Furthermore, basic immunohistological analysis did not suggest any difference in proliferation or apoptosis in C57/BL6 or FVB/N background (figure 4.1).

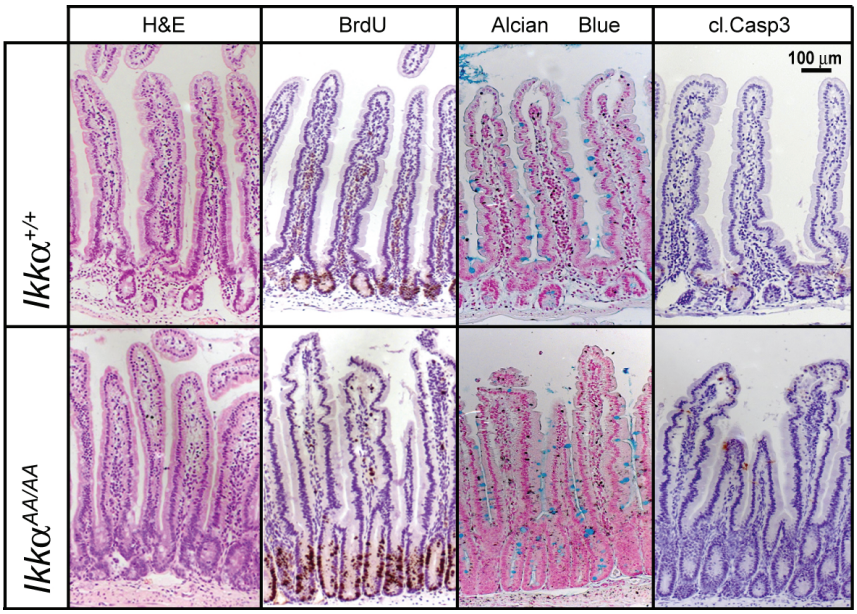

Figure 4.1 Basic Characterization of *Ikkα*$^{AA/AA}$ mouse intestine. H&E staining for basic morphology, BrdU IHC for proliferation, Alcian blue staining for goblet cell distribution and cl. Casp3 IHC for apoptosis in WT and *Ikkα*$^{AA/AA}$ mouse small intestines show no difference in morphology and proliferation of *Ikkα*$^{AA/AA}$ mice. Yet there is no significant difference in differentiation or apoptotic response at the base line.

4.2. BASIC OBSERVATIONS WITH SPORADIC AND FAMILIAL CRC MODELS

4.2.1. Azoxymethane Induced Sporadic CRC

To understand IKKα involvement in sporadic colorectal carcinogenesis, *Ikkα*$^{AA/AA}$ mice were crossed to FVB/N background for four generations and injected with AOM as described in the Materials and Methods to induce sporadic tumor formation. The mice were followed for weight loss and checked general health and sacrificed after 20-24 weeks when they show the first signs of sickness and discomfort due to blocking of intestinal passage by growing tumors (which may threat life of the mice if unchecked). Average weight measurements did not differ between the two groups in the course of 20-24 weeks (figure 4.2). Both group gained weight albeit 3 weeks older *Ikkα*$^{AA/AA}$ mice gained weight slower.

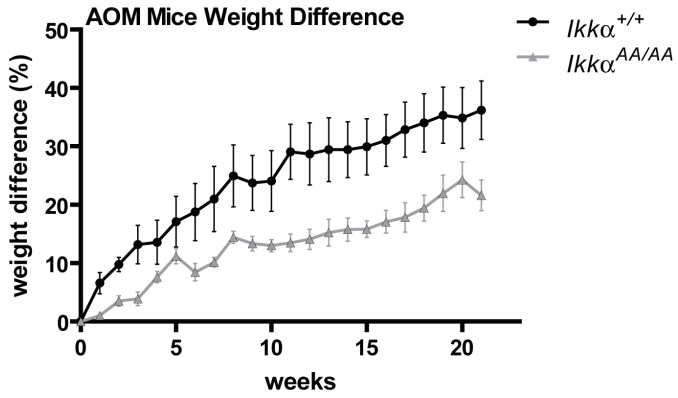

Figure 4.2: AOM Induced Mice Weight Difference Curve

4.2.1.2. Tumor Number, Size and Proliferation in AOM Induced CRC

Although mice did not show an observable weight loss pattern in any group in AOM induced CRC tumorigenesis model, histological examination of colons from these animals proved that

Ikkα$^{AA/AA}$ mice had less tumor burden (3.00±0.71 vs. 5.80±0.86, p=0.0361) and smaller tumors (0.16±0.04mm^2 vs. 1.00±0.27mm^2, p=0.0343) compared to the control group (figure 4.3.A and B respectively). Tumor distribution according to size was suggesting that control group has any size of tumors with more or less equal distribution while *Ikkα*$^{AA/AA}$ mice had only smaller tumors of 0.5mm^2 or smaller (figure 4.3.C). Further examination via serial sections showed that proliferation index of tumors were lower in *Ikkα*$^{AA/AA}$ mice albeit being insignificant (0.35±0.01 vs. 0.38±0.05, p=0.5859) and average proliferation in normal crypts was also less yet statistically insignificant (0.12±0.01 vs. 0.14±0.01, p=0.1497) (figure 4.3.D).

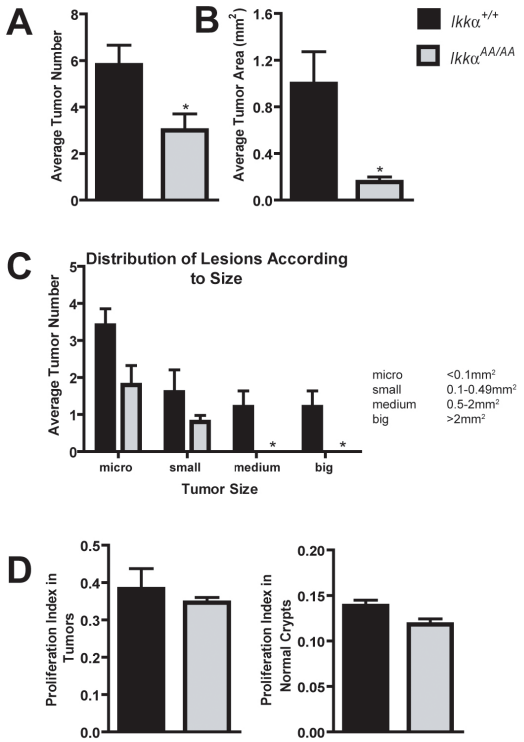

Figure 4.3: **Basic Tumor Characterization in AOM Induced Mice.** (A) Average tumor number; (B) average tumor size; (C) tumor distribution by size; (D) proliferation in normal colon and tumor in AOM induced WT and *Ikkα*$^{AA/AA}$ mice.

4.2.1.3. Tumor Morphology in AOM Induced CRC

Comparison between tumor sizes and morphology in these two groups can be seen in figure 4.4.A where a typical *Ikkα*$^{AA/AA}$ tumor was usually much smaller than wt tumors (as it was presented in figure 4.3.B). Proliferating cells in tumors was marginally different and microscopic observation of proliferating cells by BrdU IHC does not reveal a significant difference either (figure 4.4.B). Furthermore, apoptotic response of tumors was checked by TUNEL assay and it demonstrated a marginal increase in apoptosis in control mice (figure 4.4.C).

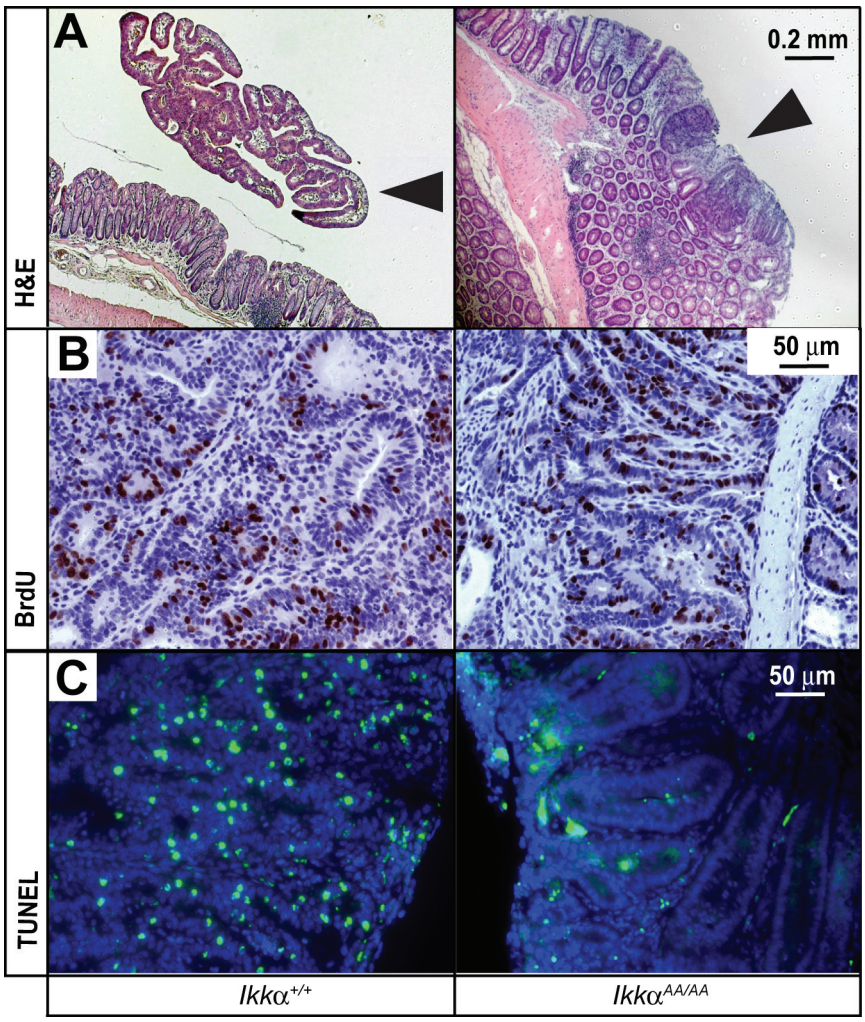

Figure 4.4: Tumor Morphology in AOM induced Mice. H&E staining (A); BrdU IHC (B) and TUNEL assay (C) in AOM induced *Ikkα*$^{AA/AA}$ and control mice in FVB/N background.

4.2.2. APC Loss Induced Genetic Intestinal Adenocarcinoma

4.2.2.1. Survival in *Apc$^{min/+}$* Mice

To understand IKKα involvement in this genetic model of adenocarcinoma we crossed *Ikkα$^{AA/AA}$* mice to *Apc$^{min/+}$* mice to generate C57/BL6-*Apc$^{min/+}$Ikkα$^{AA/AA}$* mice while using C57/BL6-*Apc$^{min/+}$Ikkα$^{+/+}$* mice as control group. The mice were monitored until theydeveloped rectal prolapse or rectal bleedings due to tumors. Survival curves for these two groups of animals have shown a big difference with *Apc$^{min/+}$Ikkα$^{AA/AA}$* mice had an extended survival advantage over control group (median survival of 236.5 vs. 166 respectively, p<0.0001) (figure 4.5). Interestingly, mice heterozygous for *Ikkα* (*Ikkα$^{+/AA}$*) also had a slight survival advantage over control mice (median survival of 184.5 vs. 166, p=0.0365) (figure 4.5). However, extended survival with heterozygous mice was only limited to this observation and no other significant differences in further analysis were obtained.

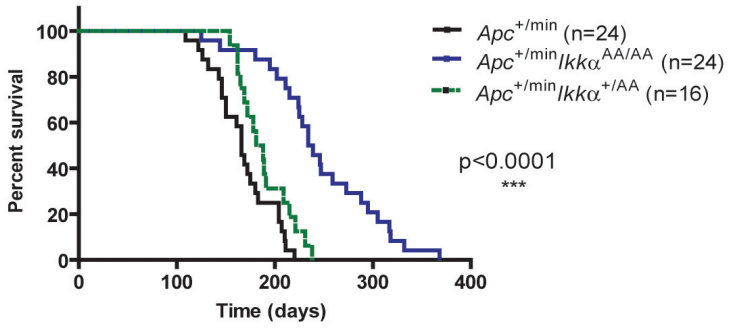

Figure 4.5: Survival of *Apc$^{min/+}$Ikkα$^{AA/AA}$* mice. *Apc$^{min/+}$Ikkα$^{AA/AA}$* mice showed a remarkable survival advantage over wt *Apc$^{min/+}$* *or heterozygous* *Apc$^{min/+}$Ikkα$^{+/AA}$* mice (236.5 vs. 166 vs 184.5 respectively, p<0.0001).

4.2.2.3. Tumor Number, Size and Distribution in 4 Months Old *Apc*$^{min/+}$ Mice

Although a decrease in tumor numbers was observed, tumor sizes were still comparable at the time of sacrifice (data not shown) so we wanted to investigate earlier time points in the course of polyp development. Then month 4 was identified as the time of separation in *Ikkα*$^{AA/AA}$ and control group not only in tumor numbers but also in tumor sizes and overall health as measured by anemic status of the animals (see figure 4.6.A for representative tumor morphologies). Tumor numbers were already remarkably different (29.27±7.49 n=22 vs. 4.17±0.98 n=19, p=0.0279) (figure 4.6.A) so do tumor sizes (1.70±0.34 vs. 0.58±0.08, p=0.0471) (figure 4.6.B). Tumor distribution by compartment, unlike to dying animals, has shown great reduction in tumor numbers in each compartment of the intestine in *Ikkα*$^{AA/AA}$ mice as well (figure 4.6.C).

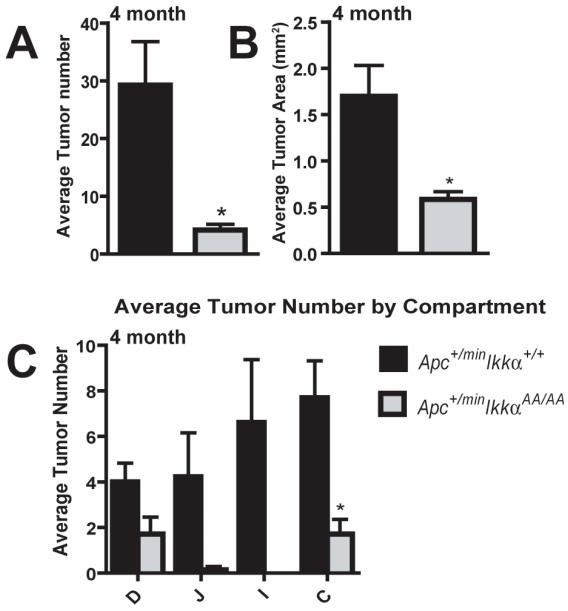

Figure 4.6: Basic Tumor Characterization in *Apc*$^{min/+}$*Ikkα*$^{AA/AA}$ Mice at month 4. (A) Average tumor number; (B) average tumor area; (C) tumor distribution by intestinal compartment (D: duodenum; J: jejunum; I: ileum; C: colon.

4.2.2.4. Anemia in 4 Months Old *Apc*$^{min/+}$ Mice

At month 4 control mice were already highly anemic while *Ikkα*$^{AA/AA}$ mice were having normal hemoglobin (9.16±1.24g/dL vs. 14.04±0.17g/dL, p=0.0085), and hematocrit (HCT) (32.46± 4.27% vs. 48.00±0.48%, p=0.0128) levels with little deviation from healthy control animals. These observations were proving that *Ikkα*$^{AA/AA}$ mice were healthy compared to already anemic controls (figure 4.7) most probably due to reduced tumor sizes and resulting decreased intestinal bleedings.

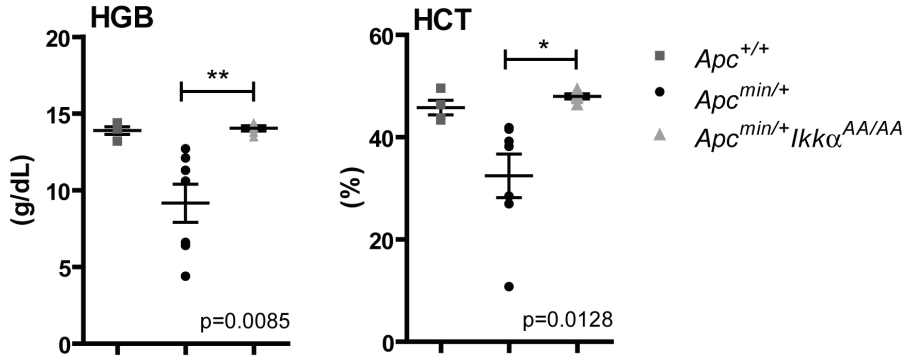

Figure 4.7: Anemic Status in *Apc*$^{min/+}$*Ikkα*$^{AA/AA}$ Mice at month 4. *Apc*$^{min/+}$*Ikkα*$^{AA/AA}$ animals were observed to be in a better health condition and with no anemia compared to *Apc*$^{min/+}$ controls as measured by above blood values (both hemoglobin and hematocrit values in *Apc*$^{min/+}$*Ikkα*$^{AA/AA}$ mice were as high as *wt* animals).

4.2.2.5. Proliferation in *Apc*$^{min/+}$ Mice Tumors at Month 4

A great difference in the tumor sizes between *Ikkα*$^{AA/AA}$ and control group of animal were observed in *Apc*$^{min/+}$model (figure 4.6.B and 4.9.A). To understand if this difference is arising from proliferative differences, BrdU IHC is performed and proliferating cells per crypt and proliferation index of the tumors were measured. BrdU IHC for proliferating cells (figure 4.9.B) has shown a slight decrease in proliferation index (0.3195 ± 0.004315 n=2 vs. 0.2772 ± 0.008544 n=2, p=0.0475) in the tumors from colon at 4 month for *Ikkα*$^{AA/AA}$ (figure 4.8.C). Furthermore, an insignificant decrease of proliferation (11.00±1.00 vs. 9.40±0.40, p= 0.2757) in the adjacent

non-tumor colonic crypts was observed (figure 4.8.A). Nevertheless, in the duodenum, no difference in proliferation rate was observed in normal crypts (15.50±0.70 vs. 15.75±0.65, p=0.8180) (figure 4.8.B) yet considering the size difference in the duodenal tumors this result is most probably due to lack of comparable sized tumors which were quite few to derive a statistically significant conclusions. Apoptosis as measured by TUNEL assay positive cells suggested not a major difference in controlled cell death yet more apoptotic cells were evident in the control group (figure 4.9.C). This observation with less apoptosis in *Ikkα*$^{AA/AA}$ intestinal tumors suggests that dying cells do not contribute regression of tumor development or any specific cell killing is debatable by current observations.

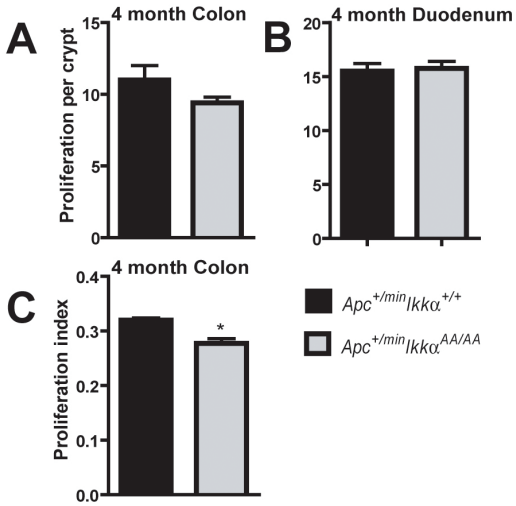

Figure 4.8: Proliferation in *Apc*$^{min/+}$*Ikkα*$^{AA/AA}$ Mice Intestines at Month 4. Average proliferation per crypt in normal colon (A) is slightly reduced in *Ikkα*$^{AA/AA}$ mice but not affected in duodenum (B). Proliferation index in colon tumors from *Apc*$^{min/+}$ mice shows a significant decrease in *Ikkα*$^{AA/AA}$ mice compared to WT (C) n=3 for all groups.

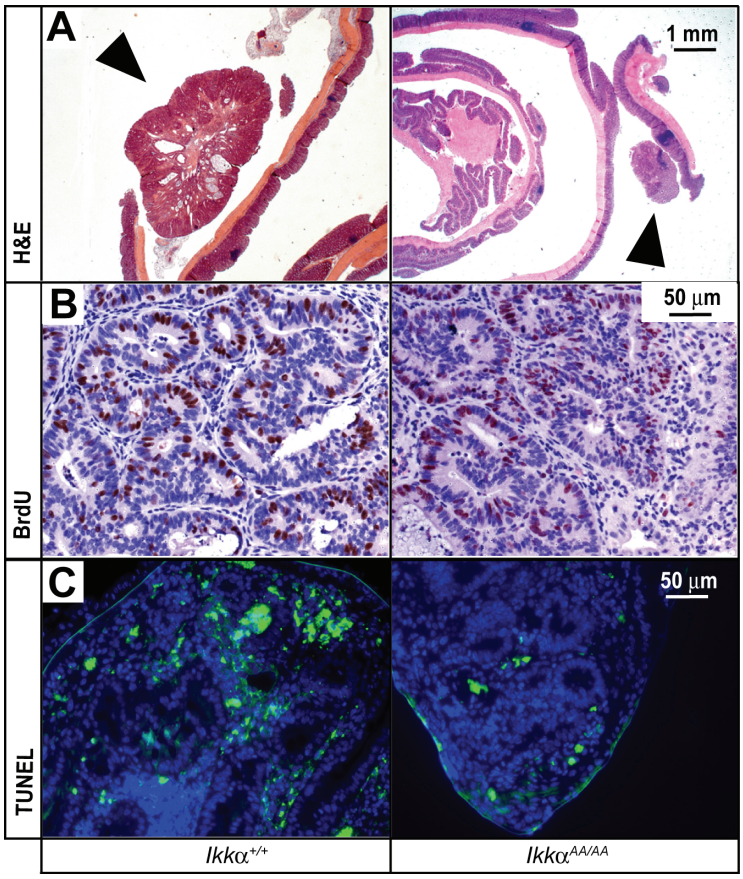

Figure 4.9: General morphology of *Apc*$^{min/+}$*Ikkα*$^{AA/AA}$ tumors at 4 months. (A) H&E staining for general tumor morphology and tumor size (B) BrdU for proliferation in tumors (C) TUNEL staining for apoptosis in *Apc*$^{min/+}$ tumors in wt and *Ikkα*$^{AA/AA}$ animals.

4.2.3. Constitutive β-catenin Activation Induced Genetic Intestinal Adenoma

4.2.3.1. *Vil-Cre-ER*^{T2}*Ctnnb1*$^{+/lox(ex3)}$as a Good Representation of *Apc*$^{min/+}$ Model

Because of the long time requirements for generation of *Apc*$^{min/+}$ mice and combination of these mice to other genetic backgrounds, we have utilized another genetic model of intestinal tumorigenesis to identify underlying molecular mechanism behind the phenotype we observed in previous models with *Ikkα*$^{AA/AA}$ mice. This model comprises constitutive activation of β-catenin via conditional and tissue specific deletion of phosphoregulatory domain. *Villin-CreER*^{T2} mice

previously described with its enterocyte specificity and tamoxifen dependent induction properties. By the use of this model otherwise lethal to embryos β-catenin activation is achieved in the intestines of adult mice. *Vil-Cre-ER^{T2}Ctnnb1$^{+/lox(ex3)}$* (for short *β-cat^{CA}*) is a fast model for mimicking the hyperproliferative phenotype similar to the loss of *Apc*. This model is a good representative of *Apc$^{fl/fl}$* mice as shown by GSEA (Subramanian et al., 2005) with a very high confidence (figure 4.10) yet we obtained results in very short time and with high confidence interval due to sensitivity of the model to different phenotypic or chemical interventions. Once the animals are induced, they survive with a median survival of 21 days (mean survival is 21.36± 0.66) (figure 4.11). Histological examinations revealed high proliferation throughout duodenum and partially in jejunum at the time of sacrifice (figure 4.12). Especially proliferation and cell cycle markers show a great difference due to highly elevated proliferation (see below in figure 4.14 and 4.15).

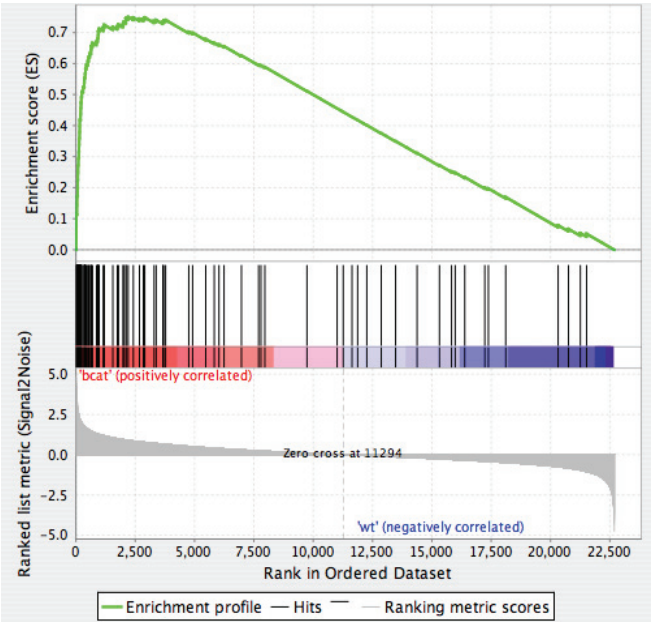

Figure 4.10: GSEA Enrichment Plot for Comparing *β-cat^{CA}* Model with *Apc$^{fl/fl}$* Upregulated Genes. Here *Vil-Cre-ER^{T2}Ctnnb1$^{+/lox(ex3)}$*at day 15 and wt mice microarray data analyzed against WNT targets in *Apc$^{fl/fl}$* mice (Sansom et al., 2007) and control group shows a high correlation showing good representation of the model (NES= 2.891, nominal p<0.001, FDR q<0.001). Therefore, *β-cat^{CA}* model is a good representation of *Apc$^{fl/fl}$*.

4.2.3.2. Survival of *β-cat*^{CA}*Ikkα*$^{AA/AA}$ Mice

To understand the role of IKKα involvement in this genetic model of intestinal tumorigenesis, we crossed *Ikkα*$^{AA/AA}$ mice to C57/BL6 background *β-cat*^{CA} mice to generate tamoxifen inducible enterocytes specific β-catenin activation system with activation deficient IKKα (*Ikkα*$^{AA/AA}$). Similar to *Apc*$^{min/+}$ model we observed a survival advantage in *Ikkα*$^{AA/AA}$ mice (median survival of 21 days n=11 vs. 34.5 n=10, p=0.0002) of about 60.87% (figure 4.12). Unlike to *Apc*$^{min/+}$ mice *Ikkα*$^{+/AA}$ did only provide a small survival advantage (figure 4.12) implying that heterozygousity does not have a significant contribution to the phenotype (median survival of 23 days n=7, p=0.3491). When we compared the weight difference curves for the both groups (until the median survival of *β-cat*^{CA} mice) we observed a rapid decrease in *β-cat*^{CA} animal weights while *β-cat*^{CA}*Ikkα*$^{AA/AA}$ mice sustained a stable weight for a couple of more days before hyperproliferation becomes dominated at a later time point. Therefore, *β-cat*^{CA}*Ikkα*$^{AA/AA}$ mice had a survival advantage with better health condition in the early stages of hyperproliferation.

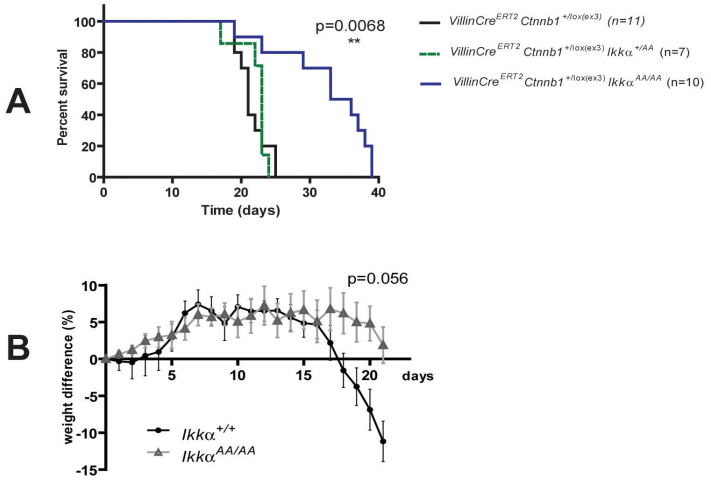

Figure 4.11: Survival of *β-cat*^{CA}*Ikkα*$^{AA/AA}$ *mice.* (A) Survival curves for *β-cat*^{CA}, *β-cat*^{CA}*Ikkα*$^{AA/AA}$ and *β-cat*^{CA}*Ikkα*$^{+/AA}$ animals show a clear survival advantage for *β-cat*^{CA}*Ikkα*$^{AA/AA}$ animals compared to other groups (median survival of 34 days vs. 21 or 23 days with p=0.0068 (*β-cat*^{CA}*Ikkα*$^{AA/AA}$ vs *β-cat*^{CA} p<0.0001). (B) Difference in weight curve for the first 21 days indicates great weight loss for *β-cat*^{CA} mice after day 15 while *β-cat*^{CA}*Ikkα*$^{AA/AA}$ mice are still stable (*β-cat*^{CA}*Ikkα*$^{AA/AA}$ vs *β-cat*^{CA} p=0.056).

4.2.3.3. Morphology of *β-cat*^{CA}*Ikkα*$^{AA/AA}$ Mice

Although we observed a sharp difference in survival of these two groups, histological examination of *β-cat*^{CA} mice did not give any hints about underlying mechanism at the time of their sacrifice. General morphology (figure 4.12), proliferation and apoptosis were all looking similar in histological sections (not shown). Yet basic examination via RT-PCR of cell cycle, differentiation and apoptosis markers has yielded similar results for both groups (data not shown). Hence we could not see any differences at the end of survival and continued our experiments in early time points.

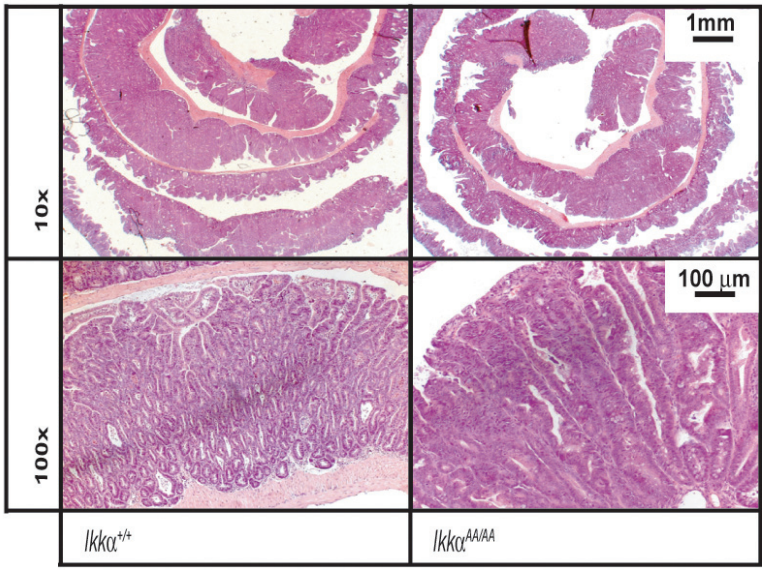

Figure 4.12: Morphology of duodenum at the time of sacrifice in *β-cat*^{CA}*Ikkα*$^{AA/AA}$ mice. Regardless of the extended survival we could not see any difference in duodenal morphologies in terms of proliferation or apoptosis (further stainings were done but no difference was observed as well).

4.2.3.4. General Morphology of *β-cat*^{CA}*Ikkα*$^{AA/AA}$ Mice at Day 15

Altogether, above data has suggested no sign of decrease in initiation or tumor progression at the time of sacrifice, regardless of the extended survival at the time, hence we extended our experimentation whether we can find a time point where we can see a difference in the phenotypes of both groups. After checking mice at different time points we have found that day 15 (figure 4.11.B) is the time where control group is already showing major differences in proliferation and resulting weight loss to those of wild type animals. However, $\beta\text{-}cat^{CA}Ikk\alpha^{AA/AA}$ mice were still very low in hyperproliferation with only a few animals shown hyperproliferative phenotype limited to only a fraction of the duodenum (usually proximal duodenum) while most of the animals did not show extensive hyperproliferation observed in $\beta\text{-}cat^{CA}$ mice (figure 4.13, and 14).

H&E stainings show that $\beta\text{-}cat^{CA}Ikk\alpha^{AA/AA}$ villi were still quite intact with the exception of extended proliferative crypt area. Control group in most cases have shown aberrant villi formation due to increased proliferation rate (figure 4.13). Further examination with proliferation marker BrdU and c-Myc has confirmed our histological examinations and proved that proliferation was still highly limited to crypt area (figure 4.14.A and B respectively). Furthermore, cell cycle markers like cyclin D1 and cyclin D2 were also reduced in the histological sections of 15-day $\beta\text{-}cat^{CA}Ikk\alpha^{AA/AA}$ animals (former was only slightly reduced compared to control group see in figure 4.15.A and B respectively). Altogether these observations were suggesting decreased proliferation in $\beta\text{-}cat^{CA}Ikk\alpha^{AA/AA}$ as a possible reason for retarded proliferation leading to better health outcomes in these mice.

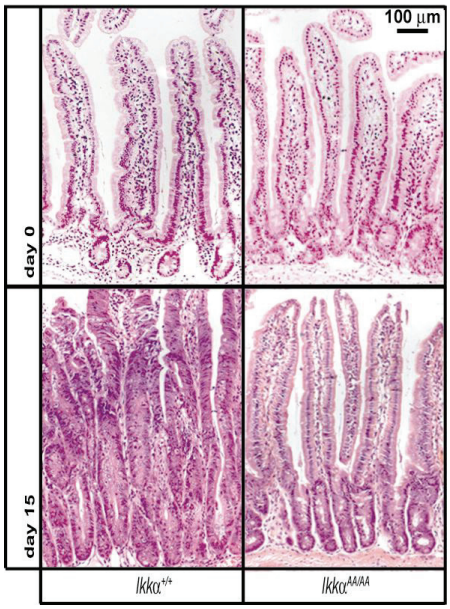

Figure 4.13: H&E Staining of *β-cat*^{CA}*Ikkα*$^{AA/AA}$ Mice at Day 15. Villi in *β-cat*^{CA} and *β-cat*^{CA}*Ikkα*$^{AA/AA}$ mice 15 day after β-catenin induction demonstrate a big difference due to increased proliferation in the control group while *β-cat*^{CA}*Ikkα*$^{AA/AA}$ mice has little increase in proliferative disturbance limited to crypt area. Non-induced controls (day 0) were also included for reference.

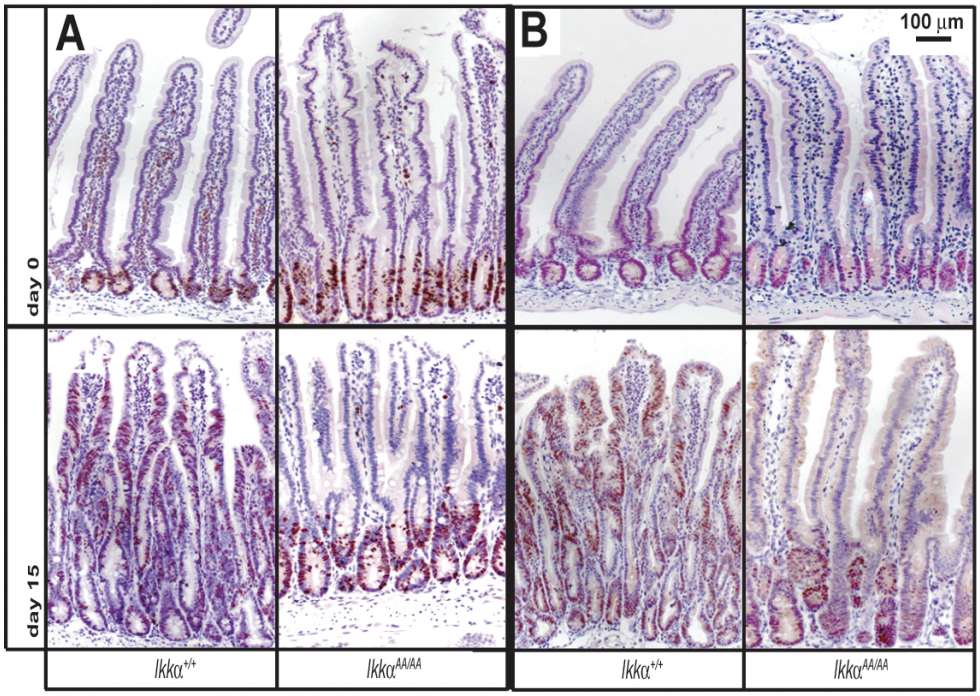

Figure 4.14: BrdU (A) and c-Myc (B) IHC of *β-cat*^{CA}*Ikkα*$^{AA/AA}$ Mice at Day 15. Although day 0 samples show thicker crypts in non-induced *Ikkα*$^{AA/AA}$ mice, at day 15 much less proliferation is observed in *β-cat*^{CA}*Ikkα*$^{AA/AA}$ mice compared to control group (all pictures are from 100x magnification).

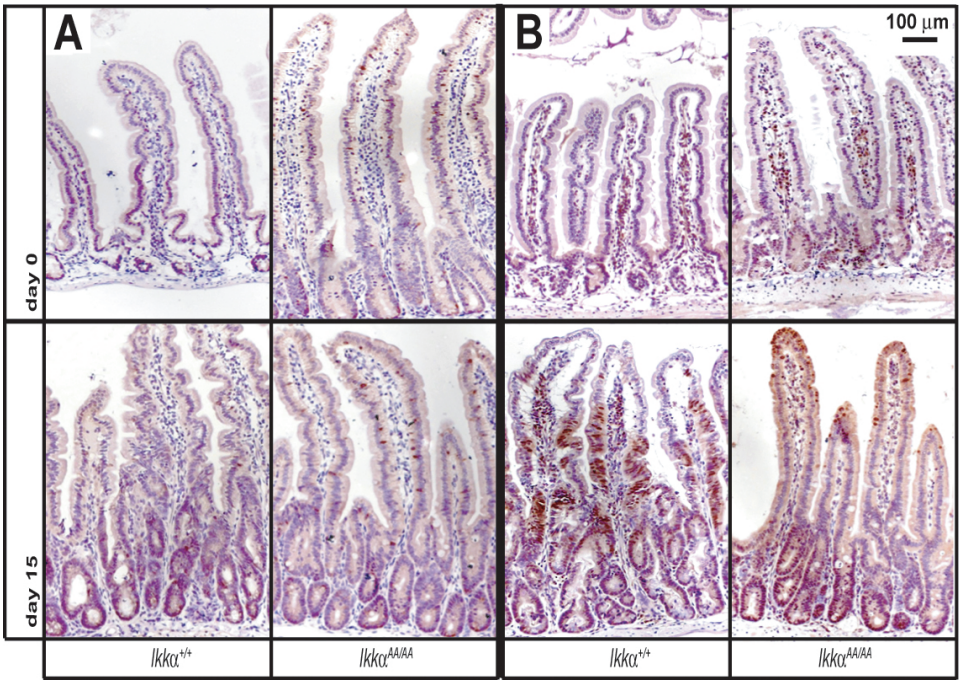

Figure 4.15: Cyclin D1 (A) and Cyclin D2 (B) IHC of *β-cat*^{CA}*Ikkα*$^{AA/AA}$ Mice at Day 15. *β-cat*^{CA}*Ikkα*$^{AA/AA}$ mice at day 15 had reduced Cyclin D1 and D2 levels supporting reduced cell cycle entry and proliferation (all pictures are from 100x magnification).

4.3. IDENTIFICATION OF MOLECULAR MECHANISM BEHIND IKKα INACTIVATION IN CRC

4.3.1. Involvement of Alternative NF-κB Activation in IKKα Inactivation

To check the possibility of the alternative NF-κB activation in the epithelial cells to explain observed phenotype, baseline NF-κB2 activation levels were checked via immunoblotting in epithelial samples of *β-cat*^{CA} mice. Similar levels of NF-κB activation for both groups were observed (figure 4.16.C). According to the expression data *β-cat*^{CA}*Ikkα*$^{AA/AA}$ mice did show have any difference of activation of alternative NF-κB activation as marked by proteolytic cleavage of p100 to p52 to that of *β-cat*^{CA} mice. To further investigate the role of its involvement whole body knockout for p52 and enterocyte specific *Relb*$^{fl/fl}$ were crossed to *β-cat*^{CA} background and survival

curves for these animals were generated (figure 4.16.A and B). Both model provided marginal survival advantages over *β-cat*^{CA} (*β-cat*^{CA}*p52*$^{\Delta IEC}$: median of 23 vd. 21; n=8, p=0.2357/*β-cat*^{CA}*Relb*$^{\Delta IEC}$: median of 24 vs. 21; n=6, p=0.0338) while they were still way too less than *β-cat*^{CA}*Ikkα*$^{AA/AA}$ mice survival (vs. 34.5 p=0.0019 and p=0.004 respectively). Therefore, the contribution of alternative NF-κB activation should be marginal and not enough to explain full phenotype associated with reduced proliferation and tumors sizes in *β-cat*^{CA}*Ikkα*$^{AA/AA}$ mice.

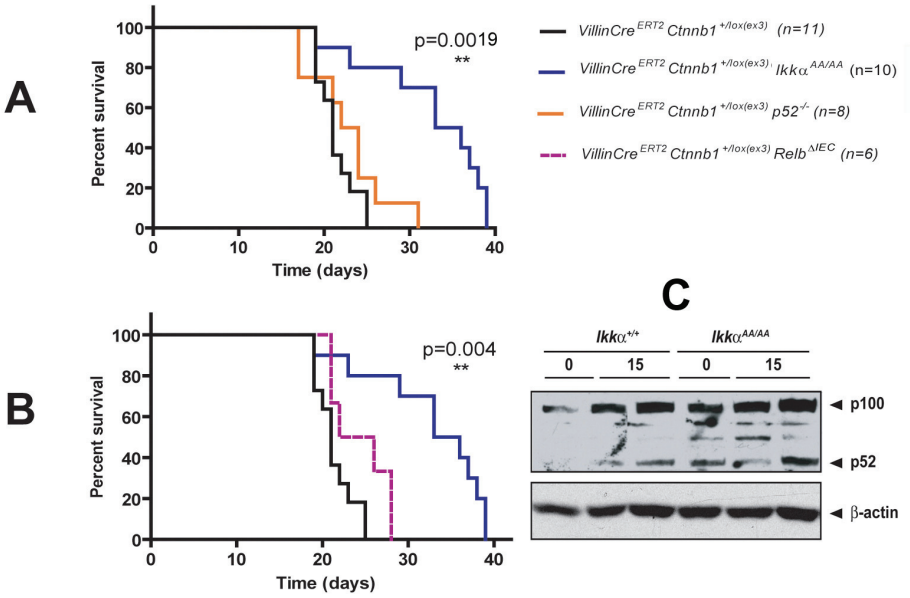

Figure 4.16: Survival of *β-cat*^{CA}*p52*$^{-/-}$ and *β-cat*^{CA}*Relb*$^{\Delta IEC}$ mice. Survival curves for *β-cat*^{CA}, *β-cat*^{CA}*Ikkα*$^{AA/AA}$ and *β-cat*^{CA}*p52*$^{-/-}$ animals (A) again show a clear survival advantage for *β-cat*^{CA}*Ikkα*$^{AA/AA}$ animals compared to other p52 KO (23 vs. 34.5days with p=0.0019). (B) On the other hand *β-cat*^{CA}*Relb*$^{\Delta IEC}$ mice has a slight survival advantage over *β-cat*^{CA} mice (24 vs. 21 p=0.038) while it is still much less than *β-cat*^{CA}*Ikkα*$^{AA/AA}$ mice (24 vs. 34.5 days with p=0.004). (C) Alternative NF-κB activation was also the same in IEC samples from 15-day animals as checked by immunoblot.

4.3.2. General Expression Analysis in *β-cat*^{CA} Mice

4.3.2.1. Hightroughput Expression Analysis in *β-cat*^{CA} Mice via Microarray

To explain proliferation difference we observed in *β-cat*^{CA}*Ikkα*$^{AA/AA}$ mice, we decided to screen overall gene expression profiles in a DNA chip based assay. For this purpose we used Affymetrix 20K mouse chip and screened over 23K transcript expressions in 1: WT 2: *Ikkα*$^{AA/AA}$ 3: *β-cat*^{CA} (day 15) 4: *β-cat*^{CA}*Ikkα*$^{AA/AA}$ (day 15) mice with 2 samples per group. GSEA of all gene profiles to Wnt signaling targets (Sansom et al., 2007) has shown that *β-cat*^{CA} mice resembles more to *Apc*$^{fl/fl}$ phenotype (figure 4.10) while almost all of the genes normally upregulated in *Apc*$^{fl/fl}$ mice were downregulated in *β-cat*^{CA}*Ikkα*$^{AA/AA}$ mice.

4.3.2.1.1. Hierarchical Clustering of Expression Data

To identify possible mechanisms hierarchical clustering of the significantly regulated genes by Z-score to plot a heat map of relative expressions (figure 4.17) or by k-means (figure 4.18) to plot relative rank score graphs were done. Hierarchical clustering with k-means algorithm yielded 10 clusters with differential expression patterns. Among these clusters, *β-cat*^{CA} at day 15 (cluster IV and VI) or *β-cat*^{CA}*Ikkα*$^{AA/AA}$ at day 15 (cluster VIII) upregulated ones were further analyzed to identify targets of β-catenin activation (in general) and reduced proliferation (in *β-cat*^{CA}*Ikkα*$^{AA/AA}$ mice). Clusters upregulated in *β-cat*^{CA} mice but downregulated in *β-cat*^{CA}*Ikkα*$^{AA/AA}$ mice were suggesting direct involvement of IKKα in Wnt signaling. However, the Wnt target genes downregulated in *β-cat*^{CA}*Ikkα*$^{AA/AA}$ at day 15 were quite different from that of described before (Fingerle et al., 2009) and were not suggesting a clear role in the control of Wnt signaling unlike to the correlation described in that manuscript. Consequently, these results suggested that neither

β-catenin (by protein expression) nor c-Myc (via promoter activity assays-data not shown) was directly affected from IKKα. This phenomenon will be clarified by the comparison of Wnt target gene expression to that of analyzed in Fingerle et al. in related discussion chapter (see section 5.2.2).

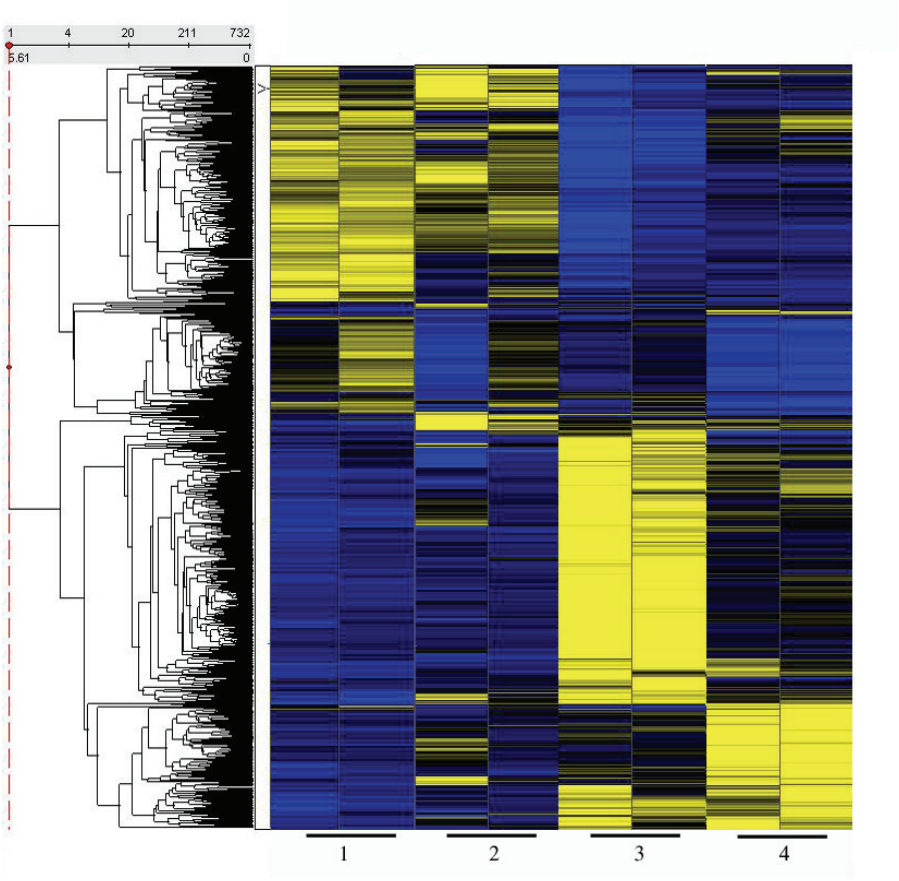

Figure 4.17: Hierarchical Clustering of 732 Significantly Regulated Genes in Heatmap and Dendogram. Microarray data is filtered for significantly regulated genes and 732 genes were found to be altered at least in one of the groups ($p<0.05$). Then these genes were hierarchically clustered and plotted for similarly expressed genes according to their Z-scores (a score for relative expression). Yellow is used for upregulation and blue for downregulation (Z-scores between -3.12 to 3.13). Above for each cluster: 1: WT 2: $Ikk\alpha^{AA/AA}$ 3: $\beta\text{-}cat^{CA}$ (day 15) 4: $\beta\text{-}cat^{CA}Ikk\alpha^{AA/AA}$ (day 15).

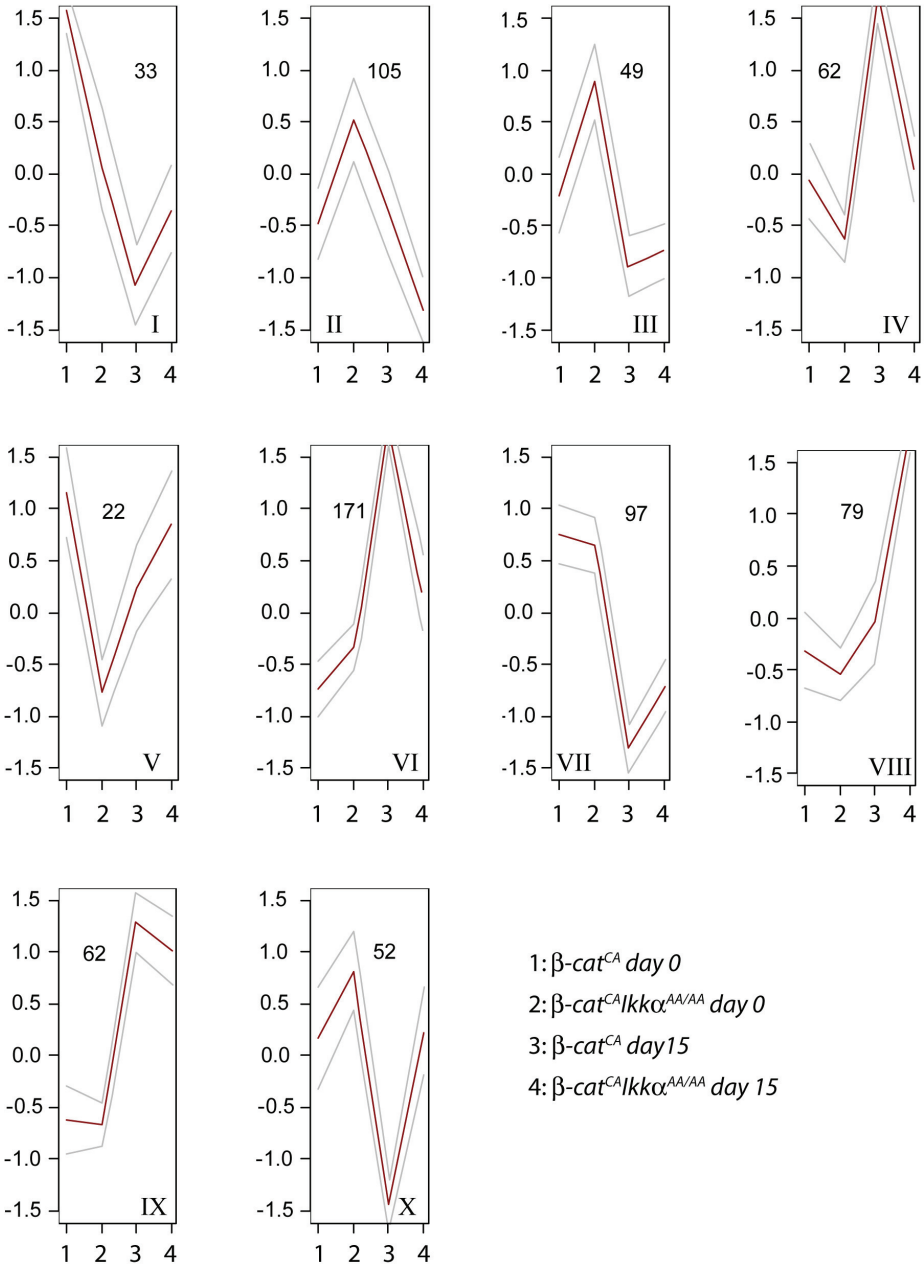

Figure 4.18: K-Means Clustering of Significantly Regulated 732 Genes in Microarray Analysis. Microarray data is filtered for significantly regulated genes and 732 genes were found to be altered at least in one of the genotypes ($p<0.05$). Then these genes were hierarchically clustered with k-means algorithm according to expression patterns. The algorithm divided these genes into 10 expressional co-regulated clusters (these graphs are regenerated by faithfully preserving the original data to exclude some genotypes unnecessary for this project).

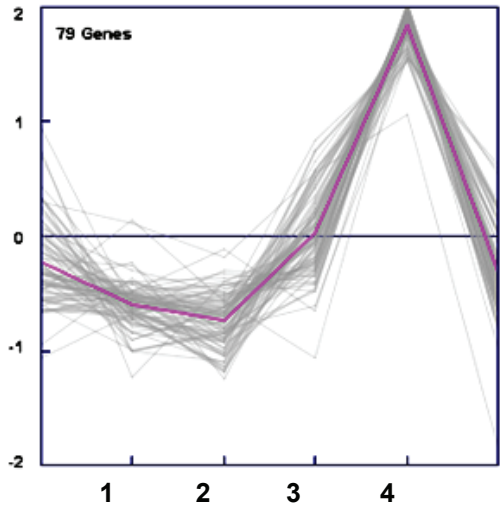

Figure 4.19: Closer look at the cluster with 79 transcripts that are upregulated in 15 day *β-cat*^{CA}*Ikkα*$^{AA/AA}$ mice. The above cluster shows 79 genes with significant upregulation in *β-cat*^{CA}*Ikkα*$^{AA/AA}$ mice. These genes are uniquely upregulated in *β-cat*^{CA}*Ikkα*$^{AA/AA}$ mice while all other phenotypes have similar levels of regulation. 1: WT 2: *Ikkα*$^{AA/AA}$ 3: *β-cat*^{CA} 4: *β-cat*^{CA}*Ikkα*$^{AA/AA}$ mice.

4.3.2.1.2. Functional Classification of Expression Data and Identifying Molecular Signatures

When we analyzed *β-cat*^{CA}*Ikkα*$^{AA/AA}$ upregulated genes we have found that a cluster of 79 genes (cluster VIII in figure 4.18 and 19) 42% of the genes within this cluster (figure 4.20 table 4.1) are involved in immune response or inflammation (see gene identities in supplementary microarray data in Appendices chapter).

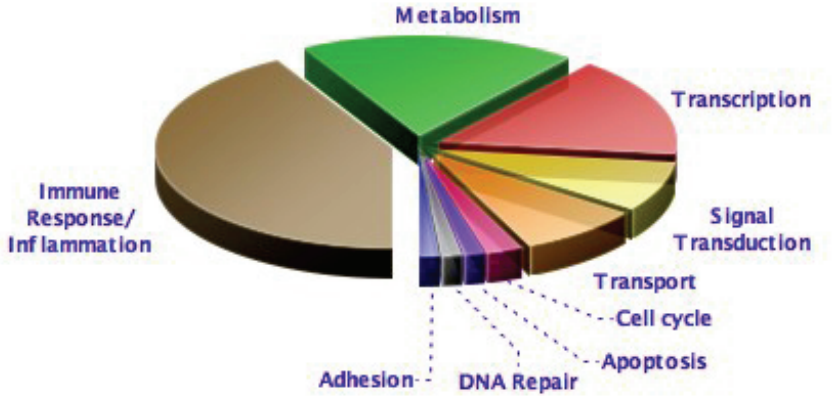

Figure 4.20: Functional Classification of the Genes in *β-cat*^{CA}*Ikkα*$^{AA/AA}$ Mice Upregulated Cluster. Functional classification of the genes in this cluster made it apparent that most of these genes are related to immune response or inflammation (41.89%).

Gene Function	Number of Genes	Percentage
Immune Response/Inflammation	31	41.89
Metabolism	14	18.92
Transcription	12	16.22
Signal Transduction	6	8.11
Transport	6	8.11
Cell Cycle	2	2.7
Apoptosis	1	1.35
DNA Repair	1	1.35
Adhesion	1	1.35

Table 4.1: Data for functional classification of *β-cat*^{CA}*Ikkα*$^{AA/AA}$ mice upregulated cluster (supplementary to figure 4.21). Only genes with known functional associations are included and some genes may have more than one function.

Since previously known IFN targets were found within this cluster, GSEA (Subramanian et al., 2005) was performed with molecular signatures from previously confirmed molecular targets of IFN stimulation in various human epithelial cell lines to verify these associations. These signature genes were chosen on the basis of their availability in GSEA MSigDB and their relevance due to their coverage of epithelial tissue IFN downstream upregulation. Although there

were other IFN signature lists related to downstream upregulation which gave similar results as we will present shortly, we have just used these representative analysis for the sake of clarity. We have found signature genes that are upregulated in mice upon IFNα, β or γ stimulation and run an analysis for our chip results to compare *β-cat^{CA}Ikkα$^{AA/AA}$* with all the rest. In all runs we have obtained significant association of upregulation of these signatures only with *β-cat^{CA}Ikkα$^{AA/AA}$* samples (figure 4.21). For IFNα signature genes (Radaeva et al., 2002) we compared *β-cat^{CA}Ikkα$^{AA/AA}$* with all the rest and we obtained a high correlation of upregulated genes almost exclusively in *β-cat^{CA}Ikkα$^{AA/AA}$* mice (with NES score of 2.228, $p<0.01$). Similarly IFNβ (Der et al., 1998) and IFNγ (Sana et al., 2005) signatures were again exclusively upregulated in *β-cat^{CA}Ikkα$^{AA/AA}$* mice (NES of 2.232 and 1.736 respectively, $p<0.01$ for both). Here the NES scores were lower due to smaller population size of our significantly regulated genes. Still these results suggested that the genes in cluster VIII can be of utmost importance because of belonging to interferon signaling which is central to immune regulation and responses.

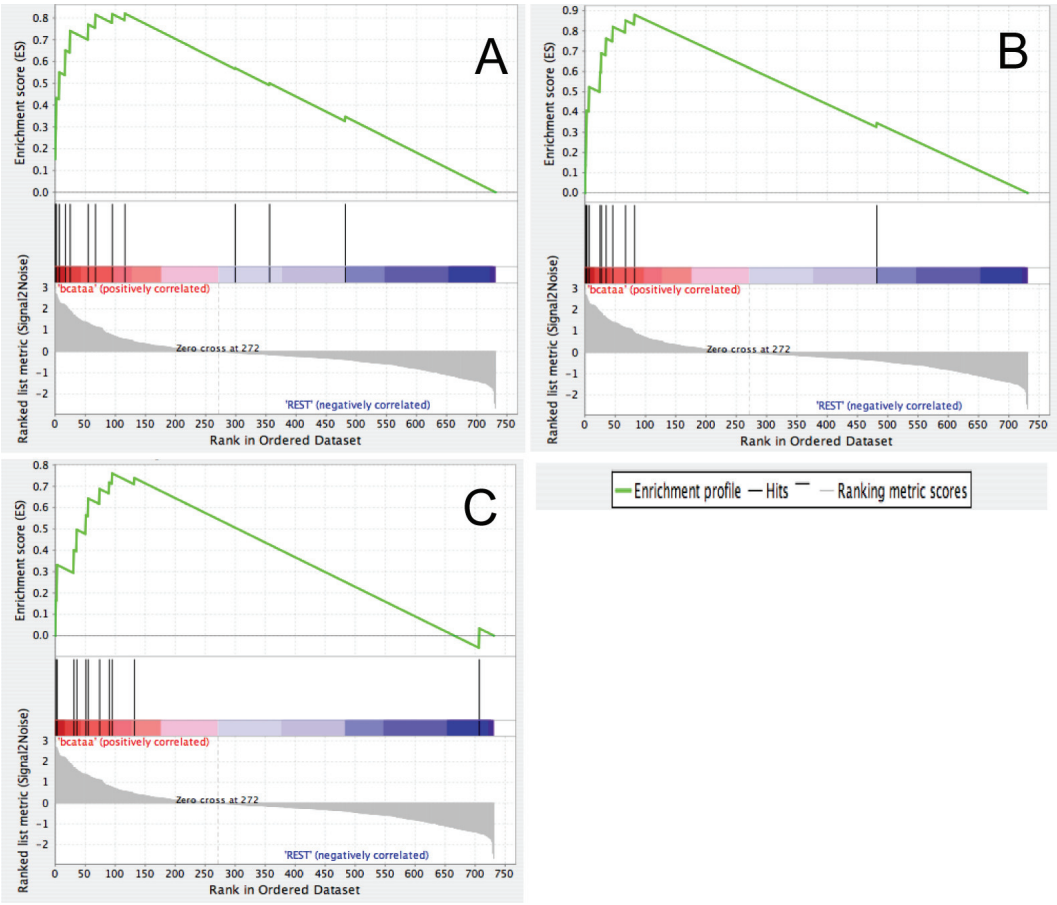

Figure 4.21: GSEA of Microarray Data with Interferon Induction Signature Genes. Genesets were used from previously described signatures of interferon induction gene profiles. Genes upregulated upon (A) IFN-α (B) IFN-β (C) IFN-γ stimulations from respective signature sets (Der et al., 1998; Radaeva et al., 2002; Sana et al., 2005) were selected and analyzed against our significantly regulated gene list. On the left always *β-cat*^{CA}*Ikkα*$^{AA/AA}$ mice were compared to the all other groups and we have found almost all the hits of upregulation obtained in *β-cat*^{CA}*Ikkα*$^{AA/AA}$ mice with high enrichment scores and statistical significance ($p<0.01$, FDR<0.01 for all analysis).

Similarly GSEA was run for *Apc*$^{fl/fl}$ mice upregulated genes to associate *β-cat*^{CA}*Ikkα*$^{AA/AA}$ mice with Wnt target expression. As a result of this analysis, *β-cat*^{CA} mice has shown a great correlation with Wnt targets while *β-cat*^{CA}*Ikkα*$^{AA/AA}$ mice at day 15 were showing downregulation or negative correlation with almost all Wnt signature genes with very high NES score and significance (NES=2.628, nominal $p<0.001$, FDR $q<0.001$) (figure 4.22) which was quite similar to the result

we obtained in wt mice (figure 4.10). Although some of these genes were also upregulated in *β-cat*^{CA}*Ikkα*$^{AA/AA}$ mice, a general downregulation of Wnt targets was evident relative to *β-cat*^{CA} mice.

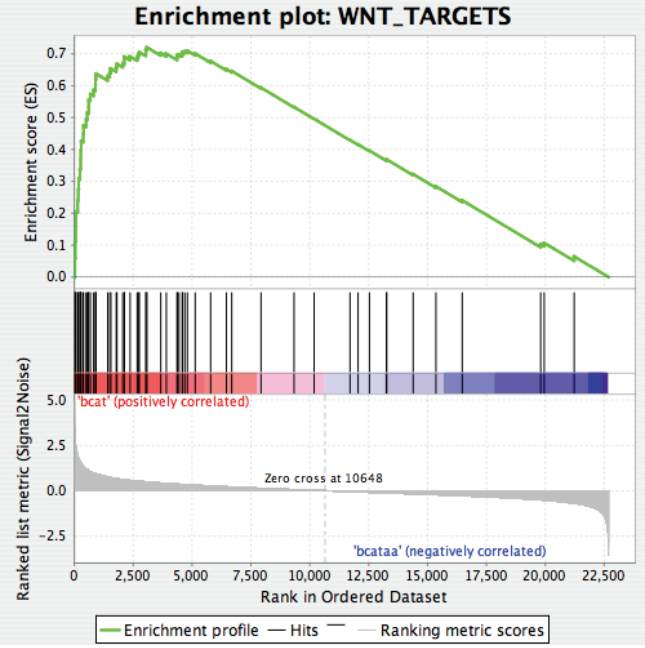

Figure 4.22: GSEA Enrichment Plot for Comparing *β-cat*^{CA} Model with *Apc*$^{fl/fl}$ Upregulated Genes (WNT_TARGETS). These two models are looking highly correlated in upregulated gene hits so our model is good representation of *Apc*$^{fl/fl+}$. Here *Vil-Cre-ER*^{T2}*Ctnnb1*$^{+/lox(ex3)}$and *Vil-Cre-ER*^{T2}*Ctnnb1*$^{+/lox(ex3)}$ *Ikkα*$^{AA/AA}$ 15 day induced mice microarray data analyzed against WNT targets in *Apc*$^{fl/fl}$ mice (Sansom et al., 2007) and control group shows a high correlation showing good representation of the model.

4.3.2.2. Expression Analysis in *β-cat*^{CA} Mice via RT-PCR

Following our initial Microarray analysis results, we performed a series of RT-PCR expression analysis with highly upregulated genes of interferon downstream targets to verify our observations (figure 4.23). Results were mostly supporting our initial observation of interferon downstream activation from the cluster of *β-cat*^{CA}*Ikkα*$^{AA/AA}$ upregulated genes or general upregulated genes in *β-cat*^{CA}*Ikkα*$^{AA/AA}$ mice. Almost all the genes we looked in *β-cat*^{CA}*Ikkα*$^{AA/AA}$ mice were upregulated relative to *β-cat*^{CA} mice. Consequently, we thought interferon signaling and immune cell

activation may play a role in extended survival as a result of reduced proliferation in *β-cat*^{CA}*Ikkα*$^{AA/AA}$ mice. Especially increase in IFNγ targets were more notable and indicating a strong IFNγ downstream activation in *β-cat*^{CA}*Ikkα*$^{AA/AA}$ IEC.

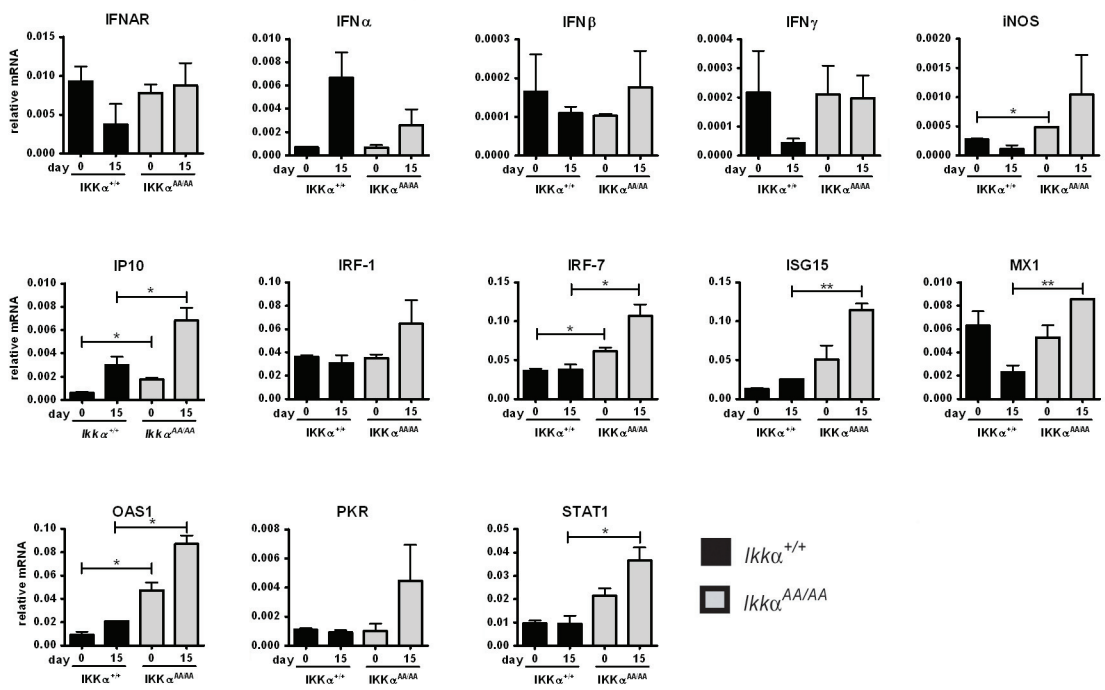

Figure 4.23: RT-PCR Analysis in Interferon Targets in *β-cat*^{CA}*Ikkα*$^{AA/AA}$ IEC. Interferon downstream target upregulations were confirmed in IEC from *β-cat*^{CA}*Ikkα*$^{AA/AA}$ mice at day 15 by RT-PCR analysis.

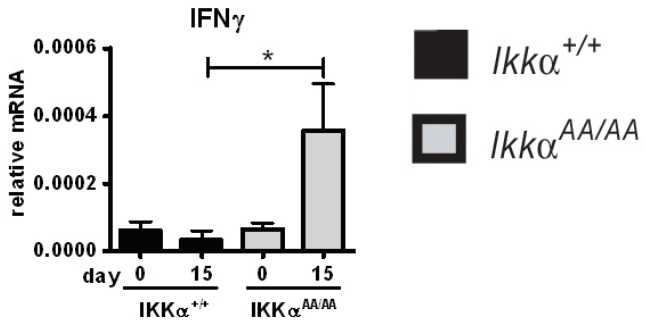

Figure 4.24: IFNγ production is increased in *β-cat*^{CA}*Ikkα*$^{AA/AA}$ mice. RT-PCR analysis results from whole mucosa samples.

4.3.2.3. Expression Analysis in *β-cat*^{CA} Mice via Protein Immunoblotting

β-catenin activation was complete in *β-cat*^{CA} mice at day 15 and there were no change in their relative expression in *β-cat*^{CA}*Ikkα*$^{AA/AA}$ mice (figure 4.25). Still we observed a decrease of c-Myc which was parallel to decrease in proliferation as shown by histology (figure 4.14). IKKα levels were also not affected by the specific knock-in. We further checked IFNγ downstream activation in IEC lysates from *β-cat*^{CA} mice samples. Similar to our previous observations with mRNA expressions we observed a strong IFNγ downstream activation unique to *β-cat*^{CA}*Ikkα*$^{AA/AA}$ mice. Hence these results have verified that IFNγ secretion via activated immune cells were either increased or more effective in *β-cat*^{CA}*Ikkα*$^{AA/AA}$ mice. Again there was an increase in STAT1 and IRF1 levels while specifically STAT1 phosphorylation or iNOS activation were specifically occurred in *Ikkα*$^{AA/AA}$ mice samples (increased upon β-catenin activation) while STAT3 levels and activation was unaffected. Still we thought that our expression data was solid enough to conclude the upregulation of IFNγ levels in *β-cat*^{CA}*Ikkα*$^{AA/AA}$ mice. Exclusion of IFNα or β involvement will be much clear when we will present further data regarding whole body knockouts and hematopoietic cell characterization in the following sections. We will continue exploring the mechanism regarding IFNγ downstream targets upregulation and the importance of this upregulation in tumor growth suppression in the following parts.

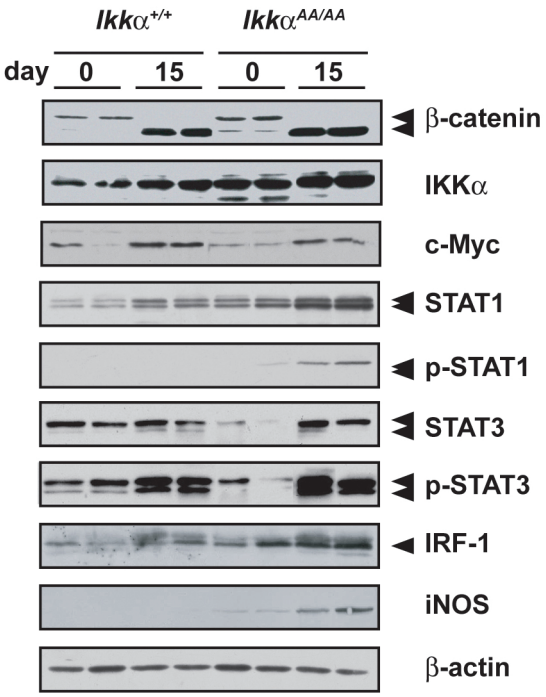

Figure 4.25: WB Analysis in *β-cat^{CA}Ikkα$^{AA/AA}$* Mice at day 15. Decrease in proliferation and c-Myc levels were not due to β-catenin expression and knock-in did not affect IKKα expression in IEC samples. On the other hand, IEC cell lysates have shown upregulation of IFNγ downstream targets like STAT1, IRF-1 and activation of iNOS and phosphorylation of STAT1 in *β-cat^{CA}Ikkα$^{AA/AA}$* mice while STAT3 activation was indifferent in both groups.

Gene expression levels for IFNγ downstream targets like IRF-1 and STAT1 were also checked in *Apc$^{min/+}$* and *Apc$^{min/+}$Ikkα$^{AA/AA}$* mice tumors collected at month 4 (figure 4.26). Once more upregulation in these targets were observed for *Apc$^{min/+}$Ikkα$^{AA/AA}$* mice tumors. These observations strongly suggested that interferon signature observed in *β-cat^{CA}Ikkα$^{AA/AA}$* mice is model independent and a general phenomenon for the reduced proliferation and resulting extended survival in these mice.

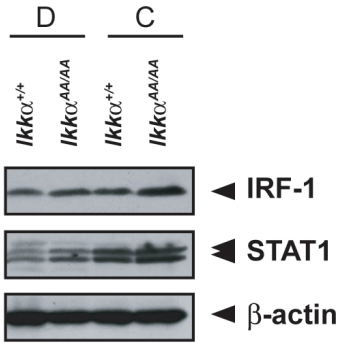

Figure 4.26: WB analysis in *Apc*$^{min/+}$ tumors at month 4. Duodenal and colon tumors (D and C respectively) were analyzed for IRF-1 and Stat1 expression in *Apc*$^{min/+}$ and *Apc*$^{min/+}$*Ikkα*$^{AA/AA}$ mice. These IFNγ downstream targets were also upregulated in *Apc*$^{min/+}$*Ikkα*$^{AA/AA}$ mice as in the case of *β-cat*^{CA}*Ikkα*$^{AA/AA}$ mice. Therefore, previous observations with IFN signature is model independent and elongated survival and reduced proliferation in AOM and *Apc*$^{min/+}$ mice should be due to the same phenomenon in *β-cat*^{CA}*Ikkα*$^{AA/AA}$ mice.

4.2.3.4. Cell Cycle Arrest as a Result of IFNγ Upregulation in *β-cat*^{CA}*Ikkα*$^{AA/AA}$ Mice

Once it becomes apparent that a strong IFNγ downstream activation is ongoing in *β-cat*^{CA}*Ikkα*$^{AA/AA}$ mice, we wanted to know how the proliferation in *β-cat*^{CA}*Ikkα*$^{AA/AA}$ mice is reduced in the absence of IKKα activation. Furthermore, it is also known that IFNγ induced cell cycle arrest may be the key mechanism in reduced proliferation in *β-cat*^{CA}*Ikkα*$^{AA/AA}$ mice. Therefore, kinase activities of major IFNγ downstream targets regulating cell cycle were checked. Finally, it was confirmed that Cdk1 (Cdc2) and Cdk2 kinase activities on histone H1 were reduced (figure 4.27) in IEC lysates of *β-cat*^{CA}*Ikkα*$^{AA/AA}$ mice at day 15 relative to *β-cat*^{CA} at day 15 and were comparable to baseline levels in control animals (figure 4.27.A and B). Consequently, IFNγ was acting on IECs to cause cell growth arrest which was the reason for reduced proliferation observed in *β-cat*^{CA}*Ikkα*$^{AA/AA}$ mice.

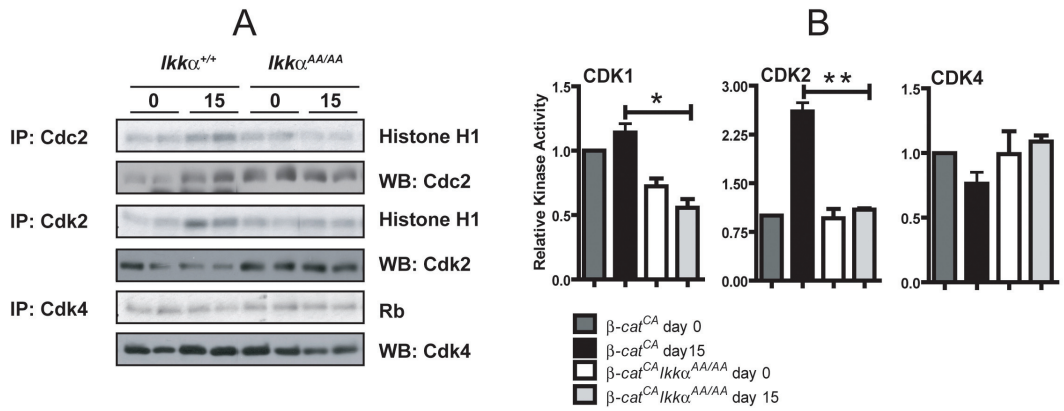

Figure 4.27: Cell Cycle Arrest in *β-cat^{CA}Ikkα$^{AA/AA}$* Mice at day 15. (A) KA for CDK1 (Cdc2), CDK2 and CDK4 were performed by pulling them down from IEC lysates against using Histine H1 or Rb as substrates. CDK1 and CDK2 kinase activities were reduced in 15-day *β-cat^{CA}Ikkα$^{AA/AA}$* mice but Cdk4 activity was retained. This shows that IFNγ acts on *Ikkα$^{AA/AA}$* tumor cell via causing G0 or S phase cell cycle arrest. (B) Normalized relative kinase activities in bar graphs as measured by light densitometry.

4.3.3. Understanding Regulation of Downstream Targets of IKKα Inactivation

4.3.3.1. Reversion of Extended Survival in *β-cat^{CA}Ikkα$^{AA/AA}$* Mice via *Ifng* Deletion

After the observation of increased IFNγ downstream targets in *β-cat^{CA}Ikkα$^{AA/AA}$* mice and proving that reduced proliferation is due to cell cycle arrest caused by increased IFNγ downstream effectiveness in IECs, we wanted to identify whether the whole *Ikkα$^{AA/AA}$* phenotype is dependent on IFN activation. For this purpose, *Ifnγ$^{-/-}$* and *Ifnar1$^{-/-}$* knock-out (see discussion for this model) mice were crossed to *β-cat^{CA}Ikkα$^{AA/AA}$* background to generate triple mutants. As a result of these breedings and formed survival data upon β-catenin activation, only *Ifnγ$^{-/-}$* knock-out completely reverted the *Ikkα$^{AA/AA}$* phenotype after β-catenin activation and survived as short as control group (median survival of 20.5 vs. 21 (*β-cat^{CA}*) p=0.2812 vs. 34.5 (*β-cat^{CA}Ikkα$^{AA/AA}$*) p<0.0001) (figure 4.28). Therefore, IFNγ should be the ultimate target of *Ikkα$^{AA/AA}$* phenotype leading to decreased proliferation and cell cycle arrest in *β-cat^{CA}Ikkα$^{AA/AA}$* mice intestines.

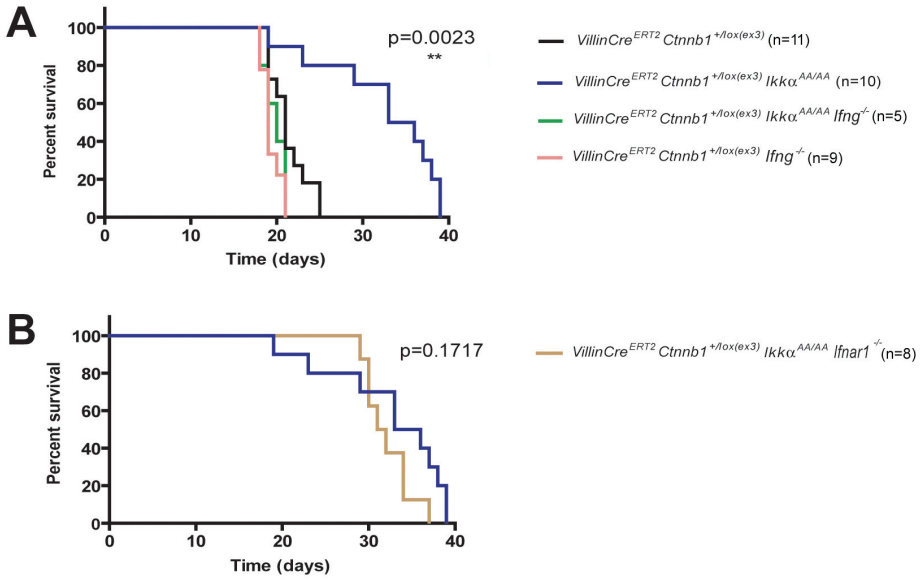

Figure 4.28: *Ifnγ*$^{-/-}$ but not *Ifnar1*$^{-/-}$ Reverts Extended Survival in *β-cat*^{CA}*Ikkα*$^{AA/AA}$ Mice. When we coupled *Ifnγ*$^{-/-}$ mice to our *Vil-Cre-ER*^{T2}*Ctnnb1*$^{+/lox(ex3)}$*Ikkα*$^{AA/A}$ it reverts all extended survival and mice behave like control group (median survival of 20.5 vs. 21 p=0.2812) (A) but we did not see the same phenomenon in *Ifnar1*$^{-/-}$ mice coupled to our *β-cat*^{CA}*Ikkα*$^{AA/AA}$ model (median survival of (median 31.5 vs. 21 p<0.0001) which was similar to *β-cat*^{CA}*Ikkα*$^{AA/AA}$ survival (31.5 vs. 34.5 p=0.1717) (B).

4.3.3.2. Contribution of Epithelial and Hematopoietic Cell Compartments

Initially observing that the interferon downstream targets are strongly upregulated in *β-cat*^{CA}*Ikkα*$^{AA/AA}$ mice, this regulation was tried to be identified whether it is due to activated hematopoietic cells or increased sensitivity to interferons in epithelial cells. To separate these roles conditional *Ikkα*$^{fl/fl}$ mice were mated to *β-cat*^{CA} background to generate epithelial specific deletion of *Ikkα* and activation of β-catenin at the same time. After generating these mice *Ikkα*$^{\Delta IEC}$ mutation and β-catenin activation were induced by tamoxifen and survival data was obtained to compare with previous phenotypes. It is observed that IEC specific deletion only marginally increased (median survival of 24 vs 21 p=0.07) (figure 4.29.A). This shows that epithelial IKKα has a partial contribution in the increased survival but not enough to explain whole phenotype.

To separate the roles of epithelial and hematopoietic cells bone marrow (b.m.) transplantations

were performed from *Ikkα*$^{AA/AA}$ to WT mice in β-catenin activation model. BMD cells were isolated and transplanted from uninduced *β-cat*^{CA}*Ikkα*$^{AA/AA}$ to uninduced *β-cat*^{CA} mice while using *β-cat*^{CA} bone marrow transplants as control. After confirming successful replacement of bone marrows by genotyping animals from blood samples (figure 4.29.C) to check myeloid cell DNA, β-catenin activation was induced by tamoxifen injections. Upon sacrifice of the animals, survival curves were plotted and it was observed that *Ikkα*$^{AA/AA}$ b.m. transplanted mice had extended survival advantage over control group (27 vs. 21 p=0.03) (figure 4.29.B) yet still not as much as *β-cat*^{CA}*Ikkα*$^{AA/AA}$ mice. Therefore, these results suggested that IKKα dysfunction in both IEC and hematopoietic cells has contribution in extended survival of these mice and neither of them is self-sufficient to recapitulate the phenotype.

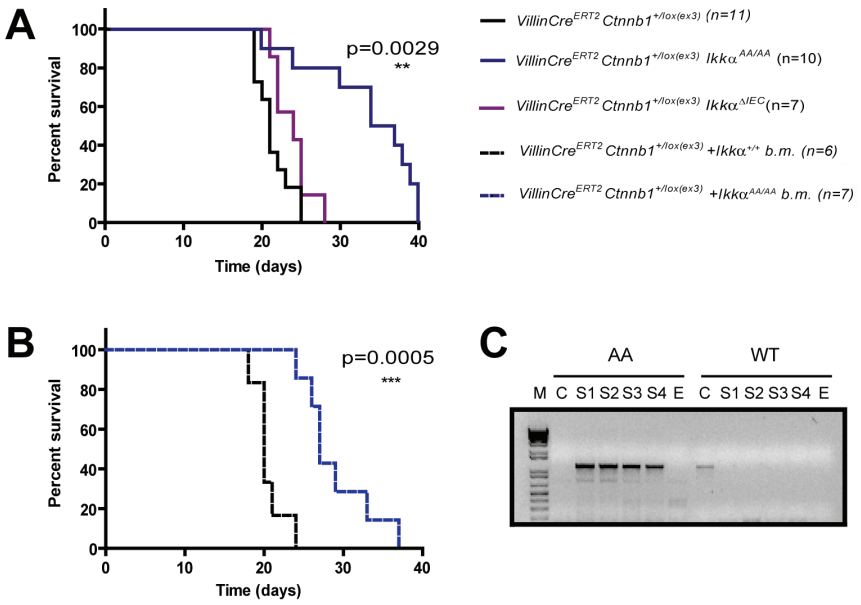

Figure 4.29: Survival Graphs for intestinal specific *Ikkα* deletion model *β-cat*^{CA}*Ikkα*$^{\Delta IEC}$ mice (A) and *Ikkα*$^{AA/AA}$ bone marrow transplanted mice (B). Both *Ikkα*$^{\Delta IEC}$ mice (median survival of 24 vs. 21 p=0.007) and *Ikkα*$^{AA/AA}$ bone marrow transplanted *β-cat*^{CA} mice (median survival of 27 vs. 21.5 p=0.0286) had extended survivals compared to control groups but not as long as whole body knock-in *β-cat*^{CA}*Ikkα*$^{AA/AA}$ mice (median survival of 34.5 vs. 21) suggesting that the effect we see is additive of both tissues. Genotypings from blood isolated genomic DNAs confirms complete reversion of hematopoietic cell line to *Ikkα*$^{AA/AA}$ in bone marrow transplanted mice (C): M marker C control (WT transplanted sample), E no DNA and S1-S4 AA transplanted samples.

4.3.3.3. Analysis of Hematopoietic Cells to Identify Molecular Machinery behind IFNγ Activation

Once it is proven that IFNγ is the ultimate target of *Ikkα*$^{AA/AA}$ phenotype by the reversion of the phenotype, the next step was to identify upstream events leading to increased IFNγ secretion. The first job was to identify the source and then the type of activation that leads to immune responses. For this purpose, a series of expression analysis were performed to identify molecular pathways leading to IFNγ secretion. In epithelial cells IFNγ downstream was active and there was an increased IFNγ secretion in whole mucosa samples (figure 4.24). Furthermore, these results showed that hematopoietic compartment contributes more to the survival of *β-cat*^{CA}*Ikkα*$^{AA/AA}$ mice. Primary source of IFNγ production is known to be activated Th1 cells and NK cells. For this purpose in the following parts this possibility of adaptive immune cell involvement in upregulated IFNγ levels in *β-cat*^{CA}*Ikkα*$^{AA/AA}$ mice will be investigated.

4.3.3.3.1. Lack of Th1 Activation Regardless of Increase in IL-12

Activation of T-cells by tumor specific antigens and induction of Th1 phenotype in CD4^{+} T-cells can induce maturation of APCs and better IL-12 production which leads to increased IFNγ production by CD8^{+} T-cells and NK-cells. Further, these activations may initiate adaptive cytotoxic immunity towards tumor cells. Therefore, T-cells and Th1 activation is the principal source of IFNγ production in pro-inflammatory environment. For this purpose, activation of T-cells was the first mechanism to be checked to understand upregulated IFNγ signaling. T-cell specific marker expression is checked by RT-PCR or FACS (figure 4.30.A and B). A sharp increase in CD4^{+} cells were observed in RT-PCR but only a slight increase was evident in FACS results in *β-cat*^{CA}*Ikkα*$^{AA/AA}$ mice MLN. On the other hand, CD8^{+} T-cells were not higher in the

whole mucosa but slightly lower in MLNs of *β-cat*^{CA}*Ikkα*$^{AA/AA}$ mice. These initial observations suggested no CD8^{+} T-cell amplification. Still a better way to understand their activation was looking activation markers rather than absolute numbers. For this purpose, CD4^{+} or CD8^{+} T-cells were sorted for different activation markers which have shown that there were increase in CD69^{+} and FoxP3^{+} in CD4^{+} T cells (figure 4.30.C) in *β-cat*^{CA}*Ikkα*$^{AA/AA}$ mice at day 15. These FACS data coupled to increase in CD4 cells in RT-PCR and in MLN suggested that there can be an increase in CD4^{+} activities which should be investigated with further analysis. However, increase in FoxP3 regulatory cells do not help explaining tumor specific cytotoxicity in*β-cat*^{CA}*Ikkα*$^{AA/AA}$ mice yet RT-PCR data did not support its increase in whole mucosa samples (figure 4.30.E). On the other hand no significant activation was observed for CD8+ cells except from a prominent increase in activation signal Ly6c in mucosa isolated cells. However, this upregulation was absent in MLN samples to support any activation in their status. Still further data is required to conclude about their tumor specific activities.

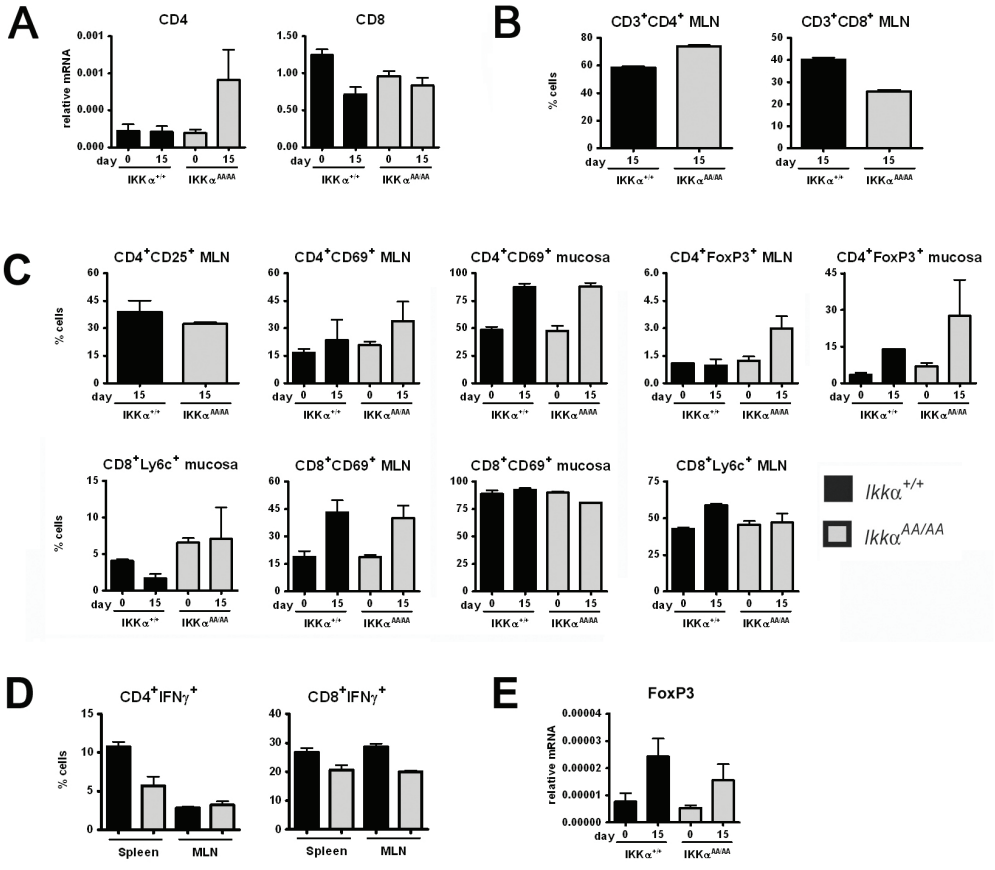

Figure 4.30: Investigation of T-cell Activation in *β-cat^{CA}Ikkα$^{AA/AA}$* Mice. Similar to innate immune cells, we sorted CD4$^+$ and CD8$^+$ isolated from MLN or intestinal mucosa with different markers for activating or suppressing phenotypes via using FACS. Interestingly we observed an increase in suppressive T-cells in *β-cat^{CA}Ikkα$^{AA/AA}$* mice while there was no evidence of CD8$^+$ activation. (D) Neither CD4$^+$ nor CD8$^+$ cells were producing higher amounts of IFNγ. Coupled to their slight or no increase in numbers, T-cells cannot explain the increase in IFNγ production in *β-cat^{CA}Ikkα$^{AA/AA}$* mice. (E) Foxp3 expression in whole mucosa samples as measured by RT-PCR.

After observing some signals with T-cell activation, it was further checked if they were really shifting to Th1 phenotype to mount tumor specific immunity. To verify this, cytokines profiles related to Th1/Th2 were obtained. Cytokines responsible for Th1 and Th2 were checked by RT-PCR and no preference into any of the phenotypes was observed (figure 4.31) in *β-cat^{CA}Ikkα$^{AA/AA}$* mice whole mucosa samples at day 15. Even increase in IL-4 and IL-10 in *β-cat^{CA}Ikkα$^{AA/AA}$* was contradictory to expected Th1 phenotype. Therefore, tumor specific adaptive immunity was seemed not be to be induced in *β-cat^{CA}Ikkα$^{AA/AA}$* mice since there was no expected cytokine signature to identify Th1 shift.

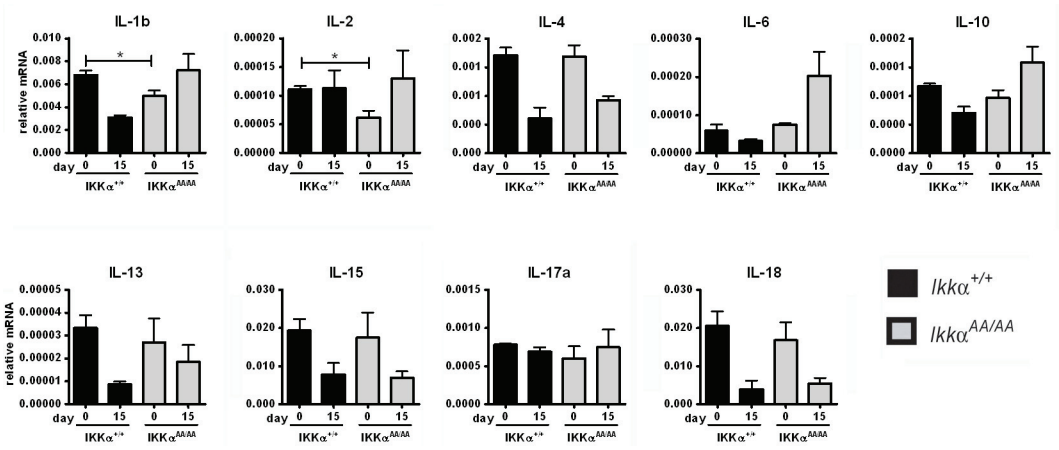

Figure 4.31: Interleukin Expressions in *β-cat^{CA}Ikkα$^{AA/AA}$* Mice at day 15. Interleukin expression profiles were obtained from whole mucosa samples. There was no clear shift towards Th1 or Th2 phenotypes evident.

Still, there was an increase in IL-12 levels as measured by RT-PCR and ELISA (figure 4.32). Since no activation in T-cells to shift into Th1 phenotype was observed by the above cytokine profiles, it was unlikely to observe any effect as a result of elevated IL-12. Lacking T-cell deficient mutant data (*Rag1*$^{-/-}$ mice) to rule out their involvement, it was addressed whether increase in IL-12 was inducing T-cell activation in *β-cat*^{CA}*Ikkα*$^{AA/AA}$ mice leading to increased IFNγ production. Upon activation, *β-cat*^{CA}*Ikkα*$^{AA/AA}$ mice were injected with anti-IL-12p40 neutralizing antibody (every 5th day 250μg Ab) to deplete IL-12 in their body. Nevertheless, IL-12p40 neutralization did not affect *β-cat*^{CA}*Ikkα*$^{AA/AA}$ mice survival (survival of 37 days vs. 34.5 in *β-cat*^{CA}*Ikkα*$^{AA/AA}$ mice, p=0.5118) (figure 4.33). Therefore, increase in IL-12 in *β-cat*^{CA}*Ikkα*$^{AA/AA}$ mice does not account for the decreased proliferation in *β-cat*^{CA}*Ikkα*$^{AA/AA}$ mice and most probably there is no tumor specific adaptive immune activation by T-cells. Finally, FACS analysis of CD4+ and CD8+ cells for IFNγ production made it clear that they are not involved in IFNγ production in *β-cat*^{CA}*Ikkα*$^{AA/AA}$ mice at day 15 (figure 4.30.D).

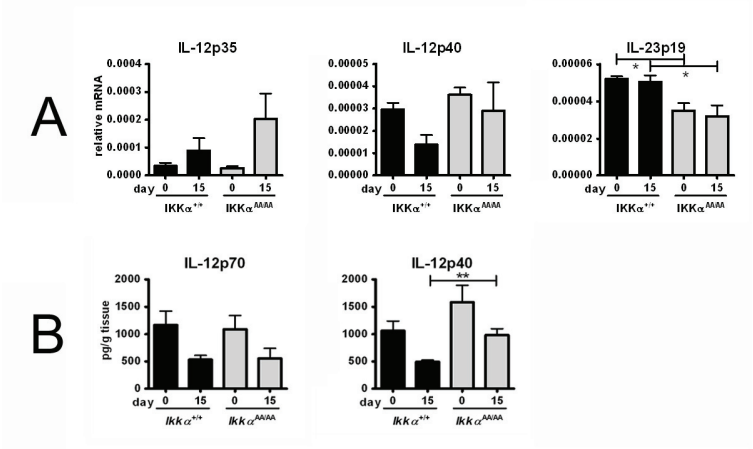

Figure 4.32: IL-12 Expression in Whole Mucosa of *β-cat*^{CA}*Ikkα*$^{AA/AA}$ Mice. RT-PCR (A) and ELISA in *β-cat*^{CA} mice whole mucosa samples (B) shows slight increase in IL-12p40 in *Ikkα*$^{AA/AA}$ mice while IL-12p70 ELISA does not confirm increase we observed in IL-12p35 in mRNA analysis. On the other hand, IL-23p19, specific IL-23 subunit, is slightly decreased in *Ikkα*$^{AA/AA}$ samples. All results are representative of 3 independent experiments.

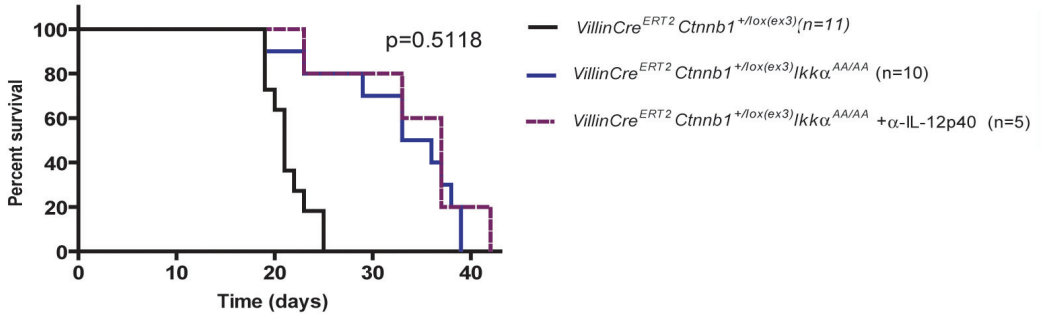

Figure 4.33: Survival of *β-cat*^{CA}*Ikkα*$^{AA/AA}$ Mice is not affected from IL-12 neutralization. Ultimately we neutralized IL-12p40 in *β-cat*^{CA}*Ikkα*$^{AA/AA}$ mice via injection of anti-IL-12p40 Ab (250μg/mouse) every 5th day until the end of their survival. Neutralization did not affect the survival. Therefore, IL-12 activation does not play any role in canonical T-cell activation and probably in upregulation of IFNγ production.

4.3.3.3.2. NK Cell Involvement and Lack of Tumor Specific Cytotoxicity

NK cells are know with their high capacity to recognize tumor cells and secrete IFNγ and can be an important source of it in *β-cat*^{CA}*Ikkα*$^{AA/AA}$ mice in the absence of T-cell responses. Although NK cells did not show any upregulation of activation like other cells of innate immunity, they are still important to cause strong cytotoxic response due to their activity via different cytotoxic agents. Therefore, they were checked for IFNγ production and shown that they were not increased their IFNγ production in *β-cat*^{CA}*Ikkα*$^{AA/AA}$ mice (figure 4.34.E) suggesting that NK cells do not further activate T-cell responses by IFNγ. Still they could be a strong source of anti-tumor cytotoxicity by different agents. Different cytotoxicity markers like perforin, granzyme, FasL and killer did not show any increase in whole mucosa samples from *β-cat*^{CA}*Ikkα*$^{AA/AA}$ mice (figure 4.34.A). Only TRAIL and *Klrk1b* (NKG2D) exhibited increase in their expression in *β-cat*^{CA}*Ikkα*$^{AA/AA}$ mice. More interestingly there was no increase in apoptotic rates in*β-c at*^{CA}*Ikkα*$^{AA/AA}$

mice as shown by TUNEL or Casp3 IHC stainings (4.34.B) (confirming the previous observations with AOM and *Apc*$^{min/+}$ mice) Finally, NK involvement is in *β-cat*^{CA}*Ikkα*$^{AA/AA}$ mice phenotype is ruled out by NK depletion. NK cells are depleted in *β-cat*^{CA}*Ikkα*$^{AA/AA}$ mice via using injection of anti-asialo GM1 (Habu et al., 1981) Ab (α-ASGM1) every 4th day as 200μg per mice. Although a rapid loss of NK cells from *β-cat*^{CA}*Ikkα*$^{AA/AA}$ mice spleen samples were achieved (figure 4.34.D), no difference in the survival of *β-cat*^{CA}*Ikkα*$^{AA/AA}$ mice (35.5 vs. 34.5 in *β-cat*^{CA}*Ikkα*$^{AA/AA}$ mice, p=0.4039) (figure 4.34.C) were observed. This reflected that NK cell also do not play a role in *Ikkα*$^{AA/AA}$ phenotype. In conclusion, the data strongly suggested that tumor specific adaptive immune responses and cytotoxicity are absent in *β-cat*^{CA}*Ikkα*$^{AA/AA}$ mice.

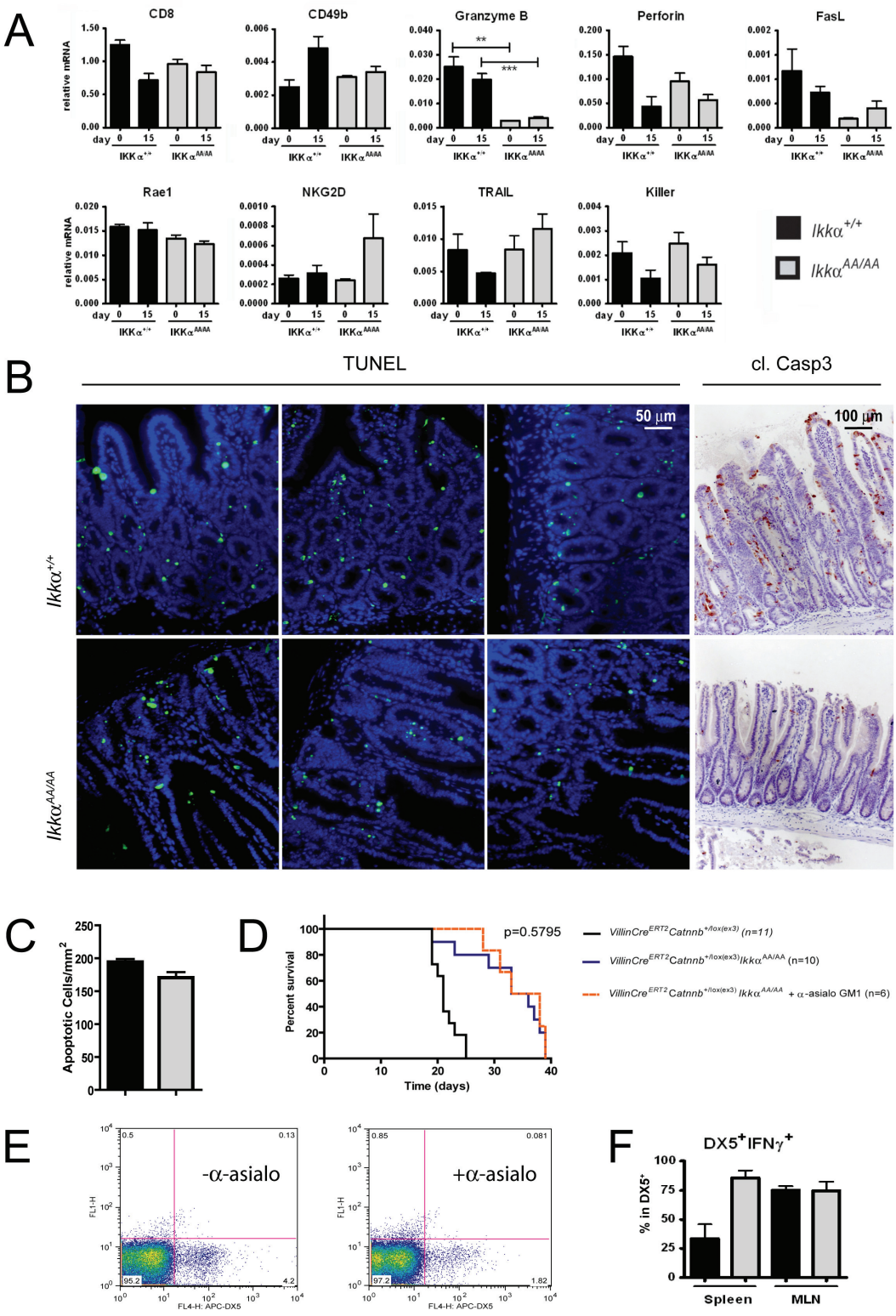
A
CD8
CD49b
Granzyme B
Perforin
FasL
Rae1
NKG2D
TRAIL
Killer
relative mRNA
day 0 15 0 15
IKKα+/+ IKKαAA/AA
Ikkα+/+
IkkαAA/AA
B
TUNEL
cl. Casp3
50 μm
100 μm
Ikkα+/+
IkkαAA/AA
C
Apoptotic Cells/mm2
D
p=0.5795
Percent survival
Time (days)
VillinCreERT2Catnnb+/lox(ex3) (n=11)
VillinCreERT2Catnnb+/lox(ex3)IkkαAA/AA (n=10)
VillinCreERT2Catnnb+/lox(ex3) IkkαAA/AA + α-asialo GM1 (n=6)
E
-α-asialo
+α-asialo
FL1-H
FL4-H: APC-DX5
F
DX5+IFNγ+
% in DX5+
Spleen
MLN

Figure 4.34: Tumor Cytotoxicity and Apoptosis in *β-cat^{CA}Ikkα$^{AA/AA}$* mice at day15. (A) Cytotoxic gene expression profiles has shown an increase for TRAIL and Klrk1b but more important cytotoxicity factors like perforin and FasL were absent (B) there was no increase in apoptosis in *β-cat^{CA}Ikkα$^{AA/AA}$* mice as shown by TUNEL and Casp3 stainings (C) Quantification of apoptotic cells per unit area showing slightly more apoptosis in *β-cat^{CA}* samples at day 15 (D) NK Cells Are Not Responsible from IFNγ Related Phenotype in *Vil-Cre-ER^{T2}Ctnnb1$^{+/lox(ex3)}$Ikkα$^{AA/AA}$* Mice. Depletion of NK cells via anti-asialo GM1 antibody did not revert survival in *β-cat^{CA}Ikkα$^{AA/AA}$* mice (35.5 vs. 34.5 p=0.5795) unlike in the case of *Ifnγ* KO. (E) NK depletion after anti-asialo Ab as measured by FACS. (F) NK cells from spleen had more IFNγ secreting cells in *β-cat^{CA}Ikkα$^{AA/AA}$* mice at day15 yet no such relation was observed in NKs isolated from MLN samples.

4.3.3.3.3. Myeloid Cell Activation and Expansion in *β-cat^{CA}Ikkα$^{AA/AA}$* Mice

Having ruled out adaptive immune cell or tumor specific cytotoxicity in *β-cat^{CA}Ikkα$^{AA/AA}$* mice, there was only one more potential source for IFNγ secretion to be investigated. Activation of myeloid cells could be the source of IFNγ production in *β-cat^{CA}Ikkα$^{AA/AA}$* mice at day 15. For this purpose, the next step was to identify whether myeloid cells were activated and amplified to produce higher levels of IFNγ. Relative numbers of all myeloid cells were observed to be increased in *β-cat^{CA}Ikkα$^{AA/AA}$* mice as measured by cell specific cell surface marker expressions (figure 4.35.A). Increases in macrophages and DCs were further confirmed by FACS where macrophages were showing a dramatic increase in *β-cat^{CA}Ikkα$^{AA/AA}$* mice MLNs (figure 4.35.B) at day 15.

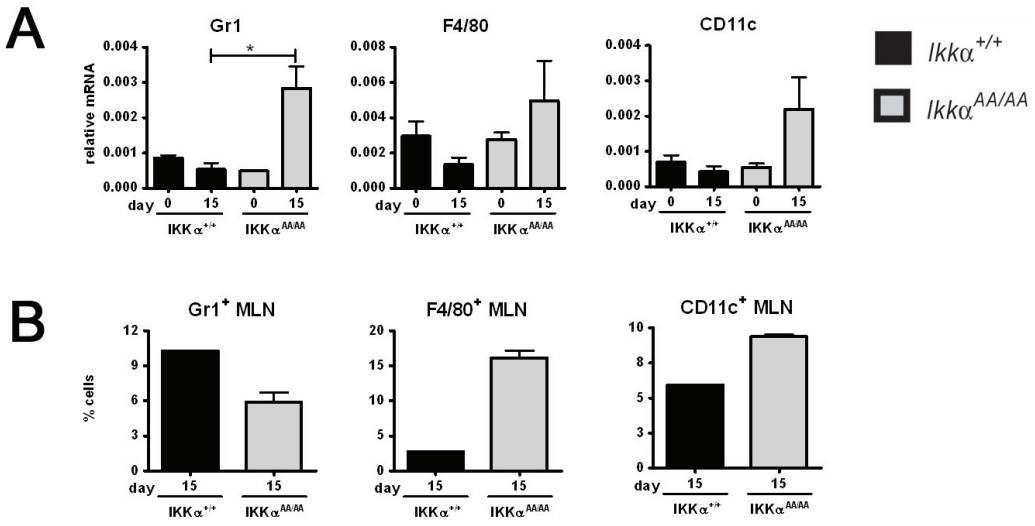

Figure 4.35: Increase in Myeloid Cells in *β-cat^{CA}Ikkα$^{AA/AA}$* Mice at day 15. (A) RT-PCR or (B) FACS analysis for APC specific markers has shown overall increase in numbers in *β-cat^{CA}Ikkα$^{AA/AA}$* mice.

Since we observed an overall increase in macrophage and dendritic cell numbers, we wanted to clarify if their numbers are increased due to better recruitment by the cytokines secreted from hyperproliferating IECs. Histological examination of DCs did not give a specific pattern for any of the groups and DCs did not show increased numbers in hyperproliferating areas of *β-cat^{CA}Ikkα$^{AA/AA}$* mice (not shown). However, macrophages and neutrophils showed distinct intraepitlelial localization in *β-cat^{CA}Ikkα$^{AA/AA}$* mice samples (figure 4.36). This observation was strongly suggesting the preferred recruitment of macrophages to the target tissue.

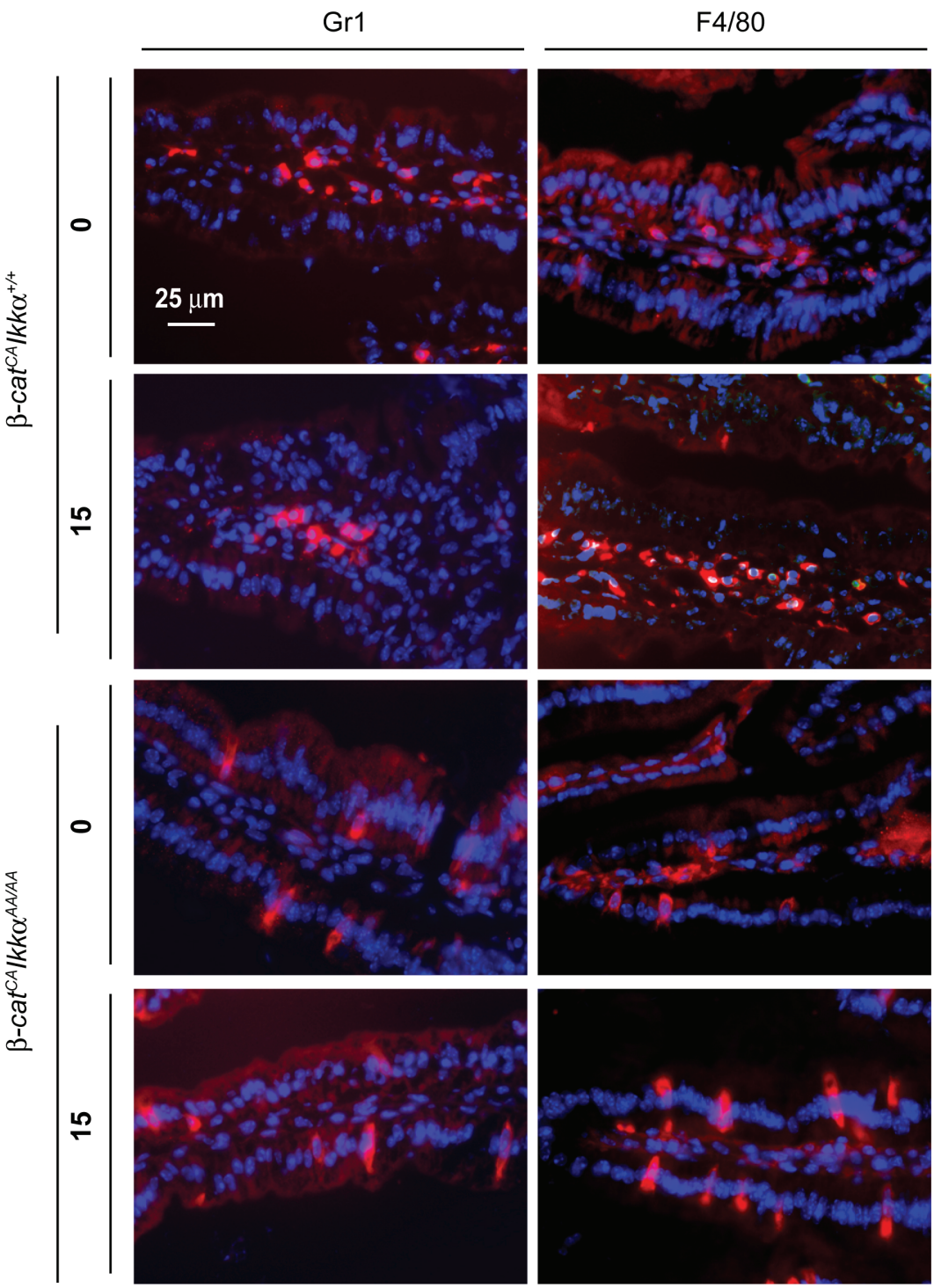

Figure 4.36: Intraepithelial Localization of Macrophages and Neutrophils in *β-cat*^{CA}*Ikkα*$^{AA/AA}$ Intestines at day 15. Immunofluorescent stainings of duodenal sections show that in *β-cat*^{CA}*Ikkα*$^{AA/AA}$ mice samples macrophages and neutrophils had distinct localization to within enterocytes (at 400x magnification).

Furthermore, macrophages and neutrophils were checked for activation specific marker. For this purpose, macrophages and neutrophils were isolated from spleen (only MΦ) and MLNs and were sorted for activation specific markers like TNF-α, IL-10 and IL-12. (figure 4.37). From this analysis macrophages did not exhibit any difference in activation (slight decrease in IL-10 was not supported by further regulation of TNF-α and IL-12) whereas neutrophils were actively secreting TNF-α, IL-10 and IL-12 in increased amount in $\beta\text{-}cat^{CA}Ikk\alpha^{AA/AA}$ mice. Moreover, activation of M1/M2 phenotypes were further examined in $Ikk\alpha^{AA/AA}$ or WT BMD (G-CSF induced) macrophages by arginase and citrulline assays and we could not observe any kind of shift towards expected M1 phenotype for the adaptive immune activation (data not shown).

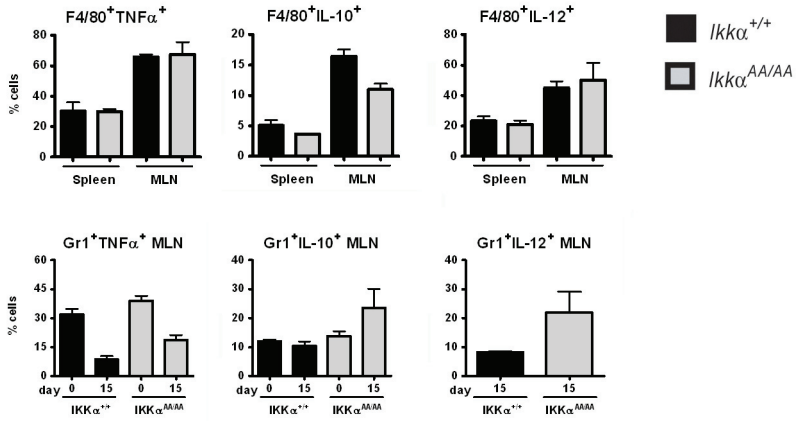

Figure 4.37: Macrophage and Neutrophil Activation in $\beta\text{-}cat^{CA}Ikk\alpha^{AA/AA}$ mice at day 15. (A) Hematopoietic cells isolated from spleen or MLNs are sorted for macrophage or neutrophil markers coupled to different activation signals in FACS. Macrophages has shown a decrease in IL-10 for $\beta\text{-}cat^{CA}Ikk\alpha^{AA/AA}$ mice while neutrophils were looking active with increased IL-10, Il-12 and TNF-α levels for the same group (all percentages are given as the fraction of the whole $F4/80^+$ or $Gr1^+$ cell populations).

Similarly, DCs were checked for their activation status from 15 day $\beta\text{-}cat^{CA}Ikk\alpha^{AA/AA}$ mice samples (figure 4.38). This time DCs isolated from MLN or whole mucosa were sorted for DC activation markers. $CD11c^+B220^+$ cells are pDC population and $CD11c^+CD86^+$ matured DCs. These markers has shown that there is similar levels of maturation and activation in both groups

On the other hand, IL-10 and TNF-α was higher for MLN but lower for mucosal DCs (figure 4.38).

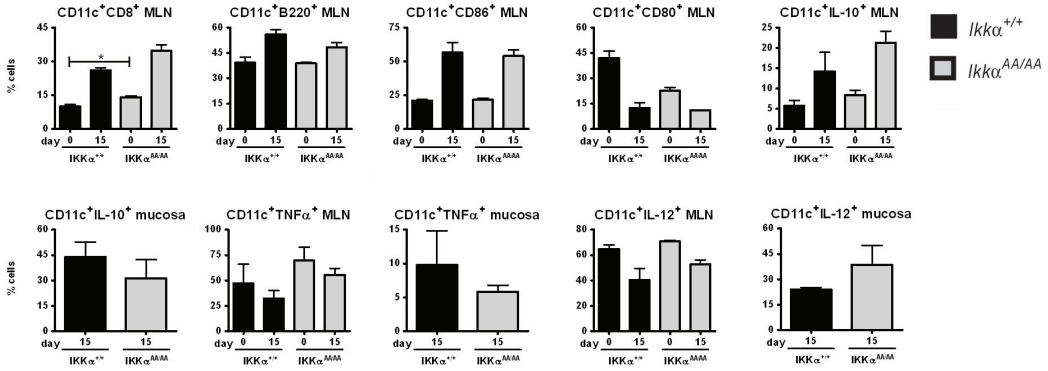

Figure 4.38: Dendritic Cell Activation in *β-cat^{CA}Ikkα$^{AA/AA}$* Mice at day 15. After looking expression of stimulated DCs, we also isolated hematopoietic cells from spleen, MLN or intestinal mucosa and sorted them for different DC activation markers in FACS. For Dc classes only CD8+ DCs were elevated yet expression of TNF-α (in whole mucosa) and IL-12 was higher in *β-cat^{CA}Ikkα$^{AA/AA}$* mice.

Altogether, above data suggested that amplification and intraepithelial localization of myeloid cells is a good indicator of their activation upon hyperproliferative stress in *β-cat^{CA}Ikkα$^{AA/AA}$* mice. They were also shown to be the source of IL-12 production which does not translate into adaptive immune activation. If adaptive immunity is not responsible from IFNγ production, dramatic amplification of APCs should account for the increase in IFNγ levels. Although they are lesser sources of IFNγ in proinflammatory environment, still dramatic increases in macrophages secreting IFNγ can explain increased IFNγ levels in *β-cat^{CA}Ikkα$^{AA/AA}$* mice. To examine if APCs are the source of IFNγ, hematopoietic cells isolated from spleen or MLN and they were sorted for cell APC specific markers and IFNγ expression at the same time (figure 4.39). According to this analysis only CD11c^{+}B220^{+}Dx5^{+} cell population, called as IKDCs, were highly increased in their IFNγ production in *β-cat^{CA}Ikkα$^{AA/AA}$* mice. These cells are specified with their IFNγ production and NK cell like properties within pDC population. However, they only constitute 5% of all DCs even in 10 times increased amounts in *β-cat^{CA}Ikkα$^{AA/AA}$* mice. Therefore, they alone may not be

enough to explain increased IFNγ production. However, this increase in IFNγ can trigger already amplified macrophages to express IFNγ. Already macrophages were shown to be massively increased in number (about 8 times in *β-cat*^{CA}*Ikkα*$^{AA/AA}$ mice (figure 4.35.B)). Although IFNγ production per cell may not be increased, still such an increase in macrophage numbers can contribute increased IFNγ levels. Consequently, activated IKDCs and amplified macrophages are the only source of IFNγ in *β-cat*^{CA}*Ikkα*$^{AA/AA}$ mice.

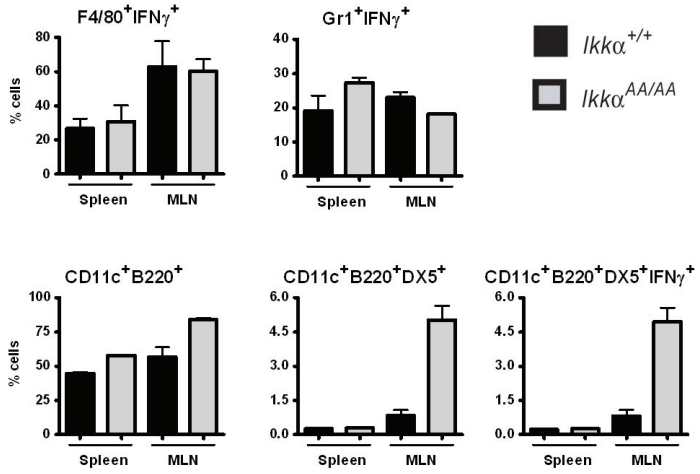

Figure 4.39: Activated Myeloid Cells are the Source of IFNγ. After showing that activated adaptive cells are not the main source of IFNγ we have sorted all immune cell types responsible from IFNγ production and identified CD11c$^+$B220$^+$NK1.1$^+$ (DX5) IKDCs as a major source of IFNγ production (almost all IKDCs are positive for IFNγ as well). The other and more prominent source should be macrophages, their massive amplification should account for increase in IFNγ levels in whole mucosa.

4.3.3.3.3.1. Recruitment of Myeloid Cells to the Site of Hyperproliferation

So far the results has shown that myeloid cells are activated and amplified in *β-cat*^{CA}*Ikkα*$^{AA/AA}$ mice and this relative increase in their numbers account for IFNγ upregulation. However, still it was not answered how myeloid cells are activated upon hyperproliferation. As mentioned before, increased sensitivity towards epithelial secreted cytokines may be the other pathway leading to myeloid cell activation and amplification in tumor specific responses. For this purpose, epithelial secreted monocyte chemoattractant expressions were examined in epithelial and whole mucosa

samples. Chemoattractants like *Ccl20, Ccl28, Cxcl1, Cxcl2, Cxcl5* and *Tslp* were highly elevated in *β-cat*^{CA}*Ikkα*$^{AA/AA}$ mice both in epithelial and whole mucosa samples (figure 4.40.B and A respectively). These observations were suggesting that all these chemokines are secreted by the hyperproliferating epithelia in *β-cat*^{CA}*Ikkα*$^{AA/AA}$ mice. Finally, *Mcp-1* is only upregulated in whole mucosa samples and its upregulation was absent in epithelial total RNA samples from *β-cat*^{CA}*Ikkα*$^{AA/AA}$ mice. Especially, Mcp-1 activation is important for the activation and amplification of macrophages and account for increased macrophage numbers in *β-cat*^{CA}*Ikkα*$^{AA/AA}$ mice. Similarly, all other chemokines secreted by the epithelia should account for specific recruitment of the myeloid cells to the hyperproliferating area leading to increased numbers and specific localization observed with macrophages and neutrophils.

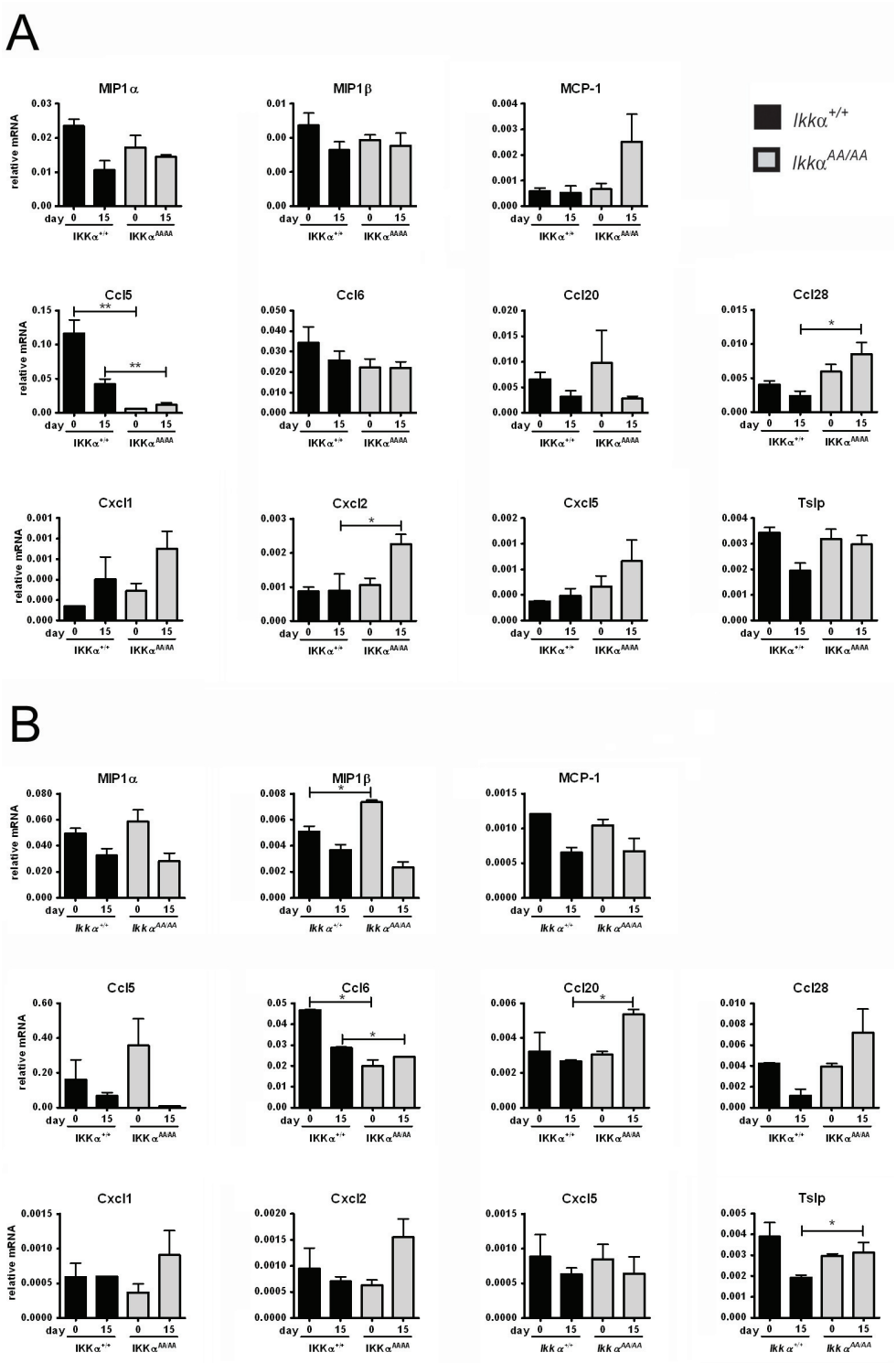

Figure 4.40: RNA Expression profiles for NF-κB Target Cytokines. Whole mucosa (A) and IEC (B) expression profiles immune cell attracting chemokines show increased expression levels for most of the factors leading to better recruitment of myeloid cells and their amplification in *β-cat^{CA}Ikkα$^{AA/AA}$* mice.

4.3.3.4. Requirement of Active NF-κB Signaling in IKKα Inactivation

So far activation of myeloid cells by epithelia secreted chemokines is shown to be followed by monocyte induction and amplification by Mcp-1 caused increase in the production of IFNγ that result in cell cycle arrest on hyperproliferating cells in *β-cat*^{CA}*Ikkα*$^{AA/AA}$ mice. Although all the downstream machinery regarding IFNγ production and cell cycle arrest was identified, still no evidence for the exact machinery concerning chemokine productions and the exact role of IKKα in this machinery were presented. Close examination of these chemoattractants secreted by IEC reveals that most of them are regulated by pro-inflammatory NF-κB signaling. Since it was previously shown in bacteria challenged mice that IKKβ compensates IKKα loss to prime immune activation via extended promoter binding of NF-κB subunits (but not increased binding activity) (Lawrence et al., 2005) it was investigated whether the same mechanism is responsible from increased NF-κB target production to mount immune cell recruitment and activation. For this purpose, *β-cat*^{CA}*Ikkα*$^{AA/AA}$ mice were crossed with *Ikkβ*$^{-/-}$ conditional knock-outs to introduce epithelial specific deletion of IKKβ in our model (*Ikkβ*$^{\Delta IEC}$) to verify if these effects are the result of NF-κB activation. As a result of this extra knock-out, *β-cat*^{CA}*Ikkα*$^{AA/AA}$*Ikkβ*$^{\Delta IEC}$ mice did not survive as long as *β-cat*^{CA}*Ikkα*$^{AA/AA}$ mice (28 vs. 34.5, p=0.0015) (figure 4.41.A). Nevertheless, this observation only made sense when we compared it to the results of *β-cat*^{CA}*Ikkβ*$^{\Delta IEC}$ mice (figure 4.41.B) (Fingerle et al., 2009) which had similar survival (27 vs. 28 p=0.6141, figure 4.41.C) to our triple mutants. Consequently, extended survival of *β-cat*^{CA}*Ikkα*$^{AA/AA}$ mice was dependent on IKKβ and in the absence of active NF-κB signaling the mice were behaving as if they are only *Ikkβ*$^{\Delta IEC}$ knock-outs. So these observations made it clear that IKKβ is required and compensates the loss of IKKα to generate starting signals for extended survival and its role should be crucial for immune activation.

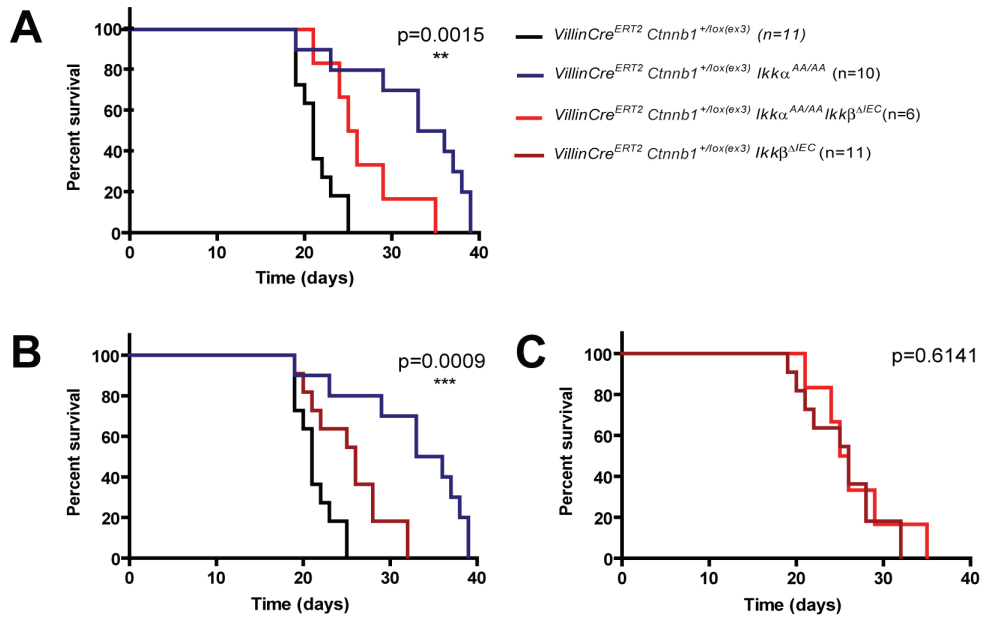

Figure 4.41: Survival Graphs for *Ikkβ*$^{\Delta IEC}$ Knock-out with or without *Ikkα*$^{AA/AA}$ in *Vil-Cre-ER*^{T2}*Ctnnb1*$^{+/lox(ex3)}$ Model. *β-cat*^{CA}*Ikkα*$^{AA/AA}$ mice were crossed with *Ikkβ*$^{\Delta IEC}$ to generate doubly mutant mice for *Ikkα* and *Ikkβ*. We observed that they were not surviving as long as *Ikkα* single mutants (median survival of 25.5 vs. 34.5) (A) yet more than control grup (25.5 vs. 21 p=0.0097). When we compared their survival to that of *Ikkβ*$^{\Delta IEC}$ alone (B) we observed that they were almost the same (C) (median survival of 25.5 vs. 26 p=0.6141).

If the hypothesis with NF-κB activation and the involvement of IKKα in this activation is correct then it should be observed that all upregulations in these genes should be absent in *β-cat*^{CA}*Ikkα*$^{AA/AA}$ *Ikkβ*$^{\Delta IEC}$ mice. To investigate this, whole mucosa samples from 15-day *β-cat*^{CA}*Ikkα*$^{AA/AA}$*Ikkβ*$^{\Delta IEC}$ mice were isolated, and were compared for gene expression to that of *β-cat*^{CA}*Ikkα*$^{AA/AA}$ mice (figure 4.42). As expected, all the immune activations from myeloid chemoattraction to IFNγ production were lost in *β-cat*^{CA}*Ikkα*$^{AA/AA}$ *Ikkβ*$^{\Delta IEC}$ mice. Therefore, intact NF-κB activation is required for the production of these monocyte chemoattractants secreted by IEC and myelod cells (like Mcp-1). In turn, these chemoattractants activate myeloid cells and they secrete either higher amounts of IFNγ (IKDCs) or increase in numbers (MΦs) which suppress tumor growth in *Ikkα*$^{AA/AA}$ mice.

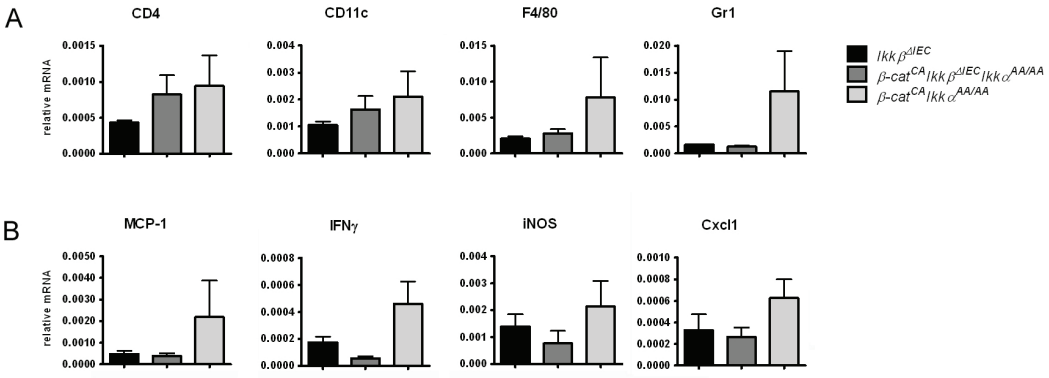

Figure 4.42: Active NF-κB Signaling is Required for Myeloid Cell Recruitment. Additional *Ikkβ*$^{\Delta IEC}$ has cancelled upregulation of almost all chemoattractants in *β-cat*^{CA}*Ikkα*$^{AA/AA}$ mice as shown by RT-PCR (B). As a result of chemoattractant decline all amplified hematopoietic cell lines were diminished in *β-cat*^{CA}*Ikkα*$^{AA/AA}$*Ikkβ*$^{\Delta IEC}$ mice (A).

5. DISCUSSION

5.1. CHARACTERIZATION OF PHENOTYPE ASSOCIATED WITH IKKα INACTIVATION IN CRC

Given the potential role of IKKα in colorectal tumorigenesis, we started our experimentation with examining IKKα activation deficient mice (Cao et al., 2001) in three different cancer models. The first model was featuring a sporadic distal tumor formation via a chemical carcinogen AOM (Druckrey and Lange, 1972). The latter two models were relying on conventional genetic model of CRC development. Both models were initiating tumorigenesis via elimination of control over Wnt signaling either via *Apc* loss (Moser et al., 1990) or via β-catenin stabilization (Harada et al., 1999). Regardless of the model used a reduction in tumor sizes, numbers and proliferation rate were observed in $Ikk\alpha^{AA/AA}$ mice models of colorectal carcinogenesis. As a result of elimination of IKKα activation, longer survival and better health in $Ikk\alpha^{AA/AA}$ mice were among the other observations. Following all these observations, a series of analysis were performed to understand molecular mechanism behind retarded tumor growth. Extension of analysis to further gene knockout models was utilized to obtain genetic evidences to molecular hypotheses derived from these observations. As a result of these experiments, the major molecular pathways and vast amount of details regarding the role of IKKα in colorectal tumorigenesis were identified and mostly clarified. In the following sections results obtained during this project will be presented in a sequential manner.

5.1.1. AOM Induced *Ikkα*$^{AA/AA}$ Mice Have Tumors with Reduced Size and Number

AOM is a well established chemical carcinogen for rodent colorectal carcinogenesis. This model is a very good approximation for sporadic nature of human colorectal tumorigenesis which occurs in later ages due to requirement of different mutations (Druckrey and Lange, 1972). Further studies have shown that AOM causes DNA mutations by causing double strand breaks and by interfering in DNA repair machinery (Caderni et al., 1997). Increased mutation rates lead to quicker accumulation of mutations (Fearon and Vogelstein, 1990) which in turn disturb the control over cell cycle and apoptosis in a similar way as sporadic carcinogenesis develops (Taketo, 2006). This model has been used in many different studies to develop sporadic cancers. When combined with DSS it can be a useful model to mimic colitis associated carcinogenesis (Tanaka et al., 2003).

By applying AOM induced colorectal carcinogenesis to genetic model of activation deficient IKKα mutants, a great deal of reduction in colorectal tumor numbers and slow down in tumor growth were observed. Although weight curves for WT and *Ikkα*$^{AA/AA}$ animals did not differ significantly, a considerable decrease in tumor sizes and numbers in *Ikkα*$^{AA/AA}$ mice at the end of 24 weeks of induction was evident. 24 weeks was chosen effective for tumor development while the animals were still alive. Tumor sizes were reduced in *Ikkα*$^{AA/AA}$ mice considerably and no large tumors were observed. Since both groups of animals had the same time to develop tumors, a decrease in proliferation index in *Ikkα*$^{AA/AA}$ mice was expected. Decreased proliferation in *Ikkα*$^{AA/AA}$ mice indicates that tumor promotion is delayed in these mice so that fewer and smaller tumors were observed. Another important factor that may contribute to tumor suppression is apoptosis which can be important (Townson et al., 2003) if there is any activation in apoptotic machinery by upregulation of cell death machinery by intrinsic factors (Chu et al., 1997) or hematopoietic cytotoxic effect (Hung et al., 1998). For this purpose, apoptotic rates were also checked and found not to be increased in *Ikkα*$^{AA/AA}$ mice. This phenomenon suggested that cell death cannot account for the regressed tumor sizes while proliferation rate was marginally decreased both in

tumor and non-tumor epithelia. Consequently, smaller and fewer tumors in *Ikkα*$^{AA/AA}$ mice were observed due to suppression of proliferation rather than induction of apoptosis.

5.1.2. *Apc*$^{min/+}$*Ikkα*$^{AA/AA}$ Mice Have Retarded Tumor Initiation and Development

Applications of other genetic models were required at this point to understand the mechanism behind this phenomenon and possible life extending potential of elimination of IKKα phospho-activation. The most important target of sporadic colorectal tumorigenesis is the loss of control over Wnt signaling which provides homeostasis and differentiation in intestinal epithelia (Gregorieff and Clevers, 2005; Pinto et al., 2003). APC and β-catenin are the most prominent molecules in this regulation (Liu et al., 2002; Morin et al., 1997). It is known that β-catenin is an important transcription factor that controls proliferation and differentiation of intestinal epithelial cells (Van de Wetering et al., 2002). Since our initial observation with AOM mice was the reduction in proliferation rather than increased apoptotic rate, any control over β-catenin activation would be invaluable to investigate.

The next model used for understanding the role of IKKα in colorectal tumorigenesis was widely used genetic model of Apc loss. *Apc*$^{min/+}$ mice were previously reported to develop multiple intestinal neoplasia which result in early loss of the mice at around month 6 (Moser et al., 1990). This phenotype is morphologically and pathologically very similar to heritable FAP disease seen in human juveniles (Su et al., 1992). Indeed, both are caused by the orthologous *Apc* gene mice and human. For this purpose use of *Apc*$^{min/+}$ mice is a very good model for understanding genetic basis of colorectal carcinogenesis (Taketo, 2006) and the results will most probably applicable to human disease as well. Most sporadic colorectal cancers has APC loss as a distinctive background (Fodde et al., 2001). Still they require further mutations to make tumors cross adenoma to carcinoma barrier (Fearon and Vogelstein, 1990). It was also shown that loss of APC is a priming event for CI (Powell et al., 1992). Moreover, CI is an important propelling force behind increased mutational rate (Fodde et al., 2001; Munemitsu et al., 1994). Therefore, *Apc*$^{min/+}$ mice can be regarded as a good model for both genetic and sporadic colorectal tumorigenesis.

Apc$^{min/+}$ mice were crossed to *Ikkα*$^{AA/AA}$ background and monitored until the first signs of sickness. Once the survival curves for these animals were derived, a 42.5% increase in the survival of these animals than that of control group (236.5 vs. 166) was observed. Even heterozygous *Apc*$^{min/+}$*Ikkα*$^{AA/+}$ mice have proved a marginal increase in survival (184.5 vs. 166: 11.1%) suggesting that the effect of *Ikkα*$^{AA/AA}$ is dose dependent yet not proportional and requires the loss of both activation alleles to fully pronounce the effects on survival. These results strongly suggested that the extended survival observed in *Apc*$^{min/+}$*Ikkα*$^{AA/AA}$ mice was independent of the model used but influenced by the loss of IKKα activation. Although one can argue that the time required to attain similar sized tumors are much longer in *Apc*$^{min/+}$*Ikkα*$^{AA/AA}$ mice, it was still required to show that the proliferation of tumors were less in *Apc*$^{min/+}$*Ikkα*$^{AA/AA}$ mice and this was the reason for fewer tumor in these mice. For this purpose, an earlier time point where differences in proliferation and tumor sizes can be readily seen was to be found.

Indeed, it was month 4 where the differences in proliferation which resulted in smaller tumor sizes and fewer tumor numbers were readily observed. Investigation of proliferative rates yielded that *Apc*$^{min/+}$*Ikkα*$^{AA/AA}$ mice had reduced proliferation but not increased apoptosis. This reduction in proliferation was explaining the differences in tumor numbers leading to better survival of the animals. Due to this retardation in proliferation not only tumor numbers were fewer but and their sizes were smaller at month 4. Another support for the reduction in tumor sizes at month for was the almost reversed anemic status of the animals. Since *Apc*$^{min/+}$ animals suffer from chronic anemia caused by intestinal hemorrhages (Hinoi et al., 2007; Taketo, 2006), anemia is a good indication of tumor development and general health. Measurement of different blood values yielded that *Apc*$^{min/+}$*Ikkα*$^{AA/AA}$ mice had better overall HGB and HCT levels than that of *Apc*$^{min/+}$ mice at month 4. Given the fact that chronic anemia is an intrinsic property of *Apc*$^{min/+}$ mice, increased anemia can be only explained by bleeding into intestinal lumen in WT mice due to larger tumors while *Apc*$^{min/+}$*Ikkα*$^{AA/AA}$ mice were still non-anemic due to diminished tumor size and reduced tumor numbers. Moreover, *Apc*$^{min/+}$*Ikkα*$^{AA/AA}$ mice attained similar anemic level 2-3 months later than wt mice just before their death. However, tumor numbers were almost halved in *Apc*$^{min/+}$*Ikkα*$^{AA/AA}$ mice at death. Altogether, these observations suggested that chronic anemia is

inevitable yet reduction in tumor numbers lessened the tumor burden of *Apc*$^{min/+}$*Ikkα*$^{AA/AA}$ mice and improved their life quality.

5.1.3. Extended Survival and Reduced Proliferation of *β-cat*^{CA}*Ikkα*$^{AA/AA}$ Mice

The use and generation of *Apc*$^{min/+}$ mice require long time periods due to time of adenoma formation and poor breeding with homozygous males (Hinoi et al., 2007). For this purpose, another model of genetic colorectal carcinogenesis was utilized to shorten adenoma formation and to maximize different genetic combinations to understand molecular basis of IKKα involvement in colorectal carcinogenesis. This model was previously described *Vil-Cre-ER*^{T2}*-Ctnnb1*$^{+/lox(ex3)}$ (*β-cat*^{CA} for short) (Harada et al., 1999) to generate conditional and intestinal specific activation of β-catenin which cannot be phospho-regulated due to lacking phosphorylation sites. Continuously active β-catenin molecule is active and freely translocates into nucleus to activate a hyperproliferative program in enterocytes (Harada et al., 1999). This model is extremely severe when used homozygous that is why it is used in heterozygous form to ease follow up of the mice (Fingerle et al., 2009). Also, Analysis of Microarray data for gene expression profiles confirmed that β-catenin activation in these mice is quite similar to APC loss in *Apc*$^{fl/fl}$ mice in terms of Wnt targets regulation (Fingerle et al., 2009). Still a median survival of 21 days is considerably rapid and sensitive to the changes that are contributed by other genetic alterations. Rapid production of this colorectal carcinogenesis model enabled us to produce mice with different genetic backgrounds and to question contribution of different genes or pathways easily by obtaining survival curves and producing high numbers of samples to perform further biochemical analysis. For these purposes, the rest of the analysis was performed in this model.

To investigate molecular mechanism behind IKKα inactivation, *Ikkα*$^{AA/AA}$ mice were crossed to *β-cat*^{CA} mice (Harada et al., 1999) for the generation of survival data. As in the case of *Apc*$^{min/+}$ model, extended survivals in *β-cat*^{CA}*Ikkα*$^{AA/AA}$ mice were observed. However, this time survival advantage of *β-cat*^{CA}*Ikkα*$^{AA/AA}$ mice was slightly higher (%64.2) compared to control group (34.5

vs. 21) to that of *Apc*$^{min/+}$ mice. Similarly postmortem examination did not yield any differences in morphology or physiology of the mice at the time of death. These two groups started to separate in weight loss characteristics from day 15 on which control group dramatically started to lose weight while *Ikkα*$^{AA/AA}$ mice were more stable. For this reason, morphological and physiological changes at day 15 in *β-cat*^{CA} mice were addressed for further analysis and day 15 was identified as the time point when major differences in the pathology of the two groups were distinguished. Macroscopic and microscopic analysis suggested less proliferation and preservation of crypt villus axis in *β-cat*^{CA}*Ikkα*$^{AA/AA}$ mice at day 15. Proliferation was still limited to already elongated crypts while *β-cat*^{CA} mice had proliferation throughout the villus axis. This suggested that extended survival occurs due to slowed proliferation as in the case of *Apc*$^{min/+}$ mice and delayed tumor initiation evident by less proliferating cells. Similar to previous models no increased apoptosis was observed in epithelial cells, concluding that apoptosis is not responsible in any of these CRC models (we will discuss molecular details of apoptosis in the following parts).

So far the results suggested that tumor initiation is slowed down in *Ikkα*$^{AA/AA}$ mice regardless of the model used. All models used for CRC have shown that *Ikkα*$^{AA/AA}$ mice have a survival advantage over control mice which is caused by suppression of the tumor growth. Furthermore, this suppression was due to retarded proliferation rather than increased apoptosis. In the following sections the molecular machinery behind retarded proliferation in the absence of IKKα activation will become clear.

5.2. IDENTIFICATION OF THE ROLE OF IKKα IN CRC

5.2.1. Survival in *Ikkα*$^{AA/AA}$ Mice is Independent of Alternative NF-κB Signaling

IKKα is known to be an important regulator of alternative NF-κB signaling (Cao et al., 2001). Under the control of diverse signaling machinery related to immune activation, cell proliferation and immune cell maturation, IKKα forms activated homodimers which

phosphorylate p100 to induce its proteolytic cleavage to p52 and following activation of RelB/p52 heterodimers (Karin and Greten, 2005). Phospho-activation of IKKα was shown to be crucial for alternative NF-κB activation (Cao et al., 2001). Given that canonical NF-κB signaling is primary regulated by IKKβ rather than IKKα (Zandi et al., 1997), tumor suppressive phenotype in *Ikkα*$^{AA/AA}$ mice may arise from abrogation of alternative NF-κB in *β-cat*^{CA}*Ikkα*$^{AA/AA}$ mice. To investigate involvement of alternative pathway, whole body knock-outs for both *p52* (Paxian et al., 2002) and epithelial specific *Relb*$^{fl/fl}$ (Weih et al. unpublished) were crossed to *β-cat*^{CA} mice and their survival curves were formed upon conditional β-catenin activation. *β-cat*^{CA}*p52*$^{-/-}$ mice survived marginally longer than *β-cat*^{CA} mice (24 days vs. 21 days) while their survival was far from *β-cat*^{CA}*Ikkα*$^{AA/AA}$ mice (vs. 34.5 days). Similarly, *β-cat*^{CA}*RelB*$^{\Delta IEC}$ mice survived a bit longer than *β-cat*^{CA} mice (25 days vs. 21 days) and again their survival was much less than *β-cat*^{CA}*Ikkα*$^{AA/AA}$ mice. Although both knockout models survived longer than WT *β-cat*^{CA} mice, still their survival was not comparable to that of *β-cat*^{CA}*Ikkα*$^{AA/AA}$ mice. Therefore, the contribution of alternative NF-κB signaling is minimal and most probably limited to effect on IEC and it is not enough to explain tumor growth suppression in *Ikkα*$^{AA/AA}$ mice.

5.2.2. Decreased Proliferation in *Ikkα*$^{AA/AA}$ Mice is not due to Direct Control over Wnt Signaling

Since proliferation machinery in intestinal epithelia is strictly regulated via Wnt signaling (Pinto and Clevers, 2005), this fact raised the question if there is any regulation of Wnt signaling or β-catenin via IKKα in CRC development. Indeed, it was previously noted that IKKs regulate β-catenin directly via phosphorylation (Lamberti et al., 2001) yet the possible phosphorylation sites were given the same as the ones used by GSK3β and CK-I (S41 and S45 and surrounding amino acids fit perfectly into canonical recognition site for IKKs which is also found on IκBs and other specific substrates (Karin and Greten, 2005; Rothwarf and Karin, 1999)). However, the phosphorylation by IKKs in these sites has reverse effect than canonical phosphorylation of β-

catenin (Carayol and Wang, 2006). Eventually it was questioned whether elimination of IKKα activation has negative effect on β-catenin activation and resulting proliferation. However, this continuously active β-catenin molecule also lacks previously addressed phosphorylation sites for IKKs. Therefore, IKK direct regulation over β-catenin may not be the key factor in decreased proliferation in the models of CRC presented here. Alternative sites of phosphorylation might be existed. However, previously presented phosphorylation analysis data (Lamberti et al., 2001) and sequence analysis on β-catenin for finding alternative phosphorylation sites suggested that the possibility of finding an alternative phospho-activation domain is improbable.

On the other hand, it was suggested that cyclin D1 is controlled via IKKα through Wnt/β-catenin (Albanese et al., 2003), a more recent study has argued that cyclin D1 is not an immediate target of IKKα and elevated much later in *Apc* loss (Sansom et al., 2005). Current results support the latter argument and suggested that cyclin D1 is not a direct target of IKKα in *β-cat*^{CA} model as evident by unaltered protein concentrations. Consequently, direct regulation of cyclin D1 by IKKα is either absent or other co-regulators are involved to compensate the absence of IKKα. On the other hand, absence of cyclin D1 direct regulation still does not rule out the possibility of Wnt/β-catenin regulation by IKKα. However, β-catenin levels were affected neither in *β-cat*^{CA}*Ikkα*$^{AA/AA}$ mice at day 15 nor in *Apc*$^{min/}$*Ikkα*$^{AA/AA+}$ mice at month 4 relative to *Ikkα*$^{AA/AA}$ counterparts. If Wnt signaling and β-catenin levels are not regulated by IKKα, then decrease in c-Myc levels observed in *β-cat*^{CA}*Ikkα*$^{AA/AA}$ mice should be due to another mechanism.

To explain this phenomenon, expression profile from *β-cat*^{CA}*Ikkα*$^{AA/AA}$ mice at day 15 were obtained and analyzed for Wnt signaling targets. Hierarchical clustering of Microarray data by K-means algorithm yielded 10 distinct clusters within these significantly regulated genes. Among these there were two clusters (#IV&VI) that were upregulated in *β-cat*^{CA} mice at 15 day but not in *β-cat*^{CA}*Ikkα*$^{AA/AA}$ mice at 15 day. These clusters were notable such that there were a number of Wnt targets that were upregulated in *β-cat*^{CA} mice at day 15 relative to *β-cat*^{CA}*Ikkα*$^{AA/AA}$ mice at day 15. When GSEA was run to compare *β-cat*^{CA} mice with *β-cat*^{CA}*Ikkα*$^{AA/AA}$ mice at day 15, *β-cat*^{CA}*Ikkα*$^{AA/AA}$ mice showed downregulation of numerous Wnt targets in *Apc* loss phenotype (described in (Sansom et al., 2007)). This observation suggested that *β-cat*^{CA}*Ikkα*$^{AA/AA}$ mice have reduced Wnt target expressions compared to *β-cat*^{CA} mice at day 15. Nevertheless, the genes that

are downregulated in Wnt signaling in *β-cat*^{CA}*Rela*$^{\Delta IEC}$ mice at day 15 (Fingerle et al., 2009) were quite different than those of *β-cat*^{CA}*Ikkα*$^{AA/AA}$ mice at day 15. Since in that paper it was argued that β-catenin is regulated via p65 whose absence influenced proliferation by direct Wnt regulation, the genes downregulated in *β-cat*^{CA}*Ikkα*$^{AA/AA}$ mice do not support that discussion. In that paper it was shown that β-catenin targets like *Ascl2, Olfm4, Sox9* (expression of which was found to be important for a stem cell like reprogramming in proliferating epithelial cells in *β-cat*^{CA} mice) were downregulated. However, none of these genes related to Wnt stem cell program were downregulated in *β-cat*^{CA}*Ikkα*$^{AA/AA}$ mice at day 15. Therefore, these results signified that these two genotypes have totally different effects on Wnt target expression profiles and IKKα does not have a direct control over Wnt signaling and its downstream targets concerning retarded proliferation in *Ikkα*$^{AA/AA}$ mice in different CRC models.

5.2.3. General Expression Analysis Revealed Interferon Related Gene Upregulation in *β-cat*^{CA}*Ikkα*$^{AA/AA}$ Mice

Histological observations and survival data has suggested reduced proliferation as the basis of reduced tumor growth and extended survival in *Ikkα*$^{AA/AA}$ mice. To understand molecular machinery regarding reduced proliferation in *Ikkα*$^{AA/AA}$ mice, more biochemical data was required. To understand molecular pathways and their possible signatures on *Ikkα*$^{AA/AA}$ phenotype, total RNA extracts were analyzed in Affymetrix Mouse Microarray to see genome wide expression profiles. Expression analysis in *β-cat*^{CA} mice at day 15 yielded expression data for over 23k transcripts. According to statistical analysis the genes significantly regulated in at least one of the genotypes were identified (normalized expression data (Z-scores) was compared for absolute expressions and clustered by K-means (MacQueen, 1967) algorithm where $p>0.05$ were excluded as insignificant). As a result of these criteria, a set of 732 genes all of which were found to be significantly regulated in at least one of the genotypes in comparison to others were identified.

Hierarchical clustering of significantly regulated genes yielded 10 distinct clusters. Three of the clusters were notable since they contained genes up or down regulated in $\beta\text{-}cat^{CA}Ikk\alpha^{AA/AA}$ mice at day 15 relative to $\beta\text{-}cat^{CA}$ mice at day 15. Two of these clusters were containing numerous Wnt targets downregulated in $\beta\text{-}cat^{CA}Ikk\alpha^{AA/AA}$ mice at day 15 and their role in relation to direct Wnt signaling control has already been discussed in the previous topic. At this point the importance of the second unique cluster was more pronounced. The second cluster (#VIII) was consisting of 79 transcripts which were solely upregulated in $\beta\text{-}cat^{CA}Ikk\alpha^{AA/AA}$ mice at day 15. Close examination of these genes has shown that most of these genes were involved in immune regulation or inflammation. Even some of these genes were interferon downstream targets. Given the importance of interferons in immune activation and tumor suppression (McConnell and Yang, 2009), the rest of the analysis was focused on this issue to verify initial observations with Microarray data. GSEA (Subramanian et al., 2005) was run to verify various interferon signatures (IFNα, β or γ) which were previously described to be upregulated in response to these cytokines in different cell lines (Der et al., 1998; Radaeva et al., 2002; Sana et al., 2005). As a result of this analysis, a good correlation of upregulations in interferon signature genes associated with reduced proliferation in $\beta\text{-}cat^{CA}Ikk\alpha^{AA/AA}$ mice at day 15 were observed. These observations strongly suggested that $\beta\text{-}cat^{CA}Ikk\alpha^{AA/AA}$ mice at day 15 have better interferon activation which in turn may lead to specific immune activation to suppress tumor growth (Goldstein and Laszlo, 1988). Further analysis of certain interferon downstream targets with RT-PCR verified increased expression of these markers in $\beta\text{-}cat^{CA}Ikk\alpha^{AA/AA}$ mice at day 15 relative to $\beta\text{-}cat^{CA}$ mice at day 15. Especially there was a strong IFNγ downstream (Schroder et al., 2004) activation in genes like *Stat1* (Kaplan et al., 1998), *Irf1* (Matsuyama et al., 1993), *Nos2* (Goldstein and Laszlo, 1988), *Oas1* (Schiller et al., 1990), *Eif2ak2 (Pkr)* (Kumar et al., 1997), *Isg15* (Clauss et al., 1990) and *Cxcl10* (*Ip10)* (Luster et al., 1985) in $\beta\text{-}cat^{CA}Ikk\alpha^{AA/AA}$ mice IECs at day 15. Furthermore, protein expression from $\beta\text{-}cat^{CA}Ikk\alpha^{AA/AA}$ mice IEC extracts for IRF-1, STAT1 and NOS2 (iNOS) confirmed all previous observations with increased interferon downstream expression profiles and more significantly phospho-activation of STAT1 was specific to $\beta\text{-}cat^{CA}Ikk\alpha^{AA/AA}$ samples at day 15. All these data from Microarray data to protein expressions strongly suggested that IFNγ

signaling is active in *β-cat*^{CA}*Ikkα*$^{AA/AA}$ mice and can account for the retarded tumor growth leading to better survival.

5.2.4. IFNγ Induced Cell Cycle Arrest is the Key Mechanism in Reduced Proliferation in *β-cat*^{CA}*Ikkα*$^{AA/AA}$ Mice

IFNγ is the only type II interferon and it is differentially regulated than type I interferons and induces downstream activation via its specific receptor. IFNγ can also be induced via toll-like receptors, APCs via MHC class I dependent manner, via cytokines like IL-12 or by-self induction from previously activated cells (Schroder et al., 2004). IFNγ is versatile cytokine with profound effects on Th1 activation, lymphocyte development and tumor regression (Dalton et al., 1993; Mattner et al., 1996). IFNγ can be produced from different immune cells like dendritic cells, T-cells, and NK cells (Shankaran et al., 2001). IFNγ can induce downstream activation in both immune cells and target tissue since epithelial cells also contain IFNγR. Differently from type I interferons it has its tumor regressive activity on epithelial and endothelial tissues and have little effect on cancers of myeloid origin (Prendergast and Jaffee, 2007). IFNγ induces IFNγR downstream signaling via JAK/STAT dependent manner (Takaoka et al., 2008). Usually JAKs are found to be in structural association with IFNγR and tyrosine kinase activity induces STAT1 or 2. STAT1 homodimers or STAT1/STAT2 heterodimers translocate to the nucleus to activate IFNγ downstream targets like IRF-1, iNOS, STAT1 or other cytokines which are related to specific T-cell activation (Takaoka et al., 2008). These cytokines coupled to IL-12p70 strongly promotes Th1 phenotype and inhibits Th2 activation (Mattner et al., 1996). Th1 activation is important in some viral infections and tumor specific immunity for elimination of malignant cells (Smyth et al., 2006). Especially, IFNγ secretion from T-cells and NK-cells are found to be very important in tumor regression and activation of tumor specific cell killing via NK-cells or $CD8^+$ T-cells (Shankaran et al., 2001). Perforin specific tumor cell elimination is found to be IFNγ dependent and in the absence of IFNγ tumor derived from these mice are found to be highly

immunogenic which is less pronounced in perforin deficient mice (Curcio et al., 2003). Otherwise, IFNγ is a strong activator of STAT1 in epidermal and endothelial tissues which in turn slows down cell cycle and cause tumor regression independent of immune specific tumor cell killing via upregulation of p21 which in turn causes cell cycle arrest in target cells (Burke et al., 1997; Shankaran et al., 2001).

Although no upregulation in relative p21 levels were observed, still the best way to verify its activity indirectly was checking Cdk activities to phosphorylate their downstream targets. In the present study it was already presented that both Cdk1 (Boxem et al., 1999) and Cdk2 (Yam et al., 1999) phosphorylation on their respective substrates were decreased in *β-cat^{CA}Ikkα$^{AA/AA}$* IEC samples at day 15. These observations verified that IFNγ casuses cell cycle arrest in *β-cat^{CA}Ikkα$^{AA/AA}$* mice intestines. As a result of this cycle arrest, *β-cat^{CA}Ikkα$^{AA/AA}$* mice exhibited slowed proliferation evident by histological stainings and proliferation marker downregulation. These results can also account for reduced c-Myc levels where no direct involvement of Wnt signaling regulation is required. Consequently, cell cycle arrest in *β-cat^{CA}Ikkα$^{AA/AA}$* mice may explain the phenotype associated with decreased proliferation leading to retarded tumor growth and better survival.

After proving that IFNγ upregulation may explain all the phenotype related to tumor suppression by gene expression profiles and downstream kinase activities this phenomenon was further verified by the use of genetic models. For this purpose, *ifng$^{-/-}$* and *Ifnar1$^{-/-}$* mice were crossed to *β-cat^{CA}Ikkα$^{AA/AA}$* background to see whether IFNs are the real target of survival mechanism in this model of CRC by the examination of the survival of these animals. *β-cat^{CA}Ikkα$^{AA/AA}$Ifnar1$^{-/-}$* mice survived similar to *β-cat^{CA}Ikkα$^{AA/AA}$* mice (31.5 vs. 34.5). Hence the additional loss of type I interferon signaling did not affect survival of *β-cat^{CA}Ikkα$^{AA/AA}$* mice. Although there were a subset of type I interferon downstream molecules that were upregulated as observed in gene expression profiles, it was evident with this result that IFNα does not play any role in extended survival of *Ikkα$^{AA/AA}$* phenotype. These results was particularly important while considering specific APC activation leading to adaptive immunity could utilize type I interferons as well through activated DCs which was not observed in the context of current data. On the other hand, *β-cat^{CA}Ikkα$^{AA/AA}$ifng$^{-/-}$* mice gave an astonishing result of reversion of all extended

survival observed in *β-cat*^{CA}*Ikkα*$^{AA/AA}$ only mice (20 vs. 34.5 days). At the baseline levels *β-cat*^{CA}*ifng*$^{-/-}$ mice had a lower survival than that of *β-cat*^{CA} mice (19 vs. 21). However, even the addition of *Ikkα*$^{AA/AA}$ knock-in did not provide almost any survival advantage (19 vs. 20 days). Moreover, IFNγ downstream targets were highly upregulated in epithelial cells of *β-cat*^{CA}*Ikkα*$^{AA/AA}$ mice leading to cell cycle arrest which accounted for reduced proliferation in them. Consequently, all the positive effect of *Ikkα*$^{AA/AA}$ phenotype is reversed by the removal of *Ifng* from the *β-cat*^{CA}*Ikkα*$^{AA/AA}$ model because IFNγ is the ultimate target of IKKα inactivation in *β-cat*^{CA}*Ikkα*$^{AA/AA}$ mice leading to reduced proliferation and extended survival.

5.2.5. Both Epithelial and Hematopoietic Cells Contribute to the *Ikkα*$^{AA/AA}$ Phenotype

Once it became clear that IFNγ upregulation and resulting cell cycle arrest are the key points in reduced proliferation and extended survival in *β-cat*^{CA}*Ikkα*$^{AA/AA}$ mice, the next step was to identify molecular mechanism in which IKKα inactivation leads to IFNγ downstream. One possible explanation was the increased sensitivityof IECs to IFNγ which leads them to the cell cycle arrest (Burke et al., 1997; Shankaran et al., 2001) while other possibility was the increased levels of IFNγ from activated immune cells (Hung et al., 1998). In either way, identification of contributions from both compartments was required. To address the origin of mechanism and to separate the roles between epithelial and hematopoietic compartments, *Ikkα*$^{\Delta IEC}$ mice were combined with *β-cat*^{CA} background to generate *β-cat*^{CA}*Ikkα*$^{\Delta IEC}$ mice and also bone marrow transplantation from *Ikkα*$^{AA/AA}$ mice to *β-cat*^{CA} mice was performed. In the epithelial specific deletion of *Ikkα* in *β-cat*^{CA}, epithelial cells had a marginal contribution to the survival (24 vs. 21 days) but latency of survival was much less compared to *β-cat*^{CA}*Ikkα*$^{AA/AA}$ mice (24 vs. 34.5 days). Other than survival no other differences in histological examinations were observed from wt *β-cat*^{CA} mice at the time of sacrifice. Yet no further analysis with 15 days samples were performed. Still these results strongly suggested that epithelial intrinsic role of IKKα has a marginal contribution in the survival most probably due to increased sensitivity to interferons or alteration

of alternative NF-κB signals. The first point is supported by preliminary observations of increased STAT1 and IRF-1 levels in *β-cat*^{CA}*Ikkα*$^{\Delta IEC}$ mice yet this increase was not leading to cell cycle arrest observed in *β-cat*^{CA}*Ikkα*$^{AA/AA}$ mice at day 15 to extend their survival. As mentioned before, whole body abrogation of *p52* or epithelial specific *Relb* deletion resulted in similar survival to *β-cat*^{CA}*Ikkα*$^{\Delta IEC}$ mice. Therefore, contribution of alternative NF-κB signaling may account for epithelial IKKα abrogation yet further experimentation like epithelial specific IKKα inactivation (by bone marrow transplantation from wt mice to *β-cat*^{CA}*Ikkα*$^{AA/AA}$ mice) is needed to clarify this phenomenon. However, one can argue that this effect was still not enough to recapitulate the longer survival in whole body *Ikkα*$^{AA/AA}$ knock-ins. Therefore, the majority of the effect regarding reduced proliferation should be coming from the hematopoietic cells.

It was actually what was observed when bone marrow transplantations were performed to *β-cat*^{CA} mice to assess hematopoietic loss of IKKα activation. Both *β-cat*^{CA} and *Ikkα*$^{\Delta IEC}$ use cre recombinase which would cause unwanted side effect like activation of β-catenin in hematopoietic cells. For this purpose, bone marrow transplantation from *Ikkα*$^{AA/AA}$ mice was performed to obtain bone marrow specific inactivation of IKKα. Consequently, bone marrow transplantation experiments yielded a survival advantage slightly longer than *β-cat*^{CA}*Ikkα*$^{\Delta IEC}$ mice (27 vs. 24 days) but still significantly lower than that of *β-cat*^{CA}*Ikkα*$^{AA/AA}$ mice (27 vs. 34.5 days). Although these observations suggested a more significant role of hematopoietic cells in the reduced prolifetion, it was still not enough to explain the extended survival in *β-cat*^{CA}*Ikkα*$^{AA/AA}$ mice alone.

Even though inactivation of IKKα in epithelial or hematopoietic cells has resulted longer survival in *β-cat*^{CA} mice, still their survivals do not sum up the longer survival in *β-cat*^{CA}*Ikkα*$^{AA/AA}$ mice. Therefore, the effect which was witnessed in *Ikkα*$^{AA/AA}$ mice is an additive result of both epithelial and hematopoietic compartments and it seemed that contribution from both sides was crucial. Since summing up of the contributions are far from the *Ikkα*$^{AA/AA}$ whole body knock-ins, one can argue that the effect of both tissues is amplified in respond to each other or a feedback mechanism which operates between these two compartments is responsible for the extended survival in *Ikkα*$^{AA/AA}$ mice. In the following parts, the possible mechanism that causes the

communication between these two compartments and the role of different immune cells in the activation of immune responses leading to amplified IFNγ response will be discussed.

5.2.6. Hematopoietic Origin of IFNγ Secretion in *β-cat^{CA}Ikkα$^{AA/AA}$* Mice

After proving that reduced proliferation and resulting phenotype in *β-cat^{CA}Ikkα$^{AA/AA}$* mice were dependent on IFNγ activation, the next step was to identify molecular machinery regarding upregulated IFNγ levels in *β-cat^{CA}Ikkα$^{AA/AA}$* mice. Moreover, it was clarified that IFNγ upregulation was mostly contributed by hematopoietic cells, then the major challenge was to identify molecular mechanism leading to its upregulation and the cell types related to its secretion. As IFNγ is concerned in immune activation, there are different sources of it within hematopoietic compartment and different immunoregulatory mechanisms that may lead to its secretion. One way of increased IFNγ downstream activation was the increased sensitivity of IECs to IFNγ. This phenomenon was discussed within the context of separating the roles between epithelial and hematopoietic compartment. Although being crucial it was shown to be having fewer shares than hematopoietic cells. The next possibility was the increased IFNγ production by the immune cells. In the rest of the discussion different possibilities with immune activation and resulting sources of IFNγ secretion will be investigated in the light of current findings.

5.2.6.1. Adaptive Immunity is not Involved in the Suppression of Proliferation in *β-cat^{CA}Ikkα$^{AA/AA}$* Mice

The canonical Th1 activation pathway begins with tumor recognition by APCs which in turn activate lymphocytes by presenting tumor specific antigens. Active Th1 cells can produce IFNγ or other inflammatory cytokines like IL-2, IL-15, IL-18 or IL-21 (Smyth et al., 2005). This IFNγ coupled to other inducing cytokines trigger APC maturation or higher IL-12 secretion (Hung et

al., 1998). Moreover, these cytokines has a positive loop on APCs to activate their antigen presentation or phagocytic abilities (Smyth et al., 2006). In turn, IL-12 further activates $CD4^+$ T-cells to increase IFNγ production (Mattner et al., 1996). These cytokines coupled to IFNγ can also induce cytotoxic T-cells or NK cells to produce even more IFNγ to amplify the signal and cytotoxic molecules targeting tumor cells (Shankaran et al., 2001; Street et al., 2001). Altogether, secretion of proinflammatory cytokines central to Th1 activation orchestrates cytotoxic immune responses towards tumor cells (Beckhove et al., 2004; Dhodapkar et al., 2002).

The first step was to identify whether T-cell activation was existed by the analysis of activation specific markers. As a result FACS analysis, activation specific markers like CD69 and Foxp3 in $CD4^+$ and Ly6c in $CD8^+$ cells (Cambiaggi et al., 1992; Johnson et al., 1993; Körholz et al., 1997; Robb et al., 1981; Zhang and Zhao, 2007) were upregulated in $\beta\text{-}cat^{CA}Ikk\alpha^{AA/AA}$ mice at day 15. Further analysis of Foxp3 in whole mucosa by RT-PCR failed to support FACS results (which would otherwise be controversial to observe Th1 activation in the presence of suppressive activity by Tregs (Zhang and Zhao, 2007)). Although these increases in activation markers can suggest an increased T-cell activity in $\beta\text{-}cat^{CA}Ikk\alpha^{AA/AA}$ mice at day 15, further data was required to confirm these preliminary data. Furthermore, T-cell specific cytokine profiles were analyzed via RT-PCR. Upon these analyses, no clear Th1 shift was observed in $\beta\text{-}cat^{CA}Ikk\alpha^{AA/AA}$ mice. Moreover, lack of increased IFNγ production in lymphocytes was confirming these observations. Consequently, these observations strongly suggested that Th1 activation in $CD4^+$ T-cells was absent in $\beta\text{-}cat^{CA}Ikk\alpha^{AA/AA}$ mice.

Although no Th1 activation was evident, involvement of NK cells and activation of tumor cytotoxicity was to be clarified. Neither of these two cells types were upregulated in $\beta\text{-}cat^{CA}Ikk\alpha^{AA/AA}$ mice. NK cells were not producing higher IFNγ like $CD8^+$ cells in $\beta\text{-}cat^{CA}Ikk\alpha^{AA/AA}$ mice at day 15. Furthermore, cytotoxic factors upregulated in activated $CD8^+$ or NK cells like granzymes and perforin were not upregulated in $\beta\text{-}cat^{CA}Ikk\alpha^{AA/AA}$ mice at day 15. On the contrary, there was a clear reduction in perforin and granzyme levels in $\beta\text{-}cat^{CA}Ikk\alpha^{AA/AA}$ mice. Analysis of other cytotoxic markers like NKG2D (Raulet, 2003) and TRAIL and its receptor Killer (DR5) (Takeda et al., 2002) gave a slight increase in $\beta\text{-}cat^{CA}Ikk\alpha^{AA/AA}$ mice except from FasL (Kim et al.,

2006; Prendergast and Jaffee, 2007). Although these elevations in TRAIL and its receptor DR5 can suggest a TRAIL mediated cytotoxicity, upregulations in their absolute concentrations did not translate into higher cell death figures in *β-cat^{CA}Ikkα$^{AA/AA}$* mice at day 15 as measured by TUNEL and cleaved Caspase3 IHC. Moreover, previous observations with other models of CRC were confirming this result and no increase in apoptosis evident in *Ikkα$^{AA/AA}$* mice. Even there was a slight decrease in apoptosis in some samples in *β-cat^{CA}Ikkα$^{AA/AA}$* mice, *Apc$^{min/+}$Ikkα$^{AA/AA}$* and AOM-*Ikkα$^{AA/AA}$* tumors. As a last proof for lack of NK involvement, NK cells were depleted in *β-cat^{CA}Ikkα$^{AA/AA}$* mice and their survival upon this effect is measured. As a result of NK depletion no change in *β-cat^{CA}Ikkα$^{AA/AA}$* mice survivals were observed. Therefore, NK cells do not contribute to the reduced proliferation leading to increased survival in these mice. In conclusion, absence of Th1 shift and NK cell responses suggested that there is no adaptive immune activation leading to tumor specific cytotoxicity in *β-cat^{CA}Ikkα$^{AA/AA}$* mice.

5.2.6.2. Myeloid Cell Activation as a Source of IFNγ in *β-cat^{CA}Ikkα$^{AA/AA}$* Mice

In current analysis, myeloid cells were lacking activation in antigen presentation and following adaptive immune activation. Macrophages were checked for M0 to M1 shift via arginase and NOS activities and no increase in their activation was observed. Moreover, their expression levels for M1/M2 specific markers like IL-10, IL-12 and TNF-α (Condeelis and Pollard, 2006) did not suggest a shift towards any phenotype. Therefore, antigen presenting and adaptive immune promoting characteristic of macrophage was absent in *β-cat^{CA}Ikkα$^{AA/AA}$* mice regardless of their increased numbers. Neutrophils on the other hand were specifically activated and producing IL-12 in higher amounts. DCs cells were showing increased IL-12 and TNF-α production in *β-cat^{CA}Ikkα$^{AA/AA}$* mice, while their antigen presentation was not affected. BMD DCs were subjected to different activating ligands for their activation status and they were observed to be slightly elevated in IL-12 expression. However, IL-12 neutralization in *β-cat^{CA}Ikkα$^{AA/AA}$* mice showed that IL-12 does not have any direct role in increased survival of *β-cat^{CA}Ikkα$^{AA/AA}$* mice but can still have an indirect role which will become clear shortly in the context of macrophage activation.

Regardless the absence of adaptive immune activation by APCs, myeloid cells were observed to be highly active and amplified in *β-cat*^{CA}*Ikkα*$^{AA/AA}$ mice. Absolute numbers of macrophages, DCs and neutrophils showed an increase in *β-cat*^{CA}*Ikkα*$^{AA/AA}$ mice as measured by specific marker expression in RT-PCR and FACS. Furthermore, IHC analysis has show intraepithelial localization for macrophages and neutrophils while DCs did not show any specific tissue localization in *β-cat*^{CA}*Ikkα*$^{AA/AA}$ mice at day 15. Since the direct involvement of IL-12 and adaptive immune activation were ruled out, this specific localization pattern observed in *β-cat*^{CA}*Ikkα*$^{AA/AA}$ mice at day 15 could be the result of better recruitment of APCs via chemokines secreted by epithelial cells to the site of hyperproliferation. To address this phenomenon, gene expression profiles for monocyte chemoattractants were checked both in IEC and in whole mucosa RNA samples. As a result of this analysis, a high correlation of increased cytokine production in *β-cat*^{CA}*Ikkα*$^{AA/AA}$ mice was observed. *Cxcl1, Cxcl2 , Cxcl5, Ccl20, Ccl28* and *Tslp* RNA expressions were increased in both tissues while *Mcp-1* was found to be elevated only in whole mucosa. All these cytokines, with the exeption of MCP-1, can be produced by IEC in the case of injury or infection to attract monocytes (Furuichi et al., 2006; Huang et al., 2001; Li et al., 2005; Luu et al., 2000). On the other hand, chemokines like *Ccl5* and *Ccl6* were persistently downregulated in *β-cat*^{CA}*Ikkα*$^{AA/AA}$ samples in both compartments. *Ccl5* downregulation is most probably due to lack of T-cell activation leading to tumor specific cytotoxicity (Song et al., 2000). *Ccl6* downregulation is on the other hand is the only controversial example because it is reduced only in the presence of T-cell activity (Ma et al., 2004). According to our model, hyperproliferating IECs secrete these chemokines (due to disturbed epithelial barrier and infiltrating bacteria) to attract myeloid cells and these cells further activate themselves by autocrine factors like MCP-1 (Huang et al., 2001; Lu et al., 1998). The other source of monocyte activation is IFNγ (Brucet et al., 2004; Shi et al., 2003; Wesemann and Benveniste, 2003; Wesemann et al., 2004). It was reported that a small subset of pDCs can secrete high levels of IFNγ and can lyse tumor in TRAIL dependent manner (Taieb et al., 2006), which was probably absent in *β-cat*^{CA}*Ikkα*$^{AA/AA}$ mice at day 15. Especially numbers of IKDCs were dramatically higher in *β-cat*^{CA}*Ikkα*$^{AA/AA}$ mice at day 15. Moreover, they were the only group of hematopoietic cells with increased IFNγ production. IKDC produced IFNγ and already elevated IL-12 (Munder et al., 1998; Schindler et al., 2001) may further help

the promotion and activation of macrophages which further expand in numbers to produce even higher amounts of IFNγ (Di Marzio et al., 1994; Puddu et al., 1997). Though per cell production is not observed to be altered in our analysis (further proof is required), this dramatically increase in macrophage numbers may account for increased IFNγ production. Therefore, amplification in myeloid cells especially in macrophages can make them a significant source of IFNγ in *β-cat*^{CA}*Ikkα*$^{AA/AA}$ mice.

5.2.7. NF-κB Activation is Required for Reduced Proliferation in *Ikkα*$^{AA/AA}$ Mice

Although myeloid cells were identified as a source of amplified IFNγ response with the current data, still the basic role of IKKα in their activation was to be clarified. Close examination of monocyte chemoattractants upregulated in *β-cat*^{CA}*Ikkα*$^{AA/AA}$ mice at day 15 revealed that they were regulated by canonical NF-κB signaling (Bonizzi and Karin, 2004). Since they are NF-κB targets, IKKα should play an inhibitory role in NF-κB activities leading to immune suppression which was already shown in macrophage activation upon bacterial challenge (Lawrence et al., 2005; Li et al., 2005). Indeed, recent literature was suggesting that IKKα is regulator of pro-inflamatory signaling pathways in different cell types varying from macrophages to T-cells (Gloire et al., 2007; Lawrence et al., 2005). When the case of *Ikkα*$^{AA/AA}$ mice challenged with bacteria which produces macrophage recruiting cytokines like MIP-1α, CCL20, CCL28, CXCL1 and CXCL5 was considered, the increase in prolonged NF-κB binding (Lawrence et al., 2005) seems to be crucial for chemoattraction of APC to the site of hyperproliferation. Indeed, the elevations of these cytokines were occurring in our *β-cat*^{CA}*Ikkα*$^{AA/AA}$ at day 15 in IEC samples. Therefore, all upregulation of these factors could be NF-κB dependent also in the case of hyperproliferation.

To investigate this possibility *β-cat*^{CA}*Ikkβ*$^{\Delta IEC}$ mouse model was generated for introduction of epithelial specific deletion of IKKβ. The first important observation with this model was such that *β-cat*^{CA}*Ikkβ*$^{\Delta IEC}$ mice had a limited survival advantage over wt mice (26 vs. 21) through a mechanism unrelated to our *Ikkα*$^{AA/AA}$ model (Fingerle et al., 2009). Nevertheless, when these

mice were coupled to *Ikkα*$^{AA/AA}$ to generate *β-cat*^{CA}*Ikkα*$^{AA/AA}$*Ikkβ*$^{\Delta IEC}$ mice, the extra survival observed in *β-cat*^{CA}*Ikkα*$^{AA/AA}$ mice was lost regardless of the positive effect of *Ikkβ*$^{\Delta IEC}$. On the contrary, the survival of both *β-cat*^{CA}*Ikkβ*$^{\Delta IEC}$ and *β-cat*^{CA}*Ikkα*$^{AA/AA}$*Ikkβ*$^{\Delta IEC}$ mice were almost the same (25.5 vs. 26). This strongly suggested that the anti-proliferative effect observed in *Ikkα*$^{AA/AA}$ mice was dependent on IKKβ and most probably on canonical NF-κB activity regardless of unaffected binding levels. The extra survival in *β-cat*^{CA}*Ikkβ*$^{\Delta IEC}$ mice (Fingerle et al., 2009) depends on alteration of Wnt signaling and downregulation of Wnt target that give differentiated epithelial cells a stem cell like phenotype in the constitutive activation of NF-κB by *Nfkbia*$^{\Delta IEC}$ (IκBα) mice (Rupec et al., 2005). However, *β-cat*^{CA}*Ikkα*$^{AA/AA}$ mice on the other hand require active NF-κB signaling to have longer survival which suggests that the survival in *β-cat*^{CA}*Ikkα*$^{AA/AA}$ and *β-cat*^{CA}*Rela*$^{\Delta IEC}$ mice (Fingerle et al., 2009) are completely due to different mechanisms. The first reason of this divergence is the need for active NF-κB which is completely absent in *Ikkβ*$^{\Delta IEC}$ or *Rela*$^{\Delta IEC}$ mice (which is even more strong in *Rela*$^{\Delta IEC}$ mice) but is still there in *Ikkα*$^{AA/AA}$ mice. The other important difference is the alteration of Wnt targets which is not observed in *Ikkα*$^{AA/AA}$ mice at all (by Microarray data). Nevertheless, abolishment of extra survival in *β-cat*^{CA}*Ikkβ*$^{\Delta IEC}$*Ikkα*$^{AA/AA}$ double knockouts strongly suggested the requirement of NF-κB activation in *Ikkα*$^{AA/AA}$ mice.

If this hypothesis was correct all the upregulations in chemoattractants and resulting APC amplifications should be absent in *β-cat*^{CA}*Ikkβ*$^{\Delta IEC}$*Ikkα*$^{AA/AA}$ mice. Expression profiles of these cytokines have shown complete reversion of cytokine profiles in *β-cat*^{CA}*Ikkβ*$^{\Delta IEC}$*Ikkα*$^{AA/AA}$ mice. As a result of decreased chemokines, *β-cat*^{CA}*Ikkβ*$^{\Delta IEC}$*Ikkα*$^{AA/AA}$ mice also reduced in myeloid cell numbers. Macrophage, neutrophil and DC numbers returned back to basal levels in *β-cat*^{CA} mice. Therefore, prolonged NF-κB activation in *β-cat*^{CA}*Ikkα*$^{AA/AA}$ mice is responsible for the production of chemokines which further attract and amplify myeloid cells to produce IFNγ which suppresses tumor growth via cell cycle arrest. In conclusion, removal of *Ikkβ* is sufficient to reverse all these positive effect associated with *Ikkα*$^{AA/AA}$ mice.

5.2.8. Identifying Kinase Specific and Structural Roles of IKKα in Immune Suppression

Current data suggested that the presence of intact IKKα is important in terms of proper functioning of NF-κB in epithelial and hematopoietic cells. Furthermore, the absence of IKKα activation in *β-cat*^{CA}*Ikkα*$^{AA/AA}$ mice has shut down the mechanism which feedback inhibits extended promoter binding of p65. Without control, NF-κB promoter binding was prolonged to upregulate proinflammatory monocyte chemoattractants in *β-cat*^{CA}*Ikkα*$^{AA/AA}$ mice. These upregulations resulted in increased myeloid populations which further secrete IFNγ respectively. Moreover, in myeloid cells intrinsic autocrine factors like MCP-1 and IL-12 are also controlled by NF-κB. Therefore, further activation of myeloid cells is also dependent on prolonged NF-κB activity in the absence of IKKα phospho-activation (Lawrence et al., 2005). This mechanism strongly suggests the involvement of NF-κB activation both in epithelial cells and hematopoietic cells to obtain strong tumor suppression observed in *β-cat*^{CA}*Ikkα*$^{AA/AA}$ mice.

Epithelial specific deletion of IKKα did not yield a comparable survival advantage as in the case of bone marrow transplantation into *β-cat*^{CA} mice. Although monocyte chemoattractants are required for amplified macrophage activation, they are still not enough to impose full effect without hematopoietic cell involvement without *Ikkα*$^{AA/AA}$ replacement in these cells. One possible explanation is the cell intrinsic factors in hematopoietic cells that provide better activation in the absence of IKKα activation (Lawrence et al., 2005; Li et al., 2005). In *Ikkα*$^{AA/AA}$ b.m. transplanted animals there were still a significant survival advantage, most probably due to the same mechanism that increased chemoattractant expression by the epithelial cells. In fact, activation of macrophages and their apoptotic resistance to proinflammatory stress stimuli may account for the increased numbers of IFNγ secreting myeloid cells. One important point is the requirement of IKKα in proper p65 functioning (Gloire et al., 2007). Although it is known that IKKα kinase activity is important for the functioning of several factors for its action as a transcriptional co-activator or repressor, another important function of IKKα is its structural

association in some p65 promoters unrelated to kinase function (Chariot, 2009; Gloire et al., 2007).

For this reason, the reduced survival in epithelial specific *β-cat^{CA}Ikkα$^{\Delta IEC}$* mice may be due to the structural absence of IKKα protein rather than its inactivation in *β-cat^{CA}Ikkα$^{AA/AA}$* mice. In other words, IKKα is required in the nucleus for the proper functioning of NF-κB signaling and p65 binding to its related promoters (Chariot, 2009). However, it was not checked whether chemoattractants were reduced or myeloid cell recruitment is abrogated in *β-cat^{CA}Ikkα$^{\Delta IEC}$* mice at day 15. Still there is a possibility that these chemoatractants which are amplified in *β-cat^{CA}Ikkα$^{AA/AA}$* mice can be missing in *β-cat^{CA}Ikkα$^{\Delta IEC}$* mice at day 15. Only after obtaining the expression profiles for these chemokines in *β-cat^{CA}Ikkα$^{\Delta IEC}$* mice at day 15 this statement can be verified. Still recruitment of myeloid cells may not guarantee increased IFNγ levels. In fact without involvement of right signaling activation, recruited myeloid cells can increase TNF-α and cause proinflammatory immune activation favoring tumor promotion as in the case of *β-cat^{CA}Nfkbia$^{\Delta IEC}$* mice (Fingerle et al., 2009). Therefore, activation and recruitment of IFNγ secreting myeloid cells should be crucial in the longer survival of *β-cat^{CA}Ikkα$^{AA/AA}$* mice and this phenomenon is an important possibility to explain reduced proliferation in *β-cat^{CA}Ikkα$^{\Delta IEC}$*. For this purpose, performing b.m. transplantation from wt mice to *β-cat^{CA}Ikkα$^{AA/AA}$* mice is required for complete understanding of kinase specific and structural roles of IKKα in epithelial and myeloid cells.

Regardless of this phenomenon, an increase in the survival of *β-cat^{CA}Ikkα$^{\Delta IEC}$* mice which was very similar to that of *Nfkb2* or *Relb$^{\Delta IEC}$* mice was observed (24 vs. 24 and 25 respectively). Therefore, rather than increased chemoattractants as in the case of *β-cat^{CA}Ikkα$^{AA/AA}$* mice, slightly longer survival in *β-cat^{CA}Ikkα$^{\Delta IEC}$* mice may also be the result of complete abrogation of alternative NF-κB signaling in epithelial cells. One evidence is the base line activation of p52 which is still present in *β-cat^{CA}Ikkα$^{AA/AA}$* mice (most probably due to baseline kinase activity of IKKα also consider that alternative signaling is specifically activated with certain receptors). Therefore, alternative NF-κB activation may also contribute the extended survival in *Ikkα$^{AA/AA}$* mice but most probably by a different mechanism which needs to be verified with further experimentation with 15 day samples.

Another important point to be clarified is the absence of adaptive immune responses regardless of myeloid cell activation and increased IL-12 levels. It was previously shown that superrepression of NF-κB activation in T-cells has retarded Th1 subset development in lymphocytes and reduced Th1 specific expression of IFNγ and IL-12 (Aronica et al., 1999; Seetharaman et al., 1999). Moreover, lymphocytes preferentially shifted towards Th2 in the absence of NF-κB activation (Aronica et al., 1999). These observations suggest that IKKα can also suppress Th1 activation which may be unrelated to its kinase activity yet promoter specific structural role can be important. Still detailed analysis of NF-κB activation in T-cells should be examined to derive further conclusions.

In this thesis, it was shown that kinase specific role of IKKα is responsible for elongated promoter binding of NF-κB on certain gene promoters. Therefore, inactivation of IKKα leads to elongated promoter binding of NF-κB in IECs to promote proinflammatory chemokine production leading to better attraction of monocytes. Similarly, absence of IKKα activation in myeloid cells most probably trigger longer NF-κB promoter binding which induce cell intrinsic factors like MCP-1 and IL-12. Coupled to IKDC derived IFNγ, these factors further promote macrophages to amplify and impose their IFNγ producing effect better without increase in expression (which also needs to be clarified). Recent literature was suggesting the kinase specific role is governing the prolonged NF-κB promoter binding while structural role is required for proper functioning of NF-κB itself. Therefore, kinase specific role of IKKα suppresses prolonged NF-κB binding to resolve inflammation. While structural role is important in APC activation, still it may suppress Th1 activation and adaptive immune responses. By the use of T-cell specific IKKα abrogation it may be possible to reach better tumor suppression in $\beta\text{-}cat^{CA}Ikk\alpha^{AA/AA}$ mice.

6. CONCLUSION

Here we presented evidence for tumor promoting role of IKKα in the development of CRC by the suppression of immune activation at different levels. By the use of activation deficient IKKα mutants in three different genetic and pharmacologic CRC models, we identified a distinct phenotype of tumor retardation due to cell cycle arrest resulting in extended survival of the animals. These results strongly suggested a tumor promoting function for IKKα in normal intestinal tumorigenesis with a model independent manner. By further investigations to understand molecular machinery we have shown that this tumor promoting effect of IKKα is most probably due to its NF-κB suppressive role to resolve elongated inflammation. According to our model (figure 6.1), IKKα suppresses elongated NF-κB promoter activity in hyperproliferating IECs to block proinflammatory immune responses by acting separately in enterocytes and myeloid cells.

In the absence of IKKα phospho-activation, prolonged NF-κB activity enhanced expression of a set of monocyte chemoattractants secreted by hyperproliferating enterocytes to facilitate recruitment of myeloid cells to the site of hyperproliferation. Furthermore, prolonged NF-κB activation in myeloid cells induced upregulation of intrinsic factors like MCP-1 and IL-12 for autocrine activation of already recruited myeloid cells to expand in numbers and to produce IFNγ. Regardless of the absence of adaptive immune activation and tumor specific cytotoxicity, increased numbers of IFNγ producing myeloid cells built up a sufficient pool of IFNγ to suppress tumor growth in IECs.

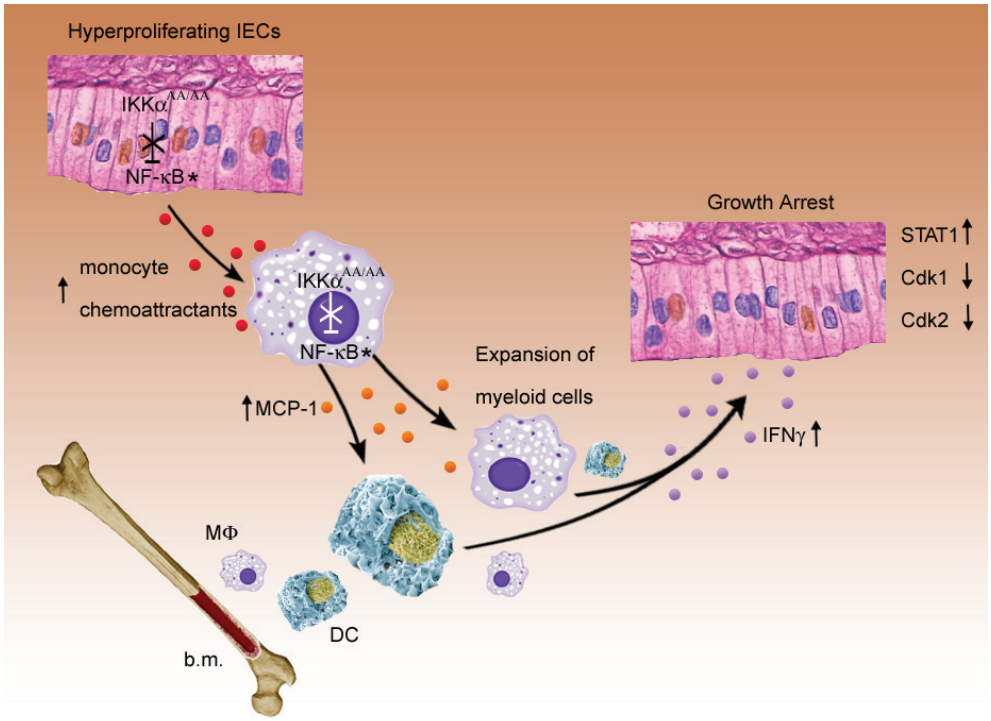

Figure 6.1: Proposed Mechanism of IKKα Involvement in CRC.

In conclusion, here it has been shown that anti-inflammatory role of IKKα to limit macrophage activation has a profound role in initiation and progression of colorectal tumorigenesis. Although this effect mostly depends on direct suppression of myeloid activation to block increased levels of IFNγ production, suppression of epithelial cells to block myeloid cell chemoattraction also has a crucial contribution in preventing amplification of tumor specific immune responses. Therefore, we provided evidence that specific inhibition of IKKα activation can be a potent therapeutic target for inhibiting colorectal tumor growth. Even coupled to adaptive immune activation to induce tumor cytotoxicity and tumor lysis, specific phospho-inactivation of IKKα may prove to be a powerful strategy to overcome colorectal tumors.

7. REFERENCES

Agou, F., Ye, F, Goffinont, S, Courtois, G, Yamaoka, S, Israël, A and Véron, M. (2002). NEMO trimerizes through its coiled-coil C-terminal domain. *J Biol Chem*, **277**, 17464-17475.

Albanese, C., Wu, K, D'Amico, M, Jarrett, C, Joyce, D, Hughes, J, Hulit, J, Sakamaki, T, Fu, M, Ben-Ze'ev, A, Bromberg, J.F, Lamberti, C, Verma, U, Gaynor, R.B, Byers, S.W and Pestell, R.G. (2003). IKKalpha regulates mitogenic signaling through transcriptional induction of cyclin D1 via Tcf. *Mol Biol Cell*, **14**, 585-599.

Amit, S., Hatzubai, A, Birman, Y, Andersen, J.S, Ben-Shushan, E, Mann, M, Ben-Neriah, Y and Alkalay, I. (2002). Axin-mediated CKI phosphorylation of beta-catenin at Ser 45: a molecular switch for the Wnt pathway. *Genes Dev*, **16**, 1066-1076.

Andreu, P., Colnot, S, Godard, C, Gad, S, Chafey, P, Niwa-Kawakita, M, Laurent-Puig, P, Kahn, A, Robine, S, Perret, C and Romagnolo, B. (2005). Crypt-restricted proliferation and commitment to the Paneth cell lineage following Apc loss in the mouse intestine. *Development*, **132**, 1443-1451.

Arnott, C.H., Scott, K.A, Moore, R.J, Hewer, A, Phillips, D.H, Parker, P, Balkwill, F.R and Owens, D.M. (2002). Tumour necrosis factor-alpha mediates tumour promotion via a PKC alpha- and AP-1-dependent pathway. *Oncogene*, **21**, 4728-4738.

Aronica, M.A., Mora, A.L, Mitchell, D.B, Finn, P.W, Johnson, J.E, Sheller, J.R and Boothby, M.R. (1999). Preferential role for NF-kappa B/Rel signaling in the type 1 but not type 2 T cell-dependent immune response in vivo. *J Immunol*, **163**, 5116-5124.

Baeuerle P.A., Baltimore D. (1996). NF-kappa B: ten years after. *Cell* , **87** (1), 13-20.

Baldwin, A.S.J.. (1996). The NF-kappa B and I kappa B proteins: new discoveries and insights. *Annu Rev Immunol*, **14**, 649-683.

Balkwill, F. and Mantovani, A. (2001). Inflammation and cancer: back to Virchow?. *Lancet*, **357**, 539-545.

Barker, N., van Es, J.H, Kuipers, J, Kujala, P, van den Born, M, Cozijnsen, M, Haegebarth, A, Korving, J, Begthel, H, Peters, P.J and Clevers, H. (2007). Identification of stem cells in small intestine and colon by marker gene Lgr5. *Nature*, **449**, 1003-1007.

REFERENCES

Batlle, E., Henderson, J.T, Beghtel, H, van den Born, M.M.W, Sancho, E, Huls, G, Meeldijk, J, Robertson, J, van de Wetering, M, Pawson, T and Clevers, H. (2002). Beta-catenin and TCF mediate cell positioning in the intestinal epithelium by controlling the expression of EphB/ephrinB. *Cell*, **111**, 251-263.

Beckhove, P., Feuerer, M, Dolenc, M, Schuetz, F, Choi, C, Sommerfeldt, N, Schwendemann, J, Ehlert, K, Altevogt, P, Bastert, G, Schirrmacher, V and Umansky, V. (2004). Specifically activated memory T cell subsets from cancer patients recognize and reject xenotransplanted autologous tumors. *J Clin Invest*, **114**, 67-76.

Behrens, J., von Kries, J.P, Kühl, M, Bruhn, L, Wedlich, D, Grosschedl, R and Birchmeier, W. (1996). Functional interaction of beta-catenin with the transcription factor LEF-1. *Nature*, **382**, 638-642.

Billiau, A., Heremans, H, Vandekerckhove, F, Dijkmans, R, Sobis, H, Meulepas, E and Carton, H. (1988). Enhancement of experimental allergic encephalomyelitis in mice by antibodies against IFN-gamma. *J Immunol*, **140**, 1506-1510.

Bollrath, J., Phesse, T.J, von Burstin, V.A, Putoczki, T, Bennecke, M, Bateman, T, Nebelsiek, T, Lundgren-May, T, Canli, O, Schwitalla, S, Matthews, V, Schmid, R.M, Kirchner, T, Arkan, M.C, Ernst, M and Greten, F.R. (2009). gp130-mediated Stat3 activation in enterocytes regulates cell survival and cell-cycle progression during colitis-associated tumorigenesis. *Cancer Cell*, **15**, 91-102.

Bonizzi, G. and Karin, M. (2004). The two NF-kappaB activation pathways and their role in innate and adaptive immunity. *Trends Immunol*, **25**, 280-288.

Boxem, M., Srinivasan, D.G and van den Heuvel, S. (1999). The Caenorhabditis elegans gene ncc-1 encodes a cdc2-related kinase required for M phase in meiotic and mitotic cell divisions, but not for S phase. *Development*, **126**, 2227-2239.

Brandes, M., Willimann, K and Moser, B. (2005). Professional antigen-presentation function by human gammadelta T Cells. *Science*, **309**, 264-268.

Brucet, M., Marqués, L, Sebastián, C, Lloberas, J and Celada, A. (2004). Regulation of murine Tap1 and Lmp2 genes in macrophages by interferon gamma is mediated by STAT1 and IRF-1. *Genes Immun*, **5**, 26-35.

Burke, F., East, N, Upton, C, Patel, K and Balkwill, F.R. (1997). Interferon gamma induces cell cycle arrest and apoptosis in a model of ovarian cancer: enhancement of effect by batimastat. *Eur J Cancer*, **33**, 1114-1121.

Burnet, F.M.. (1958). The biology of the cancer cell. *Fed Proc*, **17**, 687-690.

Caderni, G., De Flippino, D, Luceri, C, Briani, C, Fazi, M, Dolara, P and Bazzicalupo, M. (1997). *APC mutations in aberrant crypt foci and colonic tumors induced by azomethane in rats*. AACR, San Diego, CA.

Cahill, D.P., Kinzler, K.W, Vogelstein, B and Lengauer, C. (1999). Genetic instability and darwinian selection in tumours. *Trends Cell Biol*, **9**, M57-60.

References

Cahill, D.P., Lengauer, C, Yu, J, Riggins, G.J, Willson, J.K, Markowitz, S.D, Kinzler, K.W and Vogelstein, B. (1998). Mutations of mitotic checkpoint genes in human cancers. *Nature*, **392**, 300-303.

Cambiaggi, C., Scupoli, M.T, Cestari, T, Gerosa, F, Carra, G, Tridente, G and Accolla, R.S. (1992). Constitutive expression of CD69 in interspecies T-cell hybrids and locus assignment to human chromosome 12. *Immunogenetics*, **36**, 117-120.

Cao, Y., Bonizzi, G, Seagroves, T.N, Greten, F.R, Johnson, R, Schmidt, E.V and Karin, M. (2001). IKKalpha provides an essential link between RANK signaling and cyclin D1 expression during mammary gland development. *Cell*, **107**, 763-775.

Capecchi, M.R.. (1989). Altering the genome by homologous recombination. *Science*, **244**, 1288-1292.

Carayol, N. and Wang, C. (2006). IKKalpha stabilizes cytosolic beta-catenin by inhibiting both canonical and non-canonical degradation pathways. *Cell Signal*, **18**, 1941-1946.

Chariot, A.. (2009). The NF-kappaB-independent functions of IKK subunits in immunity and cancer. *Trends Cell Biol*, **19** (8), 404-413 .

Chen, L., Egan, L, Li, Z, Greten, F.R, Kagnoff, M.F and Karin, M. (2003). The two faces of IKK and NF-kappaB inhibition: prevention of systemic inflammation but increased local injury following intestinal ischemia-reperfusion. *Nat Med*, **9**, 575-581.

Chen, W., ten Berge, D, Brown, J, Ahn, S, Hu, L.A, Miller, W.E, Caron, M.G, Barak, L.S, Nusse, R and Lefkowitz, R.J. (2003). Dishevelled 2 recruits beta-arrestin 2 to mediate Wnt5A-stimulated endocytosis of Frizzled 4. *Science*, **301**, 1391-1394.

Chu, Z.L., McKinsey, T.A, Liu, L, Gentry, J.J, Malim, M.H and Ballard, D.W. (1997). Suppression of tumor necrosis factor-induced cell death by inhibitor of apoptosis c-IAP2 is under NF-kappaB control. *Proc Natl Acad Sci U S A*, **94**, 10057-10062.

Clarke, A.R.. (2006). Wnt signalling in the mouse intestine. *Oncogene*, **25**, 7512-7521.

Claudio, E., Brown, K, Park, S, Wang, H and Siebenlist, U. (2002). BAFF-induced NEMO-independent processing of NF-kappa B2 in maturing B cells. *Nat Immunol*, **3**, 958-965.

Clauss, I.M., Wathelet, M.G, Szpirer, J, Content, J, Islam, M.Q, Levan, G, Szpirer, C and Huez, G.A. (1990). Chromosomal localization of two human genes inducible by interferons, double-stranded RNA, and viruses. *Cytogenet Cell Genet*, **53**, 166-168.

Condeelis, J. and Pollard, J.W. (2006). Macrophages: obligate partners for tumor cell migration, invasion, and metastasis. *Cell*, **124**, 263-266.

Coope, H.J., Atkinson, P.G.P, Huhse, B, Belich, M, Janzen, J, Holman, M.J, Klaus, G.G.B, Johnston, L.H and Ley, S.C. (2002). CD40 regulates the processing of NF-kappaB2 p100 to p52. *EMBO J*, **21**, 5375-5385.

Curcio, C., Di Carlo, E, Clynes, R, Smyth, M.J, Boggio, K, Quaglino, E, Spadaro, M, Colombo, M.P, Amici, A, Lollini, P, Musiani, P and Forni, G. (2003). Nonredundant roles of antibody, cytokines, and perforin in the eradication of established Her-2/neu carcinomas. *J Clin Invest*, **111**, 1161-1170.

Curiel, T.J., Coukos, G, Zou, L, Alvarez, X, Cheng, P, Mottram, P, Evdemon-Hogan, M, Conejo-Garcia, J.R, Zhang, L, Burow, M, Zhu, Y, Wei, S, Kryczek, I, Daniel, B, Gordon, A, Myers, L, Lackner, A, Disis, M.L, Knutson, K.L, Chen, L and Zou, W. (2004). Specific recruitment of regulatory T cells in ovarian carcinoma fosters immune privilege and predicts reduced survival. *Nat Med*, **10**, 942-949.

Dalton, D.K., Pitts-Meek, S, Keshav, S, Figari, I.S, Bradley, A and Stewart, T.A. (1993). Multiple defects of immune cell function in mice with disrupted interferon-gamma genes. *Science*, **259**, 1739-1742.

Darrasse-Jèze G, Bergot AS, Durgeau A, Billiard F, Salomon BL, Cohen JL, Bellier B, Podsypanina K, Klatzmann D.(2009). Tumor emergence is sensed by self-specific CD44hi memory Tregs that create a dominant tolerogenic environment for tumors in mice. *J Clin Invest.* **119**(9):2648-2662

Dejardin, E., Droin, N.M, Delhase, M, Haas, E, Cao, Y, Makris, C, Li, Z, Karin, M, Ware, C.F and Green, D.R. (2002). The lymphotoxin-beta receptor induces different patterns of gene expression via two NF-kappaB pathways. *Immunity*, **17**, 525-535.

Delhase, M., Hayakawa, M, Chen, Y and Karin, M. (1999). Positive and negative regulation of IkappaB kinase activity through IKKbeta subunit phosphorylation. *Science*, **284**, 309-313.

Der, S.D., Zhou, A, Williams, B.R and Silverman, R.H. (1998). Identification of genes differentially regulated by interferon alpha, beta, or gamma using oligonucleotide arrays. *Proc Natl Acad Sci U S A*, **95**, 15623-15628.

Descargues, P., Sil, A.K and Karin, M. (2008). IKKalpha, a critical regulator of epidermal differentiation and a suppressor of skin cancer. *EMBO J*, **27**, 2639-2647.

Dhodapkar, K.M., Krasovsky, J, Williamson, B and Dhodapkar, M.V. (2002). Antitumor monoclonal antibodies enhance cross-presentation ofcCellular antigens and the generation of myeloma-specific killer T cells by dendritic cells. *J Exp Med*, **195**, 125-133.

Di Marzio, P., Puddu, P, Conti, L, Belardelli, F and Gessani, S. (1994). Interferon gamma upregulates its own gene expression in mouse peritoneal macrophages. *J Exp Med*, **179**, 1731-1736.

Druckrey, H. and Lange, A. (1972). Carcinogenicity of azoxymethane dependent on age in BD rats. *Fed Proc*, **31**, 1482-1484.

Dunn, G.P., Bruce, A.T, Ikeda, H, Old, L.J and Schreiber, R.D. (2002). Cancer immunoediting: from immunosurveillance to tumor escape. *Nat Immunol*, **3**, 991-998.

Dunn, G.P., Old, L.J and Schreiber, R.D. (2004). The immunobiology of cancer immunosurveillance and immunoediting. *Immunity*, **21**, 137-148.

Eckmann, L., Nebelsiek, T, Fingerle, A.A, Dann, S.M, Mages, J, Lang, R, Robine, S, Kagnoff, M.F, Schmid, R.M, Karin, M, Arkan, M.C and Greten, F.R. (2008). Opposing functions of IKKbeta during acute and chronic intestinal inflammation. *Proc Natl Acad Sci U S A*, **105**, 15058-15063.

Egan, L.J., Eckmann, L, Greten, F.R, Chae, S, Li, Z, Myhre, G.M, Robine, S, Karin, M and Kagnoff, M.F. (2004). IkappaB-kinasebeta-dependent NF-kappaB activation provides radioprotection to the intestinal epithelium. *Proc Natl Acad Sci U S A*, **101**, 2452-2457.

Ekbom, A.. (1998). Risk of cancer in ulcerative colitis. *J Gastrointest Surg*, **2**, 312-313.

El Marjou, F., Janssen, K, Chang, B.H, Li, M, Hindie, V, Chan, L, Louvard, D, Chambon, P, Metzger, D and Robine, S. (2004). Tissue-specific and inducible Cre-mediated recombination in the gut epithelium. *Genesis*, **39**, 186-193.

Elwood, P.C., Gallagher, A.M, Duthie, G.G, Mur, L.A.J and Morgan, G. (2009). Aspirin, salicylates, and cancer. *Lancet*, **373**, 1301-1309.

Evans, M.J. and Kaufman, M.H. (1981). Establishment in culture of pluripotential cells from mouse embryos. *Nature*, **292**, 154-156.

Exner, M., Hartemann, P and Kistemann, T. (2001). Hygiene and health - the need for a holistic approach. *Am J Infect Control*, **29**, 228-231.

Fattovich, G., Stroffolini, T, Zagni, I and Donato, F. (2004). Hepatocellular carcinoma in cirrhosis: incidence and risk factors. *Gastroenterology*, **127**, S35-50.

Fausto, N.. (1999). Mouse liver tumorigenesis: models, mechanisms, and relevance to human disease. *Semin Liver Dis*, **19**, 243-252.

Fearon, E.R. and Vogelstein, B. (1990). A genetic model for colorectal tumorigenesis. *Cell*, **61**, 759-767.

Fingerle, A.A., Schwitalla, S, Göktuna, S.I, Rupec, R.A, Gerhard, M, Lang, R, Schmid, R.M, Taketo, M.M, Arkan, M.C and Greten, F.R. (2009). NF-kappaB and constitutive Wnt-activation cooperate to induce crypt stem cell expansion during initiation of intestinal tumorigenesis. *In progress*, , .

Fiorentino, D.F., Bond, M.W and Mosmann, T.R. (1989). Two types of mouse T helper cell. IV. Th2 clones secrete a factor that inhibits cytokine production by Th1 clones. *J Exp Med*, **170**, 2081-2095.

Fodde, R., Smits, R and Clevers, H. (2001). APC, signal transduction and genetic instability in colorectal cancer. *Nat Rev Cancer*, **1**, 55-67.

Freese, E.. (1959). The difference between spontaneous and base-analogue induced mutations of phage T4. *Proc Natl Acad Sci U S A*, **45**, 622-633.

Furuichi, K., Wada, T, Iwata, Y, Kokubo, S, Hara, A, Yamahana, J, Sugaya, T, Iwakura, Y, Matsushima, K, Asano, M, Yokoyama, H and Kaneko, S. (2006). Interleukin-1-dependent sequential chemokine expression and inflammatory cell infiltration in ischemia-reperfusion injury. *Crit Care Med*, **34**, 2447-2455.

Gardner, E.J.. (1951). A genetic and clinical study of intestinal polyposis, a predisposing factor for carcinoma of the colon and rectum. *Am J Hum Genet*, **3**, 167-176.

Gareus, R., Huth, M, Breiden, B, Nenci, A, Rösch, N, Haase, I, Bloch, W, Sandhoff, K and Pasparakis, M. (2007). Normal epidermal differentiation but impaired skin-barrier formation upon keratinocyte-restricted IKK1 ablation. *Nat Cell Biol*, **9**, 461-469.

Ghosh, S., May, M.J and Kopp, E.B. (1998). NF-kappa B and Rel proteins: evolutionarily conserved mediators of immune responses. *Annu Rev Immunol*, **16**, 225-260.

Gilmore, T.D.. (1999). The Rel/NF-kappaB signal transduction pathway: introduction. *Oncogene*, **18**, 6842-6844.

Girardi, M., Oppenheim, D.E, Steele, C.R, Lewis, J.M, Glusac, E, Filler, R, Hobby, P, Sutton, B, Tigelaar, R.E and Hayday, A.C. (2001). Regulation of cutaneous malignancy by gammadelta T cells. *Science*, **294**, 605-609.

Gloire, G., Horion, J, El Mjiyad, N, Bex, F, Chariot, A, Dejardin, E and Piette, J. (2007). Promoter-dependent effect of IKKalpha on NF-kappaB/p65 DNA binding. *J Biol Chem*, **282**, 21308-21318.

Goldstein, D. and Laszlo, J. (1988). The role of interferon in cancer therapy: a current perspective. *CA Cancer J Clin*, **38**, 258-277.

Gregorieff, A. and Clevers, H. (2005). Wnt signaling in the intestinal epithelium: from endoderm to cancer. *Genes Dev*, **19**, 877-890.

Greten, F.R. and Karin, M. (2004). The IKK/NF-kappaB activation pathway-a target for prevention and treatment of cancer. *Cancer Lett*, **206**, 193-199.

Greten, F.R., Arkan, M.C, Bollrath, J, Hsu, L, Goode, J, Miething, C, Göktuna, S.I, Neuenhahn, M, Fierer, J, Paxian, S, Van Rooijen, N, Xu, Y, O'Cain, T, Jaffee, B.B, Busch, D.H, Duyster, J, Schmid, R.M, Eckmann, L and Karin, M. (2007). NF-kappaB is a negative regulator of IL-1beta secretion as revealed by genetic and pharmacological inhibition of IKKbeta. *Cell*, **130**, 918-931.

Greten, F.R., Eckmann, L, Greten, T.F, Park, J.M, Li, Z, Egan, L.J, Kagnoff, M.F and Karin, M. (2004). IKKbeta links inflammation and tumorigenesis in a mouse model of colitis-associated cancer. *Cell*, **118**, 285-296.

Grivennikov, S., Karin, E, Terzic, J, Mucida, D, Yu, G, Vallabhapurapu, S, Scheller, J, Rose-John, S, Cheroutre, H, Eckmann, L and Karin, M. (2009). IL-6 and Stat3 are required for survival of intestinal epithelial cells and development of colitis-associated cancer. *Cancer Cell*, **15**, 103-113.

Groden, J., Thliveris, A, Samowitz, W, Carlson, M, Gelbert, L, Albertsen, H, Joslyn, G, Stevens, J, Spirio, L, Robertson, M and et al.. (1991). Identification and characterization of the familial adenomatous polyposis coli gene. *Cell*, **66**, 589-600.

Guttridge, D.C., Albanese, C, Reuther, J.Y, Pestell, R.G and Baldwin, A.S.J. (1999). NF-kappaB controls cell growth and differentiation through transcriptional regulation of cyclin D1. *Mol Cell Biol*, **19**, 5785-5799.

Habu, S., Fukui, H, Shimamura, K, Kasai, M, Nagai, Y, Okumura, K and Tamaoki, N. (1981). In vivo effects of anti-asialo GM1. I. Reduction of NK activity and enhancement of transplanted tumor growth in nude mice. *J Immunol*, **127**, 34-38.

Harada, N., Tamai, Y, Ishikawa, T, Sauer, B, Takaku, K, Oshima, M and Taketo, M.M. (1999). Intestinal polyposis in mice with a dominant stable mutation of the beta-catenin gene. *EMBO J*, **18**, 5931-5942.

Hasegawa, Y., Takanashi, S, Kanehira, Y, Tsushima, T, Imai, T and Okumura, K. (2001). Transforming growth factor-beta1 level correlates with angiogenesis, tumor progression, and prognosis in patients with nonsmall cell lung carcinoma. *Cancer*, **91**, 964-971.

Hayden, M.S. and Ghosh, S. (2008). Shared principles in NF-kappaB signaling. *Cell*, **132**, 344-362.

Hicks, A.M., Riedlinger, G, Willingham, M.C, Alexander-Miller, M.A, Von Kap-Herr, C, Pettenati, M.J, Sanders, A.M, Weir, H.M, Du, W, Kim, J, Simpson, A.J.G, Old, L.J and Cui, Z. (2006). Transferable anticancer innate immunity in spontaneous regression/complete resistance mice. *Proc Natl Acad Sci U S A*, **103**, 7753-7758.

Hinoi, T., Akyol, A, Theisen, B.K, Ferguson, D.O, Greenson, J.K, Williams, B.O, Cho, K.R and Fearon, E.R. (2007). Mouse model of colonic adenoma-carcinoma progression based on somatic Apc inactivation. *Cancer Res*, **67**, 9721-9730.

Hu, Y., Baud, V, Delhase, M, Zhang, P, Deerinck, T, Ellisman, M, Johnson, R and Karin, M. (1999). Abnormal morphogenesis but intact IKK activation in mice lacking the IKKalpha subunit of IkappaB kinase. *Science*, **284**, 316-320.

Huang, D.R., Wang, J, Kivisakk, P, Rollins, B.J and Ransohoff, R.M. (2001). Absence of monocyte chemoattractant protein 1 in mice leads to decreased local macrophage recruitment and antigen-specific T helper cell type 1 immune response in experimental autoimmune encephalomyelitis. *J Exp Med*, **193**, 713-726.

Huang, S., Pettaway, C.A, Uehara, H, Bucana, C.D and Fidler, I.J. (2001). Blockade of NF-kappaB activity in human prostate cancer cells is associated with suppression of angiogenesis, invasion, and metastasis. *Oncogene*, **20**, 4188-4197.

Huang, S., Robinson, J.B, Deguzman, A, Bucana, C.D and Fidler, I.J. (2000). Blockade of nuclear factor-kappaB signaling inhibits angiogenesis and tumorigenicity of human ovarian cancer cells by suppressing expression of vascular endothelial growth factor and interleukin 8. *Cancer Res*, **60**, 5334-5339.

Huang, W., Ju, T, Hung, M and Chen, C. (2007). Phosphorylation of CBP by IKKalpha promotes cell growth by switching the binding preference of CBP from p53 to NF-kappaB. *Mol Cell*, **26**, 75-87.

Hung, K., Hayashi, R, Lafond-Walker, A, Lowenstein, C, Pardoll, D and Levitsky, H. (1998). The central role of CD4(+) T cells in the antitumor immune response. *J Exp Med*, **188**, 2357-2368.

Hunter, C.A.. (2005). New IL-12-family members: IL-23 and IL-27, cytokines with divergent functions. *Nat Rev Immunol*, **5**, 521-531.

Häcker, H. and Karin, M. (2006). Regulation and function of IKK and IKK-related kinases. *Sci STKE*, **2006**, re13.

Jemal, A., Siegel, R, Ward, E, Hao, Y, Xu, J, Murray, T and Thun, M.J. (2008). Cancer statistics, 2008. *CA Cancer J Clin*, **58**, 71-96.

Jensen, J., Pedersen, E.E, Galante, P, Hald, J, Heller, R.S, Ishibashi, M, Kageyama, R, Guillemot, F, Serup, P and Madsen, O.D. (2000). Control of endodermal endocrine development by Hes-1. *Nat Genet*, **24**, 36-44.

Johnson, L.N., Noble, M.E and Owen, D.J. (1996). Active and inactive protein kinases: structural basis for regulation. *Cell*, **85**, 149-158.

Johnson, R., Lancki, D.W and Fitch, F.W. (1993). Accessory molecules involved in antigen-mediated cytolysis and lymphokine production by cytotoxic T lymphocyte subsets. I. Identification of functions for the T cell surface molecules Ly-6C and Thy-1. *J Immunol*, **151**, 2986-2999.

Kaplan, D.H., Shankaran, V, Dighe, A.S, Stockert, E, Aguet, M, Old, L.J and Schreiber, R.D. (1998). Demonstration of an interferon gamma-dependent tumor surveillance system in immunocompetent mice. *Proc Natl Acad Sci U S A*, **95**, 7556-7561.

Karin, M.. (1990). Too many transcription factors: positive and negative interactions. *New Biol*, **2**, 126-131.

Karin, M.. (2008). The IkappaB kinase - a bridge between inflammation and cancer. *Cell Res*, **18**, 334-342.

Karin, M. and Greten, F.R. (2005). NF-kappaB: linking inflammation and immunity to cancer development and progression. *Nat Rev Immunol*, **5**, 749-759.

Katz, J.P., Perreault, N, Goldstein, B.G, Lee, C.S, Labosky, P.A, Yang, V.W and Kaestner, K.H. (2002). The zinc-finger transcription factor Klf4 is required for terminal differentiation of goblet cells in the colon. *Development*, **129**, 2619-2628.

Kenny, P.A., Enver, T and Ashworth, A. (2005). Receptor and secreted targets of Wnt-1/beta-catenin signalling in mouse mammary epithelial cells. *BMC Cancer*, **5**, 3.

Kim, R., Emi, M, Tanabe, K and Arihiro, K. (2006). Tumor-driven evolution of immunosuppressive networks during malignant progression. *Cancer Res*, **66**, 5527-5536.

Kinzler, K.W., Nilbert, M.C, Su, L.K, Vogelstein, B, Bryan, T.M, Levy, D.B, Smith, K.J, Preisinger, A.C, Hedge, P, McKechnie, D and et al.. (1991). Identification of FAP locus genes from chromosome 5q21. *Science*, **253**, 661-665.

Kitagawa, M., Hatakeyama, S, Shirane, M, Matsumoto, M, Ishida, N, Hattori, K, Nakamichi, I, Kikuchi, A, Nakayama, K and Nakayama, K. (1999). An F-box protein, FWD1, mediates ubiquitin-dependent proteolysis of beta-catenin. *EMBO J*, **18**, 2401-2410.

Kopf, M., Baumann, H, Freer, G, Freudenberg, M, Lamers, M, Kishimoto, T, Zinkernagel, R, Bluethmann, H and Köhler, G. (1994). Impaired immune and acute-phase responses in interleukin-6-deficient mice. *Nature*, **368**, 339-342.

Korinek, V., Barker, N, Morin, P.J, van Wichen, D, de Weger, R, Kinzler, K.W, Vogelstein, B and Clevers, H. (1997). Constitutive transcriptional activation by a beta-catenin-Tcf complex in APC-/- colon carcinoma. *Science*, **275**, 1784-1787.

Kumar, A., Yang, Y.L, Flati, V, Der, S, Kadereit, S, Deb, A, Haque, J, Reis, L, Weissmann, C and Williams, B.R. (1997). Deficient cytokine signaling in mouse embryo fibroblasts with a targeted deletion in the PKR gene: role of IRF-1 and NF-kappaB. *EMBO J*, **16**, 406-416.

Körholz, D., Banning, U, Bönig, H, Grewe, M, Schneider, M, Mauz-Körholz, C, Klein-Vehne, A, Krutmann, J and Burdach, S. (1997). The role of interleukin-10 (IL-10) in IL-15-mediated T-cell responses. *Blood*, **90**, 4513-4521.

Lamberti, C., Lin, K.M, Yamamoto, Y, Verma, U, Verma, I.M, Byers, S and Gaynor, R.B. (2001). Regulation of beta-catenin function by the IkappaB kinases. *J Biol Chem*, **276**, 42276-42286.

Langowski, J.L., Zhang, X, Wu, L, Mattson, J.D, Chen, T, Smith, K, Basham, B, McClanahan, T, Kastelein, R.A and Oft, M. (2006). IL-23 promotes tumour incidence and growth. *Nature*, **442**, 461-465.

Latchman, D.S.. (1997). Transcription factors: an overview. *Int J Biochem Cell Biol*, **29**, 1305-1312.

Lawrence, T., Bebien, M, Liu, G.Y, Nizet, V and Karin, M. (2005). IKKalpha limits macrophage NF-kappaB activation and contributes to the resolution of inflammation. *Nature*, **434**, 1138-1143.

Li, A.G., Lu, S, Han, G, Hoot, K.E and Wang, X. (2006). Role of TGFbeta in skin inflammation and carcinogenesis. *Mol Carcinog*, **45**, 389-396.

Li, M., Carpio, D.F, Zheng, Y, Bruzzo, P, Singh, V, Ouaaz, F, Medzhitov, R.M and Beg, A.A. (2001). An essential role of the NF-kappa B/Toll-like receptor pathway in induction of inflammatory and tissue-repair gene expression by necrotic cells. *J Immunol*, **166**, 7128-7135.

Li, Q., Lu, Q, Bottero, V, Estepa, G, Morrison, L, Mercurio, F and Verma, I.M. (2005). Enhanced NF-kappaB activation and cellular function in macrophages lacking IkappaB kinase 1 (IKK1). *Proc Natl Acad Sci U S A*, **102**, 12425-12430.

Lin, E.Y., Gouon-Evans, V, Nguyen, A.V and Pollard, J.W. (2002). The macrophage growth factor CSF-1 in mammary gland development and tumor progression. *J Mammary Gland Biol Neoplasia*, **7**, 147-162.

Ling, L., Cao, Z and Goeddel, D.V. (1998). NF-kappaB-inducing kinase activates IKK-alpha by phosphorylation of Ser-176. *Proc Natl Acad Sci U S A*, **95**, 3792-3797.

Liu, B., Park, E, Zhu, F, Bustos, T, Liu, J, Shen, J, Fischer, S.M and Hu, Y. (2006). A critical role for I kappaB kinase alpha in the development of human and mouse squamous cell carcinomas. *Proc Natl Acad Sci U S A*, **103**, 17202-17207.

Liu, B., Xia, X, Zhu, F, Park, E, Carbajal, S, Kiguchi, K, DiGiovanni, J, Fischer, S.M and Hu, Y. (2008). IKKalpha is required to maintain skin homeostasis and prevent skin cancer. *Cancer Cell*, **14**, 212-225.

Liu, C., Li, Y, Semenov, M, Han, C, Baeg, G.H, Tan, Y, Zhang, Z, Lin, X and He, X. (2002). Control of beta-catenin phosphorylation/degradation by a dual-kinase mechanism. *Cell*, **108**, 837-847.

Liyanage, U.K., Moore, T.T, Joo, H, Tanaka, Y, Herrmann, V, Doherty, G, Drebin, J.A, Strasberg, S.M, Eberlein, T.J, Goedegebuure, P.S and Linehan, D.C. (2002). Prevalence of regulatory T cells is increased in peripheral blood and tumor microenvironment of patients with pancreas or breast adenocarcinoma. *J Immunol*, **169**, 2756-2761.

Lu, B., Rutledge, B.J, Gu, L, Fiorillo, J, Lukacs, N.W, Kunkel, S.L, North, R, Gerard, C and Rollins, B.J. (1998). Abnormalities in monocyte recruitment and cytokine expression in monocyte chemoattractant protein 1-deficient mice. *J Exp Med*, **187**, 601-608.

Luo, J., Tan, W, Ricono, J.M, Korchynskyi, O, Zhang, M, Gonias, S.L, Cheresh, D.A and Karin, M. (2007). Nuclear cytokine-activated IKKalpha controls prostate cancer metastasis by repressing Maspin. *Nature*, **446**, 690-694.

Luster, A.D., Unkeless, J.C and Ravetch, J.V. (1985). Gamma-interferon transcriptionally regulates an early-response gene containing homology to platelet proteins. *Nature*, **315**, 672-676.

Luu, N.T., Rainger, G.E and Nash, G.B. (2000). Differential ability of exogenous chemotactic agents to disrupt transendothelial migration of flowing neutrophils. *J Immunol*, **164**, 5961-5969.

Ma, B., Zhu, Z, Homer, R.J, Gerard, C, Strieter, R and Elias, J.A. (2004). The C10/CCL6 chemokine and CCR1 play critical roles in the pathogenesis of IL-13-induced inflammation and remodeling. *J Immunol*, **172**, 1872-1881.

MacQueen, J.. (1967). *Some methods for classification and analysis of multivariate observations*. Uni. of Calif. Press.

Maeda, S., Chang, L, Li, Z, Luo, J, Leffert, H and Karin, M. (2003). IKKbeta is required for prevention of apoptosis mediated by cell-bound but not by circulating TNFalpha. *Immunity*, **19**, 725-737.

Maeda, S., Kamata, H, Luo, J, Leffert, H and Karin, M. (2005). IKKbeta couples hepatocyte death to cytokine-driven compensatory proliferation that promotes chemical hepatocarcinogenesis. *Cell*, **121**, 977-990.

Martinez, F.O., Sica, A, Mantovani, A and Locati, M. (2008). Macrophage activation and polarization. *Front Biosci*, **13**, 453-461.

Martínez, M.E., Marshall, J.R and Giovannucci, E. (2008). Diet and cancer prevention: the roles of observation and experimentation. *Nat Rev Cancer*, **8**, 694-703.

Massagué, J.. (1998). TGF-beta signal transduction. *Annu Rev Biochem*, **67**, 753-791.

Matsuyama, T., Kimura, T, Kitagawa, M, Pfeffer, K, Kawakami, T, Watanabe, N, Kündig, T.M, Amakawa, R, Kishihara, K, Wakeham, A and et al.. (1993). Targeted disruption of IRF-1 or IRF-2 results in abnormal type I IFN gene induction and aberrant lymphocyte development. *Cell*, **75**, 83-97.

Mattner, F., Magram, J, Ferrante, J, Launois, P, Di Padova, K, Behin, R, Gately, M.K, Louis, J.A and Alber, G. (1996). Genetically resistant mice lacking interleukin-12 are susceptible to infection with Leishmania major and mount a polarized Th2 cell response. *Eur J Immunol*, **26**, 1553-1559.

May, M.J., D'Acquisto, F, Madge, L.A, Glöckner, J, Pober, J.S and Ghosh, S. (2000). Selective inhibition of NF-kappaB activation by a peptide that blocks the interaction of NEMO with the IkappaB kinase complex. *Science*, **289**, 1550-1554.

May, M.J., Marienfeld, R.B and Ghosh, S. (2002). Characterization of the Ikappa B-kinase NEMO binding domain. *J Biol Chem*, **277**, 45992-46000.

McConnell, B.B. and Yang, V.W. (2009). The Role of Inflammation in the Pathogenesis of Colorectal Cancer. *Curr Colorectal Cancer Rep*, **5**, 69-74.

Mercurio, F., Zhu, H, Murray, B.W, Shevchenko, A, Bennett, B.L, Li, J, Young, D.B, Barbosa, M, Mann, M, Manning, A and Rao, A. (1997). IKK-1 and IKK-2: cytokine-activated IkappaB kinases essential for NF-kappaB activation. *Science*, **278**, 860-866.

Mimori-Kiyosue, Y., Shiina, N and Tsukita, S. (2000). Adenomatous polyposis coli (APC) protein moves along microtubules and concentrates at their growing ends in epithelial cells. *J Cell Biol*, **148**, 505-518.

Miyamoto, S. and Verma, I.M. (1995). Rel/NF-kappa B/I kappa B story. *Adv Cancer Res*, **66**, 255-292.

Moore, R.J., Owens, D.M, Stamp, G, Arnott, C, Burke, F, East, N, Holdsworth, H, Turner, L, Rollins, B, Pasparakis, M, Kollias, G and Balkwill, F. (1999). Mice deficient in tumor necrosis factor-alpha are resistant to skin carcinogenesis. *Nat Med*, **5**, 828-831.

Morin, P.J., Sparks, A.B, Korinek, V, Barker, N, Clevers, H, Vogelstein, B and Kinzler, K.W. (1997). Activation of beta-catenin-Tcf signaling in colon cancer by mutations in beta-catenin or APC. *Science*, **275**, 1787-1790.

Moser, A.R., Pitot, H.C and Dove, W.F. (1990). A dominant mutation that predisposes to multiple intestinal neoplasia in the mouse. *Science*, **247**, 322-324.

Muncan, V., Sansom, O.J, Tertoolen, L, Phesse, T.J, Begthel, H, Sancho, E, Cole, A.M, Gregorieff, A, de Alboran, I.M, Clevers, H and Clarke, A.R. (2006). Rapid loss of intestinal crypts upon conditional deletion of the Wnt/Tcf-4 target gene c-Myc. *Mol Cell Biol*, **26**, 8418-8426.

Munder, M., Mallo, M, Eichmann, K and Modolell, M. (1998). Murine macrophages secrete interferon gamma upon combined stimulation with interleukin (IL)-12 and IL-18: A novel pathway of autocrine macrophage activation. *J Exp Med*, **187**, 2103-2108.

Munemitsu, S., Souza, B, Müller, O, Albert, I, Rubinfeld, B and Polakis, P. (1994). The APC gene product associates with microtubules in vivo and promotes their assembly in vitro. *Cancer Res*, **54**, 3676-3681.

Müller, U., Steinhoff, U, Reis, L.F, Hemmi, S, Pavlovic, J, Zinkernagel, R.M and Aguet, M. (1994). Functional role of type I and type II interferons in antiviral defense. *Science*, **264**, 1918-1921.

Naugler, W.E., Sakurai, T, Kim, S, Maeda, S, Kim, K, Elsharkawy, A.M and Karin, M. (2007). Gender disparity in liver cancer due to sex differences in MyD88-dependent IL-6 production. *Science*, **317**, 121-124.

Nenci, A., Becker, C, Wullaert, A, Gareus, R, van Loo, G, Danese, S, Huth, M, Nikolaev, A, Neufert, C, Madison, B, Gumucio, D, Neurath, M.F and Pasparakis, M. (2007). Epithelial NEMO links innate immunity to chronic intestinal inflammation. *Nature*, **446**, 557-561.

Ng, A.Y., Waring, P, Ristevski, S, Wang, C, Wilson, T, Pritchard, M, Hertzog, P and Kola, I. (2002). Inactivation of the transcription factor Elf3 in mice results in dysmorphogenesis and altered differentiation of intestinal epithelium. *Gastroenterology*, **122**, 1455-1466.

Oshima, M., Dinchuk, J.E, Kargman, S.L, Oshima, H, Hancock, B, Kwong, E, Trzaskos, J.M, Evans, J.F and Taketo, M.M. (1996). Suppression of intestinal polyposis in Apc delta716 knockout mice by inhibition of cyclooxygenase 2 (COX-2). *Cell*, **87**, 803-809.

Pahl, H.L.. (1999). Activators and target genes of Rel/NF-kappaB transcription factors. *Oncogene*, **18**, 6853-6866.

Park, J.M., Greten, F.R, Li, Z and Karin, M. (2002). Macrophage apoptosis by anthrax lethal factor through p38 MAP kinase inhibition. *Science*, **297**, 2048-2051.

Parkin, D.M., Bray, F, Ferlay, J and Pisani, P. (2005). Global cancer statistics, 2002. *CA Cancer J Clin*, **55**, 74-108.

Paxian, S., Merkle, H, Riemann, M, Wilda, M, Adler, G, Hameister, H, Liptay, S, Pfeffer, K and Schmid, R.M. (2002). Abnormal organogenesis of Peyer's patches in mice deficient for NF-kappaB1, NF-kappaB2, and Bcl-3. *Gastroenterology*, **122**, 1853-1868.

Pham, C.G., Bubici, C, Zazzeroni, F, Papa, S, Jones, J, Alvarez, K, Jayawardena, S, De Smaele, E, Cong, R, Beaumont, C, Torti, F.M, Torti, S.V and Franzoso, G. (2004). Ferritin heavy chain upregulation by NF-kappaB inhibits TNFalpha-induced apoptosis by suppressing reactive oxygen species. *Cell*, **119**, 529-542.

Pinto, D. and Clevers, H. (2005). Wnt, stem cells and cancer in the intestine. *Biol Cell*, **97**, 185-196.

Pinto, D., Gregorieff, A, Begthel, H and Clevers, H. (2003). Canonical Wnt signals are essential for homeostasis of the intestinal epithelium. *Genes Dev*, **17**, 1709-1713.

Potter, J.D.. (1999). Colorectal cancer: molecules and populations. *J Natl Cancer Inst*, **91**, 916-932.

Powell, S.M., Zilz, N, Beazer-Barclay, Y, Bryan, T.M, Hamilton, S.R, Thibodeau, S.N, Vogelstein, B and Kinzler, K.W. (1992). APC mutations occur early during colorectal tumorigenesis. *Nature*, **359**, 235-237.

Prendergast, G.C. and Jaffee, E.M. (2007). *Cancer Immunotherapy: Immune Supression and Tumor Growth*. Academic Press, Baltimore, MD.

Preston, S.L., Wong, W, Chan, A.O, Poulsom, R, Jeffery, R, Goodlad, R.A, Mandir, N, Elia, G, Novelli, M, Bodmer, W.F, Tomlinson, I.P and Wright, N.A. (2003). Bottom-up histogenesis of colorectal adenomas: origin in the monocryptal adenoma and initial expansion by crypt fission. *Cancer Res*, **63**, 3819-3825.

Puddu, P., Fantuzzi, L, Borghi, P, Varano, B, Rainaldi, G, Guillemard, E, Malorni, W, Nicaise, P, Wolf, S.F, Belardelli, F and Gessani, S. (1997). IL-12 induces IFN-gamma expression and secretion in mouse peritoneal macrophages. *J Immunol*, **159**, 3490-3497.

Radaeva, S., Jaruga, B, Hong, F, Kim, W, Fan, S, Cai, H, Strom, S, Liu, Y, El-Assal, O and Gao, B. (2002). Interferon-alpha activates multiple STAT signals and down-regulates c-Met in primary human hepatocytes. *Gastroenterology*, **122**, 1020-1034.

Raulet, D.H.. (2003). Roles of the NKG2D immunoreceptor and its ligands. *Nat Rev Immunol*, **3**, 781-790.

Rensing, L.. (1972). Periodic geophysical and biological signals as Zeitgeber and exogenous inducers in animal organisms. *Int J Biometeorol*, **16 Suppl**, 113-125.

Robb, R.J., Munck, A and Smith, K.A. (1981). T cell growth factor receptors. Quantitation, specificity, and biological relevance. *J Exp Med*, **154**, 1455-1474.

Roder, D.M.. (2002). The epidemiology of gastric cancer. *Gastric Cancer*, **5 Suppl 1**, 5-11.

Rothwarf, D.M. and Karin, M. (1999). The NF-kappa B activation pathway: a paradigm in information transfer from membrane to nucleus. *Sci STKE*, **1999**, RE1.

Rothwarf, D.M., Zandi, E, Natoli, G and Karin, M. (1998). IKK-gamma is an essential regulatory subunit of the IkappaB kinase complex. *Nature*, **395**, 297-300.

Rubinfeld, B., Albert, I, Porfiri, E, Fiol, C, Munemitsu, S and Polakis, P. (1996). Binding of GSK3beta to the APC-beta-catenin complex and regulation of complex assembly. *Science*, **272**, 1023-1026.

Rupec, R.A., Jundt, F, Rebholz, B, Eckelt, B, Weindl, G, Herzinger, T, Flaig, M.J, Moosmann, S, Plewig, G, Dörken, B, Förster, I, Huss, R and Pfeffer, K. (2005). Stroma-mediated dysregulation of myelopoiesis in mice lacking I kappa B alpha. *Immunity*, **22**, 479-491.

Sadava, D., Heller, H.C, Orians, G.H, Purves, W.K and Hillis, D.M. (2006). *Life: The Science of Biology*. Sinauer Associates, Inc., and W. H. Freeman and Company.

Saito, H., Tsujitani, S, Oka, S, Kondo, A, Ikeguchi, M, Maeta, M and Kaibara, N. (1999). The expression of transforming growth factor-beta1 is significantly correlated with the expression of vascular endothelial growth factor and poor prognosis of patients with advanced gastric carcinoma. *Cancer*, **86**, 1455-1462.

Sakaguchi, S., Sakaguchi, N, Shimizu, J, Yamazaki, S, Sakihama, T, Itoh, M, Kuniyasu, Y, Nomura, T, Toda, M and Takahashi, T. (2001). Immunologic tolerance maintained by CD25+ CD4+ regulatory T cells: their common role in controlling autoimmunity, tumor immunity, and transplantation tolerance. *Immunol Rev*, **182**, 18-32.

Sakurai, T., Maeda, S, Chang, L and Karin, M. (2006). Loss of hepatic NF-kappa B activity enhances chemical hepatocarcinogenesis through sustained c-Jun N-terminal kinase 1 activation. *Proc Natl Acad Sci U S A*, **103**, 10544-10551.

Sana, T.R., Janatpour, M.J, Sathe, M, McEvoy, L.M and McClanahan, T.K. (2005). Microarray analysis of primary endothelial cells challenged with different inflammatory and immune cytokines. *Cytokine*, **29**, 256-269.

Sansom, O.J., Meniel, V.S, Muncan, V, Phesse, T.J, Wilkins, J.A, Reed, K.R, Vass, J.K, Athineos, D, Clevers, H and Clarke, A.R. (2007). Myc deletion rescues Apc deficiency in the small intestine. *Nature*, **446**, 676-679.

Sansom, O.J., Reed, K.R, van de Wetering, M, Muncan, V, Winton, D.J, Clevers, H and Clarke, A.R. (2005). Cyclin D1 is not an immediate target of beta-catenin following Apc loss in the intestine. *J Biol Chem*, **280**, 28463-28467.

Schiller, J.H., Horisberger, M.A, Bittner, G, Carlin, J.M, Storer, B, Byrne, G.I, Willson, J.K and Borden, E.C. (1990). Effects of combinations of interferon-beta ser and interferon-gamma on interferon-inducible proteins and on the cell cycle. *J Biol Response Mod*, **9**, 368-377.

Schindler, H., Lutz, M.B, Röllinghoff, M and Bogdan, C. (2001). The production of IFN-gamma by IL-12/IL-18-activated macrophages requires STAT4 signaling and is inhibited by IL-4. *J Immunol*, **166**, 3075-3082.

Schneider, G., Saur, D, Siveke, J.T, Fritsch, R, Greten, F.R and Schmid, R.M. (2006). IKKalpha controls p52/RelB at the skp2 gene promoter to regulate G1- to S-phase progression. *EMBO J*, **25**, 3801-3812.

Schneikert, J. and Behrens, J. (2007). The canonical Wnt signalling pathway and its APC partner in colon cancer development. *Gut*, **56**, 417-425.

Schonhoff, S.E., Giel-Moloney, M and Leiter, A.B. (2004). Neurogenin 3-expressing progenitor cells in the gastrointestinal tract differentiate into both endocrine and non-endocrine cell types. *Dev Biol*, **270**, 443-454.

Schroder, K., Hertzog, P.J, Ravasi, T and Hume, D.A. (2004). Interferon-gamma: an overview of signals, mechanisms and functions. *J Leukoc Biol*, **75**, 163-189.

Seetharaman, R., Mora, A.L, Nabozny, G, Boothby, M and Chen, J. (1999). Essential role of T cell NF-kappa B activation in collagen-induced arthritis. *J Immunol*, **163**, 1577-1583.

Senftleben, U., Cao, Y, Xiao, G, Greten, F.R, Krähn, G, Bonizzi, G, Chen, Y, Hu, Y, Fong, A, Sun, S.C and Karin, M. (2001). Activation by IKKalpha of a second, evolutionary conserved, NF-kappa B signaling pathway. *Science*, **293**, 1495-1499.

Shankaran, V., Ikeda, H, Bruce, A.T, White, J.M, Swanson, P.E, Old, L.J and Schreiber, R.D. (2001). IFNgamma and lymphocytes prevent primary tumour development and shape tumour immunogenicity. *Nature*, **410**, 1107-1111.

Shariat, S.F., Kim, J.H, Andrews, B, Kattan, M.W, Wheeler, T.M, Kim, I.Y, Lerner, S.P and Slawin, K.M. (2001). Preoperative plasma levels of transforming growth factor beta(1) strongly predict clinical outcome in patients with bladder carcinoma. *Cancer*, **92**, 2985-2992.

Shevach, E.M.. (2004). Fatal attraction: tumors beckon regulatory T cells. *Nat Med*, **10**, 900-901.

Shi, S., Nathan, C, Schnappinger, D, Drenkow, J, Fuortes, M, Block, E, Ding, A, Gingeras, T.R, Schoolnik, G, Akira, S, Takeda, K and Ehrt, S. (2003). MyD88 primes macrophages for full-scale activation by interferon-gamma yet mediates few responses to Mycobacterium tuberculosis. *J Exp Med*, **198**, 987-997.

Shih, I.M., Wang, T.L, Traverso, G, Romans, K, Hamilton, S.R, Ben-Sasson, S, Kinzler, K.W and Vogelstein, B. (2001). Top-down morphogenesis of colorectal tumors. *Proc Natl Acad Sci U S A*, **98**, 2640-2645.

Shih, I.M., Zhou, W, Goodman, S.N, Lengauer, C, Kinzler, K.W and Vogelstein, B. (2001). Evidence that genetic instability occurs at an early stage of colorectal tumorigenesis. *Cancer Res*, **61**, 818-822.

Shinkai, Y., Rathbun, G, Lam, K.P, Oltz, E.M, Stewart, V, Mendelsohn, M, Charron, J, Datta, M, Young, F, Stall, A.M and et al.. (1992). RAG-2-deficient mice lack mature lymphocytes owing to inability to initiate V(D)J rearrangement. *Cell*, **68**, 855-867.

Siebenlist, U., Franzoso, G and Brown, K. (1994). Structure, regulation and function of NF-kappa B. *Annu Rev Cell Biol*, **10**, 405-455.

Sizer, F. and Whitney, E. (2005). *Nutrition: Concepts and Controversies*. Brooks Cole.

Smyth, M.J., Crowe, N.Y and Godfrey, D.I. (2001). NK cells and NKT cells collaborate in host protection from methylcholanthrene-induced fibrosarcoma. *Int Immunol*, **13**, 459-463.

Smyth, M.J., Dunn, G.P and Schreiber, R.D. (2006). Cancer immunosurveillance and immunoediting: the roles of immunity in suppressing tumor development and shaping tumor immunogenicity. *Adv Immunol*, **90**, 1-50.

Smyth, M.J., Thia, K.Y, Street, S.E, Cretney, E, Trapani, J.A, Taniguchi, M, Kawano, T, Pelikan, S.B, Crowe, N.Y and Godfrey, D.I. (2000). Differential tumor surveillance by natural killer (NK) and NKT cells. *J Exp Med*, **191**, 661-668.

Smyth, M.J., Wallace, M.E, Nutt, S.L, Yagita, H, Godfrey, D.I and Hayakawa, Y. (2005). Sequential activation of NKT cells and NK cells provides effective innate immunotherapy of cancer. *J Exp Med*, **201**, 1973-1985.

Song, A., Nikolcheva, T and Krensky, A.M. (2000). Transcriptional regulation of RANTES expression in T lymphocytes. *Immunol Rev*, **177**, 236-245.

Stoler, D.L., Chen, N, Basik, M, Kahlenberg, M.S, Rodriguez-Bigas, M.A, Petrelli, N.J and Anderson, G.R. (1999). The onset and extent of genomic instability in sporadic colorectal tumor progression. *Proc Natl Acad Sci U S A*, **96**, 15121-15126.

Street, S.E., Cretney, E and Smyth, M.J. (2001). Perforin and interferon-gamma activities independently control tumor initiation, growth, and metastasis. *Blood*, **97**, 192-197.

Su, L.K., Kinzler, K.W, Vogelstein, B, Preisinger, A.C, Moser, A.R, Luongo, C, Gould, K.A and Dove, W.F. (1992). Multiple intestinal neoplasia caused by a mutation in the murine homolog of the APC gene. *Science*, **256**, 668-670.

Subramanian, A., Tamayo, P, Mootha, V.K, Mukherjee, S, Ebert, B.L, Gillette, M.A, Paulovich, A, Pomeroy, S.L, Golub, T.R, Lander, E.S and Mesirov, J.P. (2005). Gene set enrichment analysis: a knowledge-based approach for interpreting genome-wide expression profiles. *Proc Natl Acad Sci U S A*, **102**, 15545-15550.

Taieb, J., Chaput, N, Ménard, C, Apetoh, L, Ullrich, E, Bonmort, M, Péquignot, M, Casares, N, Terme, M, Flament, C, Opolon, P, Lecluse, Y, Métivier, D, Tomasello, E, Vivier, E, Ghiringhelli, F, Martin, F, Klatzmann, D, Poynard, T, Tursz, T, Raposo, G, Yagita, H, Ryffel, B, Kroemer, G and Zitvogel, L. (2006). A novel dendritic cell subset involved in tumor immunosurveillance. *Nat Med*, **12**, 214-219.

Takaoka, A., Tamura, T and Taniguchi, T. (2008). Interferon regulatory factor family of transcription factors and regulation of oncogenesis. *Cancer Sci*, **99**, 467-478.

Takeda, K., Smyth, M.J, Cretney, E, Hayakawa, Y, Kayagaki, N, Yagita, H and Okumura, K. (2002). Critical role for tumor necrosis factor-related apoptosis-inducing ligand in immune surveillance against tumor development. *J Exp Med*, **195**, 161-169.

Takeda, K., Takeuchi, O, Tsujimura, T, Itami, S, Adachi, O, Kawai, T, Sanjo, H, Yoshikawa, K, Terada, N and Akira, S. (1999). Limb and skin abnormalities in mice lacking IKKalpha. *Science*, **284**, 313-316.

Taketo, M.M.. (2006). Mouse models of gastrointestinal tumors. *Cancer Sci*, **97**, 355-361.

Tanaka, T., Kohno, H, Suzuki, R, Yamada, Y, Sugie, S and Mori, H. (2003). A novel inflammation-related mouse colon carcinogenesis model induced by azoxymethane and dextran sodium sulfate. *Cancer Sci*, **94**, 965-973.

Tappenden, P., Jones, R, Paisley, S and Carroll, C. (2007). Systematic review and economic evaluation of bevacizumab and cetuximab for the treatment of metastatic colorectal cancer. *Health Technol Assess*, **11**, 1-128, iii-iv.

Tegethoff, S., Behlke, J and Scheidereit, C. (2003). Tetrameric oligomerization of IkappaB kinase gamma (IKKgamma) is obligatory for IKK complex activity and NF-kappaB activation. *Mol Cell Biol*, **23**, 2029-2041.

Tergaonkar, V., Pando, M, Vafa, O, Wahl, G and Verma, I. (2002). p53 stabilization is decreased upon NFkappaB activation: a role for NFkappaB in acquisition of resistance to chemotherapy. *Cancer Cell*, **1**, 493-503.

Toi, M., Taniguchi, T, Yamamoto, Y, Kurisaki, T, Suzuki, H and Tominaga, T. (1996). Clinical significance of the determination of angiogenic factors. *Eur J Cancer*, **32A**, 2513-2519.

Townson, J.L., Naumov, G.N and Chambers, A.F. (2003). The role of apoptosis in tumor progression and metastasis. *Curr Mol Med*, **3**, 631-642.

Van Es, J.H., Jay, P, Gregorieff, A, van Gijn, M.E, Jonkheer, S, Hatzis, P, Thiele, A, van den Born, M, Begthel, H, Brabletz, T, Taketo, M.M and Clevers, H. (2005). Wnt signalling induces maturation of Paneth cells in intestinal crypts. *Nat Cell Biol*, **7**, 381-386.

Van Ginderachter, J.A., Movahedi, K, Hassanzadeh Ghassabeh, G, Meerschaut, S, Beschin, A, Raes, G and De Baetselier, P. (2006). Classical and alternative activation of mononuclear phagocytes: picking the best of both worlds for tumor promotion. *Immunobiology*, **211**, 487-501.

Van de Wetering, M., Sancho, E, Verweij, C, de Lau, W, Oving, I, Hurlstone, A, van der Horn, K, Batlle, E, Coudreuse, D, Haramis, A.P, Tjon-Pon-Fong, M, Moerer, P, van den Born, M, Soete, G, Pals, S, Eilers, M, Medema, R and Clevers, H. (2002). The beta-catenin/TCF-4 complex imposes a crypt progenitor phenotype on colorectal cancer cells. *Cell*, **111**, 241-250.

Wang, C.Y., Mayo, M.W and Baldwin, A.S.J. (1996). TNF- and cancer therapy-induced apoptosis: potentiation by inhibition of NF-kappaB. *Science*, **274**, 784-787.

Wang, C.Y., Mayo, M.W, Korneluk, R.G, Goeddel, D.V and Baldwin, A.S.J. (1998). NF-kappaB antiapoptosis: induction of TRAF1 and TRAF2 and c-IAP1 and c-IAP2 to suppress caspase-8 activation. *Science*, **281**, 1680-1683.

Waterman, M.L.. (2004). Lymphoid enhancer factor/T cell factor expression in colorectal cancer. *Cancer Metastasis Rev*, **23**, 41-52.

Watson, J.D. and Crick, F.H. (1953). Molecular structure of nucleic acids; a structure for deoxyribose nucleic acid. *Nature*, **171**, 737-738.

Wells, J.M. and Melton, D.A. (1999). Vertebrate endoderm development. *Annu Rev Cell Dev Biol*, **15**, 393-410.

References

Wesemann, D.R. and Benveniste, E.N. (2003). STAT-1 alpha and IFN-gamma as modulators of TNF-alpha signaling in macrophages: regulation and functional implications of the TNF receptor 1:STAT-1 alpha complex. *J Immunol*, **171**, 5313-5319.

Wesemann, D.R., Qin, H, Kokorina, N and Benveniste, E.N. (2004). TRADD interacts with STAT1-alpha and influences interferon-gamma signaling. *Nat Immunol*, **5**, 199-207.

[Wikipedia Free Encyclopedia] Human gastrointestinal system. Retrieved on 12.06.2009. http://en.wikipedia.org/wiki/File:Digestive_system_diagram_en.svg.

[Wikipedia Free Encyclopedia2] K-means clustering. Retrieved on 15.09.2009. http://en.wikipedia.org/wiki/k-means_clustering.

[Wikipedia Free Encyclopedia3] Standard score. Retrieved on 15.09.2009. http://en.wikipedia.org/wiki/standard_score.

Willimsky, G. and Blankenstein, T. (2005). Sporadic immunogenic tumours avoid destruction by inducing T-cell tolerance. *Nature*, **437**, 141-146.

Wong, H., Bourdelas, A, Krauss, A, Lee, H, Shao, Y, Wu, D, Mlodzik, M, Shi, D and Zheng, J. (2003). Direct binding of the PDZ domain of Dishevelled to a conserved internal sequence in the C-terminal region of Frizzled. *Mol Cell*, **12**, 1251-1260.

Xiao, G., Harhaj, E.W and Sun, S.C. (2001). NF-kappaB-inducing kinase regulates the processing of NF-kappaB2 p100. *Mol Cell*, **7**, 401-409.

Yam, C.H., Ng, R.W, Siu, W.Y, Lau, A.W and Poon, R.Y. (1999). Regulation of cyclin A-Cdk2 by SCF component Skp1 and F-box protein Skp2. *Mol Cell Biol*, **19**, 635-645.

Yamaoka, S., Courtois, G, Bessia, C, Whiteside, S.T, Weil, R, Agou, F, Kirk, H.E, Kay, R.J and Israël, A. (1998). Complementation cloning of NEMO, a component of the IkappaB kinase complex essential for NF-kappaB activation. *Cell*, **93**, 1231-1240.

Yang, Q., Bermingham, N.A, Finegold, M.J and Zoghbi, H.Y. (2001). Requirement of Math1 for secretory cell lineage commitment in the mouse intestine. *Science*, **294**, 2155-2158.

Yost, C., Farr, G.H.3, Pierce, S.B, Ferkey, D.M, Chen, M.M and Kimelman, D. (1998). GBP, an inhibitor of GSK-3, is implicated in Xenopus development and oncogenesis. *Cell*, **93**, 1031-1041.

Zandi, E., Chen, Y and Karin, M. (1998). Direct phosphorylation of IkappaB by IKKalpha and IKKbeta: discrimination between free and NF-kappaB-bound substrate. *Science*, **281**, 1360-1363.

Zandi, E., Rothwarf, D.M, Delhase, M, Hayakawa, M and Karin, M. (1997). The IkappaB kinase complex (IKK) contains two kinase subunits, IKKalpha and IKKbeta, necessary for IkappaB phosphorylation and NF-kappaB activation. *Cell*, **91**, 243-252.

Zhang, L. and Zhao, Y. (2007). The regulation of Foxp3 expression in regulatory CD4(+)CD25(+)T cells: multiple pathways on the road. *J Cell Physiol*, **211**, 590-597.

Zitvogel, L., Tesniere, A and Kroemer, G. (2006). Cancer despite immunosurveillance: immunoselection and immunosubversion. *Nat Rev Immunol*, **6**, 715-727.

Zou, W.. (2005). Immunosuppressive networks in the tumour environment and their therapeutic relevance. *Nat Rev Cancer*, **5**, 263-274.

van der Flier, L.G., Haegebarth, A, Stange, D.E, van de Wetering, M and Clevers, H. (2009). OLFM4 Is a Robust Marker for Stem Cells in Human Intestine and Marks a Subset of Colorectal Cancer Cells. *Gastroenterology*, **137**, 15-17.

van der Flier, L.G., van Gijn, M.E, Hatzis, P, Kujala, P, Haegebarth, A, Stange, D.E, Begthel, H, van den Born, M, Guryev, V, Oving, I, van Es, J.H, Barker, N, Peters, P.J, van de Wetering, M and Clevers, H. (2009). Transcription factor achaete scute-like 2 controls intestinal stem cell fate. *Cell*, **136**, 903-912.

8. APPENDICES

8.1. SUPPLEMENTARY MICROARRAY DATA

8.1.1. List of Genes within Cluster VIII (15-day *β-cat*^{CA}*Ikkα*$^{AA/AA}$ Upregulated)

UniqueID	Gene Symbol
1426278_at	Ifi27
1425065_at	Oas2
1448562_at	Upp1
1421911_at	Stat2
1422006_at	Eif2ak2
1425374_at	Oas3
1450672_a_at	Trex1
1423555_a_at	Ifi44
1419042_at	Iigp1
1418191_at	Usp18
1417244_a_at	Irf7
1424921_at	Bst2
1426774_at	Parp12
1418825_at	Irgm
1425913_a_at	2810022L02Rik
1426415_a_at	Trim25
1419043_a_at	Iigp1
1451777_at	BC013672
1451644_a_at	H2-Q1
1425927_a_at	Atf5
1416051_at	C2
1451426_at	Lgp2
1425405_a_at	Adar
1417185_at	Ly6a
1418293_at	Ifit2
1451821_a_at	Sp100
1424775_at	Oas1a
1451860_a_at	Trim30
1453196_a_at	Oasl2
1421217_a_at	Lgals9
1419762_at	Ubd
1418392_a_at	Gbp4
1423619_at	Rasd1
1418021_at	C4b

1431591_s_at	Loc677168
1416016_at	Tap1
1417961_a_at	Trim30
1426971_at	Ube1l
1431008_at	0610037M15Rik
1428346_at	Trafd1
1449025_at	Ifit3
1434380_at	9830147J24RIK
1438676_at	Mpa2l
1448380_at	Lgals3bp
1418580_at	Rtp4
1427102_at	Slfn4
1425156_at	9830147J24Rik
1426970_a_at	Ube1l
1450271_at	Ptk6
1422751_at	Tle1
1449005_at	Slc16a3
1422977_at	Gp1bb
1419604_at	Zbp1
1419026_at	Daxx
1451969_s_at	Parp3
1424518_at	2310016F22Rik
1450424_a_at	Il18bp
1417470_at	Apobec3
1449875_s_at	H2-T22
1451095_at	Asns
1418536_at	Loc630509//Loc674
1423233_at	Cebpd
1450009_at	Ltf
1453393_a_at	Chst4
1451083_s_at	Aars
1429947_a_at	Zbp1
1448452_at	Irf8
1449009_at	Tgtp
1433966_x_at	Asns
1425719_a_at	Nmi
1418930_at	Cxcl10
1430005_a_at	Batf2
1424575_at	Rabl5
1421034_a_at	Il4ra
1452614_at	Gm566
1449363_at	Atf3
1426276_at	Ifih1
1436172_at	9530028C05
1423392_at	Clic4

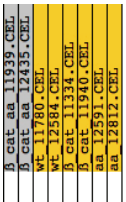

SampleName		
1426278_at	IFI27	interferon, alpha-inducible protein 27
1424921_at	BST2	bone marrow stromal cell antigen 2
1423555_a_at	IFI44	interferon-induced protein 44
1425065_at	OAS2	2'-5' oligoadenylate synthetase 2
1418191_at	USP18	ubiquitin specific peptidase 18
1423619_at	RASD1	RAS, dexamethasone-induced 1
1417185_at	LY6A	lymphocyte antigen 6 complex, locus A
1418293_at	IFIT2	interferon-induced protein with tetratricopeptide repeats 2
1419043_a_at	IIGP1	interferon inducible GTPase 1
1451644_a_at	H2-Q1 /// 0610037M15	histocompatibility 2, Q region locus 1 /// RIKEN cDNA 0610037M15 gene
1451426_at	LGP2	
1425913_a_at	2810022L02RIK	RIKEN cDNA 2810022L02 gene
1425374_at	OAS3	2'-5' oligoadenylate synthetase 3
1421911_at	STAT2	signal transducer and activator of transcription 2
1419042_at	IIGP1	interferon inducible GTPase 1
1418825_at	IRGM	immunity-related GTPase family, M
1416051_at	C2	complement component 2 (within H-2S)
1417244_a_at	IRF7	interferon regulatory factor 7
1431008_at	0610037M15RIK	RIKEN cDNA 0610037M15 gene
1418021_at	C4B /// LOC675521	complement component 4B (Childo blood group) /// similar to Complement C4 precursor
1451777_at	BC013672	cDNA sequence BC013672
1451860_a_at	TRIM30	tripartite motif protein 30
1453196_a_at	OASL2	2'-5' oligoadenylate synthetase-like 2
1424775_at	OAS1A	2'-5' oligoadenylate synthetase 1A
1425405_a_at	ADAR	adenosine deaminase, RNA-specific
1418536_at	LOC630509 /// LOC674	9; histocompatibility 2, Q region locus 7
1416016_at	TAP1	transporter 1, ATP-binding cassette, sub-family B (MDR/TAP)
1448562_at	UPP1	uridine phosphorylase 1
1426774_at	PARP12	poly (ADP-ribose) polymerase family, member 12
1419762_at	UBD	ubiquitin D
1451821_a_at	SP100	nuclear antigen Sp100
1425927_a_at	ATF5	activating transcription factor 5
1422977_at	GP1BB	glycoprotein Ib, beta polypeptide
1423233_at	CEBPD	CCAAT/enhancer binding protein (C/EBP), delta
1450424_a_at	IL18BP	interleukin 18 binding protein
1427102_at	SLFN4	schlafen 4
1425156_at	9830147J24RIK	RIKEN cDNA 9830147J24 gene
1431591_s_at	LOC677168	hypothetical protein LOC677168
1426971_at	UBE1L	ubiquitin-activating enzyme E1-like
1438676_at	MPA2L /// LOC626578	macrophage activation 2 like /// similar to macrophage activation 2 like
1434380_at	9830147J24RIK	RIKEN cDNA 9830147J24 gene
1450672_a_at	TREX1	three prime repair exonuclease 1
1449875_s_at	H2-T22 /// H2-T9	histocompatibility 2, T region locus 22 /// histocompatibility 2, T region locus 9
1418580_at	RTP4	receptor transporter protein 4
1449025_at	IFIT3	interferon-induced protein with tetratricopeptide repeats 3
1452614_at	GM566	gene model 566, (NCBI)
1426415_a_at	TRIM25	tripartite motif protein 25
1450271_at	PTK6	PTK6 protein tyrosine kinase 6
1450009_at	LTF	lactotransferrin
1421217_a_at	LGALS9	lectin, galactose binding, soluble 9
1429947_a_at	ZBP1	Z-DNA binding protein 1
1417961_a_at	TRIM30	tripartite motif protein 30
1419604_at	ZBP1	Z-DNA binding protein 1
1448380_at	LGALS3BP	lectin, galactoside-binding, soluble, 3 binding protein
1451969_s_at	PARP3	poly (ADP-ribose) polymerase family, member 3
1428346_at	TRAFD1	TRAF type zinc finger domain containing 1
1418392_a_at	GBP4	guanylate nucleotide binding protein 4
1426970_a_at	UBE1L /// D330022A01	ubiquitin-activating enzyme E1-like /// RIKEN cDNA D330022A01 gene
1424518_at	2310016F22RIK /// BC	RIKEN cDNA 2310016F22 gene /// cDNA sequence BC020489
1451095_at	ASNS	asparagine synthetase
1449005_at	SLC16A3	solute carrier family 16 (monocarboxylic acid transporters), member 3
1453393_a_at	CHST4	carbohydrate (chondroitin 6/keratan) sulfotransferase 4
1417470_at	APOBEC3	apolipoprotein B editing complex 3
1449009_at	TGTP	T-cell specific GTPase
1422006_at	EIF2AK2	eukaryotic translation initiation factor 2-alpha kinase 2
1419026_at	DAXX	Fas death domain-associated protein
1451083_s_at	AARS	alanyl-tRNA synthetase
1448452_at	IRF8	interferon regulatory factor 8
1430005_a_at	BATF2	basic leucine zipper transcription factor, ATF-like 2
1433966_x_at	ASNS	asparagine synthetase
1422751_at	TLE1	transducin-like enhancer of split 1, homolog of Drosophila E(spl)
1421034_a_at	IL4R	interleukin 4 receptor
1424575_at	RABL5	RAB, member of RAS oncogene family-like 5
1425719_a_at	NMI	N-myc (and STAT) interactor
1436172_at	9530028C05	hypothetical protein 9530028C05
1426276_at	IFIH1	interferon induced with helicase C domain 1
1418930_at	CXCL10	chemokine (C-X-C motif) ligand 10
1449363_at	ATF3	activating transcription factor 3
1423392_at	CLIC4	chloride intracellular channel 4 (mitochondrial)

Figure 8.1: Heatmap for *β-cat*^{CA}*Ikkα*$^{AA/AA}$ mice upregulated cluster of 79 genes. Ranked expression values were compared to all other phenotypes. Red is upregulation and blue is for downregulation. Two samples per each group from left to right: *β-cat*^{CA}*Ikkα*$^{AA/AA}$, WT, *β-cat*^{CA} and *Ikkα*$^{AA/AA}$.

8.1.2. Genes Upregulated More Than 2 Folds in 15-day *β-cat*^{CA}*Ikkα*$^{AA/AA}$ Mice Relative to *β-cat*^{CA}

Gene Symbol	Fold Upregulation
Ela3 /// LOC638418	52.42
Ela3 /// LOC638418	38.19
Amy2 /// 1810008N23Rik	31.03
2210010C04Rik	18.05
Ela3	11.99
Try4 /// Prss1 /// 1810049H19Rik /// LOC436522	11.62
Pnlip	11.54
Slc23a1	8.48
Ela2a	7.35
Cpb1	7.11
Pmp22	7.08
Fkbp5	7.04
Fkbp5	6.63
Ela3	6.35
Slc5a4a	6.02
Ifi44	5.93
Pck1	5.54
Ifi27	5.29
Ctrb1	5.10
Trim30	5.02
Hspa1a	4.68
2210010C04Rik	4.55
Per2	4.54
Cel	4.48
Oas2	4.48
Usp18	4.45
Hspa1b	4.22
B230342M21Rik	3.95
Oas3	3.93
Trim30	3.92
Sycn	3.87
Zbtb16	3.75
Slc13a2	3.75
Oas1d /// Oas1e	3.72
Akr1b7	3.69
Iigp1	3.65
---	3.54
H2-Q10	3.51
Iigp1	3.50
Tsc22d3	3.46
Abcb1a	3.42
2010109I03Rik	3.42
Hspa1b	3.41
Dbp	3.41
Ly6a	3.31
Ces6	3.28

Bst2	3.28
Cyp2b10	3.27
Car4	3.25
Acox2	3.24
H2-Q1 /// 0610037M15Rik	3.22
Slc5a4b	3.13
AU018778	3.10
Ifit2	3.10
Abcb1a	3.09
Susd2	3.08
Tsc22d3	3.06
Dgat2	3.05
Cyp2b10	3.05
Rbp7	3.04
Hspa1b	3.04
Car4	3.04
Ubd	3.02
Ace	3.01
Chac1	2.96
1300013J15Rik	2.96
Cpa1	2.95
Slc7a8	2.93
Dbp	2.91
2810022L02Rik	2.88
Mbl2	2.87
BC013672	2.86
Cyp2b10	2.86
Aspa	2.81
Phospho1	2.80
Oasl2	2.79
Kcnk5	2.78
0610037M15Rik	2.78
Ctrl	2.77
Mertk	2.76
Bbox1	2.75
Vwa1	2.73
Per1	2.73
Sgk	2.73
Ccrn4l	2.73
1300007C21Rik /// LOC433762	2.72
Usp2	2.72
Rasd1	2.70
Kcnk5	2.69
Ace	2.69
Usp2	2.68
Aldh1a1	2.67
Kalrn	2.64
Irgm	2.64
Prss2	2.64
Mpa2l /// LOC626578 /// LOC673101	2.63
D11Lgp2e	2.63
Trim30 /// AI451617	2.62

Casp3	2.62
Stat2	2.61
Trib3	2.60
Aldh1a7	2.60
Edg7	2.57
2310016F22Rik /// BC020489	2.54
Slfn4	2.51
Dgat2	2.50
C230093N12Rik	2.49
D11Lgp2e	2.48
AI848100	2.47
Abat	2.46
Aldh4a1	2.45
Aplp1	2.45
Sgpl1	2.43
Atf3	2.41
Entpd7	2.39
Gstm3	2.39
Stat2	2.39
C230093N12Rik	2.38
Rtp4	2.38
---	2.37
Gp1bb	2.37
Atp8a1	2.37
Prss2	2.36
Maoa	2.36
Slfn3 /// Slfn4	2.36
Herpud1	2.35
Fut4	2.35
Slc15a1	2.34
Irf7	2.34
Abca1	2.34
Gdpd2	2.33
Gstm3	2.32
Mafb	2.30
C2	2.28
LOC630509 /// LOC674192	2.28
Ifit3	2.28
Iigp2	2.26
Hpgd	2.26
Mx1	2.26
Tef	2.26
Pex11a	2.25
Ifit1	2.24
Oas1a	2.23
Ugcg	2.23
Vipr1	2.23
Mafb	2.22
Hnf4g	2.22
Gbp4	2.21
Slc1a1	2.21
Il15	2.21
Aqp3	2.20

Samd8	2.20
Cyp3a25 /// LOC622249	2.20
Eif2ak2	2.19
Sp100	2.18
Herpud1	2.18
Cyp3a11	2.18
Es22	2.18
Acot12	2.18
Cndp2	2.17
Etnk1	2.16
Clca1	2.16
LOC677168	2.16
Kalrn	2.14
Sult1d1	2.14
Pla2g1b	2.14
Igtp	2.13
Oas1e	2.13
Xlkd1	2.12
Acot12	2.12
Nr5a2	2.12
Hpgd	2.11
Ifrd1	2.10
9830147J24Rik	2.09
Hnf4g	2.09
Cubn	2.09
Mt2	2.09
Gdap10	2.08
Epb4.1l3	2.08
Ppara	2.07
Pbef1	2.07
Hist2h3c2	2.07
Atf5	2.07
Scin	2.05
Per3	2.04
Acot4	2.03
Cth	2.03
Abhd6	2.03
Rtp4	2.03
C4b /// LOC675521	2.03
Enpep	2.03
Entpd5	2.03
Pcsk5	2.02
Trib3	2.02
Cml5	2.02
Slc1a1	2.02
Upp1	2.02
Dpep1	2.02
Rorc	2.01
Sult1d1	2.01
Anpep	2.01
H2-Aa /// H2-Ea	2.01
Per2	2.00

8.2. PRIMERS

GENOTYPING PRIMERS

BCAT-EX3-F	TTCCCAGTCCTTCACGCAAG
BCAT-EX4-R	GCAAGTTCCGCGTCATCCT
Cre-370-F	ACCTGAAGATGTTCGCGATTATCT
Cre-370-R	ACCGTCAGTACGTGAGATATCTT
IFNγ-F	AGAAGTAAGTGGAAGGGCCCAGAAG
IFNγ-R	AGGGAAACTGGGAGAGGAGAAATAT
IKKa-fl-F	GGAATTAGTTCTCCTCCTCTCATATGG
IKKa-fl-R	TTAAATTGTTGAAATATCTGTAAAGGAAGG
IKKα-392-R	GGATCCGATATCTGCATGAAAAC
IKKα-AA-F	CAATGTTCCCACAAACGCTGTACAGAGCGC
IKKα-WT-F	CAATGTTCCCACAAAAGATGTACAGAGACT
IKKβ-144-F	CACAGTGCCCACATTATTTAGATAGG
IKKβ 321-R	GTCTTCAACCTCCCAAGCCTT
IKKβ 390-R	GCAATGTCTGATACAGTGTGTTAGGTT
IKKβ-93-F	TGACCCGGGAATGAATAGCA
IMR0033	GCCATCCCTTCACGTTAG
IMR0034	TTCCACTTTGGCATAAGGC
IMR0158-R	CTGAATGAACTGCAGGACGA
IMR0159-F	ATACTTTCTCGGCAGGAGCA
IMR0758	TTCTGAGAAAGACAGAAGTTA
IMR459-F	CAGCATGTGTCAATCACG
IMR460-R	TCACCATGTCATCTGTGG
NEO-AS	ATTCGCCAATGAAGGCGTTGTT
UM4-F	AAGATGTGCTGTTCCCTTCCTCTGCTCTGA
UM5-R	ATTATTAAAAGAAAAGACGAGGCGAAGTGG

RT-PCR PRIMERS

CCL20-F	TGGCAAGCGTCTGCTCTTC
CCL20-R	TTGCTGCTTCTGCCTGGC
CCL28-F	AGCAGGGCTCACACTCATGG
CCL28-R	ACCTCAGTGCAACAGCTGGA
CCL6-F	AACCCAGGTCTGTGCCGAC
CCL6-R	TGGGCCTTGCTTCAGGG
CD11c-F	AACAGAGGTGCTGTCTACATATTTCATG
CD11c-R	TGCTGAAATCCTCTGGCTGG
CD49B-F	TGGCGAGTCCCATGATGG
CD49B-R	TGCCGAACCTCAGTATCTCGT
CD4-F	GAGGCTCAGATTCCCAACCA
CD4-R	GCAGCAAGCGCCTAAGAGAG

CD8-F	CGTGGTGGTGCATGCCT
CD8-R	CCTCGAACTCAGAGAGATCCGC
C-MYC-F	AACTACGCAGCGCCTCCC
C-MYC-R	ATTTTCGGTTGTTGCTGATCTGT
CXCL1-F	TATCGCCAATGAGCTGCG
CXCL1-R	GGATGTTCTTGAGGTGAATCCC
CXCL5-F	TCCATCTCGCCATTCATGC
CXCL5-R	GATGCTGCGGCAGCGGCAGCGT
CYCLO-F	ATGGTCAACCCCACCGTGT
CYCLO-R	TTCTGCTGTCTTTGGAACTTTGTC
F4/80-F	CTTTGGCTATGGGCTTCCAGTC
F4/80-R	GCAAGGAGGACAGAGTTTATCGTG
FASL-F	ACTCCGTGAGTTCACCAACC
FASL-R	GTGGGGGTTCCCTGTTAAAT
FOXP3-F	TAGGAGCCGCAAGCTAAAAGC
FOXP3-R	TCCTTGTTTTGCGCTGAGAGT
GR1-F	GCAATGCAGCAGTTCCCACT
GR1-R	ATTGAATGGATCATCAGAGAAAGGTC
GZMA-F	ATGTGGCTATCCTTCACCTACCTAA
GZMA-R	TCCCCCATCCTGCTACTCG
GZMB-F	AAACGTGCTTCCTTTCGGG
GZMB-R	GGAAACTATGCCTGCAGCCA
IFNα-F	TGTACCTGAGAGAGAAGAAACACAGC
IFNα-R	GGAAGACAGGGTTCTCCAGACTT
IFNαR1-F	ACTCAAGCCTCCCCGCAG
IFNαR1-R	TGATGAAGCATCTTTCCGTGTG
IFNβ-F	AGCTCCAAGAAAGGACGAACAT
IFNβ-R	GCCCTGTAGGTGAGGTTGATCT
IFNγ-F	TTACTGCCACGGCACAGTCA
IFNγ-R	AGTTCCTCCAGATATCCAAGAAGAGA
IL-10-F	GGTTGCCAAGCCTTATCGGA
IL-10-R	ACCTGCTCCACTGCCTTGCT
IL-12p35-F	CACGCTACCTCCTCTTTTTG
IL-12p35-R	CAGCAGTGCAGGAATAATGTT
IL-12p40-F	AAACCAGACCCGCCCAAGAAC
IL-12p40-R	AAAAAGCCAACCAAGCAGAAGACAG
IL-15-F	TCTTCATTTTGGGCTGTGTCAG
IL-15-R	AGGCTTTCAATTTTCTCCAGGTC
IL-1b-F	GTGGCTGTGGAGAAGCTGTG
IL-1b-R	GAAGGTCCACGGGAAAGACAC
IL-2-F	GCTTTGACAGAAGGCTATCCATC
IL-2-R	CACATTTGAGTGCCAATTCGAT
IL-4-F	ACAGGAGAAGGGACGCCAT
IL-4-R	GAAGCCCTACAGACGCCAT
IL6-F	GTATGAACAACGATGATGCACTTG
IL6-R	ATGGTACTCCAGAAGACCAGAGGA
iNOS-F	CCCTCCTGATCTTGTGTTGGA
iNOS-R	CAACCCGAGCTCCTGGAAC
IP10-F	GAATCCGGAATCTAAGACCATCAA
IP10-R	GTGCGTGGCTTCACTCCAGT
IRF-1-F	GCTACCTGGGTCAGGACTTG
IRF-1-R	CAGAGAGACTGCTGCTGACG
IRF-7-F	ACAGGGCGTTTTATCTTGCG

IRF-7-R	TCCAAGCTCCCGGCTAAGT
ISG15-F	ACCCTTTCCAGTCTGGGTCT
ISG15-R	TCGCTGCAGTTCTGTACCAC
KC-F	GCCAATGAGCTGCGCTGT
KC-R	CCTTCAAGCTCTGGATGTTCTTG
MCP1-F	GGCTCAGCCAGATGCAGTTAA
MCP1-R	CCTACTCATTGGGATCATCTTGCT
MIP1α-F	CCAAGTCTTCTCAGCGCCAT
MIP1α-R	TCTTCCGGCTGTAGGAGAAGC
MIP1β-F	AGCTCTGCGTGTCTGCCCT
MIP1β-R	TGCTGAGAACCCTGGAGCA
MIP2-F	ATCCAGAGCTTGAGTGTGACGC
MIP2-R	AAGGCAAACTTTTTGACCGCC
MMP7-F	TCAGCTGGCATGAACAAACG
MMP7-R	GCAAAACCCATCCACAGCA
MX-1-F	ATGTCAGCTCCCCAAATGTCC
MX-1-R	TGCCTACAGCCACCCTGG
OAS1-F	CAAGGTGGTGAAGGGTGGC
OAS1-R	TCAAAGCTGGTGAGATTGTTAAGG
PERF1-F	CCAGAGGCAAACATGCGC
PERF1-R	GCTGCAAAATTGGCTACCTTG
PKR-F	GTTGTTGGGAGGGAGTTGACTATG
PKR-R	AAGAGGCACCGGGTTTTGTA
RANTES-F	GTGCTCCAATCTTGCAGTCGT
RANTES-R	TGAACCCACTTCTCTGGGT
STAT1-F	GACCCTGCAGCAGATCCGT
STAT1-R	GGTCGGGCTCATAGGTGAATT
TCF4-F	TTTCTTTCCGTGATACATTCTGCA
TCF4-R	CGGACGATACCTGTTTCCTATATAATAA
TGFβ1-F	GTACAGCAAGGTCCTTGCCCT
TGFβ1-R	TAGTAGACGATGGGCAGTGGC
TNFα-F	ATGAGAAGTTCCCAAATGGCC
TNFα-R	TCCACTTGGTGGTTTGCTACG
TRAIL-F	GGATATGGCCTGGCTGTAGA
TRAIL-R	GTTCCAGCTGCCTTTCTGTC
TSLP-F	CCCTGGCTGCCCTTCAC
TSLP-R	GCAGTGGTCATTGAGGGCTT

EMSA OLIGOS

NF-κBF	AGTTGAGGGGACTTTCCCAGGC
NF-κBR	GCCTGGGAAAGTCCCCTCAACT
NF-YF	GTAGGAACCAATGAAATGCGAGG
NF-YR	CCTACCCTCGCATTTCATTGGTT
P53-F	TACAGAACATGTCTAAGCATGCTGGGG
P53-R	CCCCAGCATGCTTAGACATGTTCTGTA
SIE-F	GTGCATTTCCCGTAAATCTTGTCTACA
SIE-R	TGTAGACAAGATTTACGGGAAATGCAC
STAT1-F	CATGTTATGCATATTCCTGTAAGTG
STAT1-R	CACTTACAGGAATATGCATAACATG
STAT3-F	GATCCTTCTGGGAATTCCTAGATC

STAT3-R	GATCTAGGAATTCCCAGAAGGATC

AS: antisense
F: forward
KO: knock-out
R: reverse

8.3 PLASMIDS

Plasmid Name	Function
Igk-luc	empty vector for promoter activity assay
Igk-Luc-3x*Ap1*	AP1 promoter for promoter activity assay
Igk-Luc-3x*κB*	NF-κB promoter for promoter activity assay
pBv-Luc-Del1	c-Myc full promoter for promoter activity assay
pBv-Luc-DelE	minimal c-myc promoter for promoter activity assay
pCl-*neo-Ctnnb1*	β-catenin for expression
pCl-*neo-Ctnnb1*^{S33Y}	binding deficient β-catenin^{S33Y}
pEGFP-C3	EGFP for expression and transfection efficiency control
pGEX4T3-GST-*c-jun*(1-79)	GST-c-Jun (1-79th amino acids) for expression
pGEX4T3-GST-*Fkhr*	GST-FKHR for overexpression and protein isolation
pGEX4T3-GST-*Foxo3a*	GST-FOXO3a for overexpression and protein isolation
pGEX4T3-GST-*Iκbα*(1-36)	GST-IκBα (1-36th amino acids) for expression
pGL2-*Skp2*-reporter	SKP2 reporter for promoter activity assay
pGL3-OF	mutant TCF/LEF promoter for promoter activity assay
pGL3-OT	TCF/LEF promoter for promoter activity assay
pRc	empty vector HA-tag for expression
pRc-HA-*hIkkβ*	HA-IKKβ expression vector
pRc-HA-*hIkkβ*$^{S187E/S191E}$	HA-IKKβ$^{S187E/S191E}$ for expression
pRc-HA-*Ikkα*	HA-IKKα for overexpression

pRc-HA-*Ikkβ* $^{S187A/S191A}$	HA-IKKβ$^{S187A/S191A}$ activation deficient for DN overexpression
pRc-HA-*Iκbα* $^{AA/AA}$	HA-IκBαAA/AA for expression
pRK5	empty vector FLAG-tag for expression
pRK5-FLAG-*Ikkα* $^{S186E/S190E}$	FLAG-IKKα$^{S186E/S190E}$ continuously active for overexpression
pRK5-FLAG-*Ikkα* ^{K42E}	FLAG-IKKα kinase deficient for DN overexpression
pRK-FLAG-*Ikkα*	FLAG-IKKα for overexpression

8.4. ANTIBODIES

8.4.1. Primary Antibodies

Mouse anti-mouse-actin IgG (Sigma) A 4700

Rabbit anti-mouse-asialo GM1 IgG (Wako Chemical GmbH)

Rabbit anti-mouse-Bcl-xL (BD Pharmingen) BD-556361

Rat APC-anti-mouse-B220/CD45R IgG (BD Pharmingen) BD-553092

Rat PE-aqnti-mouse-B220/CD45R IgG (BD Pharmingen) BD-553089

Rat anti-BrdU IgG (Serotec) MCA2060

Rabbit anti-mouse-Casp3(cleaved) IgG (Cell Signaling Technology Inc., USA) 9661S

Rat PE-anti-mouse-CD11b IgG (BD Pharmingen) BD-557397

Hamster FITC-anti-mouse-CD11c IgG (BD Pharmingen) BD-557400

Hamster PE-anti-mouse-CD11c IgG (BD Pharmingen) BD-557401

Rat PE-anti-mouse-CD25 (BD Pharmingen) BS-553075

Rat FITC-anti-mouse-CD3 (BD Pharmingen) BD-555274

Rat FITC-anti-mouse-CD4 IgG (BD Pharmingen) BD-557653

Rat PE-anti-mouse-CD4 IgG (BD Pharmingen) BD-553651

Rat APC-anti-mouse-CD49b IgG (eBioscience) 17-5971

Hamster FITC-anti-mouse-CD69 IgG (BD Pharmingen) BD-557392

Rat PE-anti-mouse-CD8 IgG (BD Pharmingen) BD-550798

Rat APC-anti-mouse-CD80 IgG (BD Pharmingen) BD-560016

Rat PE-anti-mouse-CD86 IgG (BD Pharmingen) BD-553692

Rabbit anti-mouse-β-catenin IgG (Upstate) 06-734

Mouse anti-CDC2 (17) IgG (Santa Cruz Biotechnology Inc., USA) SC-54

Rabbit anti-mouse-Cdk2 IgG (Santa Cruz Biotechnology Inc., USA) Sc163

Rabbit anti-mouse-Cdk4 IgG (Santa Cruz Biotechnology Inc., USA) SC-260

Rabbit anti-mouse-c-Myc IgG (Santa Cruz Biotechnology Inc., USA) SC-788

Rabbit anti-mouse-Cyclin D1 IgG (Santa Cruz Biotechnology Inc., USA) SC-718

Rabbit anti-mouse-Cyclin D2 IgG (Santa Cruz Biotechnology Inc., USA) SC-593

Rat PE-anti-mouse-F4/80 IgG (eBioscience) 12-4801

Rabbit anti-FLAG IgG (Sigma, Germany) F7425

Rat PE-anti-mouse-FoxP3 IgG (BD Pharmingen) BD-560480

Rat PE-anti-mouse-Gr1 IgG (eBioscience) 12-5931-82

Rabbit anti-HA IgG (Sigma, Germany)

Rabbit anti-mouse-ID2 IgG (Santa Cruz Biotechnology Inc., USA) SC-489

Rat PE-anti-mouse-IFNγ IgG (BD Pharmingen) BD-554412

Mouse anti-pIκBα IgG (B-9) IgG (Santa Cruz Biotechnology Inc., USA) sc8404

Rabbit anti-mouse-IκBα (FL) IgG (Santa Cruz Biotechnology Inc., USA) SC-847

Rabbit anti-mouse-IκBβ (S-20) IgG (Santa Cruz Biotechnology Inc., USA) SC-946

Mouse anti-mouse-IKKα IgG (Imgenex, USA) IMG136A

Mouse anti-mouse-IKKβ IgG (Upstate, USA) 05-535

Rat APC-anti-mouse-IL-10 IgG (BD Pharmingen) BD-554468

Rat PE-anti-mouse-IL-12 IgG (BD Pharmingen) BD-554479

Mouse anti-mouse-IL-12b IgG (Prof. David Artis, Univ. of Penn., USA)

Rabbit anti-mouse-IRF1 IgG (Santa Cruz Biotechnology Inc., USA) SC-640

Rabbit anti-mouse-p100 IgG (Cell Signaling Technology Inc., USA) 4882

Rabbit antimouse-p50 IgG (Santa Cruz Biotechnology Inc., USA) SC-7178

Rabbit anti-mouse-p65 IgG (Santa Cruz Biotechnology Inc., USA) SC-226

Rabbit anti-mouse-pSTAT1 IgG (Cell Signaling Technology Inc., USA) 9171L

Rabbit anti-mouse-STAT1 IgG (Santa Cruz Biotechnology Inc., USA) SC-473

Rabbit anti-mouse-pSTAT3 (Tyr705) IgG (Cell Signaling Technology Inc.) 9145

Mouse anti-mouse-STAT3 IgG (BD Pharmingen) BD-610190

Rat FITC-anti-mouse-TNFα IgG (eBioscience) 11-7321

8.4.2. Secondary Antibodies

Sheep anti-mouse HRP conjugated IgG (GE Healthcare) NA9310V

Donkey anti-rabbit HRP conjugated IgG (GE Healthcare) NA9340V

Donkey FITC-anti-rat IgG (Jackson Laboratories) 712-095-153

Donkey AlexaFluor488-anti-goat IgG (Molecular Probes) A11055

Donkey AlexaFluor488-anti-rabbit IgG (Molecular Probes) A21206

8.5 LIST OF INSTRUMENTS

Device	Company	Model
-80° Freezer:	Heraeus	HeraFreeze
-20° Freezers:	Siemens	GS34V420
	Liebherr	GTS2612
4° Refrigerator:	Siemens	KS38R425
4° Cooler Cupboard:	National Lab	LSTR 13006 GWU
Incubator:	Heraeus	FunctionLine
Incubator Shaker:	Edmund Bühler GmbH	TH15
Flow Hood:	Heraeus	HeraSafe KS18
Cell Culture Incubator:	Heraeus	HeraCell 2400
Water bath:	GFL mbH	GFL 1003
Power Supply:	BioRad	PowerPac Basic
Fluorescent Gel Imager:	BioRad	
Nitrogen Tanks:	Tec-Lab	K-Series 3K
	Taylor Wharton	LS4800
PCR Cyclers:	Applied Biosystems	Gene Amp PCR System 9700
RT-PCR Cycler	Applied Biosystems	Step ONE Plus
Autoradiography		
Film Processor:	Amersham Pharmacia	Hyper Processor
pH meter:	Inolab	WTW pH720
Microfuge incubator:	Eppendorf	Thermomixer Plus
Centrifuges:	Eppendorf	5702R
	Eppendorf	5415R
	Eppendorf	5415D
	Eppendorf	5810R
Microscopes:	Evacta+Optech	Mod.IB
	Zeiss	Imager A.1
	Zeiss	Axiostar Plus
	Zeiss	Axiovert 40 CFL
Fluorescent Microscope:	Zeiss	Axiovert 200M
Fluorescent Bulbs:	LEJ GmbH	mbq52 ac

	Zeiss	Apotome
Microtome:	Microm	HM355S
Cryomicrotome:	Microm	HM560
Tissue Dehydrator:	Leica	ASP 3005

8.6. STATISTICS

8.6.1. K-means (Wikipedia, 2009)[2]

In statistics and machine learning, ***k*-means clustering** is a method of cluster analysis which aims to partition n observations into k clusters in which each observation belongs to the cluster with the nearest mean. It is similar to the expectation-maximization algorithm for mixtures of Gaussians in that they both attempt to find the centers of natural clusters in the data.

Given a set of observations ($\mathbf{x}_1$, $\mathbf{x}_2$, …, $\mathbf{x}_n$), where each observation is a d-dimensional real vector, then k-means clustering aims to partition the n observations into k sets ($k < n$) $\mathbf{S}=\{S_1, S_2, \ldots, S_k\}$ so as to minimize the within-cluster sum of squares (WCSS):

$$\underset{\mathbf{S}}{\arg\min} \sum_{i=1}^{k} \sum_{\mathbf{x}_j \in S_i} \left\| \mathbf{x}_j - \boldsymbol{\mu}_i \right\|^2$$

where $\boldsymbol{\mu}_i$ is the mean of S_i.

8.6.2. Z-Score (Wikipedia, 2009)[3]

In mathematical statistics, a random variable X is standardized using the theoretical (population) mean and standard deviation:

$$Z = \frac{X - \mu}{\sigma}$$

where $\mu = \mathrm{E}(X)$ is the mean and = the standard deviation of the probability distribution of X.
If the random variable under consideration is the sample mean:

$$\bar{X} = \frac{1}{n} \sum_{i=1}^{n} X_i$$

then the standardized version is

$$Z = \frac{\bar{X} - \mu}{\sigma / \sqrt{n}}.$$

CURRICULUM VITAE

Personal Data

Name:	Serkan İsmail Göktuna	Address:	Klinikum rechts der Isar
Nationality:	Turkish		II. Med. Klinik
Date of Birth:	27.04.1980		Bau 502 3.OG R.2.3.10
Place of Birth:	Ankara		Ismaningerstr. 22
			81675 München
		Telephone:	+491635996933
		Fax:	+498941406791
		e-Mail:	serkan.goektuna@lrz.tum.de

Research Experience

1) 2005-2009 Technical University Munich, Munich, Germany
PhD Thesis: The role of IKKα in sporadic and familial colorectal tumorigenesis
2) 2003-2005 Sabanci University, Istanbul, Turkey
MS Thesis: MEKK1 and MEKK3 involvement in TNF-alpha and IL-1beta signaling in cervical carcinoma HeLa cells
3) 2003 Middle East Technical University, Ankara, Turkey
Special Project: Cloning and expression of aspartic protease gene from thermoacidophilic bacteria
4) 2002 Max-Delbrück Centrum für Molekulare Medizin, Berlin, Germany
Summer Practice: SNP analysis of KRT9 gene in palmoplantar hyperkeratosis patients

Education

1) Technical University Munich, Humanbiologie (PhD), Munich, Germany 2005-2009
2) Sabanci University, Biological Sciences and Bioengineering (MS), Istanbul, Turkey 2003-2005
3) Middle East Technical University, Molecular Biology and Genetics (BS), Ankara Turkey 1998-2003
4) Ankara Bahçelievler Deneme Lisesi, Natural Sciences (High School), Ankara Turkey 1994-1997

Awards

2007-2009 TÜBITAK Doctoral Scholarship for Foreign Countries
2005-2007 Deutsche Forschungsgemeinschaft BATIIa/2 Scholarship
2003-2005 Sabanci University Full Graduate Scholarship
1998-2003 METU (ODTÜ) Full Basic Sciences Scholarship
1998-2003 TÜBITAK Basic Sciences Scholarship

Publications

1) Greten FR, Arkan MC, Bollrath J, Hsu LC, Goode J, Miething C, Göktuna SI, Neuenhahn M, Fierer J, Paxian S, Van Rooijen N, Xu Y, O'Cain T, Jaffee BB, Busch DH, Duyster J, Schmid RM, Eckmann L, Karin M. NF-kappaB is a negative regulator of IL-1beta secretion as revealed by genetic and pharmacological inhibition of IKKbeta. Cell. 2007; 130(5):918-31.

2) Fingerle, A.A., Schwitalla, S, Göktuna, S.I, Rupec, R.A, Gerhard, M, Lang, R, Schmid, R.M, Taketo, M.M, Arkan, M.C and Greten, F.R. NF-kappaB and constitutive Wnt-activation cooperate to induce crypt stem cell expansion during initiation of intestinal tumorigenesis. Science 2010 (in progress).

LEBENSLAUF

Persönlischen Daten

Name:	Serkan İsmail Göktuna	Addresse:	Klinikum rechts der Isar
Nationalität:	Türkisch		II. Med. Klinik
Geburtsdsatum:	27.04.1980		Bau 502 3.OG R.2.3.10
Geburtsort:	Ankara		Ismaningerstr. 22
			81675 München
		Telephone:	+491635996933
		Fax:	+498941406791
		e-mail:	serkan.goektuna@lrz.tum.de

Forschung Erfahrung

1) 2005-2009 Technische Universität München, München, Deutschland
Doktorarbeit: The role of IKKα in sporadic and familial colorectal tumorigenesis
2) 2003-2005 Sabanci University, Istanbul, Türkei
Masterarbeit: MEKK1 and MEKK3 involvement in TNF-alpha and IL-1beta signaling in cervical carcinoma HeLa cells
3) 2003 Middle East Technical University, Ankara, Türkei
Speziel Projekt: Cloning and expression of aspartic protease gene from thermoacidophilic bacteria
4) 2002 Max-Delbrück Zentrum für Molekulare Medizin, Berlin, Deutschland
Praxis: SNP analysis of KRT9 gene in palmoplantar hyperkeratosis patients

Ausbildung

1) Technische Universität München, Humanbiologie (Doktorand), München, Deutschland 2005-2009
2) Sabanci University, Biological Sciences and Bioengineering (Masterabschluss), Istanbul, Türkei 2003-2005
3) Middle East Technical University, Molecular Biology and Genetics (Vordiplom), Ankara, Türkei 1998-2003
4) Ankara Bahçelievler Deneme Lisesi, Naturlisches Wissenschaften (Gymnasium), Ankara Türkei 1994-1997

Auszeichnung

2007-2009	TÜBITAK Doktorandstelle für Ausland Studium
2005-2007	Deutsche Forschungsgemeinschaft BATIIa/2 Doktorandstelle
2003-2005	Sabanci University Assistentenstelle
1998-2003	METU (ODTÜ) Stipendium
1998-2003	TÜBITAK Stipendium

Publikationen

1) Greten F.R., Arkan M.C., Bollrath J., Hsu L.C., Goode J., Miething C., Göktuna S.I., Neuenhahn M., Fierer J., Paxian S., Van Rooijen N., Xu Y., O'Cain T., Jaffee B.B., Busch D.H., Duyster J., Schmid R.M., Eckmann L., Karin M. NF-kappaB is a negative regulator of IL-1beta secretion as revealed by genetic and pharmacological inhibition of IKKbeta. Cell. 2007; 130(5):918-31.

2) Fingerle, A.A., Schwitalla, S, Göktuna, S.I, Rupec, R.A, Gerhard, M, Lang, R, Schmid, R.M, Taketo, M.M, Arkan, M.C and Greten, F.R. NF-kappaB and constitutive Wnt-activation cooperate to induce crypt stem cell expansion during initiation of intestinal tumorigenesis. Science 2010 (in progress).